



# Geometric Dilation and Halving Distance

**Dissertation**

Zur Erlangung des Doktorgrades (Dr. rer. nat.)  
der Mathematisch-Naturwissenschaftlichen Fakultät  
der Rheinischen Friedrich-Wilhelms-Universität Bonn

vorgelegt von

**Ansgar Grüne**

aus Wickede/Soest

Bonn, 2006

Angefertigt mit der Genehmigung der Mathematisch-Naturwissenschaftlichen Fakultät der Rheinischen Friedrich-Wilhelms-Universität Bonn

Gutachter: Prof. Dr. Rolf Klein, Universität Bonn  
Prof. Dr. Michael Clausen, Universität Bonn

Tag der mündlichen Prüfung: 19. September 2007

Diese Dissertation ist auf dem Hochschulschriftenserver der ULB Bonn unter [http://hss.ulb.uni-bonn.de/diss\\_online](http://hss.ulb.uni-bonn.de/diss_online) elektronisch publiziert.

Erscheinungsjahr: 2008

# Abstract

Let  $G$  be a geometric graph in the plane whose edges may be curves. For two arbitrary points on its edges, we can compare the length of the shortest path in  $G$  connecting them against their Euclidean distance. The supremum of all these ratios is called the *geometric dilation* of  $G$ . Given a finite point set  $S$ , we would like to know the smallest possible dilation of any graph that contains the given points on its edges. We call this infimum the dilation of  $S$  and denote it by  $\delta(S)$ .

The main results of this thesis are

- a general upper bound to the dilation of any finite point set  $S$ ,  $\delta(S) < 1.678$
- a lower bound for a specific set,  $\delta(P) > (1 + 10^{-11})\pi/2 \approx 1.571$

In order to achieve these results, we first consider closed curves. Their dilation depends on the *halving pairs*, pairs of points which divide the closed curve in two parts of equal length. In particular the distance between the two points is essential, the *halving distance*. A transformation technique based on halving pairs, the *halving pair transformation*, and the curve formed by the midpoints of the halving pairs, the *midpoint curve*, help us to derive lower bounds to dilation. For constructing graphs of small dilation we use *Zindler curves*. These are closed curves of constant halving distance.

To give a structured overview, the mathematical apparatus for deriving the main results of this thesis includes

- upper bound:
  - the construction of certain Zindler curves to generate a periodic graph of small dilation
  - an embedding argument based on a number theoretical result by Dirichlet
- lower bound:
  - the formulation and analysis of the halving pair transformation
  - a stability result for the dilation of closed curves based on this transformation and the midpoint curve
  - the application of a disk-packing result

In addition, this thesis contains

- a detailed analysis of the dilation of closed curves
- an overview and proofs of inequalities which relate halving distance to other important quantities from convex geometry, including four new inequalities
- the rediscovery of Zindler curves and a compact presentation of their properties
- a proof of the applied disk packing result

## Acknowledgments

I would like to thank my advisor, Prof. Rolf Klein, for introducing me to the intriguing dilation questions and for giving me the opportunity to work on them.

I am thankful to him and my other co-authors and colleagues for many helpful hints, fruitful collaboration, inspiring and motivating discussions, and a good working atmosphere. I want to mention Florian Berger, Prof. Adrian Dumitrescu, Annette Ebbers-Baumann, Andrea Eubeler, Sanaz Kamali Sarvestani, Dr. Tom Kamphans, Prof. Christian Knauer, Martin Köhler, Dr. Elmar Langetepe, Cinzia Miori, Prof. Salvador Segura Gomis, and Prof. Günter Rote. Also Mariele Knepper contributed to the nice atmosphere in Bonn and was very helpful with administrative tasks.

Additionally, I would like to acknowledge with thanks Prof. Salvador Segura Gomis and Prof. Paul Goodey for advice on known results in convex geometry, Prof. Ferran Hurtado for introducing me to the dilation center problem, Prof. John M. Sullivan for his hints regarding dilation in knot theory and differential geometry, Prof. Günter Rote for help with an article on Zindler curves, Dr. Achill Schürmann and Prof. Chuanming Zong for answering my questions concerning disk-packing results, and Prof. Salvatore Vassallo for pointing out some literature on minimal annuli.

I am especially thankful to Prof. Adrian Dumitrescu, Prof. Ferran Hurtado, and Prof. Salvador Segura Gomis. They offered me opportunities for research stays abroad. Working with them gave me new scientific insight, and they were incredibly nice hosts. I hope to have learned from them in both fields. Another important source of support was the DAAD which sponsored in parts my stay in Barcelona.

Also, I am grateful to everybody who helped me by proof-reading or with advice on layout,  $\text{\TeX}$ , or language questions. Thank you to Robert Blasum, Dr. Simone Frin-trop, Trinity Hartman, Dr. Tom Kamphans, Bettina Lademann, Andreas Ribbrock, Julia Nicholson, and Patrick Schriener.

Because I know that reviewing is not the most sought-after task, I appreciate very much that Prof. Michael Clausen agreed to be the second referee of this thesis.

Another thank you goes to all my friends who supported me and cheered me up. Above all, I am indebted to my parents, Anni and Klaus Grüne, and to my brother Marius for having been and being the family I can rely on. They gave me the inestimable gift of a secure and happy childhood. And my parents taught me the two most important traits for finishing this thesis: curiosity and esteem for academic titles.

Thanks to all of you!

# Contents

<b>1</b>	<b>Introduction</b>	<b>1</b>
1.1	Main problem . . . . .	1
1.2	Results . . . . .	3
1.2.1	Overview of the results of this thesis . . . . .	3
1.2.2	Dilation constant . . . . .	4
1.2.3	Proof of upper bound . . . . .	5
1.2.4	Proof of lower bound . . . . .	6
1.2.5	Additional results . . . . .	8
1.3	Related work . . . . .	9
1.3.1	History of dilation . . . . .	9
1.3.2	Dilation evolving from online algorithms . . . . .	11
1.3.3	Geometric dilation . . . . .	13
1.3.4	Dilation in differential geometry and knot theory . . . . .	14
1.3.5	Graph dilation . . . . .	17
1.3.6	Metric embeddings with small dilation . . . . .	24
1.3.7	Miscellaneous related research . . . . .	25
1.4	Structure of this thesis . . . . .	25
<b>2</b>	<b>Closed Curves</b>	<b>27</b>
2.1	Basic definitions . . . . .	28
2.2	Dilation attained by pair of points . . . . .	30
2.3	Breadth quantities . . . . .	32
2.4	Non-convex closed curves . . . . .	37
2.5	Dilation attained by halving pair . . . . .	40
2.6	Centrally symmetric closed curves . . . . .	44
2.7	Central symmetrization . . . . .	46
2.8	Halving pair transformation . . . . .	50

2.9	Midpoint curve . . . . .	56
2.10	Holditch's theorem . . . . .	58
2.11	Bounds to the dilation of cycles . . . . .	62
2.12	Stability result . . . . .	69
2.13	Polygons . . . . .	72
2.13.1	Triangles . . . . .	73
2.13.2	Regular polygons . . . . .	76
<b>3</b>	<b>Zindler Curves</b>	<b>81</b>
3.1	Characterization and Properties . . . . .	82
3.1.1	Constant perimeter halving distance . . . . .	83
3.1.2	Constant area halving distance . . . . .	88
3.1.3	Constant breadth . . . . .	92
3.1.4	Floating equilibrium . . . . .	98
3.2	Example curves . . . . .	100
3.2.1	Rounded triangle . . . . .	100
3.2.2	Flower . . . . .	107
3.2.3	Zindler's example . . . . .	109
<b>4</b>	<b>Halving Distance</b>	<b>115</b>
4.1	Overview . . . . .	115
4.2	Basic results . . . . .	116
4.3	$H$ and diameter $D$ . . . . .	118
4.4	$H$ and circumradius $R$ . . . . .	122
4.5	$H$ and perimeter $ C $ . . . . .	126
4.6	$H$ and width $w$ . . . . .	126
4.7	$h$ and width $w$ . . . . .	128
4.8	$h$ and inradius $r$ . . . . .	130
4.9	$H$ and area $A$ . . . . .	131
4.10	$h$ and area $A$ . . . . .	131
4.11	Continuity and approximation arguments . . . . .	133
<b>5</b>	<b>Point Sets</b>	<b>139</b>
5.1	Embedding point sets with small geometric dilation . . . . .	139
5.1.1	Optimal embeddings for particular point sets . . . . .	139
5.1.2	Bounding the worst-case dilation . . . . .	140

5.1.3	Dilation attained by mutually visible points . . . . .	140
5.2	Upper bounds . . . . .	142
5.2.1	Rectangular grid . . . . .	142
5.2.2	Square grid . . . . .	142
5.2.3	Hexagonal grid . . . . .	144
5.2.4	Improved hexagonal grid . . . . .	145
5.2.5	Embedding any point set . . . . .	148
5.3	Lower bounds . . . . .	151
5.3.1	A first lower bound . . . . .	151
5.3.2	Motivation for improved lower bound . . . . .	153
5.3.3	Disk-packing result . . . . .	154
5.3.4	Improved lower bound . . . . .	156
5.3.5	Reverse link between disk packing and dilation . . . . .	160
5.3.6	Apollonian packing . . . . .	161
<b>A</b>	<b>Parameterizations</b>	<b>165</b>
A.1	Arc-length parameterization . . . . .	165
A.2	Area-bisecting parameterization . . . . .	166
A.3	Extremal parameterization . . . . .	169
<b>B</b>	<b>Proof of Disk-Packing Result</b>	<b>173</b>
B.1	Idea of the proof . . . . .	173
B.2	Inductive construction . . . . .	174
B.2.1	Induction Base . . . . .	174
B.2.2	Induction Step: $R_n$ crescent . . . . .	175
B.2.2.1	Medium size disk intersecting $I$ . . . . .	176
B.2.2.2	No medium size disk intersecting $I$ . . . . .	182
B.2.3	Induction Step: $R_n$ circular . . . . .	185
B.3	Final Remark . . . . .	187
	<b>List of Symbols</b>	<b>188</b>
	<b>List of Open Problems</b>	<b>191</b>
	<b>List of Figures</b>	<b>193</b>
	<b>Bibliography</b>	<b>199</b>

**Index****211**





244m. The *detour* between the two points on  $G$  is defined as the ratio of these two values,

$$\delta_G(p, q) := \frac{d_G(p, q)}{|pq|}. \quad (1.1)$$

In the given example we have  $\delta_G(p, q) \approx 1.39$ .

Obviously, we would like the detour to be as small as possible, i.e. close to 1. This is what we demand of the networks of streets. However, in a city, there are usually buildings spread all along the streets. And other people might want to go from any other starting point  $p$  on any street of the network  $G$  to any other destination  $q$  on  $G$ . Therefore, a good measure of the overall quality of this network is the worst-case detour which we call (*geometric*) *dilation*. It is formally defined by

$$\delta(G) := \sup_{p, q \in G, p \neq q} \delta_G(p, q) \quad (1.2)$$

Here  $p, q \in G$  means that  $p$  and  $q$  lie on any edge of the graph  $G$ . For example a dilation value of  $\delta(G) \leq 2$  guarantees that one can reach any point  $q \in G$  from any other point  $p \in G$  by not having to walk more than twice their airline distance.

The main topic we want to discuss in this thesis is how to construct networks of small dilation. Suppose, we are given a finite point set  $S$  in the Euclidean plane. We would like to determine the geometric graph  $G$  of smallest possible dilation connecting the given points, i.e., every point of  $S$  has to be located on some edge of the graph. We say that the graph  $G$  *embeds*  $S$ . We only consider *simple* graphs. This means that there are no intersections apart from the vertices. To stay in the picture of the city example, we do not allow bridges. Streets can only intersect at crossroads.



Figure 1.2: We want to connect the given sites by a network of streets.<sup>3</sup>

The situation of our main problem resembles a little bit the popular computer game SimCity<sup>2</sup>, see Figure 1.2. The task is to build the streets of a city from scratch. With the point set  $S$  one is given some locations which have to be part of the network of streets. In Figure 1.2 these are the planned locations of the harbor, the park and the waterworks. As can be seen in Figure 1.3, houses will soon be built all along the streets, as the city develops. And the inhabitants would like to be able to go from any point of the network to any other point without having to take a big detour. Hence, we try to minimize the geometric dilation of the network.

<sup>2</sup>Contrary to the situation in SimCity however, we are not forced to obey a certain grid of cells, nor are there obstacles like lakes or rivers.



Figure 1.3: Soon there will be houses all along the streets. Therefore, we want to minimize the geometric dilation.<sup>3</sup>

We are interested in the smallest dilation value which can be attained by any graph embedding  $S$ . We call this value the (*geometric*) *dilation* of  $S$ . It is formally defined by

$$\delta(S) := \inf_{G \text{ simple, finite, } S \subset G} \delta(G). \quad (1.3)$$

## 1.2 Results

### 1.2.1 Overview of the results of this thesis

The concept of dilation has fruitful applications in various fields such as knot theory, convex geometry, metric space embedding, robot motion planning and urban planning. We give a short overview of the known results in Section 1.3.

Although it is a natural question, we are the first to formulate and study the embedding problem. Of course, for an urban planning situation in reality, one would have some additional restrictions. For example the “blocks”, the faces of the graph, should not be too big nor too small. And it makes sense to build some bigger streets where one can go faster.

However, in this thesis we develop a bunch of arguments and tools which we believe to be useful also for more general settings. This thesis is a first step and provides fundamental theoretical results which can be the basis of future research. The main results are:

- a general upper bound to the dilation of finite point sets,  $\delta(S) < 1.678$
- a lower bound for a specific set,  $\delta(P) > (1 + 10^{-11})\pi/2 \approx 1.571$

---

<sup>3</sup>I am thankful to Maxis/Electronic Arts for the permission to use these screenshots of their game SimCity 2000.

The mathematical apparatus for constructing these bounds includes

- upper bound:
  - the construction of certain Zindler curves to generate a periodic graph of small dilation
  - an embedding argument based on a number theoretical result by Dirichlet
- lower bound:
  - the formulation and analysis of the halving pair transformation
  - a stability result for the dilation of closed curves based on this transformation and the midpoint curve
  - the application of a disk-packing result

In addition, this thesis contains

- a detailed analysis of the dilation of closed curves
- an overview and proofs of inequalities which relate halving distance to other important quantities from convex geometry, including four new inequalities
- the rediscovery of Zindler curves and a compact presentation of their properties
- a proof of the applied disk packing result

### 1.2.2 Dilation constant

Our first question, which asks for a way to construct an optimal network embedding a given point set  $S$ , has computational character. A solution for two points is trivially the line segment which connects them. But for three points already, it is known that the solution is not easy anymore. Before we started the work on this thesis, Ebbers-Baumann et al. had proved that the optimal embedding graph for three given points is either a Steiner-tree with  $120^\circ$ -angles or a curve built of two line segments and a part of a logarithmic spiral. A full proof can be found in the recent manuscript [60].

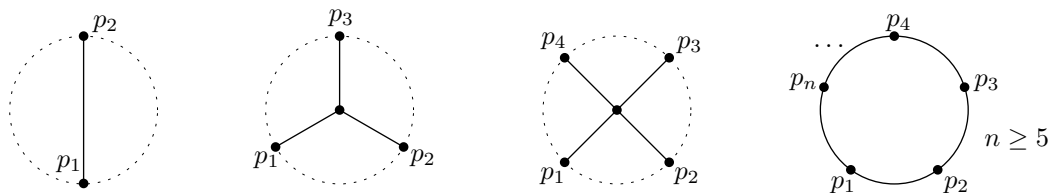


Figure 1.4: The optimal embeddings of the point sets  $S_n$ , which contain  $n$  points placed evenly on a circle.

The problem becomes much more difficult for a growing number of given points. Still, we are able to determine the optimal embeddings for particular sets, the vertex sets of regular  $n$ -gons denoted by  $S_n$ . The solutions are shown in Figure 1.4 and discussed in Section 5.1.1.

As the task to find an optimal graph for any given finite point set  $S$  turns out to be quite complicated, we look for approximate solutions which are applicable to every finite point set  $S$ . They give upper bounds to the worst dilation of any finite point set, formally defined by

$$\Delta := \sup_{S \subset \mathbb{R}^2, |S| < \infty} \delta(S). \quad (1.4)$$

The main topic of this thesis is to find and prove good bounds to this dilation constant  $\Delta$ .

### 1.2.3 Proof of upper bound

A natural idea for proving upper bounds to  $\Delta$  is to use a kind of regular grid for embedding  $S$ . Indeed this turns out to be possible. However, we have to answer two questions evolving from this approach. First, we want to find grid graphs of small dilation. And second, we have to prove that they are applicable to embed any finite  $S$ . After several attempts, each yielding

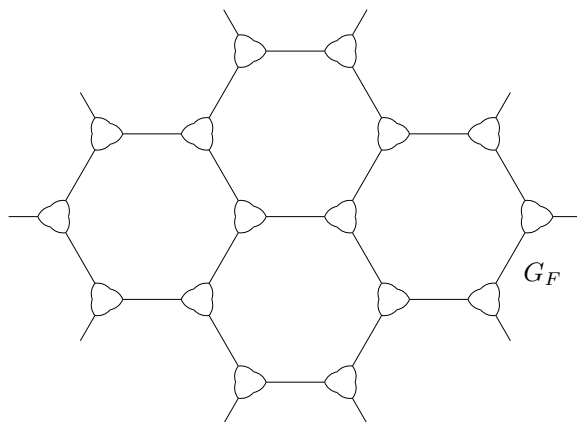


Figure 1.5: A section of the regular grid  $G_F$  based on hexagons and flower-curves which attains small dilation,  $\delta(G_F) < 1.678$ .

better dilation (Sections 5.2.2–5.2.4), we answer the first question with a hexagonal grid  $G_F$  where each vertex is replaced by a closed Zindler curve resembling a flower, see Figure 1.5. The second problem can be solved by applying a number-theoretical result from Dirichlet. All this yields the following upper bound, see Section 5.2.5.

$$\Delta < 1.678$$

We published the embedding problem and the upper bound first in [56, 58]. In Section 5.2.5, additionally, we prove a generalized version of the approximation idea, and show that it can be applied to any regular grid.

We know that the upper bound can be improved slightly. For instance one can replace the non-convex corners of the flower cycle in the grid  $G_F$  by small concave circular arcs. Or one could try to insert another kind of cycle at the vertices where one flower cycle and two hexagonal cycles meet, thereby following the iteration of the Apollonian packing presented in Section 5.3.6. But we do not see any approach promising a significant improvement.

### 1.2.4 Proof of lower bound

It is known that the dilation of any closed curve  $C$  is bounded by  $\delta(C) \geq \pi/2$ , see for instance Gromov [86, 88]. We give a new, very short proof of this result relying on Cauchy's surface area formula in Section 2.3.

The dilation of any graph  $G$  is attained by two mutually visible points  $p, q$ , i.e.  $pq \cap G = \{p, q\}$ . We extend this property, which is known for curves, to arbitrary graphs in Section 5.1.3. This shows that the dilation of any graph  $G$  which is not a tree is bounded by  $\delta(G) \geq \delta(C) \geq \pi/2$ , where  $C$  denotes the shortest cycle in  $G$ , cf. the proof of Theorem 5.4. Further arguments in the same proof show that the set  $S_5$  of five points placed evenly on the circle cannot be embedded by any tree with dilation less than  $\pi/2$ . These arguments, visualized in Figure 1.6

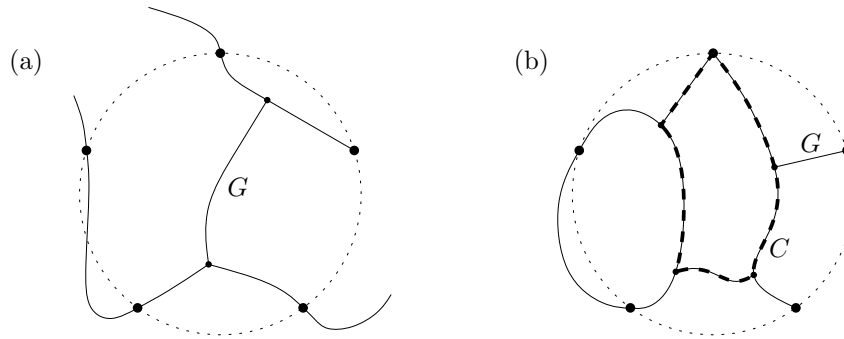


Figure 1.6: The dilation of any geometric graph  $G$  which embeds  $S_5$  is bounded by  $\delta(G) \geq \pi/2$ . The graph is a tree or it contains a cycle  $C$ .

yield a first lower bound to  $\Delta$ , namely

$$\Delta \geq \delta(S_5) \stackrel{\text{Thm. 5.4}}{=} \frac{\pi}{2} \approx 1.5707.$$

However, this lower bound, which we first presented in [56, 58], is not completely satisfactory. It is known that circles are the only closed curves attaining the optimal dilation  $\delta(C) = \pi/2$ , see Corollary 2.8. And intuitively it is clear that we cannot embed any point set with graphs where all faces have to be circular disks. Still, even if we formalized these arguments, they would not suffice to prove  $\Delta > \pi/2$ , because there could exist a sequence of embedding graphs for every point set  $S$  whose dilation tends to  $\pi/2$ .

Therefore, among other things we are interested in more specific lower bounds to the dilation of closed curves in Chapter 2. We prove that the dilation of a cycle  $C$  is never smaller than the dilation of  $\partial\text{ch}(C)$ , the boundary curve of its convex hull (Section 2.4). This restricts our search for lower bounds to convex cycles. By applying the well-known central symmetrization from convex geometry, we are able to prove a strict bound depending on the ratio of the diameter of  $C$  and its width (Theorem 2.33), but it cannot be applied immediately to prove  $\Delta > \pi/2$ .

A lower bound which turns out to be more useful in this context is based on halving pairs, which we introduced as partition pairs in [56, 58]. Two points  $p, \hat{p}$  on a closed curve  $C$  form a *halving pair* if they divide  $C$  into two paths of equal length, see Figure 1.7. In this case the distance  $|p\hat{p}|$  is called *halving distance* and the line segment  $p\hat{p}$  is called *halving chord*.

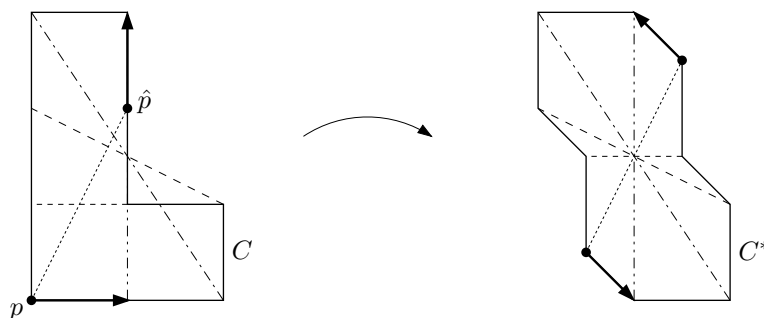


Figure 1.7: The halving pair transformation applied to an L-shaped cycle  $C$ . The chords illustrate halving pairs like  $(p, \hat{p})$ .

We prove that the dilation of any convex cycle<sup>4</sup> is attained by a halving pair (Section 2.5). Based on halving pairs, we develop the halving pair transformation (Section 2.8) shown in Figure 1.7. This transformation was mentioned very briefly by Zindler [186, p. 44] in 1921. It is similar to central symmetrization, and we prove an extensive list of its properties which might be useful in some other context as well. We apply the halving pair transformation to achieve another lower bound to the dilation of closed curves depending only on the ratio of its maximum and minimum halving distance (Theorem 2.33). We published the new lower bounds and most of the results on halving pair transformation first in [57, 59].

As a next step, we adjust this lower bound for closed curves to prove that any closed curve of dilation close to  $\pi/2$  has to be close to being a circle; it has to be contained in a thin *annulus*, a thin ring between two concentric circles (Section 2.12). This can be seen as kind of *stability result* for the inequality  $\delta(C) \geq \pi/2$ . Such results complement geometric inequalities (like the isoperimetric inequality between the area and the perimeter of a planar region) with statements of the following kind: If a certain geometric object “almost” attains equality for the considered inequality, it is “close” to the *extremal set(s)*, i.e. the object or class of objects for which the inequality is tight, see Groemer’s survey [84].

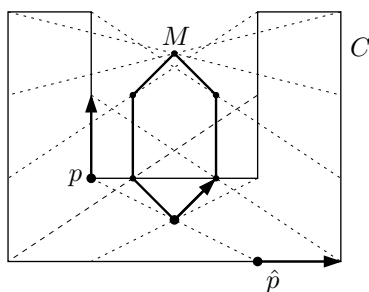


Figure 1.8: The midpoint curve  $M$  of an U-shaped cycle  $C$ .

The proof of this statement is also based on the *midpoint curve*  $M$  presented in detail in Section 2.9. It is the curve formed by the midpoints of the halving pairs, see Figure 1.8.

<sup>4</sup>In this thesis we use the notions “closed curve” and “cycle” synonymously.

Our stability result has already turned out to be useful in another setting. Denne and Sullivan [45] generalized it to higher dimensions and applied it to questions from knot theory.

The result enables us to apply a disk-packing result from Kuperberg et al. [134] (cf. Section 5.3.3) to the problem. After overcoming some additional technical problems, in Section 5.3.4, this yields the improved lower bound

$$\Delta > (1 + 10^{-11}) \frac{\pi}{2}.$$

Although this might seem a minor improvement to the previous lower bound of  $\pi/2$ , we think that it is an important step to prove a lower bound bigger than  $\pi/2$ , and it has needed the introduction of several completely new ideas. Furthermore, our arguments show that any improvement of the disk packing result immediately implies a better lower bound to  $\Delta$ . We presented the improved lower bound first in [50, 49].

### 1.2.5 Additional results

Having defined the new quantities, minimum and maximum halving distance,  $h(C)$  and  $H(C)$ , for every closed curve, it is natural to ask how they are related to other important quantities from convex geometry. These questions are also motivated by the analogy to so-called fencing problems which we describe in Section 1.3.7.

Therefore, we devote a whole chapter to list pairwise inequalities between  $h$  or  $H$  and one of the six quantities width  $w$ , diameter  $D$ , perimeter  $|C|$ , inradius  $r$ , circumradius  $R$  and area  $A$ . Some of the inequalities like  $H \leq D$  follow immediately from the definitions. Others turn out to be easy consequences of these trivial inequalities and/or known ones.

Furthermore, we prove four new inequalities with more involved proofs, namely  $H \geq w$ ,  $H \geq 2r$ ,  $h \geq \frac{1}{2}w$  and  $h > r$ .

To make this chapter self-contained, we also give full proofs of the three known not evident inequalities  $H \geq \frac{3}{2}R$ ,  $H^2 \geq \frac{4}{\pi}A$ , and  $H \geq \eta D$  where  $\eta \approx 0.843$ . For the latter inequality we present a translated and slightly corrected version of a proof in French by Radziszewski [163]. For  $H \geq \frac{3}{2}R$  we work out ideas given by Eggleston [64] based on his proof of the analogous inequality for area halving distance. However, the two cases turned out not to be as similar as expected. Therefore the proof given here is almost totally new. For  $H^2 \geq \frac{4}{\pi}A$  we reformulate Goodey's proof from [78] as an easy application of halving pair transformation.

Chapter 3 deals with *Zindler curves*, which are curves of constant halving distance. They turn out to be useful for constructing networks of small dilation, cf. Section 5.2.4 and the introduction of Chapter 3. And that is how we originally discovered this kind of curves, at first being surprised that the circle is not the only cycle of constant halving distance. The most important example is probably the rounded triangle<sup>5</sup>  $C_\Delta$  shown in Figure 1.9. We analyze it and other examples in Section 3.2.

We presented our discoveries in [48, 49]. In between the work on the conference and the journal version, we found out that these curves were first studied by Konrad Zindler in 1921 [186]. And we are not the first to rediscover them, cf. Salkowski's article [168, p. 59] from 1934.

---

<sup>5</sup>Be aware that the rounded parts of  $C_\Delta$  are not circular arcs.



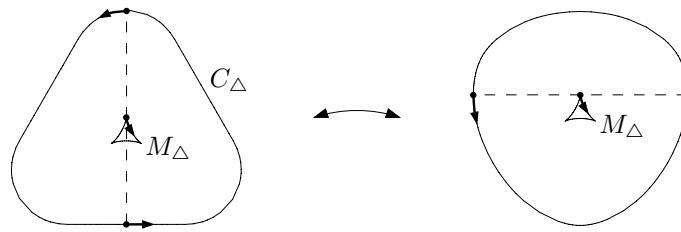


Figure 1.9: The rounded triangle  $C_\Delta$  and its dual curve of constant breadth.

Most of the properties we had proved until then turned out to be known. However, because the known results on Zindler curves are scattered over several articles, some of them quite old and sometimes not stating clearly all the necessary assumptions, I decided to devote a chapter of this thesis to this special class of curves, hoping that the point of view used here, which stresses the role of the midpoint curve, leads to a well-structured comprehensive characterization.

In that chapter it is shown that with some exceptions the halving chords of Zindler curves are always tangent to the midpoint curve. This can be used to prove that – at least in the convex case – their halving chords also bisect the area. Furthermore, there is an amazing relation to the famous curves of constant breadth. Under some additional assumptions a Zindler curve can be transformed to a curve of constant breadth and vice versa by simply rotating all the halving pairs by  $90^\circ$  around their midpoint, cf. Figure 1.9.

In addition to the results mentioned so far, in this thesis we consider the related disk-packing problem more closely. We pose some open problems (Section 5.3.3), give arguments why the link to dilation might have a one-way character (Section 5.3.5), and introduce the Apollonian packing (Section 5.3.6), a fractal disk packing which is interesting for the disk-packing questions and for the construction of graphs of small dilation.

## 1.3 Related work

The previous section has summarized the results of this thesis. This section gives an overview on related work of other authors, and on the connection to our work. It sketches how the notion of dilation has evolved from different roots, and how it was applied in different fields of research. It contains even very recent results, some of them motivated by or applying contents of this thesis.

### 1.3.1 History of dilation

The idea of dilation can be traced back to different origins. Figure 1.10 shows a rough sketch of its history and of its present state. Note that the given dates mark only the beginning of the corresponding field of research; most of them are vivid until today. In the following sections, we describe the developments in more detail.

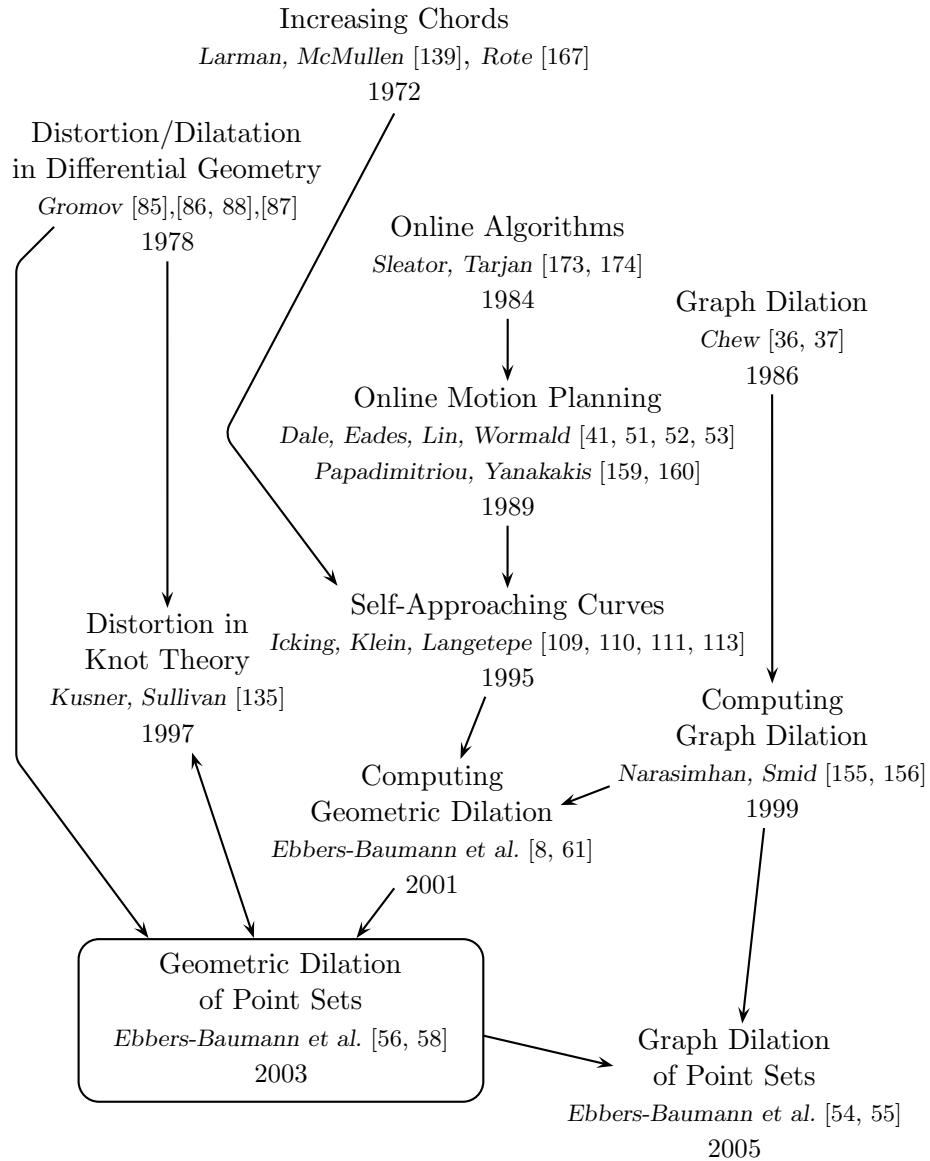


Figure 1.10: The history of dilation. The references and dates refer only to the first articles of the corresponding field of research.

### 1.3.2 Dilation evolving from online algorithms

The work group of Rolf Klein, which I joined in 2002, contributed to the branch of research starting with *online algorithms*. These are algorithms which have to make decisions without full knowledge of the situation. Because of this, in most cases they are not able to derive an optimal solution.

Let  $\Pi$  denote the considered problem, such that every member  $P \in \Pi$  is an instance of the problem. The quality of an online algorithm ALG is measured by its *competitive ratio*  $c_{\text{ALG}}$ , the maximum ratio between the costs of the online-algorithm  $\text{ALG}(P)$  and the costs of an optimal solution  $\text{OPT}(P)$ ,

$$c_{\text{ALG}} := \sup_{P \in \Pi} \frac{\text{ALG}(P)}{\text{OPT}(P)}.$$

If  $c_{\text{ALG}} < \infty$ , the algorithm is called  *$c_{\text{ALG}}$ -competitive*. Otherwise it is not competitive.

There is an obvious analogy to the definition of dilation in (1.1) and (1.2). But the first problem examined this way was not geometric. Sleator and Tarjan [173, 174] introduced the new *competitive analysis* by applying it to a list-accessing problem in 1984. This was the birth of a new field of research in computer science. Until today the technique has been applied very successfully to a variety of problems, listed for example in a survey by Fiat and Woeginger [72] and in a textbook by Borodin and El-Yaniv [23].

In 1989 Papadimitriou and Yanakakis [159, 160] and Dale et al. [41, 51, 52, 53]<sup>6</sup> were – independently from each other – the first to apply competitive analysis to robot motion planning. Here, the robot has restricted information because it does not know its environment a priori. It only gathers information while it moves through the scene and sees or bumps into obstacles. An overview of online motion planning can be found in surveys by Rao et al. [164], Icking and Klein [108], Berman [17], Icking et al. [107] and in the introduction of Kamphans' recent PhD-thesis [118].

There are several possible tasks for the robot, like finding a destination  $t$  and moving there, or exploring the whole environment. Also, the considered problems differ depending on how the robot obtains new information. For example it may have sight, possibly within a bounded radius only, or it may only have a touching sensor. It may know the location of the destination or not. It could have a compass, a GIS, or it might have to rely on measuring its own movements.

The most important cost function in this context is path length. Hence, for instance, if a robot with sight has to move inside a given polygon  $P$  to a destination  $t$  which cannot be seen from its starting position  $s$ , the competitive ratio of its strategy ALG would be

$$c_{\text{ALG}} = \sup_P \sup_{\text{polygon } s, t \in P} \frac{|\zeta_{\text{ALG}}(s, t)|}{d_P(s, t)},$$

where  $|\zeta_{\text{ALG}}(s, t)|$  denotes the length of the path of ALG in  $P$  from  $s$  to  $t$ , and  $d_P(s, t)$  is the length of the shortest path between  $s$  and  $t$  in  $P$ , see Figure 1.11.

Klein [126] introduced the expression *detour* to denote the above ratio of path-lengths, and he showed that  $c_{\text{ALG}} = \infty$  for every algorithm ALG if one considers arbitrary polygons. He defined

---

<sup>6</sup>Paul Dale has only participated in the first conference presentation [41]. The subsequent three papers are written only by Eades, Lin and Wormald.

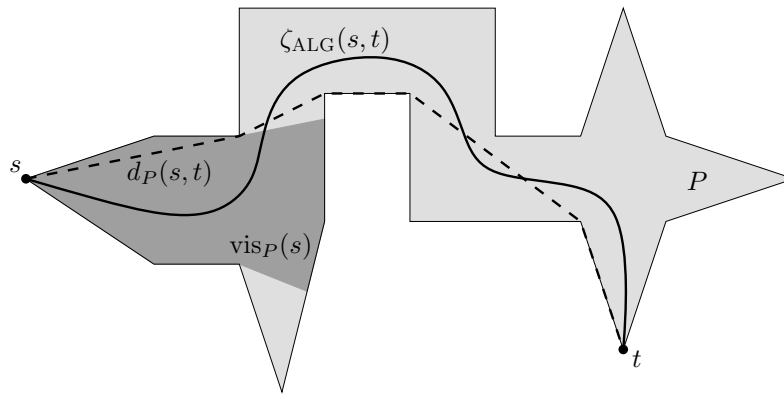


Figure 1.11: Because the robot does not know the polygon  $P$  in advance and it can only see  $\text{vis}_P(s)$  from its starting position  $s$ , it usually takes a detour before it reaches the destination  $t$ .

a special class of polygons called *streets*, and proved the existence of a strategy LAD (which minimizes the Local Absolute Detour) with competitive ratio  $c_{\text{LAD}} = 1 + \frac{3}{2}\pi \approx 5.712$  for searching the destination  $t$  in streets. He also proved the complementing lower bound  $c_{\text{ALG}} \geq \sqrt{2}$  for every strategy ALG in this problem. Several papers worked on improving the upper bound, until in 1999 Icking, Klein and Langetepe [112] and Schuierer and Semrau [171] independently from each other proved that there exists a  $\sqrt{2}$ -competitive strategy, thus matching the lower bound. The result was presented in the joint paper [114].

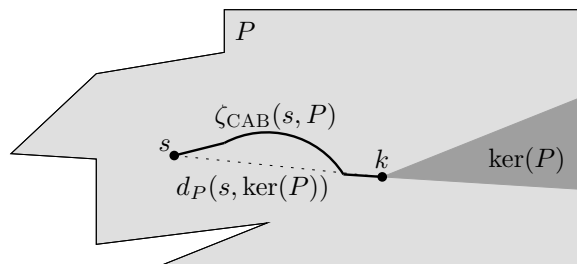


Figure 1.12: A robot starts in  $s$  and applies the strategy CAB to search for the kernel of  $P$ .

In online motion planning, the geometric dilation of closed curves was first considered in the context of searching for the kernel of a star-shaped polygon. A polygon is *star-shaped* if there exists a point  $p \in P$  from where one can see the whole polygon. The *kernel* of a star-shaped polygon is the set of all points which can see the whole polygon, see Figure 1.12. Clearly, moving to the kernel of a polygonal scene is desirable in many situations.

In 1995 Icking and Klein [109] developed the strategy CAB (Continuous Angular Bisector) for searching for the kernel of a polygon. Here, the competitive ratio is defined as

$$c_{\text{CAB}} := \sup_{P \text{ starshaped}} \sup_{s \in P} \frac{|\zeta_{\text{CAB}}(s, P)|}{d_P(s, \text{ker}(P))},$$

where  $\text{ker}(P)$  denotes the kernel of  $P$ ,  $|\zeta_{\text{CAB}}(s, P)|$  denotes the length of the path used by CAB

to go from  $s$  to  $\ker(P)$ , and  $d_P(s, \ker(P))$  is the length of the shortest path from  $s$  to  $\ker(P)$ . Klein and Icking proved that the path  $\zeta_{\text{CAB}}(s, P)$  is always *self-approaching*. This means that for any three consecutive points  $a, b, c$  on  $\zeta_{\text{CAB}}(s, P)$ , we have  $|ac| \geq |bc|$ . Furthermore, they showed that the geometric dilation<sup>7</sup> of any self-approaching curve  $C$  is bounded by  $\delta(C) \leq 5.52$ . This upper bound is improved to the tight bound 5.3331... in the subsequent articles by Icking, Klein and Langetepe [110, 111, 113], see also Klein's textbook [127]. This immediately implies the same upper bound to  $c_{\text{CAB}}$ , because  $\zeta_{\text{CAB}}$  always connects  $s$  to the nearest point in  $\ker(P)$ .

This is a very elegant way of proving an upper bound to  $c_{\text{CAB}}$ , and it reveals a surprising link to an older question stemming from complex analysis. However, in a subsequent article Lee et al. [142] introduced a different strategy of competitive ratio  $1 + 2\sqrt{2} \approx 3.8284$  which uses paths consisting of straight line segments, and later Lee and Chwa [141] improved the upper bound on the competitive ratio of CAB to  $c_{\text{CAB}} \leq \pi + 1 \approx 4.1416$ .

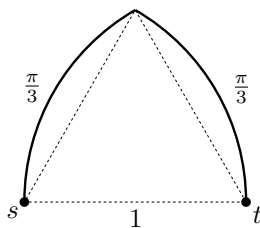


Figure 1.13: This concatenation of two circular arcs is the longest curve with increasing chords connecting  $p$  and  $q$ .

Self-approaching curves generalize arcs with increasing chords which were studied first by Larman and McMullen [139] in 1972. They call a curve  $C$  an *arc with increasing chords* if any four consecutive points  $a, b, c, d$  on  $C$  satisfy  $|ad| \geq |bc|$ . It is easy to prove that this is equivalent to saying that  $C$  is self-approaching in both directions. Larman and McMullen proved, without using any explicit name for this value, that the geometric dilation of any curve  $C$  with increasing chords is bounded by  $\delta(C) \leq 2\sqrt{3} \approx 3.464$ . If  $C$  is convex, they even showed  $\delta(C) \leq \frac{2}{3}\pi \approx 2.094$ , cf. Figure 1.13. Their research was motivated by a question from Binmore who applied a preliminary result of them to a question from complex analysis [18].

Larman and McMullen conjectured that the bound  $\delta(C) \leq \frac{2}{3}\pi$  holds for arbitrary (not necessarily convex) curves with increasing chords. For a long time the conjecture remained unproved. It is mentioned as Open Problem G3 in the collection [40] by Croft et al. Then, in 1993 Rote [167] proved the conjecture. He used the notion *minimum growth rate* which equals the inverse of geometric dilation. Later, he also collaborated with Aichholzer et al. [6] to prove a dilation bound for generalized self-approaching curves.

### 1.3.3 Geometric dilation

The results from online motion planning triggered a deeper interest in geometric dilation. In 1999 Narasimhan and Smid [155, 156] had introduced algorithms to approximate the

<sup>7</sup>The geometric dilation of curves is called 'detour' in the articles dealing with self-approaching curves.

stretch factor of some geometric graphs like paths, cycles and trees. *Stretch factor* is another name for the graph dilation we consider in detail in Section 1.3.5. At this point, naturally arose the question how to compute or at least approximate the geometric dilation of a given graph.

Ebbers-Baumann et al. [8, 61] gave the first answer in 2001. They showed how to approximate the geometric dilation, then still called detour, of an open polygonal curve with  $n$  edges in the plane in time  $O(n \log n)$ . They discuss properties of dilation which proved to be useful for several subsequent results, including this thesis. For example, in Section 5.1.3 we generalize their statement, that the pair of points attaining maximum detour is mutually visible.

Their discovery that the maximum detour is attained by a pair of points containing at least one vertex was applied again by Langerman et al. [137, 138] in 2001 and by Agarwal et al. [3] in 2002, who, independently from each other, developed similar algorithms to compute the exact geometric dilation of (open or closed) polygonal curves in the plane in time  $O(n \log n)$ . Langerman et al. gave a deterministic algorithm and additionally considered trees, while Ebbers-Baumann et al. concentrated on a randomized algorithm and added another subquadratic algorithm for polygonal curves in three dimensions. All these results were combined in the joint journal version [2].

In the same year I generalized the ideas to the more complicated problem of computing the *geometric dilation of polygons* in my diploma thesis [92]. This dilation value is defined by

$$\delta(P) := \sup_{p, q \in P, p \neq q} \frac{d_P(p, q)}{|pq|},$$

where the points  $p$  and  $q$  are taken from everywhere in the interior or on the boundary of the polygon, and  $d_P(p, q)$  denotes the length of the shortest path which stays inside of the polygon and connects  $p$  and  $q$ . It measures the jaggedness of such a polygonal “island”. I presented an  $O(n \log n)$  approximation algorithm and an  $O(n^2)$  exact algorithm. In a collaboration with Langetepe and Klein [95] we added algorithms to compute the geometric  $L_1$ -dilation of polygons in 2003.

Immediately afterwards the work on the questions of this thesis began.

### 1.3.4 Geometric dilation in differential geometry and knot theory

As mentioned in the historic overview, geometric dilation was considered before in differential geometry and knot theory. Gromov [85] considered related concepts already in 1978. He defines the *dilatation* of a mapping  $x : V \rightarrow W$  between Riemannian manifolds  $V$  and  $W$  as

$$\text{dil}(x) := \sup_{v_1, v_2 \in V, v_1 \neq v_2} \frac{d_W(x(v_1), x(v_2))}{d_V(v_1, v_2)}.$$

Note that  $\text{dil}(x)$  equals the *Lipschitz constant* of  $x$ , cf. [24], [38, p. 43]. It also reveals an analogy to our definition of geometric dilation. As we discuss later, geometric dilation can be regarded as a special case of the above definition. In the same article, Gromov defines the *distortion* of such a mapping as

$$\text{distor}(x) := \sup_{v_1, v_2 \in V, v_1 \neq v_2} \frac{d_V(v_1, v_2)}{d_W(x(v_1), x(v_2))} + \frac{d_W(x(v_1), x(v_2))}{d_V(v_1, v_2)}.$$

This is only distantly related to geometric dilation. Also, the rest of the article [85], where Gromov examines the relation between geometrical and topological invariants, does not have any important intersection with the problems we consider here.

However, as mentioned before, Gromov's subsequent book [86] from 1981, dealing with metric structures in differential geometry, and its extended translation to English [88] from 1998 have some overlapping with our results. In this book, Gromov defines dilatation as before, but in the English translation [88] the notion *distortion* now denotes a special kind of dilatation for a subset  $X$  of a metric space  $Y$  with *intrinsic metric*  $d_Y$ . Roughly speaking, a metric  $d(x, y)$  is intrinsic if it equals the infimum of the lengths of curves connecting  $x$  and  $y$ . One could call it shortest-path metric. Gromov's new definition of distortion compares the intrinsic metric of  $Y$  to the induced intrinsic metric on  $X$ . It is defined by

$$\text{distort}(X) := \sup_{x_1, x_2 \in X, x_1 \neq x_2} \frac{d_X(x_1, x_2)}{d_Y(x_1, x_2)}.$$

Clearly, if  $X$  represents a geometric graph or a curve, this kind of distortion equals geometric dilation. In the original French version [86] this value is denoted by  $\text{dil}(f)$  where  $f$  is the identity map  $f : (X, d_X) \rightarrow (X, d_Y)$ . From this point of view, geometric dilation is also a special case of Gromov's dilatation.

Gromov proves by an argument similar to our halving-pair transformation that a set  $X \subset \mathbb{R}^n$  must be simply connected if its distortion is bounded by  $\text{distort}(X) < \pi/2$ . With Corollary 2.8 we give a shorter proof of the special case where  $n = 2$  and  $X = C$  is a simple cycle; it is an immediate consequence of Cauchy's surface area formula. In this case, Gromov's statement says that  $\text{ditort}(C) = \delta(C) \geq \pi/2$ , because  $C$  is a simple cycle, hence it is not simply connected.

Gromov also remarks that  $\text{distort}(X) = \pi/2$  implies that  $X$  contains a round circle. In particular this shows that circles are the only closed curves in  $\mathbb{R}^2$  attaining  $\delta(C) = \pi/2$ , a statement we prove as an immediate consequence of our new lower bounds to the dilation of closed curves in Corollary 2.35.

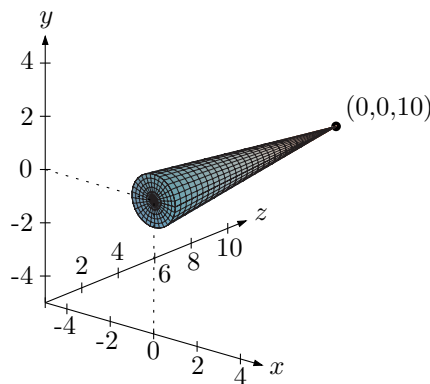


Figure 1.14: This closed *but hollow* cone, an example from Gromov [87], is a non-contractible set of dilation  $< \pi/2$ .

In two-dimensional space these results also say that every non-contractible set has distortion  $\geq \pi/2$ . This could raise the false conjecture that for every dimension  $n \in \mathbb{N}$  the distortion

of every non-contractible  $X \subset \mathbb{R}^n$  satisfies  $\text{distor}(X) \geq \pi/2$ . In [87, p. 114], Gromov gives a counter example  $X \subset \mathbb{R}^3$ , see Figure 1.14. It is the union of the unit disk  $\{(x, y, 0) | x^2 + y^2 \leq 1\}$  and the cone from the point  $(0, 0, 10)$  over the unit circle  $\{(x, y, 0) | x^2 + y^2 = 1\}$ . This means that the cone is hollow. Therefore, it is not contractible.

However, in [86, 88] Gromov proves that any  $X \subset \mathbb{R}^n$  is contractible if  $\text{distor}(X) < \pi/(2\sqrt{2})$ . Furthermore, he proves some relations between the degree of a mapping and its dilatation and examines the dilatation of mappings on spheres.

In his successive, extensive article [87] Gromov again introduces different definitions. What was called dilatation before, is now called dilation. And the *distortion* of a homeomorphism  $f : V \rightarrow W$  of a Riemannian manifold  $V$  onto a submanifold  $W \subset \mathbb{R}^n$  is defined as

$$\text{Distor}(f) := \text{dil}(f)\text{dil}(f^{-1}).$$

However, because in the cases discussed above we always have  $\text{dil}(f^{-1}) = 1$ , this does not contradict the previous definitions. Among other things, Gromov discusses the problem how to find an embedding  $f$  of a given manifold into a Euclidean space  $\mathbb{R}^N$ , where the dimension  $N$  and the distortion  $\text{Distor}(f)$  should be as small as possible. A short overview of some known answers to these kinds of questions is given in Section 1.3.6.

In [87, p. 114] Gromov also asks whether every isotopy class of knots in  $\mathbb{R}^3$  has a representative  $V$  in  $\mathbb{R}^3$  with distortion  $< 100$ . This question, a first link between dilation and knot theory, is still unanswered.

Sullivan and Kusner [135] found further interesting applications of dilation (distortion) in knot theory in 1998. They considered the question what length of rope of given radius is necessary to tie a particular knot, or equivalently, how thick may the rope be for a given length. Analogous questions can be asked for links built of several pieces of rope, see for instance Cantarella et al. [29]. Probably the simplest example is shown in Figure 1.15. The

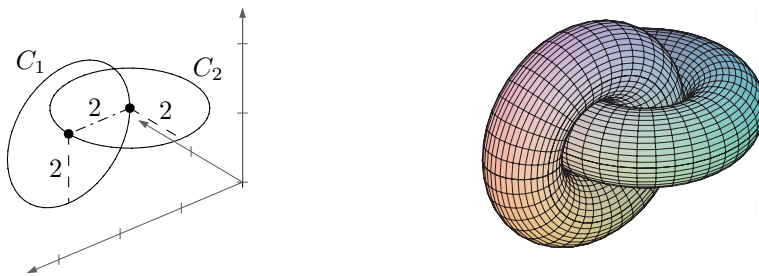


Figure 1.15: The shown configuration has total rope length  $8\pi$  and thickness radius 1. This is optimal for this link type, see Theorem 10 in [29].

total rope length of this configuration obviously equals  $8\pi$ , if the *thickness*, the radius, of the rope equals 1. This rope length is optimal by Theorem 10 in [29].

Although such questions from knot theory are intuitively easy to understand, there arises a problem if one tries to formalize them. A configuration of a knot can be represented by a sufficiently smooth curve  $C$  in  $\mathbb{R}^3$ . This curve has a well-defined length, the *rope length*. How thick can the rope be in this configuration? Clearly, pieces from different parts of the rope



are not allowed to intersect, i.e.

$$B_r(p) \cap B_r(q) = \emptyset \quad \text{for } p, q \text{ on different parts of } C,$$

where  $B_r(p) := \{z \in \mathbb{R}^3 \mid |pz| < r\}$  denotes the open ball with radius  $r$  centered at  $p$ , and  $r$  denotes the thickness of the rope. The problem is how to formalize that  $p$  and  $q$  lie on different parts of  $C$ . Clearly, we have  $B_r(p) \cap B_r(q) \neq \emptyset$  if  $p$  and  $q$  are close to each other on  $C$ , and this does not indicate a self-intersection of the rope.

Amongst different approaches, Kusner and Sullivan [135] applied dilation to solve this problem. Two points  $p$  and  $q$  are regarded as lying on different parts of  $C$ , if their detour  $\delta_C(p, q)$  is bigger than a given constant. They include a proof of the fact that the dilation of any closed curve is bounded by  $\delta(C) \geq \pi/2$ , and that only circles attain equality. Their proof uses the idea of what we call halving pair transformation. However, they do not study further properties of this transformation. Nor do they try to prove other dilation bounds or a stability result like our Lemma 2.39.

Kusner and Sullivan [135] also notice some properties of the dilation of curves which were rediscovered and proved in more detail by Ebberts-Baumann et al. [8, 61], [56, 58]. For instance, our notion of halving pair is analogous to their concept of 'opposite point'. They remark that, if the dilation of a curve is attained by a pair of points  $(p, q) \in C^2$  which is not a halving pair, the chord  $pq$  encloses the same angle with  $C$  in  $p$  and  $q$ . This is what Ebberts-Baumann et al. formalize and exploit in Lemma 1 and Lemma 2 of [8, 61]. In this thesis we prove a generalized version of these arguments in Lemma 2.11. Furthermore, Kusner and Sullivan [135] consider as an example the dilation of a wedge, which is a special case of what we prove in Lemma 2.41.

Although it seems that the kind of application of dilation in knot theory proposed by Kusner and Sullivan [135] in 1998 has been superseded by other approaches, cf. [29], dilation/distortion still plays a significant role in recent work of knot theory. It is the limit of some energy functionals applied to knots by Abrams et al. [1] in 2003. And Denne and Sullivan [45] proved a lower bound to the dilation/distortion of non-trivial knots in 2004.

Our stability result from Lemma 2.39, which we had published in a preprint in 2004, see [50, 49] for subsequent versions, turned out to be useful in this context. Denne and Sullivan generalized it to spaces  $\mathbb{R}^n$  of arbitrary finite dimension  $n \in \mathbb{N}$ , and applied it to reach their new bounds. Another ingredient of the proof is a generalized version of Kubota's inequality, Lemma 2.34 in this thesis. The same inequality was recently used to find new lower bounds to the rope length of knots by Denne et al. [44].

### 1.3.5 Graph dilation

The concept of graph dilation is closely related to geometric dilation. The only difference is that the maximum is taken only over pairs of *vertices*. Hence, the *graph dilation* of a geometric graph  $G$  with vertex set  $V$  is defined as

$$\delta_{\text{graph}} := \max_{p, q \in V, p \neq q} \frac{d_G(p, q)}{|pq|}. \quad (1.5)$$

While geometric dilation is adequate to measure the quality of an urban network of streets, graph dilation suits best to networks like railroad tracks, as access to a railway system is restricted to stations, the vertices of the corresponding graph.

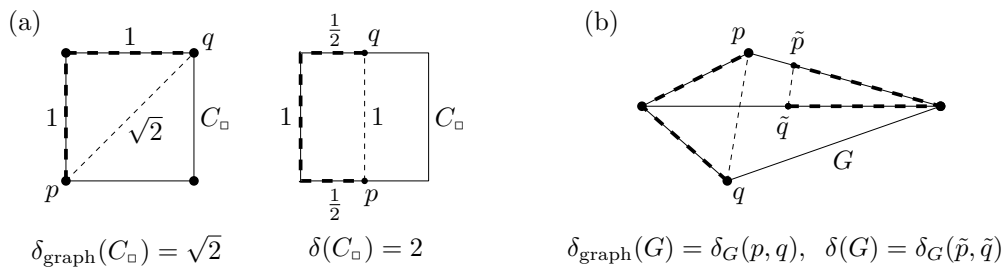


Figure 1.16: (a) The graph dilation of a square is smaller than its geometric dilation. (b) Vertices attaining graph dilation are not necessarily mutually visible.

Figure 1.16 shows differences between the two concepts of dilation. The graph dilation of a square  $C_{\square}$  equals  $\delta_{\text{graph}}(C_{\square}) = \sqrt{2}$  while its geometric dilation equals  $\delta(C_{\square}) = 2$ . Note that the inequality  $\delta_{\text{graph}}(G) \leq \delta(G)$  follows immediately from the definitions. In Section 5.1.3 we prove that there always exists a pair of mutually visible points attaining geometric dilation, but clearly this does not hold for graph dilation.

The graph dilation is also called *stretch factor* [156]. A geometric graph  $G$  is called a  $t$ -*spanner* if  $\delta_{\text{graph}}(G) \leq t$  [156], and it is said to  $t$ -approximate the complete graph [120]. A good overview of the results dealing with graph dilation known until 2000 is given by Eppstein's survey [66]. Even more recent results will be included in Narasimhan and Smid's upcoming monograph [157].

### Plane graphs of small graph dilation

The first articles dealing with graph dilation tried to construct a simple graph  $G = (V, E)$  in the plane for a given finite point set  $S$ , such that the vertex set  $V$  equals  $S$  and  $\delta_{\text{graph}}(G)$  is small. In particular, this does not allow any *Steiner-points*, i.e. additional vertices besides  $S$ . Because adding diagonals to a given graph cannot increase its graph dilation, there always exists a triangulation amongst the simple graphs with vertex set  $S$  attaining minimum graph dilation. These triangulations are called *minimum dilation triangulation*. We denote such a triangulation by  $\text{MDT}(S)$ . In his diploma thesis [125] Alexander Klein developed a Java-applet which computes  $\text{MDT}(S)$  for a small point set  $S$ . The applet [124] can be found online in our Geometry Lab, which hosts a variety of interesting applets dedicated to computational geometry.

The same arguments as above show that if one searches for graphs of small graph dilation, it suffices to consider triangulations. Chew [36] was the first to do so in 1986. He proved that for any given finite point set  $S \subset \mathbb{R}^2$  the graph dilation of the  $L_1$ -Delaunay triangulation  $\text{DT}_{L_1}(S)$  is bounded by  $\delta_{\text{graph}}(\text{DT}_{L_1}(S)) \leq \sqrt{10} \approx 3.1623$ . Figure 1.17.b shows an example of an  $L_1$ -Delaunay triangulation. In the subsequent journal version [37], Chew considered the  $\Delta$ -Delaunay triangulation  $\text{DT}_{\Delta}(S)$ , the Delaunay triangulation based on the convex distance function whose unit circle is an equilateral triangle, cf. Figure 1.17.c. The graph dilation of this triangulation is bounded by

$$\delta_{\text{graph}}(\text{DT}_{\Delta}(S)) \leq 2.$$

On the other hand he pointed out that the graph dilation of every simple graph  $G$  without

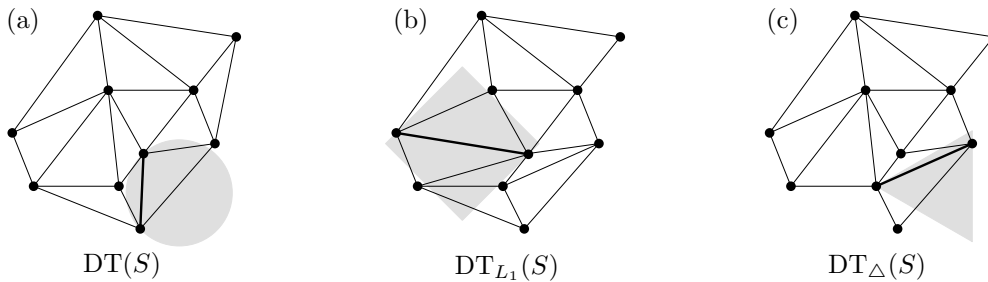


Figure 1.17: Two points  $p, q \in S$  are connected by an edge in a Delaunay triangulation, if they lie on the border of a scaled, empty unit circle.

Steiner-points, which connects the vertices of a square, is bounded by

$$\delta_{\text{graph}}(G) \geq \sqrt{2}.$$

Similarly to the roots of our own research, Chew's questions were motivated by robot motion planning. Shortest paths in graphs of bounded dilation approximate shortest paths of the original scene. And because the edge number of planar graphs is linear, they allow shortest path queries to be answered more quickly. Furthermore, the Delaunay triangulations considered in this context can be constructed quickly, in time  $O(n \log n)$ , see for instance the survey [12] by Aurenhammer and Klein.

If we define a constant  $\Delta_{\text{graph}}^{\text{no Steiner}}$  analogous to our dilation constant  $\Delta$  by

$$\Delta_{\text{graph}}^{\text{no Steiner}} := \sup_{S \subset \mathbb{R}^2, |S| < \infty} \inf_{G=(S,E) \text{ simple}} \delta_{\text{graph}}(G), \quad (1.6)$$

Chew's results can be summarized as

$$\sqrt{2} \leq \Delta_{\text{graph}}^{\text{no Steiner}} \leq 2. \quad (1.7)$$

Although his article started vivid research, and finding the exact value of  $\Delta_{\text{graph}}^{\text{no Steiner}}$  is stated as Open Problem 9 in [66], the upper bound has not been improved so far. The lower bound was improved only recently very slightly to  $\approx 1.4161$  by Mulzer [153], who in his diploma thesis in 2004 computed the minimum dilation triangulation for the vertex sets  $S_n$  of regular  $n$ -gons. The new lower bound is attained by  $S_{21}$ , see Figure 1.18.a.

Chew's original intention was to prove that the dilation of the Euclidean Delaunay triangulation is bounded by  $\delta(\text{DT}(S)) \leq \frac{\pi}{2}$ . He had observed that by considering two opposite points on the unit circle  $\mathbb{S}^1$  and by adding more and more additional points on  $\mathbb{S}^1$ , one can show that  $\pi/2$  is the best possible upper bound. In Figure 1.18.b we sketch an argumentation which omits such degenerate situations by using slightly perturbed versions of  $S_{2n}$ . In the conclusions of the journal version of his paper [37], Chew even remarks that the desired upper bound would not hold. This remark is based on a comment by Steve Fortune who seems to have had a counter example. However, unfortunately, this counter example is lost, and to our knowledge no other counter example has been published.

Dobkin et al. [47] were able to prove an upper bound of  $\approx 5.0832$ , which was subsequently improved to  $\approx 2.4184$  by Keil and Gutwin [120]. Because this is still an intriguing question, we pose it as an open problem.

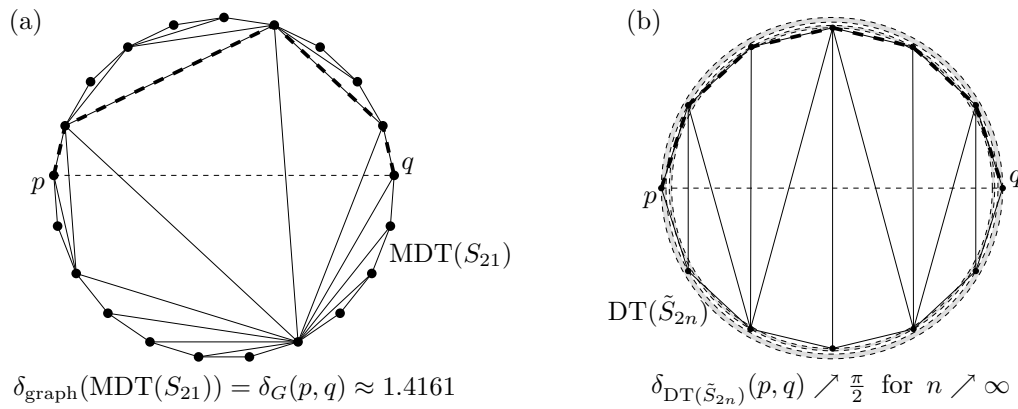


Figure 1.18: (a) Mulzer’s lower bound to  $\Delta_{\text{graph}}^{\text{no Steiner}}$ . (b) Proving that the graph dilation of all Delaunay triangulations cannot be bounded from above by a constant smaller than  $\pi/2$ .

**Open Problem 1.** *What is the worst-case dilation of any Euclidean Delaunay triangulation? Is it smaller than 2, thereby leading to a better upper bound to  $\Delta_{\text{graph}}^{\text{no Steiner}}$ ? Can one prove better lower and upper bounds than*

$$1.5708 \approx \frac{\pi}{2} \leq \sup_{S \subset \mathbb{R}^2, |S| < \infty} \delta_{\text{graph}}(\text{DT}(S)) \leq \frac{8}{3\sqrt{3}} \frac{\pi}{2} \approx 2.4184 ?$$

There is a vast variety of results originating from these questions. Das and Joseph [42] gave certain sufficient conditions for graphs to have bounded dilation. Authors like Keil [119]<sup>8</sup> showed how to construct sparse Euclidean graphs of small dilation efficiently, which may have self-intersections. For both versions, with or without self-intersections, there are results which show how to construct a graph of bounded dilation whose weight, the total edge length, is also bounded. Furthermore, there are results for higher dimensions. And graphs of small graph dilation are useful to get efficient approximate solutions for geometric NP-hard problems as traveling salesman.

Peleg and Schäffer [161] examine a different kind of graph dilation for a subgraph  $S$  of a given abstract (not geometric) graph  $G$ . It compares the shortest-path distance of  $S$  to the one in  $G$ . By definition each edge of their graphs has unit-length. And they show how to efficiently construct spanners of small dilation with few edges in this setting. We cannot list every article here, but again refer to the surveys [66], [157].

### Computing graph dilation

In 1999 Narasimhan and Smid [155, 156] were the first to give non-trivial algorithms for computing the graph dilation of geometric graphs. By applying the *well-separated pair decomposition* (WSPD) of Callahan and Kosaraju [28], which has proved useful in various problems related to dilation and approximation algorithms for geometric problems, they presented algorithms which approximate the graph dilation in sub-quadratic time. Their algorithms are not restricted to planar graphs nor to dimension 2.

<sup>8</sup>The journal version is the joint article of Keil and Gutwin [120] we have mentioned before.

As pointed out in the previous section, their result motivated Ebberts-Baumann et al. [8, 61] to consider the analogous problem for geometric dilation. As a by-product this algorithm also contains an approximation result for graph dilation. Subsequent papers, accumulated in the joint journal version [2] by Agarwal et al., showed how to compute the exact geometric *and graph dilation* for some graph classes in sub-quadratic time.

### Recent Results

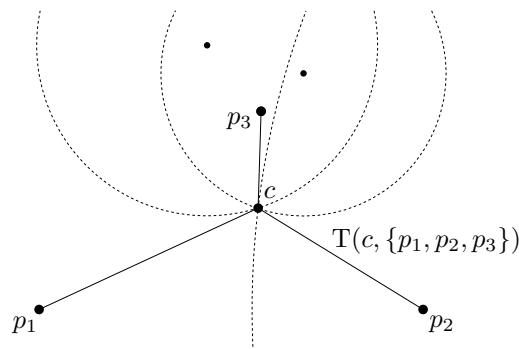


Figure 1.19: The dilation center  $c$  of a point set  $S$  minimizes the graph dilation of the tree  $T(c, S)$ . For three points it is the intersection of three circles of Apollonius.

In 2005, the research on graph dilation has experienced a new boom. Eppstein and Wortman [67] showed how to compute the dilation center of a given finite point set  $S \subset \mathbb{R}^d$  in sub-quadratic expected time. Consider Figure 1.19. The *dilation center* is the point  $c \in \mathbb{R}^d$  which minimizes the graph dilation of the tree  $T(c, S)$  resulting from connecting every point from  $S$  with  $c$  by a straight edge. Ferran Hurtado [106] raised the question, whether the dilation center of three points in  $\mathbb{R}^2$  is a new triangle center or if it appears already under a different name in the well-known collection by Kimberling [122, 123]. It is not difficult to get formulas for the ratios  $\frac{|cp_1|}{|cp_2|}$ ,  $\frac{|cp_1|}{|cp_3|}$ ,  $\frac{|cp_2|}{|cp_3|}$ . Hence the dilation center can be computed as the intersection of three *circles of Apollonius* as shown in Figure 1.19. Note that this dilation center is different from the “point of equal detour” studied by Veldkamp [179], because the latter one is defined by absolute detour values,  $d_G(p, q) - |pq|$ , whereas we consider the relative detour,  $d_G(p, q)/|pq|$ .

Farshi et al. [70] asked how to find the one additional edge which minimizes the graph dilation of a given graph, if one is only allowed to add a single edge. They give approximation algorithms which are significantly faster than the canonical exact algorithms. Gudmundsson et al. [99] showed how to prune a given geometric graph  $G = (S, E)$  so that it has  $O(|S|)$  edges, and the graph dilation increases only by less than a given factor  $(1 + \varepsilon)$  in time  $O(|E| + |S| \log |S|)$ . Klein et al. [128] presented algorithms to compute the *dilation spectrum* for some graph classes in sub-quadratic time. The dilation spectrum of a geometric graph  $G$  is the function  $f_G : [1, \infty) \rightarrow \mathbb{N}$  so that  $f(\kappa)$  equals the number of pairs of vertices whose detour value is bigger than  $\kappa$ . Aronov et al. [9] introduced algorithms which compute for a given finite point set  $S \subset \mathbb{R}^2$  a graph  $G = (V, E)$  with  $S \subseteq V$ ,  $k := |E| - n + 1$  and  $\delta_{\text{graph}}(G) \leq O(n/(k+1))$  in time  $O(n \log n)$ . Note that the graph  $G$  may contain Steiner-points.

Simultaneously and independently, we examined the graph-dilation problem which is anal-

ogous to the geometric-dilation problem of this thesis, see Ebbers-Baumann et al. [54, 55]. Given a finite point set  $S \subset \mathbb{R}^2$ , one wants to find a *simple* graph  $G = (V, E)$  of minimum graph dilation, such that  $S \subseteq V$ . This, too, allows Steiner-points. Which dilation value can we guarantee for every finite point set  $S$ ? The corresponding constant is

$$\Delta_{\text{graph}} := \sup_{S \subset \mathbb{R}^2, |S| < \infty} \inf_{\substack{G=(V,E) \text{ simple,} \\ \text{finite, } S \subseteq V}} \delta_{\text{graph}}(G). \quad (1.8)$$

The grid of equilateral triangles and an approximation result similar to Lemma 5.3 show

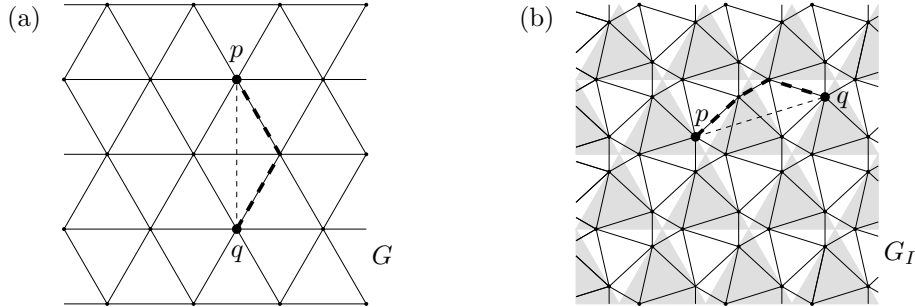


Figure 1.20: (a) The graph dilation of the grid  $G$  of equilateral triangles equals  $\frac{2}{\sqrt{3}} \approx 1.1547$ . (b) The improved grid  $G_I$  attains  $\delta_{\text{graph}}(G_I) \approx 1.1247$ .

$\Delta_{\text{graph}} \leq 2/\sqrt{3} \approx 1.1547$ , cf. Figure 1.20.a. By the improved grid shown in Figure 1.20.b we were able to prove  $\Delta_{\text{graph}} < 1.1247$ . In that article we gave lower bounds only for some graph classes.

Soon afterwards, Klein and Kutz [130] were able to prove the first general non-trivial lower bound  $\Delta_{\text{graph}} > 1.0000047$ . This leaves the following open problem.

**Open Problem 2.** Find better upper and lower bounds to  $\Delta_{\text{graph}}$  than

$$1.0000047 < \Delta_{\text{graph}} < 1.1247.$$

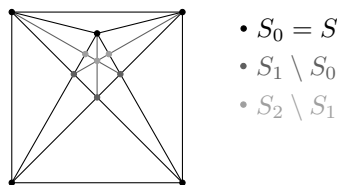


Figure 1.21: The first iterations  $S_0$ ,  $S_1$  and  $S_2$  of segment intersections.

Klein and Kutz took advantage of the following iterative construction for a given finite point set  $S$ , shown in Figure 1.21 and defined by

$$S_0 := S, \quad S_{i+1} := S_i \cup \{p \mid \{p\} = ab \cap cd, a, b, c, d \in S_i\}, \quad S_\infty := \bigcup S_i.$$

This means that during every step of the iteration, in order to construct  $S_{i+1}$  one adds the crossing points of line segments between points of  $S_i$ . It turns out that apart from some few

exceptional configurations first listed by Eppstein in his geometry junkyard [65] under the name *dilation-free graphs*, the limit set  $S_\infty$  is dense in some region. Based on her diploma thesis [117], Kamali Sarvestani and I [93, 94] proved this independently from Klein and Kutz with arguments from projective geometry. Additionally, we formulated and proved a simple representation of the density region as intersection of certain half-planes.

### NP-hardness results

In 2006 several authors considered the question, whether computing certain graphs of minimum dilation is NP-hard. For the minimum dilation triangulation this is listed as Open Problem 8 in Eppstein's survey [66]. Perhaps the recent research was also motivated by Rote and Mulzer's breakthrough [154]. They were able to prove in 2006 that computing the minimum weight triangulation is NP-hard. This is the triangulation of a given finite set  $S \subset \mathbb{R}^2$  with minimum total edge length. The question whether this problem is NP-hard was one of the few open problems from Garey and Johnson's list [74, A13].

Klein and Kutz [129] proved that the problem to compute a minimum dilation graph  $G = (S, E)$  with less than  $\frac{5920}{5919}n - \frac{7624}{5919}$  edges for a given set  $S \subset \mathbb{R}^2$  of  $n$  points is NP-hard. Additionally, they showed that the minimum dilation tree may have self-intersections, thereby answering one of the question from Open Problem 5 in [66]. Independently, Cheong et al. [34] proved that computing the minimum dilation tree is NP-hard, which completes the solution of Eppstein's Open Problem 5.

Another recent, related NP-hardness result from 2006 is due to Gudmundsson and Smid [100]. They proved that it is NP-hard to decide whether a given geometric but not necessarily simple graph in  $\mathbb{R}^d$  contains a  $t$ -spanner with at most  $K$  edges, where  $t$  and  $K$  belong to the input. A subgraph  $G'$  of  $G = (V, E)$  is a  $t$ -spanner of  $G$ , if

$$\max_{u,v \in V, u \neq v} \frac{d_{G'}(u,v)}{d_G(u,v)} \leq t.$$

### Minimum Manhattan networks

In the end of this section, we want to mention an intriguing problem which does not consider Euclidean distances but the  $L_1$ -metric. It is very easy in this setting to construct a geometric graph of graph dilation 1, which embeds a given finite point set  $S \subset \mathbb{R}^2$ . One can simply use the induced rectilinear grid, which results from drawing horizontal and vertical lines through every given point, and removing the parts which are outside of the *bounding box*

$$R(S) := \left[ \min_{p \in S} p_x, \max_{p \in S} p_x \right] \times \left[ \min_{p \in S} p_y, \max_{p \in S} p_y \right]. \quad (1.9)$$

This grid, obviously, attains  $L_1$ -dilation 1.

However, it is difficult to find, for a given finite point set  $S \subset \mathbb{R}^2$  a geometric graph  $G$  of minimum total edge length such that each two points  $p, q \in S$  are connected  $L_1$ -optimally in  $G$ , i.e.,  $d_G^{L_1}(p, q) = \|pq\|_{L_1}$ . Such a graph is called *minimum Manhattan network*. It is not known if every minimum Manhattan network can be constructed in polynomial time. Neither there exists an NP-hardness proof.

However, several polynomial-time approximation algorithms have been proposed, which construct a Manhattan network whose total edge length is bounded by a constant factor times the

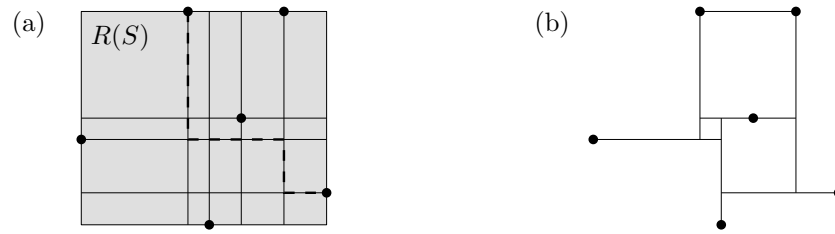


Figure 1.22: (a) The induced rectilinear grid inside the bounding box  $R(S)$  attains  $L_1$ -dilation 1. (b) A minimum Manhattan network taken from [97].

one of a minimum Manhattan network. First, in 1999, Gudmundsson et al. [97, 98] presented a 4-approximation algorithm. Then, Benkert et al. [14, 15, 16] introduced an approach which results in a 3-approximation. And finally, in 2005, Chepoi et al. [35] were able to improve the approximation factor to 2. An overview in German is offered by Köhler’s diploma thesis [131].

### 1.3.6 Metric embeddings with small dilation

In Section 1.3.4, we have mentioned that in his article [87] from 1983, Gromov discussed among other things the problem how to find an embedding  $f$  of a given manifold into a Euclidean space  $\mathbb{R}^N$ , where the dimension  $N$  and the distortion  $\text{Distor}(f)$  should be as small as possible.

Matoušek surveys answers to the analogous question for a given finite metric space in Chapter 15 of his textbook [147]. Such embeddings are very useful if dealing with similarity questions and huge amount of data. Matoušek gives the following example. Assume that we are given a set  $X$  of  $n \in \mathbb{N}$  bacterial strains, and assume that their similarity can be measured by a metric  $d(\cdot, \cdot)$  on  $X$ . This metric could be the result of various tests or of comparing their DNA, and so on.

If we found an embedding  $f : X \rightarrow \mathbb{R}^N$  of small distortion into an Euclidean space of small dimension  $N$ , we only have to store the positions  $f(x)$  for each  $x \in X$  to compare each pair of strains. The data fits into  $N \cdot n$  real numbers, whereas the original similarity data consists of  $\binom{n}{2} = n(n-1)/2$  real numbers. For big  $n$  and small  $N$  this is a huge improvement. Furthermore, the small distortion guarantees that the similarity value  $d(x, y)$  is closely approximated by the distance  $|f(x)f(y)|$ .

The most important positive result for these kind of problems is probably the *Johnson-Lindenstrauss flattening lemma* [116] which states that if  $X$  is the subset of an arbitrary Euclidean space, for any given  $\varepsilon > 0$  there exists a  $(1 + \varepsilon)$ -embedding of  $X$  into  $\mathbb{R}^k$  where  $k \in O(\varepsilon^{-2} \log n)$ .

The lemma uses another dilation-type notion. A mapping  $f : X \rightarrow Y$  between two metric spaces is called a  $D$ -embedding for a real number  $D \geq 1$ , iff

$$\exists r \in \mathbb{R} : \forall p, q \in X : r \cdot d_X(p, q) \leq d_Y(f(p), f(q)) \leq D \cdot r \cdot d_X(p, q).$$

There is a complementary negative result. Linial et al. [143] proved that for any  $n \in \mathbb{N}$  there exists a finite metric space  $X$  of  $n$  elements such that any  $D$ -embedding of  $X$  into a Euclidean



space satisfies  $D \in \Omega(\log n)$ .

For proofs, further results and references, we again refer to Chapter 15 of Matoušek’s textbook [147].

### 1.3.7 Miscellaneous related research

There is a vast literature on further results related to this thesis which does not consider primarily the concept of dilation. We have described before that some arguments which lead to our lower bounds to the dilation of closed curves stem from convex geometry. For instance, our halving pair transformation was motivated by the well-known central symmetrization, and these two transformations have similar properties. An important step is also the application of Kubota’s inequality, Lemma 2.34. The related references are given in Chapter 2.

Another related topic from convex geometry considers so called *fencing problems*. These problems ask for a best way to divide a given convex set in  $\mathbb{R}^2$  ( $\mathbb{R}^n$  resp.) into two parts of equal area (volume). There are several versions of the problem. For example, the dividing “fence” might be restricted to be a line segment (hyper-plane) or a curve (hyper-surface). Another parameter of the problem is how to measure the quality of a solution. For example, one might try to minimize the length of the fence, cf. Problem A26 in Croft, Falconer and Guy’s book [40]. A very recent result stems from Miori, Peri and Segura Gomis [151].

If one considers compact convex sets in the Euclidean plane and tries to bisect their area by a straight line segment either minimizing or maximizing the length of the segment, the optimal results are the *minimum* and *maximum area halving distance*. Those values are defined analogously to the perimeter case considered in this thesis. In a collaboration with Klein, Miori and Segura Gomis [96] we examined the relation between area halving distance and other quantities from convex geometry. Similarly to Chapter 4, we listed old inequalities and trivial ones, and contributed some new inequalities.

In Section 2.12 we prove that a closed curve of small dilation has to be contained in a thin circular annulus, a ring bounded by two concentric circles. In this context we should mention literature dealing with the problem of finding a smallest annulus which contains a given curve. The main problem was first examined by Bonnesen [21], who proved that, for every given closed convex curve  $C$  in the plane, there exists a unique annulus enclosing  $C$  with minimal difference of the radii. Nagy [178] proved that this annulus also has minimal area. The result most closely related to our work is due to Vincze [180], who showed that, with the exception of some degenerated cases, the same annulus minimizes the ratio between the outer and the inner radius. For generalizations to non-convex curves and to non-Euclidean metrics see Fuglede [73] and Peri and Vassallo [162], respectively.

Another related field of research is disk packing. We describe the relations and refer to related literature in Section 5.3.3 and Section 5.3.6.

## 1.4 Structure of this thesis

This thesis is structured as follows. In Chapter 2 we consider closed curves in the Euclidean plane. The chapter contains several results concerning their dilation and halving distance,

including the definition and analysis of the halving pair transformation and the midpoint curve, lower bounds to the dilation of cycles and the important stability result.

Chapter 3 contains an exact characterization of Zindler curves, showing that in general their halving chords bisect both, perimeter and area. It also includes a proof of the relation to curves of constant breadth, and a sorrow analysis of three important example curves.

Chapter 4 lists the inequalities between minimum and maximum halving distance and other quantities, giving proofs for all of them, the known, the trivial and the new ones.

Finally, in Chapter 5 the previous results are used to provide answers to the main question of this thesis. We prove the upper bound  $\Delta < 1.6778$  and the lower bound  $\Delta > (1 + 10^{-11})\pi/2$ . Furthermore the relation between our dilation question and disk packing problems is discussed.

Appendices provide proofs for the existence and differentiability of certain parameterizations used in Chapter 3 and a corrected proof of the disk-packing result we use in Chapter 5.

We do not have to go into more detail here, as each chapter starts with a short introduction which summarizes its intent and content.

## Chapter 2

# Closed Curves

In this chapter we provide results on the geometric dilation of simple planar closed curves. Analogously to general graphs, a curve is called *simple* if it does not have any self-intersection. Before we can prove the important results of this chapter, lower bounds to the dilation of closed curves, we have to do some quite technical preliminary work. We introduce necessary formal definitions in Section 2.1, and prove in Section 2.2 that apart from a special case, the dilation of any cycle is attained by a pair of points.

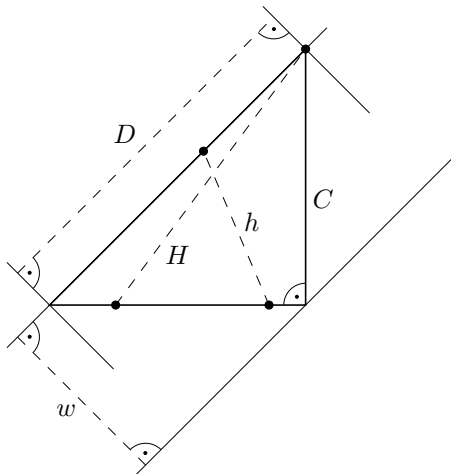


Figure 2.1: Diameter  $D$ , width  $w$ , and minimum and maximum halving distance,  $h$  and  $H$ , of an isosceles, right-angled triangle.

Next, we formally define halving pairs and halving distance and give first results by comparing halving distance to other well-known breadth quantities in Section 2.3, see Figure 2.1 for an impression. This knowledge is enough to restate the simple lower bound to the dilation of any closed curve  $C$ ,  $\delta(C) \geq \pi/2$ , which was first presented by Gromov [88]. We give a new, very short proof by applying Cauchy's surface area formula.

In Section 2.4 we show that the dilation of the convex hull  $\text{ch}(C)$  of a simple curve  $C$  in the plane is not bigger than the original dilation of  $C$ . Because of this, we can restrict the search

for lower bounds to convex curves.

In Section 2.5 we show that the dilation of any convex closed curve  $C$  is attained by a halving pair. This helps us to derive simple dilation formulas, for instance for polygons in Section 2.13.

After all the preliminary work, we are finally able to derive better lower bounds than  $\pi/2$ , which depend on  $h$  and  $H$  but also on well known quantities from convex geometry like diameter  $D$  and width  $w$ .

Bounding the dilation of centrally symmetric convex curves is quite easy, as we see in Section 2.6. This motivates us to look for transformations which map any convex cycle to a centrally symmetric one. A well-known example in convex geometry is central symmetrization, which we review in Section 2.7. It is helpful to derive new bounds to the dilation of cycles, but the most useful bounds are achieved by another technique we call halving pair transformation. It translates every halving pair, so that its midpoint is moved to the origin. Then, the translated points form a centrally symmetric curve  $C^*$ . The transformation and its various properties are presented in Section 2.8.

Because we are also interested in the area enclosed by a cycle, we cite a generalized version of Holditch's theorem due to Goodey in Section 2.10. We review its proof, and we show how it can be applied to situations appearing within this thesis. For instance these results are useful to prove that the halving pair transformation does never decrease the enclosed area, a result which was proved by Zindler [186, p. 44] only for special cases. And we will also apply the generalized Holditch's theorem in Chapter 3 and Chapter 4.

Another curve derived from  $C$  is the curve  $M$  consisting of the midpoints of the halving pairs. We analyze it in Section 2.9. Both  $C^*$  and  $M$  help us to give tight dilation bounds in Section 2.11 and an important stability result in Section 2.12. The latter one is used in Chapter 5 to prove the first lower bound to the geometric dilation of finite point sets which is bigger than  $\pi/2$ .

In the end of this chapter, we apply our knowledge to a special class of closed curves, to polygons. This results in not overly complicated dilation formulas which – nevertheless – in parts reveal some surprises.

First, we give some more formal definitions of the new notation and review well-known definitions from convex geometry.

## 2.1 Basic definitions

Throughout this chapter we consider simple, finite, regular, piecewise continuously differentiable curves in the Euclidean plane with one-sided derivatives. We denote the considered class of curves by  $\mathcal{C}$ .

A subset  $C \subset \mathbb{R}^2$  belongs to  $\mathcal{C}$ , if it is the image of an injective, continuous function  $c : [a, b] \rightarrow \mathbb{R}^2$  or  $c : [a, b) \rightarrow \mathbb{R}^2$  which satisfies additional differentiability conditions.

First, we require the existence of *one-sided derivatives* which are defined by

$$\dot{c}(t+) := \lim_{h \searrow 0} \frac{c(t+h) - c(t)}{h}, \quad \dot{c}(t-) := \lim_{h \searrow 0} \frac{c(t) - c(t-h)}{h}.$$

The right-sided derivative must exist and satisfy  $\dot{c}(t+) \neq 0$  everywhere but in  $b$ , and the

left-sided derivative has to fulfill the same conditions everywhere but in  $a$ . In the following we will say that the one-sided derivatives exist everywhere, as it is clear that  $\dot{c}(t-)$  cannot exist in  $a$  and  $\dot{c}(t+)$  cannot exist in  $b$ .

The function  $c$  is *differentiable* in  $t$ , if  $\dot{c}(t+) = \dot{c}(t-)$ . In this case, the *derivative* of  $c$  in  $t$  is  $\dot{c}(t) := \dot{c}(t+) = \dot{c}(t-)$ . The function  $c$  is *piecewise continuously differentiable* if both one-sided derivatives exist everywhere, and there exist  $n \in \mathbb{N}$  and  $a = a_0 < a_1 < \dots < a_n = b$  such that for every  $i \in \{1, \dots, n\}$ ,  $c$  is differentiable on  $(a_{i-1}, a_i)$  and  $\dot{c}$  is continuous on  $(a_{i-1}, a_i)$ .

If a function  $c : [a, b] \rightarrow C$  or  $c : [a, b) \rightarrow C$  is continuous and surjective, such that  $c^{-1}(p)$  is a closed interval for every  $p \in C$ , it is a *parameterization* of  $C$ . Note that we do not require  $c$  to be injective to be a parameterization, because in some cases it is convenient to have parameterizations which stay at a given point for a whole interval  $[t_1, t_2]$ .

If  $c$  is injective, and additionally it has non-disappearing one-sided derivatives everywhere, it is a *regular parameterization*. If a parameterization is regular, piecewise continuously differentiable and bijective, we call it a *nice parameterization* of a simple curve. The word *simple* means that the curve does not have any self-intersections, or more formally, there exists a bijective parameterization. Sometimes we will also consider non-simple curves. These are curves with self-intersections, i.e. their parameterizations are not injective.

In general, we can distinguish two types of curves. The first type has a parameterization  $c : [a, b] \rightarrow C$  and satisfies  $c(a) \neq c(b)$ . These kind of curves are called *open curves*. The second type has a parameterization  $c : [a, b) \rightarrow C$  and satisfies  $\lim_{t \nearrow b} c(t) = c(a)$ . These curves are *closed curves* or *cycles*. Note that by these definitions both types of curves can be simple or non-simple.

Most of the proofs of this thesis can be extended to a class of curves broader than  $\mathcal{C}$ , as mostly we require only the existence of one-sided derivatives, which for example is satisfied by any convex, closed curve. Convex cycles are also differentiable almost everywhere, but the set of exceptional points is not necessarily finite. It may be countably infinite, see for instance Roberts' survey [166, p. 1091] on convex functions. A class of curves which includes all convex cycles, are the *curves of finite total curvature* first presented by Milnor [149], and examined thoroughly in a survey by Sullivan [177]. We expect most of our proofs to be extendible to that class.

However, lightening the restrictions on the considered class of curves would lead to more technical efforts, in particular when proving the existence of certain parameterizations in Appendix A. And clearly,  $\mathcal{C}$  is big enough to contain the edges of every reasonable geometric graph we want to consider.

The *length* of any  $C \in \mathcal{C}$  is given by  $|C| := \int_a^b |\dot{c}(t)| dt$ . It is straight-forward to prove that this definition does not depend on the parameterization, see for instance [38, pp. 350f.]. For a closed curve  $C \in \mathcal{C}$ , let  $C^\circ$  denote the open bounded region encircled by  $C$ , called its *interior domain* or *interior* for short. The closed curve  $C$  is *convex* if its interior domain  $C^\circ$  is convex. In this case the length  $|C|$  is also called *perimeter* because it is the perimeter of  $C^\circ$ .

Dilation is defined like for arbitrary graphs. By  $d_C(p, q)$  we denote the  $C$ -distance of  $p$  and  $q$ , i.e. the length of the shortest path on  $C$  connecting  $p$  and  $q$ . The *detour*  $\delta_C(p, q)$  of  $p$  and  $q$  in  $C$  is the ratio of their  $C$ -distance and their Euclidean distance, and the (*geometric*) *dilation* of  $C$  is the supremum of these dilation values.

Sometimes we will consider an *arc-length parameterization* of a curve  $C$ , a parameterization  $\bar{c}$  of an interval  $I$  onto  $C$  so that  $|\dot{\bar{c}}(t)| = 1$  wherever the derivative exists. Such a parameterization often simplifies dilation analysis because for any open curve  $C$  and values  $t_1, t_2 \in I$  we have  $d_C(\bar{c}(t_1), \bar{c}(t_2)) = |t_2 - t_1|$ . For closed curves the same equation holds if additionally  $|t_2 - t_1| \leq |C|/2$  is granted. The existence of arc-length parameterizations for every curve  $C \in \mathcal{C}$  is shown in Appendix A.1.

For two points  $p, q$  on a simple, closed curve  $C$ , by  $C_p^q$  we denote the path from  $p$  to  $q$  on  $C$  which moves counter-clockwise. This means, that by first moving from  $p$  to  $q$  on  $C_p^q$  and then going back from  $q$  to  $p$  on  $C_q^p$ , we turn once in counter-clockwise orientation.

## 2.2 Dilation attained by pair of points

This section contains the first step of analyzing the dilation of closed curves. We observe that, with the exception of one special case, the geometric dilation of any cycle  $C$  is attained by a pair of points of  $C$ .

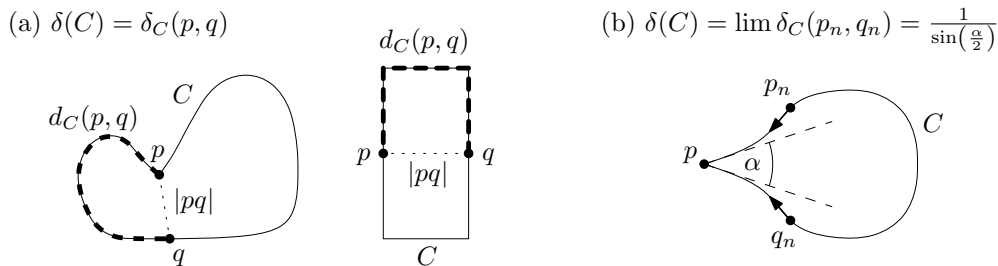


Figure 2.2: The dilation  $\delta(C)$  is attained by a pair of distinct points  $(p, q)$  or by the limit of pairs of points  $(p_n, q_n)$  approaching the same point  $p$  from opposite sides.

**Lemma 2.1.** *Let  $C \in \mathcal{C}$  be an arbitrary open or closed curve. Then, at least one of the following cases occurs:*

1. *The dilation  $\delta(C)$  is attained by a pair of points  $p, q \in C$ ,  $p \neq q$ , i.e.  $\delta(C) = \delta_C(p, q)$ .*
2. *The dilation  $\delta(C)$  is the limit of detour values of a sequence of pairs  $(p_n, q_n)_{n \in \mathbb{N}} \subset C \times C$ , so that  $(p_n)_{n \in \mathbb{N}}$  and  $(q_n)_{n \in \mathbb{N}}$  approach the same point  $p \in C$  from opposite sides. Let  $\alpha \in [0, \pi[$  denote the angle enclosed by the tangents in  $p$ . Then,*

$$\delta(C) = \lim_{n \rightarrow \infty} \delta_C(p_n, q_n) = \begin{cases} \frac{1}{\sin(\frac{\alpha}{2})} & : \alpha \in ]0, \pi[ \\ \infty & : \alpha = 0 \end{cases}$$

*If  $C$  is convex, case 1. must occur.*

*Proof.* Let  $(p_n, q_n)_{n \in \mathbb{N}}$  be a maximum sequence, i.e.  $\delta_C(p_n, q_n) \nearrow \delta(C)$ . Because  $C$  is compact in  $\mathbb{R}^2$ , so is  $C \times C$  in  $\mathbb{R}^4$ . There is a sub-sequence we will from now on denote by  $(p_n, q_n)_{n \in \mathbb{N}}$  converging to a pair  $(p, q) \in C \times C$ .

The continuity of  $d_C(\cdot, \cdot)$  implies  $d_C(p_n, q_n) \rightarrow d_C(p, q)$ . And by continuity of  $|\cdot|$  we obtain  $|p_n q_n| \rightarrow |pq|$ . If  $p \neq q$ , this implies  $\delta_C(p_n, q_n) = d_C(p_n, q_n)/|p_n q_n| \rightarrow d_C(p, q)/|pq| = \delta_C(p, q)$ . We have case 1.

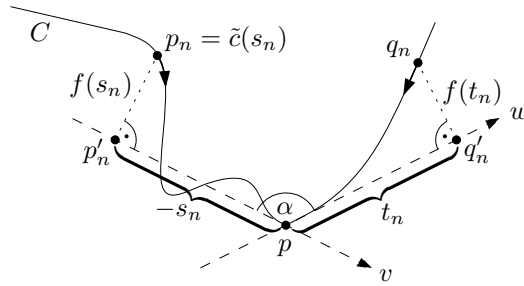


Figure 2.3: A dilation maximum sequence  $(p_n, q_n)_{n \in \mathbb{N}}$  converging to a single point.

Now we consider the remaining case  $p = q$ . Consider Figure 2.3. We choose an arbitrary orientation of  $C$ . Let  $v, w \in \mathbb{S}^1$  be the left- and right-sided normalized derivative vectors of  $C$  in  $p$ , where  $\mathbb{S}^1 := \{p \in \mathbb{R}^2 \mid |p| = 1\}$  denotes the *unit circle*. We use the following parameterization  $c$  of  $C$  in a neighborhood of  $p$ :

$$c(t) := \begin{cases} p + tv + f(t)\mathbb{R}^{90^\circ}v & \text{if } t \leq 0 \\ p + tw + f(t)\mathbb{R}^{90^\circ}w & \text{if } t > 0 \end{cases}$$

The parameter  $t$  equals the oriented length of the component of  $c(t) - p$  in direction  $v$  ( $w$  resp.), while  $f(t)$  is the oriented length of the component orthogonal to  $v$  ( $w$  resp.). The symbol  $\mathbb{R}^{90^\circ}$  denotes the matrix which turns any vector by  $90^\circ$  counter-clockwise.

Because of the one-sided differentiability and regularity of  $C$  we can choose the neighborhood of  $p$  small enough so that  $c$  is well-defined and bijective. Clearly, it is continuous at 0. We define  $s_n := c^{-1}(p_n)$  and  $t_n := c^{-1}(q_n)$ . By continuity and injectivity of  $c$  we get  $s_n \rightarrow 0$  and  $t_n \rightarrow 0$ .

By definition,  $f$  is continuously differentiable in a neighborhood of 0, and we have  $f'(t) \rightarrow 0$  for  $t \rightarrow 0$ . For any given  $\varepsilon > 0$  we can choose a small  $\delta > 0$  so that  $|f'(t)| < \varepsilon$  for every  $t \in ]-\delta, \delta[$ . And we can choose  $N$  big enough such that every  $s_n$  and  $t_n$ ,  $n \geq N$ , are contained in  $]-\delta, \delta[$ . If  $(p_n)_{n \in \mathbb{N}}$  and  $(q_n)_{n \in \mathbb{N}}$  approached  $p$  from the same side, these  $n$ -values would satisfy

$$\delta_C(p_n, q_n) = \frac{\left| \int_{s_n}^{t_n} \sqrt{1 + (f'(t))^2} dt \right|}{\sqrt{|t_n - s_n|^2 + |f(t_n) - f(s_n)|^2}} \leq \frac{\sqrt{1 + \varepsilon^2} |t_n - s_n|}{|t_n - s_n|} \xrightarrow{\varepsilon \rightarrow 0} 1.$$

This is a contradiction because  $\delta(C) = \lim \delta_C(p_n, q_n)$  cannot equal 1 for the non-degenerate closed curve  $C$ . Note that the formula for the denominator holds only if  $p_n$  and  $q_n$  lie on the same side of  $p$ .

In the remaining case, there is a sub-sequence  $(p_n, q_n)_{n \in \mathbb{N}}$  so that  $p_n$  and  $q_n$  are always on opposite sides of  $p$ . By renaming we can build a sequence of the same dilation limit where every  $p_n$  lies left of  $p$  ( $s_n < 0$ ) and every  $q_n$  lies right of  $p$  ( $t_n > 0$ ). Again, for a given  $\varepsilon > 0$  we can choose a big  $N \in \mathbb{N}$  so that for every  $n \geq N$ ,  $c(t)$  and  $f(t)$  are well-defined and

continuously differentiable on  $[s_n, 0]$  and  $[0, t_n]$ , and  $|f'(t)| < \varepsilon$  holds. Clearly, this implies  $|f(t)| \leq \int_0^t |f'(\tau)| d\tau \leq \varepsilon|t|$  for  $t \in [s_n, t_n]$ .

Keeping in mind that  $s_n < 0 < t_n$ , the shortest-path distance  $d_C(p_n, q_n)$  is bounded by

$$(t_n - s_n) \leq d_C(p_n, q_n) = \int_{s_n}^{t_n} \sqrt{1 + (f'(t))^2} dt \leq \sqrt{1 + \varepsilon^2}(t_n - s_n).$$

We define  $p'_n := p + s_nv$  and  $q'_n := p + t_nw$ , see Figure 2.3. Then, we can apply the triangle inequality to get upper and lower bounds for  $|p_nq_n|$ . Remember that  $s_n$  is negative by definition, hence  $-s_n \geq 0$ .

$$\begin{aligned} |p_nq_n| &\leq |p'_nq'_n| + |f(s_n)| + |f(t_n)| \leq |p'_nq'_n| + \varepsilon(t_n - s_n) \\ \text{and } |p_nq_n| &\geq |p'_nq'_n| - |f(s_n)| - |f(t_n)| \geq |p'_nq'_n| - \varepsilon(t_n - s_n) \end{aligned}$$

This implies

$$\frac{t_n - s_n}{|p'_nq'_n| + \varepsilon(t_n - s_n)} \leq \delta_C(p_n, q_n) \leq \frac{\sqrt{1 + \varepsilon^2}(t_n - s_n)}{|p'_nq'_n| - \varepsilon(t_n - s_n)}.$$

Hence,  $\lim \delta_C(p_n, q_n) = \lim (t_n - s_n)/|p'_nq'_n|$  which is the limit of the dilation values of  $(p'_n, q'_n)$  on the polygonal path built by the  $v$ - and the  $w$ -tangent through  $p$ . Lemma 2.41 which we prove in Section 2.13.1 shows that this value cannot be bigger than  $1/\sin(\alpha/2)$  where  $\alpha \in ]0, \pi[$  is the angle enclosed by the  $v$ - and the  $w$ -tangent. The same lemma implies that this maximum is attained by values  $s_n = -t_n$ . Case  $\alpha = 0$  yields  $\lim \delta_C(p_n, q_n) = \infty$ .

It remains to show that for convex cycles the dilation is always attained by a pair of distinct points. Assume that  $C$  is convex, and  $(p_n, q_n) \in C^2$  is a dilation maximum sequence converging to a single point  $p$ . We can choose  $\tilde{p}, \tilde{q} \in C$  close to  $p$ , so that their projections  $\tilde{p}'$  and  $\tilde{q}'$ , defined analogously to  $p'_n$  and  $q'_n$  in Figure 2.3, satisfy  $-s := |\tilde{p}'p| = |\tilde{q}'p| =: t$  and  $|\tilde{p}\tilde{q}| \leq |\tilde{p}'\tilde{q}'|$ . The last inequality can be satisfied because of the convexity of  $C$ . Hence,

$$\delta(C) \geq \delta_C(\tilde{p}, \tilde{q}) \geq \frac{t - s}{|\tilde{p}'\tilde{q}'|} \stackrel{\text{see above}}{=} \frac{1}{\sin(\alpha/2)} \stackrel{\text{see above}}{\geq} \lim_{n \rightarrow \infty} \delta_C(p_n, q_n) = \delta(C).$$

Therefore, the dilation of convex cycles is always attained by a pair of distinct points of  $C$ .  $\square$

## 2.3 Breadth quantities

In this section we want to review well-known breadth quantities from convex geometry and introduce halving distance more formally. The first step is the definition of halving pairs.

**Definition 2.2.** (*Halving Pair*) *Let  $p \in C$  be a point on a closed curve  $C \in \mathcal{C}$ . Then the unique halving partner  $\hat{p} \in C$  of  $p$  is characterized by  $d_C(p, \hat{p}) = |C|/2$ . We say that  $(p, \hat{p})$  is a halving pair of  $C$ , and the connecting segment  $p\hat{p}$  is a halving chord with direction  $(p - \hat{p})/|p - \hat{p}| \in \mathbb{S}^1$ , see Figure 2.4.*

Sometimes it is more convenient to consider the angle  $\alpha \in [0, 2\pi)$  instead of the corresponding direction  $(\cos \alpha, \sin \alpha) \in \mathbb{S}^1$ . We will use both expressions synonymously. In order to define the halving distance, the following observation is important.



**Lemma 2.3.** *For every direction  $v \in \mathbb{S}^1$  there exists a halving pair  $(p, \hat{p})$ , i.e.  $p - \hat{p} = |p - \hat{p}|v$ . For convex cycles, this halving pair is unique.*

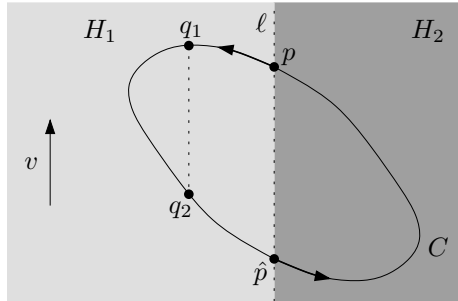


Figure 2.4: By moving  $p$  and  $\hat{p}$  we get a halving pair for every direction. These halving pairs are unique for convex cycles.

*Proof.* Consider Figure 2.4. Clearly, we can find one halving pair  $(p, \hat{p})$  of  $C$ . Next, we move  $p$  and  $\hat{p}$  continuously on  $C$  so that they keep their  $C$ -distance  $d_C(p, \hat{p}) = |C|/2$ . Eventually,  $p$  reaches the former position of  $\hat{p}$  and, at the same time,  $\hat{p}$  reaches the former position of  $p$ . Because  $C$  is simple, the vector  $p - \hat{p}$  never disappears. It changes continuously. Hence, in between, the pair must have attained all possible directions (mod  $\pi$ ). This completes the proof of the first part because, if  $(p, \hat{p})$  is a halving pair with direction  $\alpha$ , then  $(\hat{p}, p)$  is a halving pair with direction  $\alpha + \pi$ .

Now, let  $C$  be convex and let  $v \in \mathbb{S}^1$  be an arbitrary direction. Let  $(p, \hat{p})$  be a halving pair of direction  $v$ . By convexity, the line  $\ell$  through this pair can only intersect with  $C$  twice, namely in  $p$  and  $\hat{p}$ . It divides the plane  $\mathbb{R}^2$  into two half-planes  $H_1$  and  $H_2$ .

Let  $(q_1, q_2) \in C^2$  be a pair of points lying in the same half-plane, say  $H_1$ . Then, it cannot be a halving pair, since half of the length of  $C$  is contained in  $H_2$ , and there is some additional length needed to reach  $q_1$  and  $q_2$ . Thus, every halving pair  $(q, \hat{q})$  except  $(p, \hat{p})$  contains one point of  $H_1$  and one point of  $H_2$ . It cannot have direction  $v$ .  $\square$

We keep this in mind while defining halving distance and comparing it to well-known quantities from convex geometry. Within the definition of breadth, we use supporting lines. A line  $\ell$  is a *supporting line* of a closed curve  $C$  if it touches  $C$  and the curve  $C$  is fully contained in one of the closed half-planes bounded by  $\ell$ .

**Definition 2.4.** (*Breadth Quantities*) (see Figure 2.5.a) Let  $C \in \mathcal{C}$  be a closed curve, and let  $v \in \mathbb{S}^1$  be an arbitrary direction.

1. The  $v$ -length of  $C$  is the maximum distance of a pair of points with direction  $v$ , i.e.  $l_C(v) := \max \{|pq| \mid p, q \in C, q - p = |q - p|v\}$ .
2. The  $v$ -breadth ( $v$ -width) of  $C$  is the distance of the two supporting lines of  $C$  perpendicular to  $v$ , i.e.  $b_C(v) := \max_{p \in C} \langle p, v \rangle - \min_{p \in C} \langle p, v \rangle$  where  $\langle p, v \rangle$  denotes the scalar product.

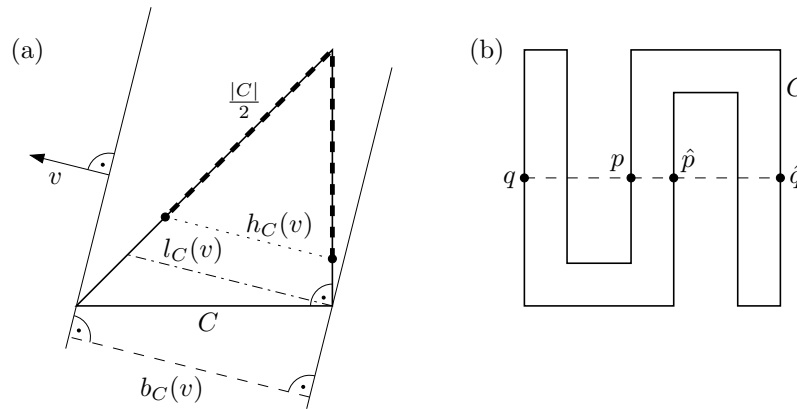


Figure 2.5: (a) The  $v$ -breadth  $b_C(v)$ ,  $v$ -length  $l_C(v)$  and  $v$ -halving distance  $h_C(v)$ . (b) There can be more than one halving pair with direction  $v$  for non-convex cycles, e.g.  $(p, \hat{p})$  and  $(q, \hat{q})$ .

3. The  $v$ -halving distance  $h_C(v)$  of  $C$  is the distance of the halving pair with direction  $v$ . Figure 2.5.b and Lemma 2.3 show that this is well-defined only for convex curves.
4. The diameter  $D(C) := \max_{v \in \mathbb{S}^1} l_C(v)$  of  $C$  is the maximum  $v$ -length. The width  $w(C) := \min_{v \in \mathbb{S}^1} l_C(v)$  of  $C$  is the minimum  $v$ -length.
5. The maximum halving distance is denoted by  $H(C) := \max_{v \in \mathbb{S}^1} h_C(v)$ . For non-convex curves we can use an arc-length parameterization  $\bar{c}$  to get a proper definition:  $H(C) := \max_{t \in [0, |C|]} |\bar{c}(t) - \bar{c}(t + |C|/2)|$ . Analogously, we define the minimum halving distance by  $h(C) := \min_{t \in [0, |C|]} |\bar{c}(t) - \bar{c}(t + |C|/2)|$ .
6. The inradius  $r(C)$  is the radius of the biggest open disk contained in the interior domain  $C^\circ$ . The circumradius  $R(C)$  is the radius of the smallest closed disk containing  $C$ .

As mentioned before, we sometimes identify  $\alpha \in \mathbb{R}$  with  $(\cos \alpha, \sin \alpha) \in \mathbb{S}^1$  and vice versa. For instance  $h_C(\alpha)$  denotes  $h_C((\cos \alpha, \sin \alpha))$ .

We introduce some additional useful standard notation. Consider a chord  $pq$  in direction  $v \in \mathbb{S}^1$  for two points  $p, q$  on a closed curve  $C \subset \mathbb{R}^2$ . The line segment  $pq$  is a *diametral chord* if it is (one of) the longest chord(s) with direction  $v$ , i.e.  $|pq| = l(v)$ . It is a *diameter* if  $|pq| = D(C)$ . It is a *w-chord*, if  $|pq| = l(v) = w(C)$ .

The next lemma gives straight forward inequalities between the main three breadth quantities. They follow immediately from the definitions, cf. Figure 2.5.a.

**Lemma 2.5.** *Let  $C \in \mathcal{C}$  be a convex closed curve, and let  $v \in \mathbb{S}^1$  be an arbitrary direction. Then the following inequalities hold:  $h_C(v) \leq l_C(v) \leq b_C(v)$ .*

Width and diameter can also be defined using the  $v$ -breadth values.

**Lemma 2.6.** *Let  $C \in \mathcal{C}$  be a closed curve in the plane, and let  $v \in \mathbb{S}^1$  be an arbitrary direction.*

1. The direction  $v$  is a direction of maximum length iff<sup>1</sup> it is a direction of maximum breadth. The maxima are equal,  $D(C) = \max_{\bar{v} \in \mathbb{S}^1} b_C(\bar{v})$ .
2. Let  $C$  be convex. Then, the direction  $v$  is a direction of minimum length iff it is a direction of minimum breadth. For every convex cycle  $C$ , the minima are equal,  $w(C) = \min_{\bar{v} \in \mathbb{S}^1} b_C(\bar{v})$ .

The equality of diameter and maximum breadth is for instance also proved in Theorem 1.3 of Lay's textbook [140, p. 76], by Eggleston [63, p. 77], and in Section 1.5 of Gritzmann and Klee's paper [83]. The latter article also shows the equality of minimum breadth and minimum length.

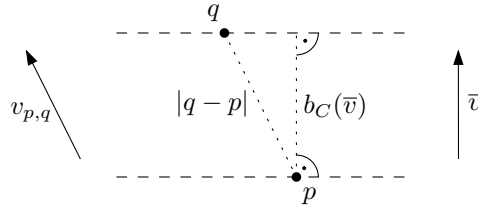


Figure 2.6: If there are points  $p, q \in C$  on the supporting lines perpendicular to  $\bar{v}$  with direction  $v_{p,q} \neq \bar{v}$ , then  $b_C(\bar{v})$  is not maximal.

*Proof.* 1. Consider Figure 2.6. Let  $\bar{v}$  be a direction of maximum breadth, and let  $(p, q)$  be a pair of points of  $C$  on the two supporting lines perpendicular to  $\bar{v}$ . This means  $\langle q - p, \bar{v} \rangle = b_C(\bar{v}) = \max_{v \in \mathbb{S}^1} b_C(v)$ .

If  $(p, q)$  did not have direction  $\bar{v}$ , it would have a distance bigger than  $b_C(\bar{v})$ . And if  $v_{p,q}$  denotes the direction of  $(q - p)$ , we could derive the following contradiction:

$$b_C(v_{p,q}) \stackrel{\text{Lemma 2.5}}{\geq} l_C(v_{p,q}) \stackrel{\text{Def.}}{\geq} |q - p| \stackrel{v_{p,q} \neq \bar{v}}{>} b_C(\bar{v}) = \max_{v \in \mathbb{S}^1} b_C(v) \geq b_C(v_{p,q})$$

Hence, the supporting lines perpendicular to  $\bar{v}$  host a pair of points  $(p, q)$  with direction  $\bar{v}$ . And the following chain of inequalities holds:

$$D(C) \geq l_C(\bar{v}) \stackrel{\text{Def.}}{\geq} |q - p| = b_C(\bar{v}) = \max_{v \in \mathbb{S}^1} b_C(v) \stackrel{\text{Lem. 2.5}}{\geq} \max_{v \in \mathbb{S}^1} l_C(v) = D(C)$$

This implies  $l_C(\bar{v}) = \max_{v \in \mathbb{S}^1} l_C(v)$  and  $D(C) = \max_{v \in \mathbb{S}^1} b_C(v)$ .

It remains to show that any direction of maximum length is also a direction of maximum breadth. So, let  $\bar{v}'$  be a direction of maximum length. Then the following chain of inequalities holds:

$$l_C(\bar{v}') = D(C) \stackrel{\text{see above}}{\geq} \max_{v \in \mathbb{S}^1} b_C(v) \geq b_C(\bar{v}') \stackrel{\text{Lemma 2.5}}{\geq} l_C(\bar{v}')$$

And the proof of the first part is completed.

<sup>1</sup>We follow the standard to abbreviate 'if and only if' by 'iff'.

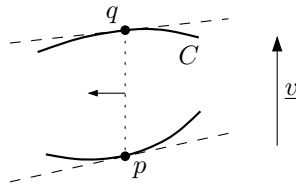


Figure 2.7: If there are no parallel supporting lines, then  $|pq| \neq l_C(\underline{v})$ .

2. The main argument of the second part is illustrated by Figure 2.7. Let  $\underline{v}$  be a direction of minimum length, and let  $(p, q)$  be a pair of points of  $C$  with direction  $\underline{v}$  attaining  $l_C(\underline{v})$ , that is  $|q - p| = l_C(\underline{v}) = \min_{v \in \mathbb{S}^1} l_C(v) = w(C)$  and  $(q - p) = |q - p| \underline{v}$ .

Because  $C$  is convex, there must exist at least one supporting line through  $p$  and one supporting line through  $q$ . Choose a pair of supporting lines through  $p$  and  $q$  enclosing the smallest possible angle, that means the lines should be closest possible to being parallel.

If the lines are not parallel, we can move  $p$  and  $q$  slightly on  $C$  preserving their direction  $\underline{v}$  and increasing their distance, see Figure 2.7. (Otherwise, we could find parallel supporting lines.) By this, we get a contradiction to  $l_C(\underline{v}) = |q - p|$ .

If the two supporting lines were parallel but not perpendicular to  $\underline{v}$ , they would have a distance smaller than  $|q - p| = \min_{v \in \mathbb{S}^1} l_C(v)$ . Thus, if  $v_\perp$  denotes a direction perpendicular to the supporting lines, we would get  $l_C(v_\perp) \leq b_C(v_\perp) < |q - p| = \min_{v \in \mathbb{S}^1} l_C(v)$ , a contradiction.

Therefore, the two supporting lines are parallel and perpendicular to  $\underline{v}$ . This implies  $b_C(\underline{v}) = l_C(\underline{v})$  and

$$w(C) = l_C(\underline{v}) \stackrel{\text{see above}}{=} b_C(\underline{v}) \geq \min_{v \in \mathbb{S}^1} b_C(v) \stackrel{\text{Lemma 2.5}}{\geq} \min_{v \in \mathbb{S}^1} l_C(v) = w(C).$$

And it follows  $b_C(\underline{v}) = \min_{v \in \mathbb{S}^1} b_C(v)$  and  $w(C) = \min_{v \in \mathbb{S}^1} b_C(v)$ .

It remains to show that any direction of minimum breadth is also a direction of minimum length. So, let  $\underline{v}'$  be a direction of minimum breadth. Then the following chain of inequalities holds:

$$b_C(\underline{v}') = \min_{v \in \mathbb{S}^1} b_C(v) \stackrel{\text{see above}}{=} w(C) \stackrel{\text{Def.}}{=} \min_{v \in \mathbb{S}^1} l_C(v) \leq l_C(\underline{v}') \stackrel{\text{Lemma 2.5}}{\leq} b_C(\underline{v}')$$

And the proof of the second part is completed.  $\square$

Lemma 2.6 might raise the question whether one of the equations  $H(C) = D(C)$  or  $h(C) = w(C)$  holds at least for convex closed curves. However, already the isosceles right-angled triangle of Figure 2.1 is clearly a counter-example.

The two-dimensional version of Cauchy's surface area formula cited below helps us to give a first lower bound to the dilation of closed curves.

**Lemma 2.7.** (Cauchy [30]) *Let  $C \in \mathcal{C}$  be a closed convex curve. Then, its length is given by*

$$|C| = \int_0^\pi b_C(\alpha) d\alpha .$$

A proof of the  $n$ -dimensional formula can be found for example in Eggleston's textbook [63]. It uses the notion of mixed volumes. An easier approach dealing only with the two-dimensional case is described on the first pages of Santaló's book on integral geometry [170] and in the textbook [20, pp. 128f.] by Blaschke and Müller. Cauchy's original proof stems from 1841 and can be found in [30], see also Sangwine-Yager's survey [169]. In differential/integral geometry Lemma 2.7 is known under the name Cauchy-Crofton formula, see Section 1-7.C of do Carmo's well-known book [46].

Lemma 2.7 immediately implies a first lower bound to the dilation of closed curves. We presented this very short proof first in [56, 58]. It was proved before by Gromov [86, 88], and dealt with in the context of knot theory by Kusner and Sullivan [135] and Abrams et al. [1].

**Corollary 2.8.** [86, 88],[56, 58] *The dilation of any closed curve  $C \in \mathcal{C}$  is bounded by  $\delta(C) \geq \pi/2$ .*

*Proof.* By  $\partial\text{ch}(C)$  we denote the boundary of the convex hull of  $C$ . Because its length cannot be bigger than the length of  $C$  and because of  $h(C) \leq h_C(v) \leq b_C(v) = b_{\partial\text{ch}(C)}(v)$  for every direction  $v \in \mathbb{S}^1$ , we get

$$|C| \geq |\partial\text{ch}(C)| \stackrel{\text{Lem. 2.7}}{=} \int_0^\pi b_{\partial\text{ch}(C)}(\alpha) d\alpha \geq \pi h(C). \quad (2.1)$$

The definitions of dilation and halving pairs imply  $\delta(C) \geq |C|/2h(C) \stackrel{(2.1)}{\geq} \pi/2$ .  $\square$

In the end of this section we want to mention another straight-forward implication of Cauchy's surface area formula, an upper and a lower bound to the perimeter of any closed convex curve. The bounds are well-known, see for instance Yaglom and Boltyanski's textbook [184, pp. 75f.], [115, pp. 218-220].

**Corollary 2.9.** *Let  $C \in \mathcal{C}$  be an arbitrary convex curve. Then, its length  $|C|$  is bounded by*

$$\pi w(C) \leq |C| \leq \pi D(C).$$

*On either side equality holds only for curves of constant breadth.*

## 2.4 Non-convex closed curves

Within this section we want to compare the dilation  $\delta(C)$  of any closed curve  $C$  to the dilation  $\delta(\partial\text{ch}(C))$  of (the boundary of) its convex hull. We will prove that the inequality  $\delta(\partial\text{ch}(C)) \leq \delta(C)$  holds. On the other hand, clearly, no such inequality can hold for the other direction, see Figure 2.8.

**Lemma 2.10.** *Let  $C \in \mathcal{C}$  be a closed curve. Then the dilation of the boundary of its convex hull is not bigger than the original dilation,  $\delta(\partial\text{ch}(C)) \leq \delta(C)$ .*

*Proof.* We will prove that for any pair of points  $p, q$  on the boundary of the convex hull we can find a corresponding pair of points  $\tilde{p}, \tilde{q}$  on the original cycle not having smaller dilation, i.e.  $\delta_C(\tilde{p}, \tilde{q}) \geq \delta_{\partial\text{ch}(C)}(p, q)$ . We distinguish 3 cases:

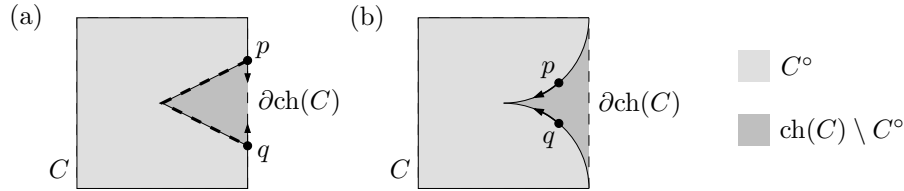


Figure 2.8: The dilation  $\delta(C)$  of a non-convex closed curve  $C$  can become (a) arbitrarily big, (b) even infinite, while  $\delta(\partial\text{ch}(C))$  stays bounded.

*Case 1:*  $p, q \in \partial\text{ch}(C) \cap C$

In this case we pick  $\tilde{p} := p$  and  $\tilde{q} := q$ . Obviously, the shortest-path distances satisfy  $d_{\partial\text{ch}(C)}(p, q) \leq d_C(p, q)$ , and this implies  $\delta_{\partial\text{ch}(C)}(p, q) \leq \delta_C(p, q) = \delta_C(\tilde{p}, \tilde{q})$ .

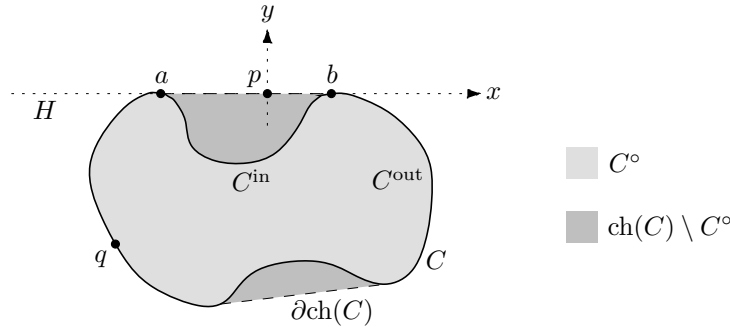


Figure 2.9: Case 2:  $p \in \partial\text{ch}(C) \setminus C$  and  $q \in \partial\text{ch}(C) \cap C$

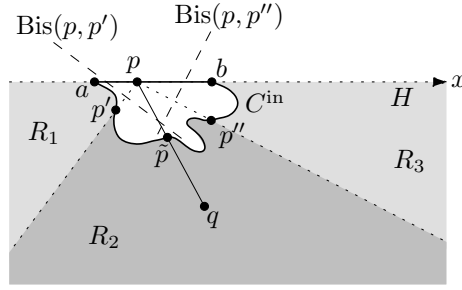
*Case 2:*  $p \in \partial\text{ch}(C) \setminus C$  and  $q \in \partial\text{ch}(C) \cap C$

Let  $ab$  be the line segment of  $\partial\text{ch}(C)$  such that  $p \in ab$  and  $ab \cap C = \{a, b\}$ , see Figure 2.9. Let  $C^{\text{in}}$  denote the path on  $C$  connecting  $a$  and  $b$  which is contained in the interior of the convex hull, and let  $C^{\text{out}} := C \setminus C^{\text{in}}$  be the other path on  $C$  connecting  $a$  and  $b$ . We can assume that  $a$  and  $b$  are located on the  $x$ -axis,  $p$  is the origin, the  $x$ -coordinates are ordered by  $a_x < p_x = 0 < b_x$ , and that  $C$  is contained in the lower half-plane  $H := \{(x, y) \in \mathbb{R}^2 \mid y \leq 0\}$ .

Then,  $q$  is contained in  $H$ . By the conditions of Case 2 the point  $q$  cannot be part of  $C^{\text{in}} \subset C \setminus \partial\text{ch}(C)$ . Hence,  $q \in C^{\text{out}}$ . Because  $C$  is simple,  $C^{\text{out}}$  cannot intersect with  $C^{\text{in}}$  and by definition of  $ab$  it cannot intersect with  $ab$ . Thus  $C^{\text{out}}$  cannot enter the region bounded by  $ab \oplus C^{\text{in}}$ , where  $\oplus$  denotes the *concatenation* of two curves. The remaining area where  $q$  could be located, can be divided into three regions  $R_1$ ,  $R_2$  and  $R_3$ , see Figure 2.10.

Let  $p'$  and  $p''$  be the points on  $C^{\text{in}}$  satisfying  $d_C(a, p') = |ap|$  and  $d_C(b, p'') = |pb|$ , respectively. Then, the  $x$ -coordinates satisfy  $p'_x < 0 = p_x < p''_x$ . Hence, the two rays emanating from  $p$  through  $p'$  and  $p''$  resp. divide  $H$  into three parts. If we remove the closed region bounded by  $C^{\text{in}} \oplus ab$ , we get three regions, (from left to right)  $R_1$ ,  $R_2$  and  $R_3$ . As we consider the closed regions, their union contains  $q$ .

If  $q \in R_2$ , then  $pq$  intersects with  $C^{\text{in}}$  at a point  $\tilde{p}$  between  $p'$  and  $p''$ . It follows that  $|\tilde{p}q| \leq |pq|$

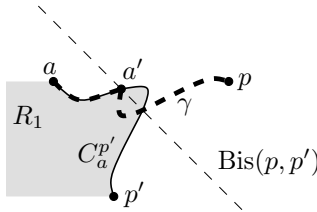
Figure 2.10: The regions  $R_1$ ,  $R_2$  and  $R_3$  containing  $q$ .

and

$$\begin{aligned}
 d_C(\tilde{p}, q) &= \min(d_C(\tilde{p}, a) + d_C(a, q), d_C(\tilde{p}, b) + d_C(b, q)) \\
 &\geq \min(d_C(p', a) + d_C(a, q), d_C(p'', b) + d_C(b, q)) \\
 &\geq \min(d_{\partial\text{ch}(C)}(p, a) + d_{\partial\text{ch}(C)}(a, q), d_{\partial\text{ch}(C)}(p, b) + d_{\partial\text{ch}(C)}(b, q)) \\
 &= d_{\partial\text{ch}(C)}(p, q).
 \end{aligned} \tag{2.2}$$

And we conclude that  $\delta_{\partial\text{ch}(C)}(p, q) \leq \delta_C(\tilde{p}, q)$ . Choosing  $\tilde{q} := q$  completes the proof in this sub-case.

If  $q \in R_1$ , we use  $d_C(p', q) \geq d_{\partial\text{ch}(C)}(p, q)$  which follows analogously to (2.2). We will show that every point included in  $R_1$  is not closer to  $p$  than to  $p'$ . This implies  $|p'q| \leq |pq|$  and, finally,  $\delta_C(p', q) \geq \delta_{\partial\text{ch}(C)}(p, q)$ . Hence, we can choose  $\tilde{p} := p'$  and  $\tilde{q} := q$  to complete the proof.

Figure 2.11:  $R_1$  must totally lie on the  $p'$ -side of  $\text{Bis}(p, p')$ .

We still have to prove that the whole region  $R_1$  lies on the side of the *bisector*  $\text{Bis}(p, p') := \{z \in \mathbb{R}^2 \mid |zp| = |zp'|\}$  belonging to  $p'$ . It is allowed to touch the bisector but not to intersect with the side which is closer to  $p'$ . Note, that by construction of  $p'$  the point  $a$  fulfills these requirements.

We use a proof by contradiction. Assume that there exists a point in  $R_1$  which is closer to  $p$  than to  $p'$ . Then, the part of  $C^{\text{in}}$  connecting  $a$  with  $p'$ , denoted by  $C_a^{p'}$ , has to intersect with the bisector  $\text{Bis}(p, p')$  at least twice. Let  $a'$  be the intersection point reached first by  $C_a^{p'}$  starting from  $a$ , see Figure 2.11. We now reflect  $C_{a'}^{p'}$ , the part of  $C_a^{p'}$  connecting  $a'$  with  $p'$ , at  $\text{Bis}(p, p')$  and denote the resulting path from  $a'$  to  $p$  by  $\tilde{C}_{a'}^p$ . Then, by concatenation we can define a path  $\gamma := C_a^{a'} \oplus \tilde{C}_{a'}^p$  connecting  $a$  and  $p$ . By construction, it has the same length

as the path  $C_a^{p'}$ , which by construction of  $p'$  has the length  $|ap|$ . Thus,  $\gamma$  has to be the line segment  $ap$  connecting  $a$  and  $p$ , and this line segment intersects with the line  $\text{Bis}(p, p')$  at most in a single point. Hence, also the not reflected path  $C_a^{p'}$  intersects with  $\text{Bis}(p, p')$  at most in a single point, contradicting our deduction that there must be at least two intersection points.

In the last sub-case of Case 2 the point  $q$  is contained in  $R_3$ . But then, due to symmetry, we can argue analogously to the case  $q \in R_1$ .

*Case 3:  $p, q \in \partial\text{ch}(C) \setminus C$*

If  $p$  and  $q$  are located on the same line segment of  $\partial\text{ch}(C)$ , we have  $\delta_{\partial\text{ch}(C)}(p, q) = 1 \leq \delta_C(p', q')$  for any  $(p', q') \in \partial\text{ch}(C)^2$ .

In the remaining case, we can apply the step of Case 2 twice. Let again  $ab$  be the line segment of  $\partial\text{ch}(C)$  such that  $p \in ab$  and  $ab \cap C = \{a, b\}$ . First, consider the cycle  $C' := (\partial\text{ch}(C) \setminus ab) \cup C^{\text{in}}$  where  $ab$  is replaced by  $C^{\text{in}}$  in  $\partial\text{ch}(C)$  and everything is defined as in Case 2. Again, we can find a point  $\tilde{p} \in C^{\text{in}} \subset C'$  so that  $\delta_{C'}(\tilde{p}, q) \geq \delta_{\partial\text{ch}(C)}(p, q)$ . Next, we can apply the arguments of Case 2 to the pair  $(q, \tilde{p})$  instead of  $(p, q)$  and  $C'$  instead of  $\text{ch}(C)$ . We get a point  $\tilde{q} \in C$  so that  $\delta_C(\tilde{p}, \tilde{q}) \geq \delta_{C'}(\tilde{p}, q) \geq \delta_{\partial\text{ch}(C)}(p, q)$ .  $\square$

## 2.5 Dilation attained by halving pair

Agarwal et al. proved in Lemma 3.1 of [3] that the dilation of planar closed polygonal curves is attained by a halving pair or by a pair of points consisting of at least one vertex. In this section we will show that an arbitrary convex, but not necessarily polygonal, closed curve  $C$  contains a halving pair attaining its dilation.

To this end, we first generalize Lemma 1 of Ebbers-Baumann et al. [61], which analyzes the angles at a local detour maximum  $(p, q) \in C^2$  of an *open* curve  $C$  as shown in Figure 2.12. A pair of points  $(p, q) \in C^2$  is a *local detour maximum* of  $C$  iff there exists a small  $\varepsilon > 0$  such that any two points  $\tilde{p} \in B_\varepsilon(p) \cap C$ ,  $\tilde{q} \in B_\varepsilon(q) \cap C$  satisfy  $\delta_C(\tilde{p}, \tilde{q}) \leq \delta_C(p, q)$ . Of course  $B_\varepsilon(p) := \{z \in \mathbb{R}^2 \mid |zp| < \varepsilon\}$  denotes the  $\varepsilon$ -*disk* centered at  $p$ .

Consider Figure 2.12. To define the decisive angles at a local detour maximum  $(p, q)$  precisely, imagine a robot moving from  $q$  towards  $p$  on  $C$ . Let  $v_1$  be the direction it is heading to when it arrives at  $p$ . And let  $v_2$  be the direction it is heading to when it leaves  $p$  to continue its journey away from  $q$ . Then we define  $\alpha_1 := \angle(v_1, q - p)$  and  $\alpha_2 := \angle(v_2, q - p)$ , where

$$\angle(v_1, v_2) := \arccos \left( \frac{\langle v_1, v_2 \rangle}{|v_1| |v_2|} \right) \in [0, \pi] \quad (2.3)$$

denotes the smaller angle between the two given vectors.

And  $\beta_1$  and  $\beta_2$  are defined analogously for a robot moving away from  $p$  and taking a rest in  $q$ .

**Lemma 2.11.** *Let  $C \in \mathcal{C}$  be an open curve, and let  $(p, q) \in C \times C$  be a local detour maximum of  $C$ . Let the angles  $\alpha_1, \alpha_2, \beta_1, \beta_2$  be defined as indicated in Figure 2.12.*

*Then,  $\alpha_1 \leq \arccos(-1/\delta_C(p, q)) \leq \alpha_2$  and  $\beta_1 \leq \arccos(-1/\delta_C(p, q)) \leq \beta_2$ .*

*Proof.* We consider a parameterization  $c$  of  $C$  in a neighborhood of  $q$  analogous to the one in



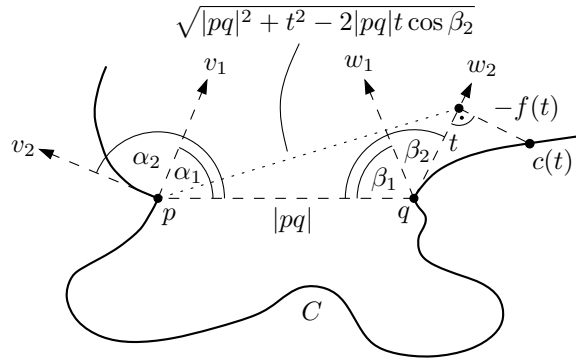


Figure 2.12: The angles between the one-sided derivative vectors at a local detour maximum  $(p, q)$  and the line segment  $pq$ .

the proof of Lemma 2.1, see Figure 2.12. It is defined by

$$c(t) := q + tw_2 + f(t)\mathbf{R}^{90^\circ} w_2$$

for small positive  $t$ -values, and  $c(0) = q$ . The parameter  $t$  represents the component of  $c(t) - q$  which is parallel to  $w_2$ , and  $f(t)$  is the orthogonal component.

We can choose the neighborhood small enough so that  $f(t)$  is differentiable. Because  $w_2$  is the one sided derivative vector of  $C$  in  $q$  we know that  $f'(t) \in O(t)$  and  $f(t) \in O(t^2)$ .

Then, by the law of cosine for small  $t > 0$  we have

$$\delta_C(p, c(t)) = \frac{d_C(p, q) + \int_0^t \sqrt{1 + (f'(\tau))^2} d\tau}{\sqrt{|pq|^2 + t^2 - 2t|pq| \cos \beta_2} \pm O(t^2)}.$$

Hence, the derivative at  $t = 0$  equals

$$\begin{aligned} \left. \frac{d}{dt} \delta_C(p, c(t)) \right|_{t=0} &= \left( \sqrt{1 + (f'(t))^2} \left( \sqrt{|pq|^2 + t^2 - 2t|pq| \cos \beta_2} \pm O(t^2) \right) \right. \\ &\quad \left. - \left( d_C(p, q) + \int_0^t \sqrt{1 + (f'(\tau))^2} d\tau \right) \left( \frac{2t - 2|pq| \cos \beta_2}{2\sqrt{|pq|^2 + t^2 - 2t|pq| \cos \beta_2}} \pm O(t) \right) \right) \\ &\quad \left/ \left( \sqrt{|pq|^2 + t^2 - 2t|pq| \cos \beta_2} \pm O(t^2) \right)^2 \right|_{t=0} \\ &= \frac{|pq| + d_C(p, q) \cos \beta_2}{|pq|^2}. \end{aligned}$$

This derivative cannot be strictly positive because in that case we could increase the dilation value by moving  $q$  slightly away from  $p$ . It follows  $\cos \beta_2 \leq -|pq|/d_C(p, q)$ . Because the cosine function is monotonously decreasing in  $[0, \pi]$ , we get

$$\beta_2 \geq \arccos \left( -\frac{|pq|}{d_C(p, q)} \right) = \arccos \left( -\frac{1}{\delta_C(p, q)} \right).$$

By using analogous arguments for the other one-sided derivatives, we get the inequalities bounding  $\alpha_1$ ,  $\alpha_2$  and  $\beta_1$ .  $\square$



with equal speed. This contradicts the fact that  $(p, q)$  is a detour maximum having maximum  $C$ -distance among all detour maxima, and the proof is completed.

For simplicity we define  $T := d_C(p, q)$ . Let  $\bar{c}$  denote an arc-length parameterization so that  $\bar{c}(0) = p$ ,  $\bar{c}(T) = q$  and  $\bar{c}([0, T]) = \xi$ . If we move  $p$  and  $q$  simultaneously away from each other on  $\xi'$  both by a distance  $t$ , the resulting dilation is  $\delta_C(\bar{c}(-t), \bar{c}(T+t)) = (d_C(p, q) + 2t)/|\bar{c}(T+t) - \bar{c}(-t)|$ .

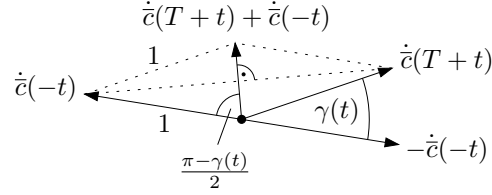


Figure 2.14: The law of cosine yields  $|\dot{c}(T+t) + \dot{c}(-t)| = 2 \cos \frac{\pi - \gamma(t)}{2}$ .

We want to find an upper bound to the denominator. Consider Figure 2.14. Let  $\gamma(t)$  denote the angle between the derivative vectors  $\dot{c}(T+t)$  and  $-\dot{c}(-t)$  for  $t$ -values where both derivatives exist. Note that  $\gamma(t)$  is strictly positive for small  $t$ , because  $\gamma(t)$  tends to  $\alpha_2 + \beta_2 - \pi$  for  $t \rightarrow 0$ , and this limit is positive because of (2.4). Then, by convexity of  $C$ , we have  $\gamma(t) \leq \alpha_2 + \beta_2 - \pi = 2 \arccos(-1/\delta(C)) - \pi$ . It follows

$$\begin{aligned} \frac{d}{d\tau} |\bar{c}(T+\tau) - \bar{c}(-\tau)| \Big|_{\tau=t} &\leq \left| \frac{d}{d\tau} |\bar{c}(T+\tau) - \bar{c}(-\tau)| \Big|_{\tau=t} \right| & (2.5) \\ &\leq \left| \frac{d}{d\tau} (\bar{c}(T+\tau) - \bar{c}(-\tau)) \Big|_{\tau=t} \right| = |\dot{c}(T+t) + \dot{c}(-t)| \\ &= 2 \cos \frac{\pi - \gamma(t)}{2} \leq 2 \cos \frac{\pi - (2 \arccos(-\frac{1}{\delta(C)}) - \pi)}{2} = \frac{2}{\delta(C)} \end{aligned}$$

wherever the left-hand side exists. By plugging everything together, we obtain

$$\begin{aligned} \delta_C(\bar{c}(T+t), \bar{c}(-t)) &= \frac{d_C(p, q) + 2t}{|\bar{c}(T+t) - \bar{c}(-t)|} \stackrel{(2.5)}{\geq} \frac{d_C(p, q) + 2t}{|pq| + \frac{2}{\delta(C)}t} \\ &\stackrel{*}{\geq} \min \left( \frac{d_C(p, q)}{|pq|}, \frac{2t}{\frac{2}{\delta(C)}t} \right) = \delta(C). \end{aligned}$$

The inequality marked by a star is valid because for arbitrary  $a, b, c, d > 0$  holds  $(a+c)/(b+d) \geq \min(a/b, c/d)$ . This is an argument used quite often within dilation analysis. It holds because of the following observation. If we have  $a/b \geq z$  and  $c/d \geq z$ , we can easily conclude  $(a+c)/(b+d) \geq z$  by multiplying each of the three inequalities by its denominator. This completes the proof of Theorem 2.12.  $\square$

## 2.6 Centrally symmetric closed curves

Another rather simple class of closed curves are the centrally symmetric closed curves. We want to examine this class now, before we introduce central symmetrization which maps convex cycles to centrally symmetric convex cycles.

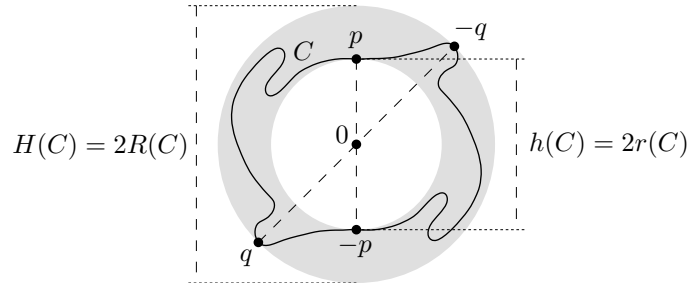


Figure 2.15: Minimum and maximum halving distance of a centrally symmetric cycle  $C$ .

We will consider a closed curve which is centrally symmetric about the origin  $0$ . Its halving pairs are the pairs  $(-p, p)$  where  $p$  is any point of  $C$ , because these pairs are connected by two paths on  $C$  which are centrally symmetric copies of each other. This implies that the minimum halving distance equals twice the *inradius*  $r(C)$ , the radius of the smallest disk contained in  $\overline{C^\circ}$ , and the maximum halving distance equals twice the *circumradius*  $R(C)$ , the radius of the smallest disk containing  $\overline{C^\circ}$ . We have:

$$h(C) = 2r(C) = 2 \min_{p \in C} |p|, \quad H(C) = 2R(C) = 2 \max_{p \in C} |p| \quad (2.6)$$

If we assume that  $C$  is convex, we get some further properties:

**Lemma 2.13.** *Let  $C \in \mathcal{C}$  be a convex closed curve which is centrally symmetric about the origin  $0$ . Then, the following holds:*

1. *For every direction  $v \in \mathbb{S}^1$  we have  $h_C(v) = l_C(v)$ . This implies  $h(C) = w(C)$  and  $H(C) = D(C)$ .*
2. *The length of  $C$  is given by*

$$|C| = \int_0^\pi \sqrt{h_C^2(\alpha) + h_C'^2(\alpha)} \, d\alpha = \int_0^\pi \sqrt{l_C^2(\alpha) + l_C'^2(\alpha)} \, d\alpha$$

*Proof.* 1. The basic inequality of Lemma 2.5 gives  $l_C(v) \geq h_C(v)$ . Consider Figure 2.16. Let  $pq$  be a diametral chord of  $C$  with direction  $v$ , i.e.  $q - p = |q - p|v = l_C(v)v$ . If  $q = -p$  holds, the pair  $(p, q)$  is a halving pair and the proof is completed. Otherwise, by symmetry, the central-symmetric copy  $(-p, -q)$  is also a pair of points of  $C$ .

Due to convexity the *closure*  $\overline{C^\circ}$  of the interior domain of  $C$  must contain the convex hull  $\text{ch}(\{p, q, -p, -q\})$ . And this parallelogram contains a pair of points  $(p', q') = (p', -p')$  of the same distance and direction as  $(p, q)$  which has the additional property of central symmetry.

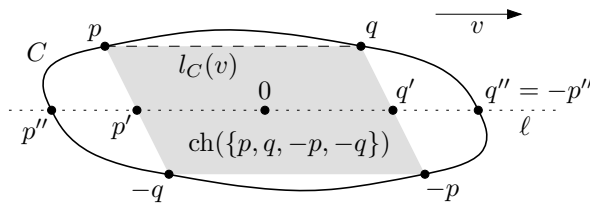


Figure 2.16: Proving  $h_C(v) \geq l_C(v)$  for a convex, centrally symmetric cycle  $C$ .

By possibly extending the line segment  $p'q'$ , which contains 0, we find intersection points  $p''$ ,  $q''$  with  $C$ . They are unique because of the convexity of  $C$ . The arguments of the beginning of this section imply that  $(p'', q'')$  is the unique halving pair with direction  $v$ . We conclude  $h_C(v) = |p''q''| \geq |p'q'| = |pq| = l_C(v)$ .

2. Let  $c : [0, 2\pi) \rightarrow C$  be a parameterization of  $C$  such that  $(c(\alpha), c(\alpha + \pi \bmod 2\pi))$  is the halving pair with direction  $\alpha$  for every  $\alpha \in [0, 2\pi)$ . Here, the curve  $C$  is centrally symmetric, which implies

$$c(\alpha) := \frac{1}{2}h(\alpha)(\cos \alpha, \sin \alpha).$$

The derivative of  $c$  is given by

$$\dot{c}(\alpha) := \frac{1}{2}h'(\alpha)(\cos \alpha, \sin \alpha) + \frac{1}{2}h(\alpha)(-\sin \alpha, \cos \alpha).$$

As the two occurring vectors are orthogonal, the norm of  $\dot{c}$  can be calculated by  $|\dot{c}(\alpha)| = \frac{1}{2}\sqrt{h^2(\alpha) + h'^2(\alpha)}$ , and we get:

$$\begin{aligned} |C| &= \int_0^{2\pi} |\dot{c}(\alpha)| \, d\alpha = \int_0^{2\pi} \frac{1}{2}\sqrt{h^2(\alpha) + h'^2(\alpha)} \, d\alpha \\ &\stackrel{h(\alpha)=h(\alpha+\pi)}{=} \int_0^\pi \sqrt{h^2(\alpha) + h'^2(\alpha)} \, d\alpha \end{aligned}$$

By applying the first part of this lemma, we also get  $|C| = \int_0^\pi \sqrt{l_C^2(\alpha) + l'_C{}^2(\alpha)} \, d\alpha$ . □

**Remark 2.14.**

1. If we plug the equation of Lemma 2.13.2 into our dilation formula for convex cycles from Theorem 2.12, we see that halving distances determine the dilation of a centrally symmetric, convex cycle. By ignoring the influence of  $h'(\alpha)$ , we get a lower bound depending only on the ratio of its mean halving distance and its smallest halving distance:

$$\delta(C) \stackrel{\substack{\text{Lem. 2.13.2,} \\ \text{Thm. 2.12}}}{=} \frac{\int_0^\pi \sqrt{h'^2_C(\alpha) + h^2_C(\alpha)} \, d\alpha}{2h(C)} \geq \frac{\pi \frac{1}{\pi} \int_0^\pi h_C(\alpha) \, d\alpha}{2 \min_\alpha h_C(\alpha)}$$

For non-convex cycles we have to replace '=' by '≥'.

2. For any centrally symmetric, convex cycle  $C$  Lemma 2.13.2 shows

$$\int_0^\pi b_C(\alpha) \, d\alpha \stackrel{\text{Lem. 2.7}}{=} |C| \stackrel{\text{Lem. 2.13.2}}{=} \int_0^\pi \sqrt{h'^2(\alpha) + h^2(\alpha)} \, d\alpha.$$

However, in general it is NOT true that  $b_C(\alpha) = \sqrt{h'^2(\alpha) + h^2(\alpha)}$ , since the right-hand side depends only on the behavior of  $C$  at the halving pair in direction  $\alpha$ , which is usually different from the points determining  $b_C(\alpha)$ , see Figure 2.17.

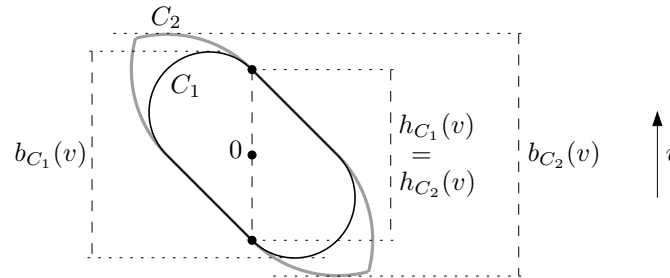


Figure 2.17: The cycles  $C_1$  and  $C_2$  have equal halving distances  $h_{C_1}(v) = h_{C_2}(v)$  and halving distance derivatives  $h'_{C_1}(v) = h'_{C_2}(v)$  but a different breadth  $b_{C_1}(v) \neq b_{C_2}(v)$  in direction  $v$ .

## 2.7 Central symmetrization

Because of the inequality  $\delta(C) \geq \delta(\text{ch}(C))$  proved in Lemma 2.10 we can restrict our search for lower dilation bounds to the case of convex cycles. This allows us to apply the well-known central symmetrization (see e.g. [63, p. 101] and [115, pp. 50–52],[184, pp. 63–66]), which maps any convex closed curve to a centrally symmetric, convex cycle.

For the convenience of the reader we review in this section the basic properties of this transformation, which will be needed later on. Then, in Section 2.8 we introduce a new transformation technique, that will be needed, too, for establishing our lower bounds.

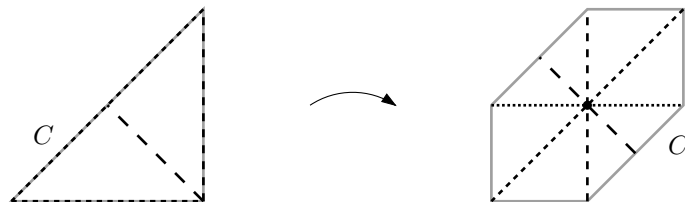


Figure 2.18: Central symmetrization of an isosceles, right-angled triangle  $C$ .

Consider Figure 2.18. The central symmetrization of a convex closed curve  $C$  can be constructed by translating the diametral chords so that its center moves to the origin. Then, the translated endpoints build the centrally symmetric curve  $C'$ . We can define this more formally.

**Definition 2.15.** Let  $C \in \mathcal{C}$  be a convex closed curve. Then, the central symmetrization of  $C$  is the cycle  $C'$  given by the parameterization<sup>2</sup>  $c' : \mathbb{S}^1 \rightarrow \mathbb{R}^2$ ,  $c'(v) := (l_C(v)/2)v$ .

The central symmetrization can also be defined by considering the interior domain  $C^\circ$  of  $C$ . To this end we use the *Minkowski sum* of two sets  $X, Y \subseteq \mathbb{R}^2$ , confer for instance [43]. It is defined by

$$X + Y := \{p + q \mid p \in X, q \in Y\} \quad (2.7)$$

With the Minkowski sum we can give an equivalent definition of the central symmetrization.

**Remark 2.16.** Let  $X$  be what Yaglom and Boltyanski [184, p. 63],[115] call the arithmetic mean of the closed region  $\overline{C^\circ}$  bounded by  $C$  and its negative  $-\overline{C^\circ}$ . It is the Minkowski sum  $\overline{C^\circ} + (-\overline{C^\circ})$  scaled by  $1/2$ . Then, the central symmetrization  $C'$  of  $C$  is the boundary of  $X$ :

$$C' = \partial \left( \frac{1}{2} \left( \overline{C^\circ} + (-\overline{C^\circ}) \right) \right) = \partial \left\{ \frac{1}{2}(q - p) \mid p, q \in \overline{C^\circ} \right\} \quad (2.8)$$

*Proof.* The proof that this second way of constructing  $C'$  is equivalent is straightforward. Let  $\overline{C'^\circ}$  denote the closed region bounded by the curve  $C'$  as defined in (2.8), and let  $v \in \mathbb{S}^1$  be an arbitrary direction. Define  $l := \sup \{k \in \mathbb{R}^{>0} \mid kv \in \overline{C'^\circ}\}$ . Then due to  $\overline{C'^\circ}$  being closed,  $lv$  is an element of  $\overline{C'^\circ}$ . And for  $k > l$  the point  $kv$  is not in  $\overline{C'^\circ}$ . Thus,  $lv \in \partial \overline{C'^\circ} = C'$ . Because  $\overline{C'^\circ}$  is convex like every Minkowski sum of convex sets, which follows directly from the definition, and because  $0 \in \overline{C'^\circ}$ , we have that for every  $k$  satisfying  $0 < k < l$  the point  $kv$  lies in  $\overline{C'^\circ}$ . Hence,  $l$  is the only positive number such that  $lv \in C'$ .

It also follows that there are  $p, q \in \overline{C^\circ}$  such that  $lv = (1/2)(q - p)$ . On the other hand, the definition of  $l$  yields that  $k > l$  implies there are no  $p, q \in \overline{C^\circ}$  satisfying  $kv = (1/2)(q - p)$ . Thus,  $l = (1/2)l_C(v)$ . This shows that  $c'$  from Definition 2.15 is a parameterization of  $C'$  as defined by (2.8).  $\square$

The following lemma lists some properties of the central symmetrization. The ones related neither to halving pairs nor to dilation are well-known. Still, we give easy proofs to make this part of the thesis self-contained.

**Lemma 2.17.** Let  $C \in \mathcal{C}$  be a convex closed curve. Then, its central symmetrization  $C'$  has the following properties:

1. The curve  $C'$  is simple and centrally symmetric about the origin.
2. The cycle  $C'$  is convex.
3. If  $C$  is a polygonal closed curve of  $n$  edges, then  $C'$  is also a polygonal closed curve and has at least  $n$  and at most  $2n$  edges.
4. For every direction  $v \in \mathbb{S}^1$ ,  $v$ -length and  $v$ -breadth are preserved and the  $v$ -halving distance cannot become smaller,  $h_{C'}(v) = l_{C'}(v) = l_C(v) \geq h_C(v)$ , and  $b_{C'}(v) = b_C(v)$ .
5. Width, diameter and perimeter are preserved by central symmetrization,  $w(C') = w(C)$ ,  $D(C') = D(C)$  and  $|C'| = |C|$ .

---

<sup>2</sup>Note that  $c'$  is not a derivative. We denote the derivative vector of a parameterization  $c$  of a curve  $C$  at time  $t$  by  $\dot{c}(t)$ .

6. The area cannot decrease by central symmetrization,  $A(C') \geq A(C)$ .
7. The circumradius cannot increase and the inradius cannot decrease by central symmetrization,  $R(C') \leq R(C)$ ,  $r(C') \geq r(C)$ .
8. The dilation of the central symmetrization  $C'$  is not bigger than the original dilation,  $\delta(C') \leq \delta(C)$ .

*Proof.* 1. This follows immediately from Definition 2.15. Obviously,  $c'(v) := (l_C(v)/2)v = -(l_C(-v)/2)(-v) = -c'(-v)$  because by definition  $l_C(v) = l_C(-v)$ .

2. The convexity of  $C'$  can best be shown by taking advantage of the arithmetic mean definition of Remark 2.16. The closed region  $(1/2)(\overline{C^\circ} + (-\overline{C^\circ}))$  bounded by  $C'$  is convex because the Minkowski sum of two convex sets is convex. This follows directly from the definition.

3. It is well-known (see e.g. de Berg et al. [43, p. 276]) that the Minkowski sum  $X := A + B$  of two convex polygons  $A$  and  $B$  having  $n_A$  and  $n_B$  edges is a convex polygon having at most  $n_A + n_B$  edges. The proof in [43] also shows that usually  $C'$  has the maximal amount of  $2n$  edges. However, for every pair of parallel edges of  $C$ , the number is reduced by one. Thus, the minimal number of edges equals  $n$ .

4. As proved in Lemma 2.13.1, the equation  $l_{C'}(v) = h_{C'}(v)$  holds for every  $v \in \mathbb{S}^1$  because  $C'$  is convex and centrally symmetric. Obviously, the halving distance  $h_{C'}(v)$  in direction  $v$  is attained by the pair of points  $(l_C(v)/2)v$ ,  $-(l_C(v)/2)v$ . Hence,  $h_{C'}(v) = l_C(v)$ . And  $l_C(v) \geq h_C(v)$  is one of the basic inequalities from Lemma 2.5.

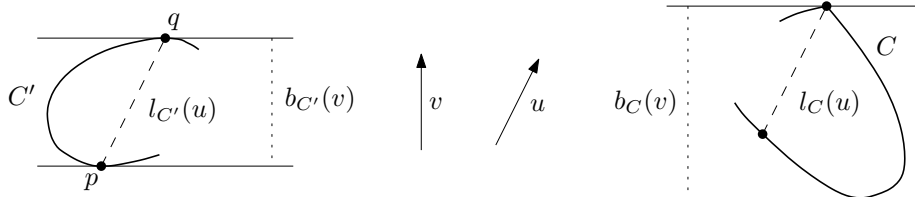


Figure 2.19: Proof of  $b_{C'}(v) \leq b_C(v)$ .

It remains to show that  $b_{C'}(v) = b_C(v)$ . We first prove that  $b_{C'}(v) \leq b_C(v)$ . Consider the left hand side of Figure 2.19. Let  $(p, q) \in C' \times C'$  be a pair of points lying on opposite supporting lines of  $C'$  perpendicular to  $v$ . Let  $u$  be the direction of  $(p, q)$ , i.e.  $q - p = |q - p|u$ . Then,  $b_{C'}(v) = \langle |q - p|u, v \rangle$ .

And, by definition,  $l_{C'}(u) \geq |q - p|$ . Above we have shown that  $l_{C'}(u) = l_C(u)$ . It follows:

$$l_C(u) \geq |q - p| \tag{2.9}$$

By definition of  $l_C(u)$ , a pair of points with direction  $u$  and distance  $l_C(u)$  has to fit between the two supporting lines of  $C$  perpendicular to  $v$ , see the right-hand side of Figure 2.19. Thus,  $b_C(v) \geq \langle l_C(u)u, v \rangle$ .



By putting everything together, we get:

$$b_{C'}(v) \stackrel{\text{Fig. 2.19, left}}{=} \langle |q-p|u, v \rangle \stackrel{(2.9)}{\leq} \langle l_{C'}(u)u, v \rangle \stackrel{\text{Fig. 2.19, right}}{\leq} b_C(v)$$

We can use the same arguments to prove  $b_C(v) \leq b_{C'}(v)$  by simply swapping the roles of  $C$  and  $C'$ . This is possible because the main argument  $l_{C'}(u) = l_C(u)$  is symmetric.

5. It follows immediately from 4. and from the definitions that width and diameters are preserved. The perimeter is preserved because all the  $v$ -breadth values are equal by 4. and Cauchy's surface area formula, Lemma 2.7, yields  $|C'| = \int_0^{2\pi} b_{C'}(\alpha) d\alpha = \int_0^{2\pi} b_C(\alpha) d\alpha = |C|$ .

6. The two-dimensional version of the *Brunn-Minkowski theorem*, see for instance [22, p. 88], [169, p. 57], [147, p. 297], says that for two convex sets  $X, Y \subset \mathbb{R}^2$  and a real value  $\vartheta \in [0, 1]$  the area of the Minkowski sum  $(1 - \vartheta)X + \vartheta Y$  satisfies the inequality

$$\sqrt{A((1 - \vartheta)X + \vartheta Y)} \geq (1 - \vartheta)\sqrt{A(X)} + \vartheta\sqrt{A(Y)}. \quad (2.10)$$

By setting  $\vartheta = 1/2$  and  $Y = -X$ , which implies  $A(Y) = A(X)$ , and by taking the squares of both sides we get

$$A\left(\frac{1}{2}(X - X)\right) \geq A(X).$$

Due to Remark 2.16 this shows  $A(C') \geq A(C)$ .

7. Because the incircle has to fit in between all pairs of parallel tangents of  $C$ , we have  $w(C) \geq 2r(C)$ . Because the line segment of length  $D(C)$  is contained in the circumcircle, we have  $D(C) \leq 2R(C)$ . Combining these facts with results we know already yields

$$\begin{aligned} 2r(C') &\stackrel{(2.6)}{=} h(C') \stackrel{\text{Lem. 2.13.1}}{=} w(C') \stackrel{\text{Lem. 2.17.4}}{=} w(C) \geq 2r(C), \\ 2R(C') &\stackrel{(2.6)}{=} H(C') \stackrel{\text{Lem. 2.13.1}}{=} D(C') \stackrel{\text{Lem. 2.17.4}}{=} D(C) \leq 2R(C). \end{aligned}$$

8. It follows easily from the results shown above that the dilation of the transformed cycle cannot be bigger than the original one:

$$\delta(C') \stackrel{\text{Thm. 2.12}}{=} \frac{|C'|}{2 \min_{v \in \mathbb{S}^1} h_{C'}(v)} \stackrel{(4), (5)}{\leq} \frac{|C|}{2 \min_{v \in \mathbb{S}^1} h_C(v)} \stackrel{\text{Thm. 2.12}}{=} \delta(C)$$

This completes the proof.  $\square$

**Corollary 2.18.** *For every convex closed curve  $C$ , there is a centrally symmetric, convex cycle  $C'$  not having bigger dilation.*

**Remark 2.19.** *The dilation ratio between the central symmetrization and the original cycle is given by:*

$$\frac{\delta(C')}{\delta(C)} \stackrel{\text{Thm. 2.12}}{=} \frac{\frac{|C'|}{2 \min_{v \in \mathbb{S}^1} h_{C'}(v)}}{\frac{|C|}{2 \min_{v \in \mathbb{S}^1} h_C(v)}} \stackrel{\text{Lem. 2.17.5}}{=} \frac{h(C)}{h(C')} \stackrel{\text{Lem. 2.17.4}}{=} \frac{h(C)}{w(C)} \quad (2.11)$$

The ratio has a value in  $(0, 1]$  (see Lemma 2.5)<sup>3</sup>. Note that the ratio is NOT a measure of the symmetry of  $C$ . If  $C$  is centrally symmetric, then the ratio equals 1 because of Lemma 2.13.1. But if the ratio equals 1,  $C$  does not have to be centrally symmetric, see Figure 2.20.

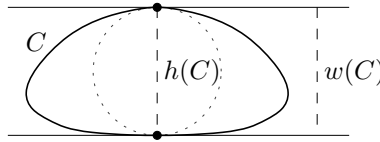


Figure 2.20: The condition  $h(C) = w(C)$  is not sufficient for  $C$  being centrally symmetric.

We now know that every convex cycle can be transformed into a centrally symmetric, convex cycle without increasing its dilation. By Remark 2.19 we even know how much the dilation decreases. Of course, this will help us in finding lower dilation bounds because we can restrict our search to the case of convex, centrally symmetric cycles. Before taking advantage of this knowledge we introduce the new halving pair transformation which will help us to derive additional important lower bounds to the dilation of cycles, and which will be essential in proving the best known lower bound to the dilation of finite point sets.

## 2.8 Halving pair transformation

The halving pair transformation translates the midpoints of the halving pairs to the origin, see Figure 2.21. As mentioned in the introduction, this transformation was first mentioned by Zindler [p. 44][186], who devoted some lines to its effect on the enclosed area of Zindler curves, a class of curves which were later named after him and which we examine in detail in Chapter 3. Gromov [88, pp. 11f.] used a similar idea to prove  $\delta(X) \geq \pi/2$  for every not simply connected set  $X \subset \mathbb{R}^n$ .

We will show that the halving pair transformation also maps convex closed curves to centrally symmetric, convex closed curves. However, it can easily be defined even for non-convex closed curves.

Consider Figure 2.21. The idea is similar to central symmetrization. One translates every halving chord in such a way that its center is moved to the origin. The curve of the translated endpoints of the halving chords is the result of the halving pair transformation. The following is a more formal definition.

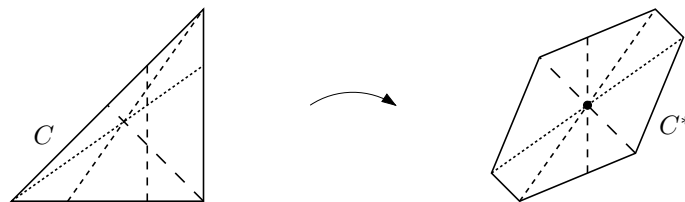


Figure 2.21: The halving pair transformation of an isosceles, right-angled triangle  $C$ .

**Definition 2.20.** Let  $C \in \mathcal{C}$  be an arbitrary closed curve. Then, the result of the halving pair transformation applied to  $C$  is the closed curve  $C^*$  given by the parameterization  $c^*(v) :=$

<sup>3</sup>Actually,  $h/w$  is even restricted to the interval  $(\frac{1}{2}, 1]$ , as we will prove in Chapter 4.

$\frac{1}{2}(\bar{c}(t) - \bar{c}(t + |C|/2))$  where  $\bar{c}(\cdot)$  is an arc-length parameterization of  $C$  and  $t + |C|/2$  is calculated modulo  $|C|$ . If  $C$  is convex, the parameterization  $c^* : \mathbb{S}^1 \rightarrow \mathbb{R}^2$ ,  $c^*(v) := \frac{h_C(v)}{2}v$ , defines the same curve  $C^*$ .

The halving pair transformation has properties similar to the central symmetrization. However, it preserves the halving distance rather than the length- and the breadth-values.

**Lemma 2.21.** *Let  $C \in \mathcal{C}$  be a closed curve. Then, the result  $C^*$  of applying the halving pair transformation to  $C$  has the following properties:*

1. The transformed curve  $C^*$  is centrally symmetric about the origin.
2. If  $C$  is convex, then  $C^*$  is simple and convex.
3. If  $C$  is a polygonal cycle of  $n$  edges, then  $C^*$  is also a polygonal cycle and has at most  $2n$  edges. If  $C$  is convex, it has at least  $n$  edges.
4. The halving distances are preserved<sup>4</sup>. The breadth values cannot increase,  $b_{C^*}(v) \leq b_C(v)$ . If  $C$  is convex, we have  $l_{C^*}(v) = h_{C^*}(v) = h_C(v) \leq l_C(v)$ , the length-values do not become bigger.
5. The width, the diameter and the length of  $C^*$  are not bigger than the original values,  $w(C^*) \leq w(C)$ ,  $D(C^*) \leq D(C)$  and  $|C^*| \leq |C|$ .
6. The area cannot decrease,  $A(C^*) \geq A(C)$ .
7. The inradius can increase and decrease by halving pair transformation, even if  $C$  is convex. The circumradius never increases,  $R(C^*) \leq R(C)$ .
8. If  $C$  is convex, the dilation of  $C^*$  is not bigger than the original dilation,  $\delta(C^*) \leq \delta(C)$ .

If  $C$  is not convex, length values and the dilation can increase, see Figures 2.22 and 2.23.

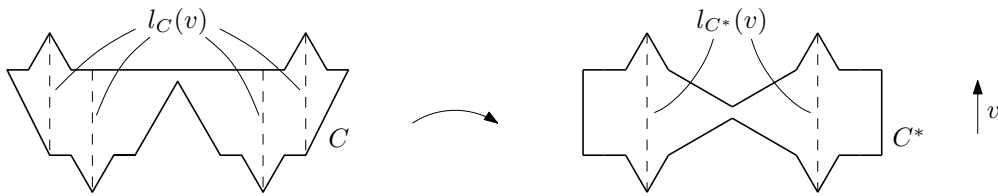


Figure 2.22: If  $C$  is not convex, the  $v$ -length can increase by halving pair transformation.

*Proof.* 1. The curve  $C^*$  is centrally symmetric about the origin because by definition  $c^*(t) = -c^*(t + |C|/2)$  holds.

<sup>4</sup>For every halving pair of  $C$  with direction  $v \in \mathbb{S}^1$  there is exactly one halving pair of  $C^*$  with direction  $v$  having the same distance. For convex closed curves we can simply write  $h_{C^*}(v) = h_C(v)$ .

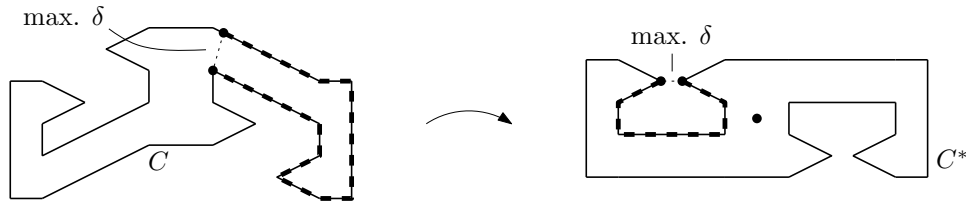


Figure 2.23: If  $C$  is not convex, the dilation can increase by halving pair transformation.

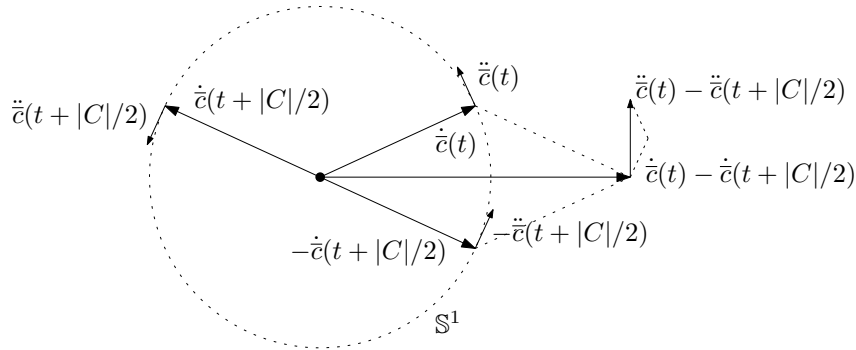


Figure 2.24: The derivative vector  $\dot{\bar{c}}(t) - \dot{\bar{c}}(t + |C|/2)$  always turns into the same direction.

2. Let  $C \in \mathcal{C}$  be a convex closed curve. We first assume that  $C$  is twice continuously differentiable. We consider an arc-length parameterization  $\bar{c} : [0, |C|) \rightarrow C$  of  $C$ . Consider Figure 2.24. Because of the assumption, the derivative  $\dot{\bar{c}}(\cdot)$  is a continuous function mapping  $[0, |C|)$  to the unit circle  $\mathbb{S}^1$ . Due to convexity the mapping is bijective, i.e. the derivative vector always turns into the same direction, say counter-clockwise. The properties carry over to  $-\dot{\bar{c}}(\cdot + |C|/2)$ , and this derivative also turns counter-clockwise.

Furthermore, the case  $\dot{\bar{c}}(t) - \dot{\bar{c}}(t + |C|/2) = 0$  cannot occur. Because of the convexity, this would imply that  $\dot{\bar{c}}(\tau) = \dot{\bar{c}}(t) = \dot{\bar{c}}(t + |C|/2)$  for all  $\tau$ -values in  $[t, t + |C|/2]$  or in  $[t + |C|/2, t + |C|]$ . But then,  $C$  would contain a line segment of length  $|C|/2$ . It would have to be a line segment and could not be simple.

Hence, the angle between  $\dot{\bar{c}}(t)$  and  $\dot{\bar{c}}(t) - \dot{\bar{c}}(t + |C|/2)$  is always smaller than  $90^\circ$ . Therefore, the component of  $\dot{\bar{c}}(t)$  which is orthogonal to  $\dot{\bar{c}}(t) - \dot{\bar{c}}(t + |C|/2)$  turns the latter vector counter-clockwise. Analogous arguments show that  $-\dot{\bar{c}}(t + |C|/2)$  turns  $\dot{\bar{c}}(t) - \dot{\bar{c}}(t + |C|/2)$  counter-clockwise. Hence,  $C^*$  is convex.

The result can be generalized to piecewise continuously differentiable curves by approximating them with smooth curves. We discuss the necessary properties in Section 4.11. It is essential that  $h_C(v)$  is continuous in  $C$  for every fixed direction  $v$  at non-degenerate closed curves  $C$ .

The simplicity of  $C^*$  follows from Lemma 2.3.

3. If  $C$  is a polygonal cycle, then  $\bar{c}(\cdot)$  and  $\bar{c}(\cdot + |C|/2)$  are piecewise affine. Hence, the parameterization  $c^*(t) = \frac{1}{2}(\bar{c}(t) - \bar{c}(t + |C|/2))$  of  $C^*$  is also piecewise affine. And there can

only be a corner at  $c^*(t)$  if there is a corner at  $\bar{c}(t)$  or  $\bar{c}(t + |C|/2)$ . This shows that  $C^*$  cannot have more than  $2n$  corners. If  $C$  is convex, corners at  $\bar{c}(t)$  and  $\bar{c}(t + |C|/2)$  cannot cancel out each other because the derivative always turns into the same direction. However, if  $C$  is not convex, indeed  $C^*$  can have less corners than  $C$ , see Figure 2.23 for an example.

4. The halving distances are preserved because of the definition of the halving pair transformation and due to the fact that for centrally symmetric cycles the halving pairs are the pairs  $(p, -p)$ ,  $p \in C$ .

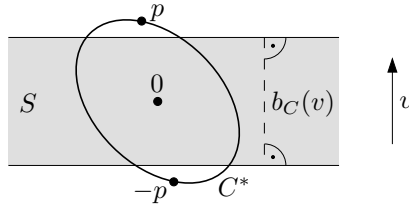


Figure 2.25: This situation is impossible:  $C^*$  cannot leave  $S$ .

We use a proof by contradiction to show  $b_{C^*}(v) \leq b_C(v)$ . Consider the strip

$$S := \{p \in \mathbb{R}^2 \mid -b_C(v)/2 \leq \langle p, v \rangle \leq b_C(v)/2\}$$

as depicted in Figure 2.25. In general, in this thesis the name *strip* denotes the closed region bounded by two parallel lines. If there was a point  $p \in C^*$  outside of  $S$ , also its halving partner  $-p$  would be in  $C^* \setminus S$ . But then, there would be a halving pair  $(q, \hat{q})$  of  $C$  of identical direction and distance. Hence,  $\langle q - \hat{q}, v \rangle = \langle p - \hat{p}, v \rangle > b_C(v)$  which contradicts the definition of  $b_C(v)$ .

Next, we prove  $l_{C^*}(v) \leq l_C(v)$  for a convex closed curve  $C$ . In this case  $C^*$  is convex and centrally symmetric. Hence, we can apply Lemma 2.13.1 and get  $l_{C^*}(v) = h_{C^*}(v)$ . Because of the arguments above,  $h_{C^*}(v) = h_C(v)$  holds. And  $h_C(v) \leq l_C(v)$  is one of the basic inequalities in Lemma 2.5.

5. The inequality  $b_{C^*}(v) \leq b_C(v)$  from above implies  $w(C^*) \leq w(C)$  and  $D(C^*) \leq D(C)$ . The length relation can be shown by considering an arc-length parameterization  $\bar{c} : [0, |C|) \rightarrow C$ . We have

$$\begin{aligned} |C| &= \int_0^{|C|} |\dot{\bar{c}}(t)| + |\dot{\bar{c}}(t + |C|/2)| dt \stackrel{\Delta\text{-inequ.}}{\geq} \int_0^{|C|} |\dot{\bar{c}}(t) - \dot{\bar{c}}(t + |C|/2)| dt \\ &\stackrel{\text{(Def. 2.20)}}{=} \int_0^{|C|} 2 |\dot{c}^*(t)| dt \stackrel{c^*(t) = -c^*(t+|C|/2)}{=} \int_0^{|C|} |\dot{c}^*(t)| dt = |C^*|. \end{aligned}$$

6. The inequality  $A(C^*) \geq A(C)$  is related to an old theorem by Holditch which we will discuss in Section 2.10. There, it will turn out to be a corollary of a more general proof result.

7. The curve in Figure 2.26 shows that the inradius can decrease by halving pair transformation. The reason is that we have

$$2r(C^*) \stackrel{(2.6)}{=} h(C^*) \stackrel{\text{Lem. 2.21.4}}{=} h(C),$$

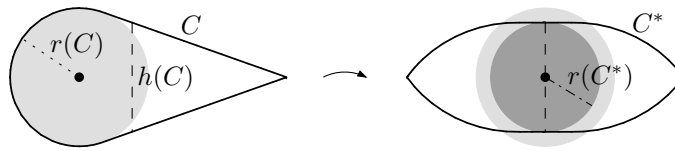


Figure 2.26: This one-sided cap-curve is an example satisfying  $r(C^*) < r(C)$ .

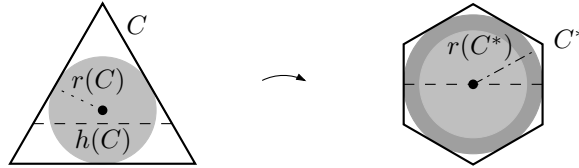


Figure 2.27: The equilateral triangle satisfies  $r(C^*) > r(C)$ .

and that there are curves satisfying  $h(C) < 2r(C)$ , cf. Section 4.8. Because there also exist curves with  $h(C) > 2r(C)$ , like the equilateral triangle displayed in Figure 2.27, the inradius can also increase.

Obviously, the circumcircle has to contain a line segment of length  $D$ . Hence we have  $D(C) \leq 2R(C)$ . This yields

$$2R(C^*) \stackrel{(2.6)}{=} H(C^*) \stackrel{\text{Lem. 2.21.4}}{=} H(C) \stackrel{\text{Lem. 2.5}}{\leq} D(C) \leq 2R(C).$$

8. The inequality between the dilation values follows immediately.

$$\delta(C^*) \stackrel{\text{Thm. 2.12}}{=} \frac{|C^*|}{2 \min_{v \in \mathbb{S}^1} h_{C^*}(v)} \stackrel{4., 5.}{\leq} \frac{|C|}{2 \min_{v \in \mathbb{S}^1} h_C(v)} \stackrel{\text{Thm. 2.12}}{=} \delta(C) \quad (2.12)$$

This concludes the proof of the properties.  $\square$

We can say a little more about the effect of halving transformation on dilation.

**Lemma 2.22.** *Let  $C \in \mathcal{C}$  be an arbitrary convex closed curve. Then, the dilation ratio between the transformed and the original cycle is given by:*

$$\frac{\delta(C^*)}{\delta(C)} \stackrel{\text{Thm. 2.12, Lem. 2.21.4}}{=} \frac{|C^*|}{|C|} \stackrel{\text{Lem. 2.13.2, Lem. 2.21.4, Lem. 2.7}}{=} \frac{\int_0^\pi \sqrt{h_C^2(\alpha) + h_C'^2(\alpha)} \, d\alpha}{\int_0^\pi b_C(\alpha) \, d\alpha} \quad (2.13)$$

*The dilation ratio has a value in  $(0, 1]$  and is a measure of the symmetry of  $C$ . The value equals 1, if and only if  $C$  is centrally symmetric, which is equivalent to  $C^* = C$  up to translation.*

*Proof.* The equations follow from the lemmata cited above the corresponding “=”-sign. We still have to prove that  $C$  is centrally symmetric iff the ratio equals 1. We consider an arc-length parameterization  $\bar{c}: [0, |C|) \rightarrow C$ .

Let  $C$  be centrally symmetric. W.l.o.g. we can assume that  $C$  is centrally symmetric about the origin. Then, the halving pairs of  $C$  are the pairs  $(p, -p)$  for every  $p \in C$ . Hence, we have  $\bar{c}(t + |C|/2) = -\bar{c}(t)$  for every  $t \in [0, |C|)$ , which implies  $C^* = C$ , and the ratio equals 1.

If, on the other hand, the ratio equals 1, we have

$$\int_0^{\frac{|C|}{2}} |\dot{\bar{c}}(t) - \dot{\bar{c}}(t + |C|/2)| dt = |C^*| = |C| = \int_0^{\frac{|C|}{2}} |\dot{\bar{c}}(t)| + |\dot{\bar{c}}(t + |C|/2)| dt .$$

As used in the proof of Lemma 2.21.5, the triangle inequality implies that the left integrand is never bigger than the right one. Hence, because the values of both integrals are equal, the integrands must be equal almost everywhere. In this case the direction and orientation of  $\dot{\bar{c}}(t)$  and  $-\dot{\bar{c}}(t + |C|/2)$  must be the same. Because both their absolute values equal 1, we obtain  $\dot{\bar{c}}(t) = -\dot{\bar{c}}(t + |C|/2)$  for almost every  $t \in [0, |C|/2)$ .

Let w.l.o.g.  $\bar{c}(0) = -\bar{c}(|C|/2)$ . This can be reached by translating  $C$ . Then, the following equation holds.

$$\begin{aligned} \bar{c}(t) &= \bar{c}(0) + \int_0^t \dot{\bar{c}}(\tau) d\tau \\ &= -\bar{c}\left(\frac{|C|}{2}\right) + \int_0^t \left(-\dot{\bar{c}}\left(\tau + \frac{|C|}{2}\right)\right) d\tau = -\bar{c}\left(t + \frac{|C|}{2}\right) \end{aligned}$$

The closed curve  $C$  is centrally symmetric. □

We know that  $\delta(C^*)/\delta(C) = |C^*|/|C| \leq 1$ . This is nice for deriving lower bounds to the dilation of cycles, as it suffices to find lower bounds for  $C^*$ . Clearly, it would be interesting to have an inequality for the other direction, too. We conjecture that the inequality  $|C^*|/|C| \geq \frac{\sqrt{3}}{2}$  holds, and that equality is attained only by equilateral triangles. A proof of this would also allow us to give a better lower bound on  $H/|C|$ , see Section 4.5. Unfortunately, so far we have only found a proof of a non-tight lower bound.

**Lemma 2.23.** *Let  $C$  be an arbitrary convex cycle in the plane. Then, the perimeter of the result of the halving pair transformation is bounded by  $|C^*| \geq \frac{1}{2}|C|$ .*

*Proof.* In Lemma 4.12 of Section 4.7 we prove the inequality  $h(v) \geq l(v)/2$  for every direction  $v \in \mathbb{S}^1$ . By the definition of central symmetrization, Definition 2.15, and by the definition of the halving pair transformation, Definition 2.20, this shows that the halving pair transformation  $C^*$  of  $C$  scaled by two contains the central symmetrization  $C'$  of  $C$ ,  $C'^{\circ} \subseteq 2C^{*\circ}$ .

This implies  $b_{C^*}(v) \geq \frac{1}{2}b_{C'}(v)$  for every direction  $v \in \mathbb{S}^1$ . Plugging this into Cauchy's surface area formula, Lemma 2.7, yields

$$|C^*| \stackrel{\text{Lemma 2.7}}{=} \int_0^\pi b_{C^*}(\alpha) d\alpha \geq \frac{1}{2} \int_0^\pi b_{C'}(\alpha) d\alpha \stackrel{\text{Lemma 2.7}}{=} \frac{1}{2}|C'| \stackrel{\text{Lemma 2.17.5}}{=} \frac{1}{2}|C|.$$

□

**Open Problem 3.** *What is the infimum of  $|C^*|/|C|$ ?*

## 2.9 Midpoint curve

Because dilation does not increase by either central symmetrization or halving pair transformation, the simple dilation formulas for centrally symmetric convex curves from Section 2.6 enable us to give lower bounds to the dilation of any convex curve depending on  $h/H$  or  $w/D$ . However, before presenting these results, we want to introduce another closed curve derived from the original curve  $C$ . Amongst other applications it will help us to get better bounds.

**Definition 2.24.** *Let again  $\bar{c} : [0, |C|) \rightarrow C$  be an arc-length parameterization of a closed curve  $C \in \mathcal{C}$ . Then, the midpoint curve  $M$  is defined by the parameterization*

$$m(t) := \frac{1}{2} \left( \bar{c}(t) - \bar{c} \left( t + \frac{|C|}{2} \right) \right).$$

*It is formed by the midpoints of the halving chords.*

The two curves  $M$  and  $C^*$  derived from  $C$  are illustrated in Figure 2.28. The midpoint curve turns out to be very useful for both, proving the stability result in Section 2.12 and analyzing the curves of constant halving distance, the Zindler curves, in Chapter 3. We have

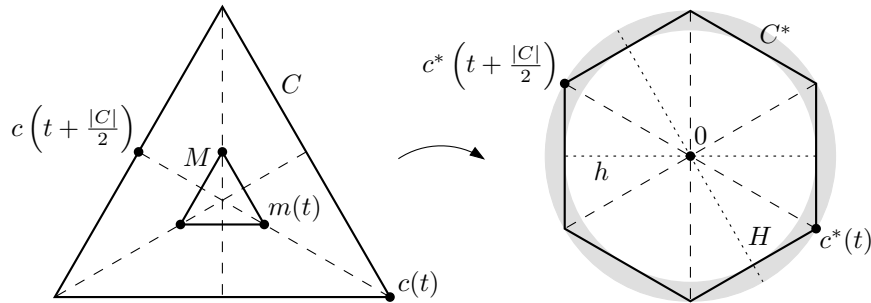


Figure 2.28: An equilateral triangle  $C$ , and the derived curves  $C^*$  and  $M$ .

$m(t) = m(t + |C|/2)$ , and thus, the curve  $M$  is traversed twice when  $C$  and  $C^*$  are traversed once. We define  $|M|$  as the length of the curve  $M$  corresponding to one traversal, i.e., the parameter interval is  $[0, |C|/2]$ .

The halving pair transformation decomposes the curve  $C$  into two components, from which  $C$  can be reconstructed:

$$c(t) = m(t) + c^*(t), \quad c \left( t + \frac{|C|}{2} \right) = m(t) - c^*(t) \quad (2.14)$$

This is analogous to the decomposition of a function into an even and an odd function, or writing a matrix as a sum of a symmetric and a skew-symmetric matrix.

In Lemma 2.21.5 we have shown the inequality  $|C^*| \leq |C|$ . By considering the midpoint curve, we can give a more specific formula, an upper bound to the length  $|M|$  of the midpoint curve, which will be a key fact in the proof of the stability result in Section 2.12. Additionally to this upper bound which we presented before in [50, 49], here we prove a complementing lower bound.



**Lemma 2.25.**  $(|C| - |C^*|)^2 \leq 4|M|^2 \leq |C|^2 - |C^*|^2$ .

*Proof.* Using the linearity of the scalar product and  $|\dot{\tilde{c}}(t)| = 1$ , we obtain

$$\begin{aligned} \langle \dot{m}(t), \dot{c}^*(t) \rangle &\stackrel{\text{Def. 2.20,}}{\stackrel{\text{Def. 2.24}}{=}} \frac{1}{4} \left\langle \dot{\tilde{c}}(t) + \dot{\tilde{c}}\left(t + \frac{|C|}{2}\right), \dot{\tilde{c}}(t) - \dot{\tilde{c}}\left(t + \frac{|C|}{2}\right) \right\rangle \\ &= \frac{1}{4} \left( |\dot{\tilde{c}}(t)|^2 - \left| \dot{\tilde{c}}\left(t + \frac{|C|}{2}\right) \right|^2 \right) = \frac{1}{4}(1 - 1) = 0. \end{aligned} \quad (2.15)$$

Here and in the whole thesis, we write  $v \perp w$  to denote that two vectors  $v$  and  $w$  are *orthogonal* to each other, i.e.  $\langle v, w \rangle = 0$ . The opposite case, where  $v$  and  $w$  are *parallel*, i.e.  $\langle v, w \rangle = |v||w|$ , is denoted by  $v \parallel w$ .

Above we have shown  $\dot{c}^*(t) \perp \dot{m}(t)$  wherever the derivatives exist, thus (2.14) yields

$$|\dot{m}(t)|^2 + |\dot{c}^*(t)|^2 = |\dot{\tilde{c}}(t)|^2 = 1. \quad (2.16)$$

This implies

$$\begin{aligned} |C| &= \int_0^{|C|} \sqrt{|\dot{m}(t)|^2 + |\dot{c}^*(t)|^2} dt \\ &\geq \sqrt{\left( \int_0^{|C|} |\dot{m}(t)| dt \right)^2 + \left( \int_0^{|C|} |\dot{c}^*(t)| dt \right)^2} = \sqrt{4|M|^2 + |C^*|^2} \end{aligned}$$

The above inequality — from which the upper bound follows — can be seen by a geometric argument: the left integral

$$\int_0^{|C|} \sqrt{|\dot{m}(t)|^2 + |\dot{c}^*(t)|^2} dt$$

equals the length of the curve

$$\gamma(s) := \left( \int_0^s |\dot{m}(t)| dt, \int_0^s |\dot{c}^*(t)| dt \right),$$

while the right expression

$$\sqrt{\left( \int_0^{|C|} |\dot{m}(t)| dt \right)^2 + \left( \int_0^{|C|} |\dot{c}^*(t)| dt \right)^2}$$

equals the distance of its end-points  $\gamma(0) = (0, 0)$  and  $\gamma(|C|)$ .

On the other hand we can use the fact that the derivative vectors  $\dot{c}^*(t)$  and  $\dot{m}(t)$  are always orthogonal to each other also for deriving a lower bound.

$$\begin{aligned} 2|M| &= \int_0^{|C|} |\dot{m}(t)| dt \stackrel{(2.16)}{=} \int_0^{|C|} \sqrt{1 - |\dot{c}^*(t)|^2} dt \\ &\stackrel{\sqrt{1-|\dot{c}^*|^2} \leq 1}{\geq} \int_0^{|C|} (1 - |\dot{c}^*(t)|^2) dt \stackrel{|\dot{c}^*| \leq 1}{\geq} |C| - \int_0^{|C|} |\dot{c}^*(t)| dt \\ &= |C| - |C^*|. \end{aligned}$$

□

## 2.10 Holditch's theorem

We still have not discussed how the halving pair transformation effects the area. This question is closely related to Holditch's theorem, which Reverent Hamnet Holditch [104] presented in 1858. In literature this article is sometimes also cited as published in "Lady's and Gentleman's diary for the year 1858", see for instance [20] and [145], but we were not able to confirm this second reference.

The theorem in its original version<sup>5</sup> reads like this.

**Theorem 2.26.** (Holditch [104]) *If a chord of a closed curve, of constant length  $a + b$ , be divided into two parts of lengths  $a, b$  respectively, the difference between the areas of the closed curve, and of the locus of the dividing point, will be  $\pi ab$ .*

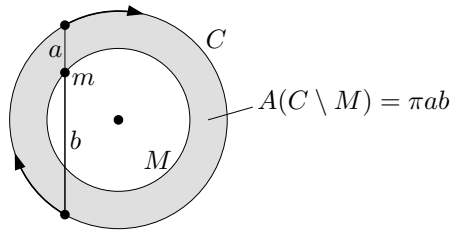


Figure 2.29: The curve<sup>6</sup> traced by the point  $m$  is another circle. And like stated by Holditch's theorem we have  $A(C \setminus M) = \pi ab$ .

A good illustration<sup>6</sup> of this theorem can be seen in Figure 2.29 where it is applied to a circle. However, Holditch did not explicitly state some assumptions which are necessary for the theorem to hold, see Broman [27] for details. That article also contains a proof and a generalized version. Holditch's theorem and different generalizations are also discussed by Edwards [62, pp. 478, 484], Kiliç and Keleş [121], Müller [152], and Blaschke and Müller [20, p. 120].

For our purpose the original version is not very helpful. Instead we use a powerful generalization by Chakerian and Goodey [32]. This section is mainly based on the ideas presented in their article.

To this end, we need the following notation. For two closed curves  $C_1$  and  $C_2$  with not necessarily simple but piecewise continuously differentiable parameterizations  $c_1 : [0, T) \rightarrow C_1$  and  $c_2 : [0, T) \rightarrow C_2$  we define

$$I(C_1, C_2) := \frac{1}{2} \int_0^T [c_1(t), \dot{c}_2(t)] dt \quad \text{and} \quad I(C_1) := I(C_1, C_1), \quad (2.17)$$

where  $[c_1, \dot{c}_2] := x_1 y_2' - y_1 x_2'$  denotes the determinant having  $c_1 = (x_1, y_1)$  and  $\dot{c}_2 = (x_2', y_2')$  as its rows.

<sup>5</sup>We denote the two lengths by  $a$  and  $b$ . Holditch used  $c$  and  $c'$  instead.

<sup>6</sup>We denote the curve of the dividing point by  $M$  to hint how we will apply Holditch's theorem. However, obviously, this curve equals the midpoint curve only if we consider halving chords and  $a = b$ .

It is not difficult to prove that the area of a simple closed curve traversed once in the interval  $[0, T]$  is given by

$$A(C) = I(C) \stackrel{\text{Def. (2.17)}}{=} \frac{1}{2} \int_0^T (x(t)y'(t) - y(t)x'(t)) dt.$$

For example, this is a corollary to Green's theorem, cf. [182]. The first proof stems from Gauss, cf. [20, p. 113].

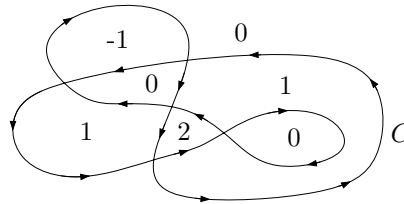


Figure 2.30: The winding numbers of an oriented closed curve  $C$ .

Also, the generalization to non-simple cycles is well-known and straight forward. To formulate it, we need the notion of winding numbers. The *winding number*  $\omega(p, C)$  of an oriented closed curve  $C$  around a point  $p \in \mathbb{R}^2 \setminus C$  counts how often the chord  $z - p$  rotates counter-clockwise if  $z$  traverses  $C$ , see Figure 2.30. A negative winding number means that  $z - p$  rotates clockwise. Clockwise and counter-clockwise rotations cancel out each other.

The definition implies the following integral formula, see for instance [38, p. 434],

$$\omega(p, C) := \frac{1}{2\pi} \int_0^T \frac{y'(t)(x(t) - p_x) - x'(t)(y(t) - p_y)}{(x(t) - p_x)^2 + (y(t) - p_y)^2} dt = \frac{1}{2\pi i} \oint_C \frac{dz}{z - p}$$

The second, simpler version results from identifying the real plane  $\mathbb{R}^2$  with the complex plane  $\mathbb{C}$  by using the map  $\pi : \mathbb{R}^2 \rightarrow \mathbb{C}$ ,  $\pi((x, y)) := x + iy$ . The equality follows easily from the fact that the right-hand side is an integer, which is shown in every textbook of complex analysis, e.g. [136, p. 114] and [5, p. 115].

With the notion of winding numbers we can easily formulate the following well-known generalization of  $I(C) = A(C)$ . It is proved for instance in [38, pp. 433f.]<sup>7</sup>.

**Lemma 2.27.** *Let  $c : [0, T] \rightarrow C$  be a piecewise continuously differentiable parameterization of a closed curve  $C$ . Then, we have*

$$I(C) = \iint_{\mathbb{R}^2 \setminus C} \omega(p, C) dp.$$

Now we are ready to state Chakerian and Goodey's generalization of Holditch's theorem. We use the notation  $C^*$  and  $M$  to hint how we will apply this theorem to the result of the halving pair transformation and the midpoint curve. However, obviously, in general the curves  $M$  and  $C^*$  appearing in this theorem are not necessarily related to those curves.

<sup>7</sup>Actually, Courant and John [38] prove only  $-\int_0^T y(t)x'(t)dt = \iint_{\mathbb{R}^2 \setminus C} \omega(p, C) dp$ , but the missing formula  $\int_0^T x(t)y'(t)dt = \iint_{\mathbb{R}^2 \setminus C} \omega(p, C) dp$  follows analogously.

**Theorem 2.28.** (cf. Chakerian and Goodey [32]) Let  $C_1$  and  $C_2$  be two closed curves in the plane given by the piecewise continuously differentiable parameterizations  $c_1 : [0, T) \rightarrow C_1$  and  $c_2 : [0, T) \rightarrow C_2$ . Let  $\lambda$  be a real value in the interval  $[0, 1]$ . Then, the functions  $m : [0, T) \rightarrow \mathbb{R}^2$ ,  $m(t) := \lambda c_1(t) + (1 - \lambda)c_2(t)$ , and  $c^* : [0, T) \rightarrow \mathbb{R}^2$ ,  $c^*(t) := \frac{1}{2}(c_1(t) - c_2(t))$ , are parameterizations of closed curves  $M$  and  $C^*$ , which satisfy

$$I(M) = \lambda I(C_1) + (1 - \lambda)I(C_2) - 4\lambda(1 - \lambda)I(C^*).$$

This is a generalization of Holditch's Theorem, Theorem 2.26, because if  $c_1$  and  $c_2$  traverse the same convex curve  $C$  in such a way that  $|c_1(t) - c_2(t)| \equiv a + b$ , then  $C^*$  is a circle with radius  $\frac{a+b}{2}$ . By choosing  $\lambda = \frac{a}{a+b}$  we derive

$$I(M) = I(C) - 4\frac{a}{a+b}\frac{b}{a+b}\pi\left(\frac{a+b}{2}\right)^2 = I(C) - \pi ab.$$

If  $C$  meets further conditions guaranteeing that the winding numbers  $\omega(z, C)$  and  $\omega(z, M)$  everywhere either equal 1 or 0<sup>8</sup>, we get Holditch's Theorem

$$A(C) - A(M) = \pi ab.$$

Now, we want to prove the generalized version, Theorem 2.28.

*Proof.* First, we prove that  $I(C_1, C_2)$  is symmetric.

$$\begin{aligned} I(C_1, C_2) &\stackrel{(2.17)}{=} \frac{1}{2} \int_0^T x_1(t)y_2'(t) - y_1(t)x_2'(t) dt & (2.18) \\ &\stackrel{\text{integr. by parts}}{=} \frac{1}{2} \left( \underbrace{[x_1(t)y_2(t)]_0^T}_0 - \int_0^T x_1'(t)y_2(t) dt \right. \\ &\quad \left. - \underbrace{[y_1(t)x_2(t)]_0^T}_0 + \int_0^T y_1'(t)x_2(t) dt \right) \\ &= \frac{1}{2} \int_0^T x_2(t)y_1'(t) - y_2(t)x_1'(t) dt \stackrel{(2.17)}{=} I(C_2, C_1) \end{aligned}$$

For the next steps we need the following lemma.

**Lemma 2.29.** Let  $C_1$  and  $C_2$  be two closed curves in the plane given by piecewise continuously differentiable parameterizations  $c_1 : [0, T) \rightarrow C_1$  and  $c_2 : [0, T) \rightarrow C_2$ . Let  $\lambda_1$  and  $\lambda_2$  be arbitrary real values. Then, the function  $c : [0, T) \rightarrow \mathbb{R}^2$ ,  $c(t) := \lambda_1 c_1(t) + \lambda_2 c_2(t)$ , is a parameterization of a closed curve  $C$ , which satisfies

$$I(C) = \lambda_1^2 I(C_1) + \lambda_2^2 I(C_2) + 2\lambda_1 \lambda_2 I(C_1, C_2).$$

---

<sup>8</sup>This means that both  $C$  and  $M$  have to be simple.

*Proof.* The proof is a straight forward application of everything we know so far.

$$\begin{aligned}
I(C) &\stackrel{\text{Def. } C,}{\stackrel{(2.17)}{=}} \frac{1}{2} \int_0^T [\lambda_1 c_1(t) + \lambda_2 c_2(t), \lambda_1 \dot{c}_1(t) + \lambda_2 \dot{c}_2(t)] dt \\
&\stackrel{\text{lin. } [\cdot, \cdot]}{=} \frac{1}{2} \lambda_1^2 \int_0^T [c_1(t), \dot{c}_1(t)] dt + \frac{1}{2} \lambda_2^2 \int_0^T [c_2(t), \dot{c}_2(t)] dt \\
&\quad + \frac{1}{2} \lambda_1 \lambda_2 \int_0^T [c_1(t), \dot{c}_2(t)] dt + \frac{1}{2} \lambda_1 \lambda_2 \int_0^T [c_2(t), \dot{c}_1(t)] dt \\
&\stackrel{(2.17),}{\stackrel{(2.18)}{=}} \lambda_1^2 I(C_1) + \lambda_2^2 I(C_2) + 2\lambda_1 \lambda_2 I(C_1, C_2)
\end{aligned}$$

□

With Lemma 2.29 we can continue to prove Theorem 2.28. We use the lemma with the values  $\lambda_1 = 1/2$  and  $\lambda_2 = -1/2$ . We get

$$I(C^*) = \frac{1}{4}I(C_1) + \frac{1}{4}I(C_2) - \frac{1}{2}I(C_1, C_2). \quad (2.19)$$

Next, we apply Lemma 2.29 with the values  $\lambda_1 = \lambda$  and  $\lambda_2 = (1 - \lambda)$ .

$$\begin{aligned}
I(M) &\stackrel{\text{Lem. } 2.29}{=} \lambda^2 I(C_1) + (1 - \lambda)^2 I(C_2) + 2\lambda(1 - \lambda)I(C_1, C_2) \\
&\stackrel{(2.19)}{=} \lambda^2 I(C_1) + (1 - \lambda)^2 I(C_2) + \lambda(1 - \lambda) \left( I(C_1) + I(C_2) - 4I(C^*) \right) \\
&= \lambda I(C_1) + (1 - \lambda)I(C_2) - 4\lambda(1 - \lambda)I(C^*).
\end{aligned}$$

This completes the proof of Theorem 2.28. □

We can apply Theorem 2.28 in a straight forward manner to the halving pair transformation by choosing  $\lambda = 1/2$ ,  $T := |C|$ ,  $c_1(t) := \bar{c}(t)$ , and  $c_2(t) := \bar{c}\left(t + \frac{|C|}{2}\right)$  for an arc-length parameterization  $\bar{c}(t)$ . We have  $I(C_1) = I(C_2) = A(C)$  and, if  $C$  is convex,  $I(C^*) = A(C^*)$ . However, so far, we do not know enough about  $I(M)$ . Goodey [78] proved that for this setting we have  $\omega(z, M) \leq 0$  everywhere. In Lemma 6 of that article he showed the statement for convex polygons, and it carries over to arbitrary convex curves by approximation arguments. We conclude that  $I(M) \leq 0$ . Goodey [78, pp. 145–149] also proves that  $I(M) = 0$  holds only for centrally symmetric cycles. This completes the proof of the following corollary, which shows another similarity between halving pair transformation and central symmetrization, cf. Lemma 2.17.6.

**Corollary 2.30.** *Let  $C \in \mathcal{C}$  be an arbitrary convex curve in the plane. Let  $C^*$  be the result of the halving pair transformation, and let  $M$  be the corresponding midpoint curve. Then, we have*

$$A(C) - A(C^*) = I(M) \leq 0.$$

*In particular, the area cannot decrease by halving pair transformation. The equality  $A(C^*) = A(C)$  is attained only by centrally symmetric cycles.*

The arguments carry over to the case where the chords  $c_1(t)c_2(t)$  are bisecting the area and not the perimeter of  $C$ . Goodey [78] has proved  $I(M) \leq 0$  also for this related situation.

Remember that by definition the midpoint curve  $M$  is traversed twice while  $C$  and  $C^*$  are traversed once in the interval  $[0, T)$ . Hence, for a simple midpoint curve, we have  $I(M) = -2A(M)$ . Zindler [186, p. 24] already proved the resulting area formula  $A(C^*) = A(C) + 2A(M)$  for the special case of midpoint curves with three cusps.

In the end of this section we want to calculate the value  $I(pq)$  for the line segment  $pq$ . This special case will be useful for applications of Holditch's theorem in Chapter 3.

**Lemma 2.31.** *Let  $p = (p_x, p_y)$  and  $q = (q_x, q_y)$  be two points in the plane. Then, we have*

$$I(pq) = \frac{1}{2}[p, q] = \frac{1}{2}(p_x q_y - q_x p_y).$$

*Proof.* We use the parameterization  $c : [0, 1] \rightarrow pq$  defined by

$$c(t) := (1 - t)p + tq.$$

The definition of  $I(C)$  in equation (2.17) and the bilinearity and anti-symmetry of the operator  $[p, q] = p_x q_y - q_x p_y$  yield

$$\begin{aligned} I(pq) &= \frac{1}{2} \int_0^1 [c(t), \dot{c}(t)] dt = \frac{1}{2} \int_0^1 [(1 - t)p + tq, q - p] dt \\ &= \frac{1}{2} \int_0^1 (1 - t)[p, q - p] + t[q, q - p] dt \\ &= \frac{1}{2} \left( [p, q - p] \int_0^1 (1 - t) dt + [q, q - p] \int_0^1 t dt \right) = \frac{1}{4} [p + q, q - p] \\ &= \frac{1}{4} \left( -\underbrace{[p, p]}_{=0} + \underbrace{[q, q]}_{=0} + [p, q] - \underbrace{[q, p]}_{=-[p, q]} \right) = \frac{1}{2} [p, q]. \end{aligned}$$

□

## 2.11 Bounds to the dilation of cycles

We have shown that the dilation of the boundary of the convex hull of any closed curve is not bigger than the original dilation (Lemma 2.10). Furthermore, for any convex closed curve we can find a centrally symmetric closed curve not having bigger dilation, by applying central symmetrization or halving pair transformation. We even obtained closed formulas telling us how much the dilation decreases by these transformations (see Remark 2.19, Lemma 2.22). We can apply this knowledge directly to get lower bounds to dilation which are more specific than the general lower bound  $\pi/2$  of Corollary 2.8.

**Theorem 2.32.** *Let  $C \in \mathcal{C}$  be a convex closed curve. Furthermore, let  $\overline{l}_C := \frac{1}{\pi} \int_0^\pi l_c(\alpha) d\alpha$  be the mean length of  $C$ . And let  $\overline{h}_C := \frac{1}{\pi} \int_0^\pi h_c(\alpha) d\alpha$  be the mean halving distance of  $C$ . As in*

Section 2.8, the result of the halving pair transformation of  $C$  is denoted by  $C^*$ . Then, the following lower bounds hold.

$$\delta(C) = \frac{|C|}{|C^*|} \frac{\frac{1}{\pi} \int_0^\pi \sqrt{h'^2(\alpha) + h^2(\alpha)} d\alpha}{h(C)} \frac{\pi}{2} \geq \frac{|C|}{|C^*|} \frac{\overline{h_C}}{h(C)} \frac{\pi}{2}, \quad (2.20)$$

$$\delta(C) = \frac{w(C)}{h(C)} \frac{\frac{1}{\pi} \int_0^\pi \sqrt{l'^2(\alpha) + l^2(\alpha)} d\alpha}{w(C)} \frac{\pi}{2} \geq \frac{w(C)}{h(C)} \frac{\overline{l_C}}{w(C)} \frac{\pi}{2}. \quad (2.21)$$

For non-convex cycles there still holds the inequality ' $\geq$ ' in (2.20).

Note that all the ratios appearing in the lower bounds of Theorem 2.32 have values in  $[1, \infty)$ . As described in Lemma 2.22, the ratio  $|C|/|C^*|$  is a measure of the symmetry of  $C$ . Its value equals 1 iff  $C$  is centrally symmetric.

The ratio  $\overline{h_C}/h(C)$  (or  $\frac{1}{\pi} \int_0^\pi \sqrt{h'^2(\alpha) + h^2(\alpha)} d\alpha/h(C)$ ) is a measure of the oscillation of the halving distance  $h_C(\cdot)$ . Its value equals 1 iff  $C$  is a cycle of constant halving distance.

As described in Remark 2.19, the ratio  $w(C)/h(C)$  equals 1 if  $C$  is centrally symmetric. However, this is not a sufficient condition.

The ratio  $\overline{l_C}/w(C)$  (or  $\frac{1}{\pi} \int_0^\pi \sqrt{l'^2(\alpha) + l^2(\alpha)} d\alpha/w(C)$ ) is a measure of the oscillation of the length values  $l_C(\cdot)$ . Its value equals 1 iff all the length-values are equal, i.e.  $C$  is a curve of constant length and breadth (remember Lemma 2.6).

By considering the integrals one can easily see that the first lower bound becomes an equality iff  $C$  is a curve of constant halving distance, and the second bound turns into an equality iff  $C$  is a curve of constant breadth.

*Proof.* First, we prove (2.21). By Remark 2.19 we know that the dilation of  $C$  satisfies  $\delta(C) = (w(C)/h(C))\delta(C')$ . Remark 2.14.1 yields a formula for the dilation of the centrally symmetric curve  $C'$ . And finally, Lemma 2.17.4 yields  $h_{C'}(\alpha) = l_C(\alpha)$ . Plugging everything together yields

$$\begin{aligned} \delta(C) &\stackrel{\text{Rem. 2.19}}{=} \frac{w(C)}{h(C)} \delta(C') \\ &\stackrel{\text{Rem. 2.14.1}}{=} \frac{w(C)}{h(C)} \frac{\frac{1}{\pi} \int_0^\pi \sqrt{h'^2_{C'}(\alpha) + h^2_{C'}(\alpha)} d\alpha}{h(C')} \frac{\pi}{2} \\ &\stackrel{\text{Lem. 2.17.4}}{=} \frac{w(C)}{h(C)} \frac{\frac{1}{\pi} \int_0^\pi \sqrt{l'^2_C(\alpha) + l^2_C(\alpha)} d\alpha}{w(C)} \frac{\pi}{2}. \end{aligned}$$

Analogously, we prove equation (2.21) by plugging together the statements from Lemma 2.22,

Remark 2.14.1 and Lemma 2.21.4:

$$\begin{aligned} \delta(C) &\stackrel{\text{Lem. 2.22}}{=} \frac{|C|}{|C^*|} \delta(C^*) \\ &\stackrel{\text{Rem. 2.14.1}}{=} \frac{|C|}{|C^*|} \frac{\frac{1}{\pi} \int_0^\pi \sqrt{h'^2_{C^*}(\alpha) + h^2_{C^*}(\alpha)} \, d\alpha}{h(C^*)} \frac{\pi}{2} \\ &\stackrel{\text{Lemma 2.21.4}}{=} \frac{|C|}{|C^*|} \frac{\frac{1}{\pi} \int_0^\pi \sqrt{h'^2_C(\alpha) + h^2_C(\alpha)} \, d\alpha}{h(C)} \frac{\pi}{2}. \end{aligned}$$

To prove the inequality for non-convex cycles, we remember that the halving distances are preserved by the halving pair transformation also in this case, see Lemma 2.21.4. Then, we can conclude

$$\delta(C) \stackrel{\text{Def.}}{\geq} \frac{|C|}{2h} = \frac{|C|}{|C^*|} \frac{|C^*|}{2h} \stackrel{\text{Rem. 2.14.1}}{\geq} \frac{|C|}{|C^*|} \frac{\frac{1}{\pi} \int_0^\pi \sqrt{h'^2(\alpha) + h^2(\alpha)} \, d\alpha}{h} \frac{\pi}{2}.$$

□

Theorem 2.32 contains tight lower dilation bounds. Still, if we want to apply these bounds to certain closed curves, we have to know something about their mean length, their mean halving distance or about the ratios  $w(C)/h(C)$ ,  $|C|/|C^*|$ . The following theorem offers an alternative which is easier to apply and which will turn out to be very useful.

**Theorem 2.33.** *Let  $C \in \mathcal{C}$  be a convex closed curve. Then the dilation of  $C$  is bounded by<sup>9</sup>*

$$\delta(C) \geq \frac{|C|}{|C^*|} \left( \arcsin\left(\frac{h}{H}\right) + \sqrt{\left(\frac{H}{h}\right)^2 - 1} \right) \quad (2.22)$$

$$\text{and} \quad \delta(C) \geq \frac{w}{h} \left( \arcsin\left(\frac{w}{D}\right) + \sqrt{\left(\frac{D}{w}\right)^2 - 1} \right). \quad (2.23)$$

*Equality in the first bound is attained only by curves whose halving pair transformation results in a cap-curve. Equality in the second bound is attained only by curves whose central symmetrization results in a cap-curve. Such a cap-curve  $\hat{C}$  is the boundary of the convex hull of a disk with radius  $w/2$  and a segment of length  $D$ , see Figure 2.31.a.*

*The first bound (2.22) holds also for non-convex cycles.*

Note once again that the ratios  $|C|/|C^*|$  and  $w/h$  can attain values in  $[1, \infty)$  depending on the symmetry of  $C$ , see Remark 2.19 and Lemma 2.22. Hence, by simply removing these fractions we receive lower bounds depending only on the ratios  $w/D$  or  $h/H$  respectively. The function  $f : [1, \infty) \rightarrow [\pi/2, \infty)$ ,  $f(x) := \arcsin(1/x) + \sqrt{x^2 - 1}$ , appearing on the right-hand side is plotted in Figure 2.31.b. It is continuous, bijective and strictly increasing. In particular it attains the minimum value  $\pi/2$  only at  $x = 1$ .

<sup>9</sup>It should be understood that  $h$  is an abbreviation of  $h(C)$  and so forth.



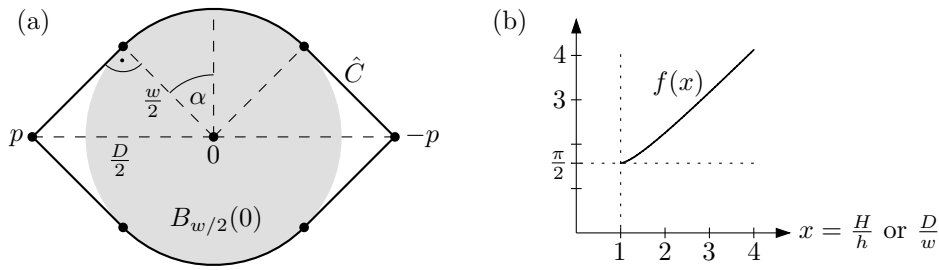


Figure 2.31: (a) The cap-curve  $\hat{C}$  is the shortest curve enclosing  $B_{\frac{w}{2}}(0)$  and connecting  $p$  and  $-p$ . (b) A plot of the lower bound  $f(x)$  depending on  $x = H/h$  or  $D/w$ .

Originally we had proved these lower bounds directly, see [57, 59]. Then, we learned about a related result by Kubota [133] from 1923, which enables us to present a reformulation of our proof as an application of his ideas. To this end, we first present Kubota’s result with a short proof. A generalized form of this lemma was recently used by Denne, Diao and Sullivan [44] to prove lower bounds to the rope length of certain knots, cf. Section 1.3.

**Lemma 2.34.** (Kubota [133]) *Let  $C \in \mathcal{C}$  be an arbitrary convex closed curve. Then, we have*

$$|C| \geq 2w \arcsin\left(\frac{w}{D}\right) + 2\sqrt{D^2 - w^2}.$$

*Equality is attained only by curves whose central symmetrization is a cap-curve  $\hat{C}$  like shown in Figure 2.31.a.*

*Proof.* Central symmetrization does not alter  $w$ ,  $D$ , nor  $|C|$ , see Lemma 2.17. Hence, for proving the inequality we can assume that the curve  $C$  is centrally symmetric about the origin 0. For such curves we know  $w(C) = 2r(C) = 2 \min_{p \in C} |p|$  and  $D(C) = 2R(C) = 2 \max_{p \in C} |p|$  by (2.6) and Lemma 2.13.1.

Hence, there exist points  $p$  and  $-p$  on  $C$  satisfying  $2|p| = D$ . On the other hand, the curve  $C$  cannot enter the open disk with radius  $w/2$  centered at 0,  $B_{w/2}(0) := \{q \in \mathbb{R}^2 \mid |q| < w/2\}$ , because that would contradict  $w = 2 \min_{q \in C} |q|$ . Hence, the convex closed curve  $C$  must encircle the convex hull of  $B_{w/2}(0) \cup -pp$ . Clearly, the unique shortest convex cycle doing so, is the corresponding cap-curve  $\hat{C}$  shown in Figure 2.31.a.

It is the concatenation of four line segments, each of length  $\sqrt{(D/2)^2 - (w/2)^2} = \frac{1}{2}\sqrt{D^2 - w^2}$ , and of four circular arcs, each of length  $(w/2)\alpha$ , where  $\sin \alpha = \cos(\pi/2 - \alpha) = (w/2)/(D/2) = w/D$ . This completes the proof of the lemma.  $\square$

Now we can prove the lower bounds in the theorem.

*Proof.* (Theorem 2.33) First, we prove inequality (2.23). The proof is an application of central

symmetrization and Kubota's inequality.

$$\begin{aligned}
\delta(C) &\stackrel{\text{Rem. 2.19}}{=} \frac{w(C)}{h(C)} \delta(C') \stackrel{\text{Thm. 2.12}}{=} \frac{w(C)}{h(C)} \frac{|C'|}{2h(C')} \\
&\stackrel{\text{Lem. 2.34}}{\geq} \frac{w(C)}{h(C)} \frac{2w(C') \arcsin\left(\frac{w(C')}{D(C')}\right) + 2\sqrt{D^2(C') - w^2(C')}}{2h(C')} \\
&\stackrel{\text{Lem. 2.17.4, Lem. 2.17.5}}{=} \frac{w(C)}{h(C)} \arcsin\left(\frac{w(C)}{D(C)}\right) + \sqrt{\left(\frac{D(C)}{w(C)}\right)^2 - 1}
\end{aligned}$$

The proof of (2.22) for convex cycles analogously uses halving pair transformation and Kubota's inequality.

$$\begin{aligned}
\delta(C) &\stackrel{\text{Lem. 2.22}}{=} \frac{|C|}{|C^*|} \delta(C^*) \stackrel{\text{Thm. 2.12}}{=} \frac{|C|}{|C^*|} \frac{|C^*|}{2h(C^*)} \\
&\stackrel{\text{Lem. 2.34}}{\geq} \frac{|C|}{|C^*|} \frac{2w(C^*) \arcsin\left(\frac{w(C^*)}{D(C^*)}\right) + 2\sqrt{D^2(C^*) - w^2(C^*)}}{2h(C^*)} \\
&\stackrel{\text{Lem. 2.21.4}}{=} \frac{|C|}{|C^*|} \left( \arcsin\left(\frac{h(C)}{H(C)}\right) + \sqrt{\left(\frac{H(C)}{h(C)}\right)^2 - 1} \right)
\end{aligned}$$

The statements about the extremal sets, the sets attaining equality, follow immediately from the corresponding statement for Kubota's inequality.

We still have to generalize (2.22) to the case of non-convex cycles. However, we can use the same ideas. The halving pair transformation results in a centrally symmetric (not necessarily simple nor convex) curve  $C^*$  which does not enter the open disk  $B_{\frac{h}{2}}(0)$  but has to connect a pair of points  $p$  and  $-p$  of distance  $| -pp | = H$  twice. By Kubota's arguments, cf. the proof of Lemma 2.34, we have

$$|C^*| \geq 2h \arcsin\left(\frac{h}{H}\right) + 2\sqrt{H^2 - h^2}. \quad (2.24)$$

We can conclude

$$\delta(C) \stackrel{\text{Def.}}{\geq} \frac{|C|}{2h} = \frac{|C|}{|C^*|} \frac{|C^*|}{2h} \stackrel{(2.24)}{\geq} \frac{|C|}{|C^*|} \left( \arcsin\left(\frac{h}{H}\right) + \sqrt{\left(\frac{H}{h}\right)^2 - 1} \right).$$

□

Theorem 2.32 or Theorem 2.33 immediately imply that circles are the only closed curves attaining dilation  $\pi/2$ , a fact which was also proved by Gromov [86, 88], Abrams et al. [1, Corollary 3.3] and Kusner and Sullivan [135].

**Corollary 2.35.** *A closed curve  $C \in \mathcal{C}$  has dilation  $\delta(C) = \frac{\pi}{2}$  if and only if it is a circle.*

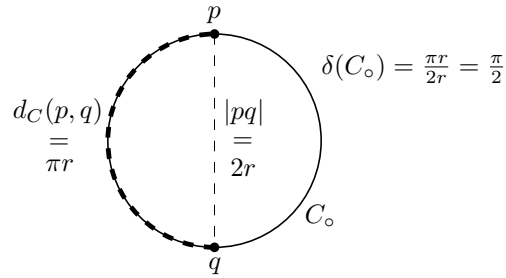


Figure 2.32: The dilation of a circle  $C_\circ$  equals  $\delta(C_\circ) = \pi/2$ .

*Proof.* We can easily calculate the dilation of a circle  $C_\circ$  with radius  $r$ , cf. Figure 2.32.

$$\delta(C_\circ) \stackrel{\text{Thm. 2.12}}{=} \frac{|C_\circ|}{2h(C_\circ)} \stackrel{(2.6)}{=} \frac{|C_\circ|}{4r} = \frac{2\pi r}{4r} = \frac{\pi}{2}$$

Now, let  $C$  be an arbitrary closed curve of dilation  $\delta(C) = \pi/2$ . Then, the inequality (2.20) or (2.22) implies  $|C| = |C^*|$ ,  $C$  has to be centrally symmetric. By the same inequalities,  $C$  has to be a closed curve of constant halving pair distance, i.e.  $h(C) = H(C)$ . Equation (2.6) from Section 2.6 shows that due to the central symmetry of  $C$  this implies that the inradius  $r(C)$  equals the circumradius  $R(C)$ ,  $C$  is a circle.  $\square$

In the end of this section we want to give an upper bound to the dilation of convex closed curves which complements the lower bound (2.23) from Theorem 2.33. Remember that the lower bound still holds if we remove the factor  $w/h$ , because  $w/h \geq 1$ . The resulting lower bound

$$\delta(C) \geq \arcsin\left(\frac{w}{D}\right) + \sqrt{\left(\frac{D}{w}\right)^2 - 1} \quad (2.25)$$

depends only on  $D/w$ . Similarly, the upper bound we present next, can be stated as a version depending only on  $D/w$  and as a version with an additional factor  $w/2h$ . Unfortunately, the first, simpler version is not tight.

To simplify notation, we give a short name to the appearing extremal sets. A *flattened circle* is the boundary of the intersection of a disk with radius  $D$  and a strip between two lines of distance  $w$  which are symmetric to each other with respect to the disk's center, see Figure 2.33.b.

**Lemma 2.36.** *If  $C \in \mathcal{C}$  is a convex closed curve, then*

$$\delta(C) \leq \frac{w}{h} \left( \frac{D}{w} \arcsin \frac{w}{D} + \sqrt{\left(\frac{D}{w}\right)^2 - 1} \right) \quad (2.26)$$

$$\text{and } \delta(C) < 2 \left( \frac{D}{w} \arcsin \frac{w}{D} + \sqrt{\left(\frac{D}{w}\right)^2 - 1} \right). \quad (2.27)$$

*The first inequality (2.26) becomes an equality only for curves whose central symmetrization is a flattened circle like defined above and like displayed in Figure 2.33.b.*

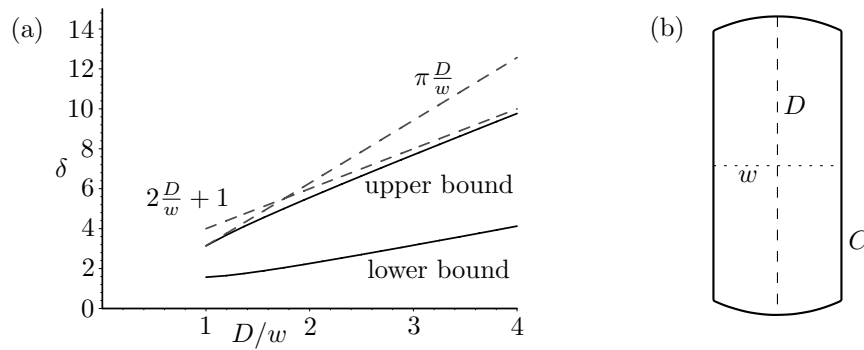


Figure 2.33: (a) A plot of the upper bound (2.27) and the lower bound (2.25). (b) A flattened disk, the extremal set of Kubota's inequality (2.28).

The second lower bound is plotted in Figure 2.33.a.

*Proof.* Kubota [133] (see also [172]) showed that perimeter  $|C|$ , diameter  $D$  and width  $w$  of a convex closed curve  $C$  satisfy

$$|C| \leq 2D \arcsin \frac{w}{D} + 2\sqrt{D^2 - w^2}. \quad (2.28)$$

The proof is similar to the one of Lemma 2.34 which stems from the same article. Central symmetrization does not alter  $|C|$ ,  $D$  nor  $w$ . And if  $C$  is centrally symmetric about the origin  $0$ , it has to be contained in the closed disk  $\overline{B_D(0)}$  with radius  $R = D$  and between two parallel lines of distance  $w$  which are centrally-symmetric with respect to  $0$ , cf. Figure 2.33.b.

The unique longest convex cycle satisfying these conditions is the corresponding flattened circle. One gets its perimeter by straight-forward application of trigonometric arguments.

Combining this with Theorem 2.12 yields

$$\delta(C) \stackrel{\text{Thm. 2.12}}{=} \frac{|C|}{2h} = \frac{w}{h} \frac{|C|}{2w} \stackrel{(2.28)}{\leq} \frac{w}{h} \left( \frac{D}{w} \arcsin \frac{w}{D} + \sqrt{\left(\frac{D}{w}\right)^2 - 1} \right).$$

And equality is only attained if there is equality in Kubota's inequality, which holds only if  $C'$  is the corresponding flattened disk.

Next, we have to refer to an inequality we prove in a later section. The inequality  $w < 2h$  from Corollary 4.13 is shown in Chapter 4, because we wanted to collect all the results relating halving distance to other quantities in one chapter. The inequality  $w < 2h$  proves the second, weaker version (2.27) of the upper bound.  $\square$

If we do not plug Kubota's inequality (2.28) but the well-known inequality  $|C| \leq D\pi$  from Corollary 2.9 or the inequality  $|C| \leq 2D + 2w$  into the dilation formula from Theorem 2.12 we get the slightly bigger but simpler dilation bounds  $\delta(C) \leq 2\left(\frac{D}{w} + 1\right)$  and  $\delta(C) \leq \pi\frac{D}{w}$ . They are also plotted in Figure 2.33.a. The inequality  $|C| \leq 2D + 2w$  follows from the fact that  $C$  has to be contained in the intersection of two strips of width  $w$  and  $D$  respectively. The longest convex cycle inside this strip is obviously the border of the parallelogram resulting from the intersection.

## 2.12 Stability result

The statement from Corollary 2.35, that only circles attain the dilation minimum of  $\pi/2$ , can be used to show that the dilation of graphs embedding certain finite point sets must be strictly bigger than  $\pi/2$ , because it has to contain faces which are not circular. However, this does not lead directly to a lower bound to the dilation of finite point sets, which is bigger than  $\pi/2$ , because, still, there could be graphs embedding such point sets whose dilation gets arbitrarily close to  $\pi/2$ .

This is why we need Lemma 2.39 presented in this section. It says that closed curves whose dilation is close to  $\pi/2$  are close to being circles. We say that curves are close to being a circle, if they are contained in a thin annulus. To this end we define an  $\eta$ -annulus as a closed region between two concentric circles where the outer radius equals  $\eta$  times the inner radius. Note that by the lower bound inequality (2.22) from Theorem 2.33 we already know that for a cycle  $C$  with dilation close to  $\pi/2$  the ratio  $H/h$  is close to 1; hence, the result of the halving pair transformation  $C^*$  is close to a circle (cf. Figure 2.28 on page 56), because by Lemma 2.21.4 and equation (2.6) in Section 2.6 it lies in an  $H/h$ -annulus.

As mentioned in the introduction, Lemma 2.39 can be regarded as a *stability result* for the inequality  $\delta(C) \geq \pi/2$ , Corollary 2.8; cf. Groemer's survey [84].

Let us now assume that we have a closed curve  $C$  whose dilation is close to  $\pi/2$ . As shown above,  $C^*$  has to be contained in a thin annulus. In order to extend this statement to the original cycle  $C$ , we need an upper bound on the length  $|M|$  of the midpoint curve. We achieve it by using Lemma 2.25.

**Lemma 2.37.** *If  $\delta(C) \leq (1 + \varepsilon)\pi/2$ , then  $|M| \leq (\pi h/2)\sqrt{2\varepsilon + \varepsilon^2}$ .*

*Proof.* By the assumption and because the dilation of  $C$  is at least the detour of a halving pair attaining minimum distance  $h$ , we have  $(1 + \varepsilon)\pi/2 \geq \delta(C) \geq |C|/2h$ , implying

$$|C| \leq (1 + \varepsilon)\pi h. \quad (2.29)$$

As used before,  $C^*$  encircles but does not enter the open disk  $B_{h/2}(0)$  with radius  $h/2$  centered at the origin 0. It follows

$$|C^*| \geq \pi h. \quad (2.30)$$

By plugging everything together, we get

$$|M| \stackrel{\text{Lem. 2.25}}{\leq} \frac{1}{2} \sqrt{|C|^2 - |C^*|^2} \stackrel{(2.29), (2.30)}{\leq} \frac{1}{2} \pi h \sqrt{(1 + \varepsilon)^2 - 1} = \frac{\pi h}{2} \sqrt{2\varepsilon + \varepsilon^2},$$

which concludes the proof of Lemma 2.37. □

Intuitively it is clear, cf. Figure 2.28 on page 56, that this bound on  $M$  and the upper bound on  $H/h$  from (2.22) in Theorem 2.33 imply that the curve  $C$  is contained in a thin annulus. This is the idea behind Lemma 2.39, the main result of this section. To prove it, we will apply the following well-known fact, see for instance [172], to  $M$ .

**Lemma 2.38.** *Every closed curve  $C$  can be enclosed in a circle with radius  $|C|/4$ .*

*Proof.* Although this fact is well-known, we want to give a short proof here which applies our notion of halving pairs.

Fix a halving pair  $(p, \hat{p})$  of  $C$ . Then by definition, for any  $q \in C$ , we have  $|pq| + |q\hat{p}| \leq d_C(p, q) + d_C(q, \hat{p}) = d_C(p, \hat{p}) = |C|/2$ . It follows that  $C$  is contained in an ellipse with foci  $p$  and  $\hat{p}$  and major axis  $|C|/2$ . This ellipse is enclosed in a circle with radius  $|C|/4$ , and the lemma follows.  $\square$

Finally, we are able to prove the main result of this section. The lemma can be extended to a larger, more practical range of  $\varepsilon$ , by increasing the coefficient of  $\sqrt{\varepsilon}$ .

**Lemma 2.39.** *Let  $C \in \mathcal{C}$  be a simple closed curve with dilation  $\delta(C) \leq (1 + \varepsilon)\pi/2$  for  $\varepsilon \leq 0.0001$ . Then  $C$  is contained in a  $(1 + 3\sqrt{\varepsilon})$ -annulus. This bound cannot be improved apart from the coefficient of  $\sqrt{\varepsilon}$ .*

*Proof.* By Lemma 2.38, the midpoint curve  $M$  can be enclosed in a circle with radius  $|M|/4$  and some center  $z$ . By the triangle inequality, we immediately obtain

$$\begin{aligned} |c(t) - z| &\stackrel{(2.14)}{=} |m(t) + c^*(t) - z| \leq |c^*(t)| + |m(t) - z| \leq \frac{H}{2} + \frac{|M|}{4}, \\ |c(t) - z| &\stackrel{(2.14)}{=} |m(t) + c^*(t) - z| \geq |c^*(t)| - |m(t) - z| \geq \frac{h}{2} - \frac{|M|}{4}. \end{aligned}$$

Thus,  $C$  can be enclosed in the annulus between two concentric circles with radii  $R = H/2 + |M|/4$  and  $r = h/2 - |M|/4$ . To finish the proof, we have to bound the ratio  $R/r$ .

The main assumption of the lemma is  $\delta(C) \leq (1 + \varepsilon)\pi/2$  for  $\varepsilon \leq 0.0001$ . We want to bound  $H/h$  and  $|M|$  in terms of  $\varepsilon$ . Assume  $H/h = (1 + \beta)$ . Inequality (2.22) in Theorem 2.33 yields the lower bound

$$\delta(C) \geq \arcsin \frac{1}{1 + \beta} + \sqrt{(1 + \beta)^2 - 1} = \arcsin \frac{1}{1 + \beta} + \sqrt{2\beta + \beta^2}.$$

We have  $\beta \leq 0.01$ , otherwise we had  $\delta(C) > 1.0001\pi/2$ , which contradicts the assumption of the lemma.

It is well known that for  $x \in [0, \pi/2]$ ,

$$\cos x \leq 1 - \frac{x^2}{2} + \frac{x^4}{24}.$$

By setting  $x = \sqrt{2\beta}$ , we obtain the following inequality, for the given  $\beta$ -range:

$$\sin\left(\frac{\pi}{2} - \sqrt{2\beta}\right) = \cos \sqrt{2\beta} \leq 1 - \beta + \frac{\beta^2}{6} \stackrel{\beta \leq 0.01 \leq 5}{\leq} 1 - \frac{\beta}{\beta + 1} = \frac{1}{\beta + 1}.$$

Thus

$$\arcsin \frac{1}{1 + \beta} \geq \frac{\pi}{2} - \sqrt{2\beta},$$

and therefore

$$\begin{aligned} \delta(C) &\geq \frac{\pi}{2} - \sqrt{2\beta} + \sqrt{2\beta + \beta^2} = \frac{\pi}{2} + \frac{\beta^2}{\sqrt{2\beta} + \sqrt{2\beta + \beta^2}} \\ &\stackrel{\beta \leq 0.01}{\geq} \frac{\pi}{2} + \frac{\beta^2}{(\sqrt{2} + \sqrt{2.01})\sqrt{\beta}} \geq \frac{\pi}{2} + \frac{\beta^{3/2}}{3}. \end{aligned}$$

With our initial assumption, we get

$$\frac{\pi}{2} + \frac{\beta^{3/2}}{3} \leq \delta(C) \leq \frac{\pi}{2}(1 + \varepsilon),$$

which yields

$$\beta \leq \left(\frac{3\pi}{2}\right)^{2/3} \varepsilon^{2/3} \stackrel{\varepsilon \leq 10^{-4}}{\leq} 2.9\varepsilon^{2/3} \stackrel{\varepsilon \leq 10^{-4}}{\leq} 0.7\varepsilon^{1/2}. \tag{2.31}$$

This bounds  $H/h$  in terms of  $\varepsilon$ . In order to find such a bound to  $|M|$ , we consider Lemma 2.37 which results in

$$|M| \stackrel{\text{Lemma 2.37}}{\leq} \frac{\pi h}{2} \sqrt{2\varepsilon + \varepsilon^2} \stackrel{\varepsilon \leq 10^{-4}}{\leq} 2.24 h\sqrt{\varepsilon}. \tag{2.32}$$

Remember that we want to bound the ratio  $R/r$  between the two concentric circles bounding  $C$ . This can be done by

$$\begin{aligned} \frac{R}{r} &= \frac{H/2 + |M|/4}{h/2 - |M|/4} = \frac{h(1 + \beta) + |M|/2}{h - |M|/2} \\ (2.32) \quad &\leq \frac{1 + \beta + 1.12\sqrt{\varepsilon}}{1 - 1.12\sqrt{\varepsilon}} \stackrel{(2.31)}{\leq} \frac{1 + 1.82\sqrt{\varepsilon}}{1 - 1.12\sqrt{\varepsilon}} \stackrel{\varepsilon \leq 10^{-4}}{\leq} 1 + 3\sqrt{\varepsilon}. \end{aligned}$$

In [50, 49] we proved the tightness of this result with a curve which is the trace of a kind of moon which moves around earth while earth itself is moving around the sun. Within this thesis we use a different curve for the same purpose, the so called flower  $C_F$ . In Remark 3.13 of Chapter 3 we prove that Lemma 2.39 does not hold if the coefficient in front of  $\sqrt{\varepsilon}$  drops below  $2\sqrt{2}/3 \approx 0.94$ .  $\square$

Lemma 2.39 naturally raises the question whether one can prove a reverse statement, saying that any cycle  $C$  contained in a thin annulus has small dilation. Clearly, we cannot expect this statement for arbitrary closed curves, because  $C$  can contain acute corners which lead to a big dilation value, see Lemma 2.1.2 and Figure 2.34.a. However, if we require convexity,

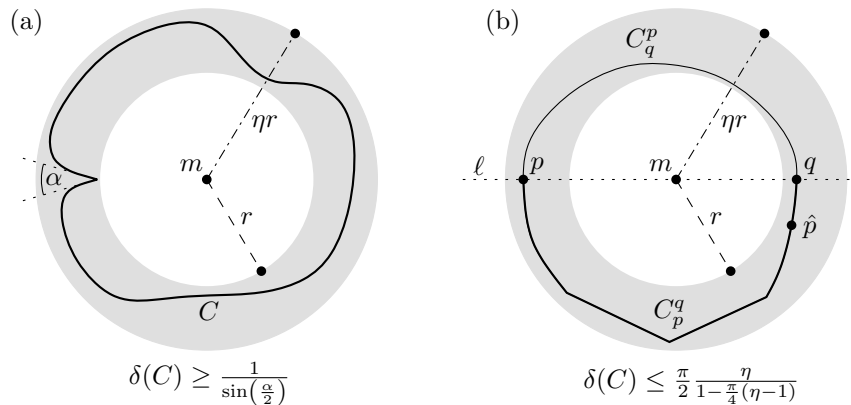


Figure 2.34: (a) The dilation of a cycle  $C$  contained in an  $\eta$ -annulus can be arbitrarily big. (b) If  $C$  is convex, the dilation is bounded.

indeed, we can prove such a result.

**Lemma 2.40.** *Let  $C \subset \mathcal{C}$  be a convex closed curve which is contained in an  $\eta$ -annulus. Then, its dilation is bounded by*

$$\delta(C) \leq \frac{\pi}{2} \frac{\eta}{1 - \frac{\pi}{4}(\eta - 1)}.$$

*Proof.* Consider Figure 2.34.b. Let  $r$  denote the inner radius of the  $\eta$ -annulus, and let  $m$  denote its center. Clearly, the perimeter of the given cycle satisfies

$$2\pi r \leq |C| \leq 2\pi\eta r. \quad (2.33)$$

We would like to apply the dilation formula  $\delta(C) = |C|/2h$  from Theorem 2.12. To this end, we need a lower bound to  $h(C)$ .

Let  $p$  be an arbitrary point on  $C$ . Let  $q$  be the other intersection point of  $C$  with the line  $\ell$  through  $p$  and  $m$ . And let  $C_p^q$  and  $C_q^p$  be the two paths on  $C$  between  $p$  and  $q$ . We may assume  $|C_p^q| \geq |C_q^p|$ . Then, the convexity of  $C$  implies

$$\pi r \leq |C_p^q| \leq |C_q^p| \leq \pi\eta r. \quad (2.34)$$

From  $q$  we have to move a distance  $(|C_p^q| - |C_q^p|)/2$  on  $C$  to reach the halving partner  $\hat{p}$  of  $p$ . Because of  $|pq| \geq 2r$  this results in

$$\begin{aligned} |p\hat{p}| &\stackrel{\Delta\text{-inequ.}}{\geq} |pq| - |q\hat{p}| \geq |pq| - \frac{|C_p^q| - |C_q^p|}{2} \\ &\stackrel{(2.34)}{\geq} 2r - \frac{\pi\eta r - \pi r}{2} = 2r \left(1 - \frac{\pi}{4}(\eta - 1)\right). \end{aligned} \quad (2.35)$$

We have proved this bound for any  $p \in C$ . Hence, it is a lower bound for  $h(C)$ , too. By plugging everything together, we get

$$\delta(C) \stackrel{\text{Thm. 2.12}}{=} \frac{|C|}{2h(C)} \stackrel{(2.33), (2.35)}{\leq} \frac{2\pi\eta r}{4r \left(1 - \frac{\pi}{4}(\eta - 1)\right)} = \frac{\pi}{2} \frac{\eta}{1 - \frac{\pi}{4}(\eta - 1)}.$$

This concludes the proof of the lemma.  $\square$

The upper bound function is plotted in Figure 2.35.

Note that if we define an *annulus constant* by

$$\eta(C) := \inf\{\eta \mid C \text{ contained in an } \eta\text{-annulus}\}, \quad (2.36)$$

the result from Lemma 2.40 above can also be regarded as a lower bound to  $\eta(C)$  depending on  $\delta(C)$  for every convex curve  $C$ , while the original stability result from Lemma 2.39 gives a corresponding upper bound to  $\eta(C)$  for every (not necessarily convex) curve.

## 2.13 Polygons

Before we apply the stability result to derive a lower bound to the dilation of finite point sets, we end this chapter by considering special closed curves, namely polygons.



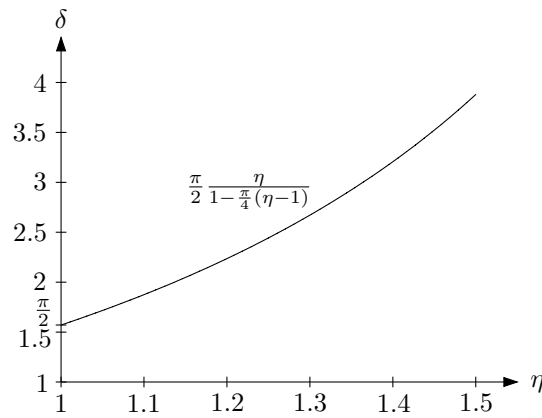


Figure 2.35: The upper bound to  $\delta(C)$  depending on the  $\eta$ -factor of an annulus, which encloses  $C$ .

### 2.13.1 Triangles

As a first step we want to consider the simplest possible polygons, triangles. Triangles are good examples because there are simple formulas for their dilation, minimum halving distance  $h$  and maximum halving distance  $H$ , and they are extremal sets of many inequalities we will analyze in Chapter 4. We need the following lemma.

**Lemma 2.41.** *Let  $r_1$  and  $r_2$  be two rays emanating from the same point  $z$  and enclosing an angle  $\alpha \in (0, \pi)$ . For a given value  $t \in (0, \infty)$  consider the pairs of points  $(p, q) \in r_1 \times r_2$  such that  $|pz| + |zq| = t$ .*

*The distance of such a pair of points depends only on  $||pz| - |qz||$  and is strictly monotonously increasing with respect to this value. In particular, the minimum distance of such a pair of points is attained by the points satisfying  $|pz| = |qz| = t/2$  and equals  $t \sin \frac{\alpha}{2}$ .*

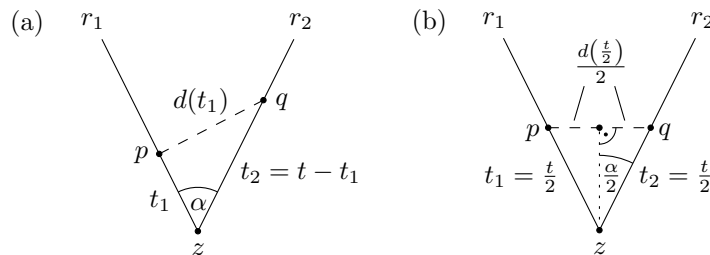


Figure 2.36: The distance  $d(t_1) := |pq|$  of points on two rays emanating from the same point  $z$ , where  $|pz| + |qz| = t_1 + t_2 \equiv t$ .

*Proof.* Consider Figure 2.36.a. We define  $t_1 := |pz|$  and  $t_2 := |qz|$ . The law of cosine yields

$$\begin{aligned} d^2(t_1) &:= |pq|^2 = t_1^2 + t_2^2 - 2 \cos(\alpha) t_1 t_2 \\ &= t_1^2 + (t - t_1)^2 - 2 \cos(\alpha) t_1 (t - t_1) \\ &= t_1^2 + t^2 - 2 t t_1 + t_1^2 + 2 \cos(\alpha) t_1 (t_1 - t) \\ &= 2 t_1 (t_1 - t) (1 + \cos \alpha) + t^2 \end{aligned}$$

We consider the derivative of  $d^2(t_1)$ :

$$\begin{aligned} \frac{d(d^2(t_1))}{dt_1} &= 2(t_1 - t)(1 + \cos \alpha) + 2t_1(1 + \cos \alpha) \\ &= 2(2t_1 - t)(1 + \cos \alpha) \end{aligned}$$

This shows that  $d^2(t_1)$  is strictly decreasing for  $t_1 \in [0, t/2)$ , attains a minimum at  $t_1 = t/2$ , and is strictly increasing for  $t_1 \in (t/2, t]$ . The value of the minimum equals

$$\begin{aligned} d\left(\frac{t}{2}\right) &= \sqrt{\left(\frac{t}{2}\right)^2 + \left(\frac{t}{2}\right)^2 - 2 \cos(\alpha) \frac{t}{2} \frac{t}{2}} \\ &= \sqrt{2 \left(\frac{t}{2}\right)^2 - 2 \cos(\alpha) \left(\frac{t}{2}\right)^2} \\ &= \frac{t}{\sqrt{2}} \sqrt{1 - \cos(\alpha)} \\ &\stackrel{\text{add. theorem}}{=} t \sin\left(\frac{\alpha}{2}\right) \end{aligned}$$

The last equation follows for instance from the addition theorem by

$$\cos \alpha = \cos\left(\frac{\alpha}{2} + \frac{\alpha}{2}\right) \stackrel{\text{add. theorem}}{=} \cos^2 \frac{\alpha}{2} - \sin^2 \frac{\alpha}{2} = 1 - 2 \sin^2 \frac{\alpha}{2}$$

which implies  $\sin(\alpha/2) = \sqrt{1 - \cos \alpha} / \sqrt{2}$ . A second option would be to apply basic trigonometry to the two right-angled triangles shown in Figure 2.36.b. The rest of the lemma follows immediately.  $\square$

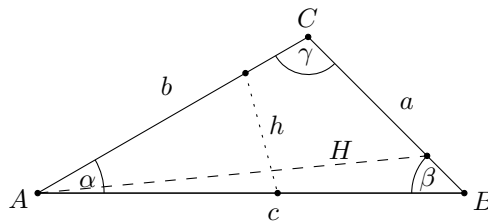


Figure 2.37: Minimum and maximum halving distance  $h$  and  $H$  of a triangle.

**Lemma 2.42.** *Given a triangle  $\Delta = \Delta(A, B, C)$  of side lengths  $a = |BC|$ ,  $b = |AC|$ ,  $c = |AB|$  and interior angles  $\alpha$ ,  $\beta$  and  $\gamma$  (in  $A$ ,  $B$  and  $C$  resp.) as shown in Figure 2.37. Let  $|\Delta| := a + b + c$  denote its perimeter. Then, the following three statements hold.*

1. The maximum halving distance  $H(\Delta)$  is attained by the halving chords through vertices with minimum interior angle.
2. The minimum halving distance  $h(\Delta)$  is attained by halving pairs  $(p, \hat{p})$  where both points have distance  $|pv| = |\hat{p}v| = |\Delta|/4$  to a vertex  $v \in \{A, B, C\}$  of minimum interior angle. This implies

$$h(\Delta) = \frac{|\Delta|}{2} \sin \frac{\min\{\alpha, \beta, \gamma\}}{2} \quad (2.37)$$

3. The dilation of  $\Delta$  is given by

$$\delta(\Delta) = \frac{1}{\sin \frac{\min\{\alpha, \beta, \gamma\}}{2}} \quad (2.38)$$

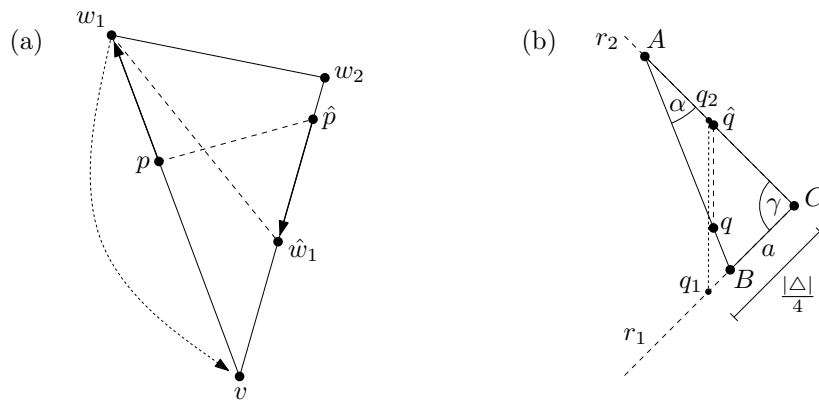


Figure 2.38: (a) The distance  $|w_1\tilde{w}_1|$  is not smaller than  $|p\hat{p}|$ . (b) If  $a \leq |\Delta|/4$ , there exists a halving pair of minimum distance on  $AB \times AC$ .

*Proof.* 1. Consider Figure 2.38.a. Let  $p\hat{p}$  be an arbitrary halving chord. Let  $v \in \{A, B, C\}$  be a vertex such that  $p$  is located on one edge  $e_p = vw_1$  adjacent to  $v$  and  $\hat{p}$  is located on the other edge  $e_{\hat{p}} = vw_2$  adjacent to  $v$ . We assume that  $|e_p| = |vw_1| \geq |vw_2| = |e_{\hat{p}}|$ . Then by Lemma 2.41 and using  $t := |\Delta|/2$  we get that the halving chord  $w_1\hat{w}_1$  is not shorter than  $p\hat{p}$ , where  $\hat{w}_1$  is the halving partner of  $w_1$ , which is clearly located on the edge  $e_{\hat{p}} = vw_2$ .

If  $vw_2$  is not an edge of minimum length, we can repeat the argument with the vertex  $w_2$  instead of  $v$  and  $w\tilde{w}_1$  instead of  $p\hat{p}$ . In this case we get  $|v\tilde{v}| \geq |w_1\tilde{w}_1| \geq |p\hat{p}|$ .

This shows that a halving chord through a vertex opposite of a shortest edge has maximum length. This vertex lies opposite of a shortest edge. Therefore, by the law of sines it is a vertex of minimum angle.

2. We assume that  $a \leq b \leq c$ . First we consider the special case that  $a < |\Delta|/4$ , see Figure 2.38.b. We assume there was a halving pair  $(p, \tilde{p})$  of minimum distance such that  $p \in BC$  and  $\tilde{p} \in AC$ . If we consider the ray  $r_1$  emanating from  $C$  along  $a$  and the ray  $r_2$  from  $C$  along  $b$ , by Lemma 2.41 there is a pair of points  $(q_1, q_2) \in r_1 \times r_2$  such that  $|q_1C| = |q_2C| = |\Delta|/4$  and  $|p\tilde{p}| \geq |q_1q_2| = 2(|\Delta|/4) \sin(\gamma/2)$ . As  $a < |\Delta|/4$  we therefore find a

halving pair  $(q, \hat{q}) \in AB \times AC$  parallel to  $q_1q_2$  such that  $|q\hat{q}| < |q_1q_2| = |\Delta| \sin(\gamma/2)/2 \leq |p\hat{p}|$ . By symmetry we can use the same arguments if  $p \in BC$  and  $\hat{p} \in AB$ . Hence, there is always a halving pair of minimum distance on  $AB \times AC$ . This combined with Lemma 2.41 proves the lemma for this case, because by the law of sines and our assumptions we have  $\min\{\alpha, \beta, \gamma\} = \alpha$ .

Now, let  $a \geq |\Delta|/4$ . This is the simpler case, because for every vertex  $v \in \{A, B, C\}$  there exists a halving pair  $(p, \hat{p})$  on its adjacent edges, such that  $|pv| = |\hat{p}v| = |\Delta|/4$ . Lemma 2.41 yields  $h = |\Delta| \sin(\min\{\alpha, \beta, \gamma\}/2)/2$  and the proof is completed.

3. This follows immediately from 2. and Theorem 2.12.  $\square$

**Corollary 2.43.** *The dilation of every triangle  $\Delta$  in the plane is bounded by*

$$\delta(\Delta) \geq 2.$$

*Equality is attained only by equilateral triangles. On the other hand, there is no upper bound; the dilation  $\delta(\Delta)$  can become arbitrarily big.*

*Proof.* This follows immediately from Lemma 2.42.3 and the fact that the minimum interior angle is less or equal  $60^\circ$ , because the sum of the three interior angles equals  $180^\circ$ . If the minimum interior angle equals  $60^\circ$ , we clearly have an equilateral triangle.

The minimum interior angle can be arbitrarily small; hence, the dilation can be arbitrarily big.  $\square$

### 2.13.2 Regular polygons

Within this thesis we want to restrict the analysis of polygons with arbitrarily many vertices to the case of regular polygons. Our article [48, 49] contains a proof that amongst polygons with an even number of vertices the regular ones attain smallest possible dilation. This shows the importance of regular polygons.

Analyzing their dilation will exemplify the intuition behind the stability result, Lemma 2.39; the closer a cycle is to being a circle the lower is its dilation value.

Additionally, the example of the regular polygons will show an interesting counter-intuitive dependence on point-symmetry. If we consider for instance the equation in (2.20) from Theorem 2.32, we would expect that a regular  $2k$ -gon has a smaller dilation than a regular  $(2k - 1)$ -gon, because the first one is point-symmetric, hence the ratio  $|C|/|C^*|$  attains its minimum 1. Point-symmetry seems to be good for small dilation, since both central symmetrization and halving pair transformation map convex cycles to point symmetric convex cycles whose dilation is less or equal. Another idea which seems to indicate this kind of dependence is that a regular  $2k$ -gon is somewhat closer to being a circle than a regular  $(2k - 1)$ -gon. Contrary to this intuition, we will prove that the dilation of a regular  $2k$ -gon is never smaller than the dilation of the corresponding regular  $(2k - 1)$ -gon. Apart from the square, i.e. the case  $k = 2$ , the dilation of a regular  $2k$ -gon is even bigger.

Let us first analyze the dilation of point-symmetric regular  $2k$ -gons.

**Lemma 2.44.** *Let  $C$  be the boundary of a regular  $n$ -gon, where  $n = 2k$ ,  $k \in \mathbb{N}$ . Then, its dilation is given by*

$$\delta(C) = \frac{n}{2} \tan\left(\frac{\pi}{n}\right)$$

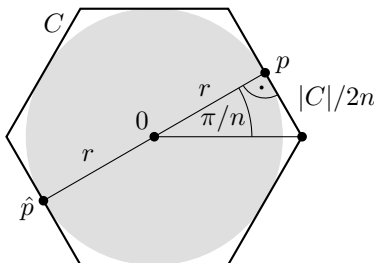


Figure 2.39: The dilation of a regular  $2k$ -gon is attained by the midpoints of edges which are central-symmetric copies of each other.

*Proof.* Consider Figure 2.39. Obviously, the  $2k$ -gon  $C$  is point-symmetric. By plugging equation (2.6),  $h = 2r$ , from Section 2.6 into Theorem 2.12,  $\delta(C) = |C|/2h$ , we know that  $\delta(C) = |C|/4r$ , where  $r$  denotes the inradius of  $C$ . On the other hand, applying basic trigonometry to the right-angled triangle in Figure 2.39 yields

$$\tan\left(\frac{\pi}{n}\right) = \frac{|C|}{2nr}, \quad \text{hence} \quad r = \frac{|C|}{2n \tan\left(\frac{\pi}{n}\right)},$$

which implies

$$\delta(C) = \frac{|C|}{4r} = \frac{2n \tan\left(\frac{\pi}{n}\right) |C|}{4|C|} = \frac{n}{2} \tan\left(\frac{\pi}{n}\right).$$

□

The dilation of regular  $(2k - 1)$ -gons is more difficult to calculate. Of course, we could try to apply the formula  $\delta(C) = |C|/2h$  from Theorem 2.12 also in this case. However, because the polygon  $C$  is not point-symmetric anymore, it is more difficult to get a formula for  $h$ . Therefore, we decide to use a different approach here, which applies the halving pair transformation in another interesting way.

**Lemma 2.45.** *Let  $C$  be the boundary of a regular  $n$ -gon, where  $n = 2k - 1$ ,  $k \in \mathbb{N}$ . Then, its dilation is given by*

$$\delta(C) = n \frac{\tan \frac{\pi}{2n}}{\cos \frac{\pi}{2n}} = n \frac{\sin \frac{\pi}{2n}}{\cos^2 \frac{\pi}{2n}}.$$

*Proof.* We will analyze the result of the halving pair transformation  $C^*$  of the regular  $n$ -gon  $C$ . Lemma 2.21.3 says that  $C^*$  is a polygonal cycle of at most  $2n$  edges. The arguments of its proof show that  $C^*$  is indeed a regular  $2n$ -gon. Because it has an even number of edges, we can calculate its dilation by the previous lemma, Lemma 2.44.

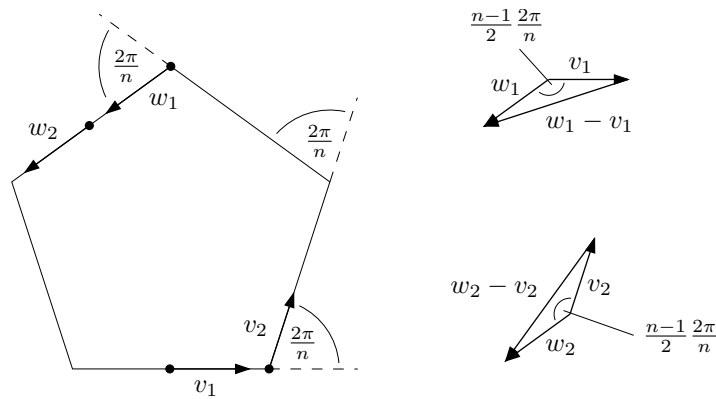


Figure 2.40: The derivative vectors of a halving pair in a regular  $(2k - 1)$ -gon enclose the angle  $((n - 1)/n)\pi$ .

Thus, we have to calculate only the ratio  $\delta(C)/\delta(C^*)$ , which can be done by applying the ideas from Lemma 2.22.

$$\frac{\delta(C)}{\delta(C^*)} \stackrel{\text{Lem. 2.22}}{=} \frac{|C|}{|C^*|} \stackrel{\text{Def. 2.20}}{=} \frac{|C|}{\int_0^{\frac{|C|}{2}} \left| \dot{\bar{c}}\left(t + \frac{|C|}{2}\right) - \dot{\bar{c}}(t) \right| dt} \quad (2.39)$$

Now consider Figure 2.40. The derivative vectors  $v := \dot{\bar{c}}(t)$  and  $w := \dot{\bar{c}}\left(t + \frac{|C|}{2}\right)$  of the arc-length parametrization  $\bar{c}$  enclose the same angle  $((n - 1)/n)\pi$  at every halving pair. This can easily be verified, because of the symmetry of  $C$ . The angle changes only if one of the points reaches a vertex. But even there, as can be seen in Figure 2.40, the smaller of the angles enclosed by the derivative vectors stays  $((n - 1)/n)\pi$ .

If we divide the triangle build by the vectors  $v$ ,  $w$  and  $w - v$  into two symmetric right-angled triangles, and apply the law of sines to the result while keeping in mind that  $|v| = |w| = 1$ , we get

$$\sin\left(\frac{n-1}{n}\frac{\pi}{2}\right) = \frac{|w-v|}{2}.$$

By plugging this into (2.39) we get

$$\frac{\delta(C)}{\delta(C^*)} = \frac{|C|}{\frac{|C|}{2} 2 \sin\left(\frac{n-1}{n}\frac{\pi}{2}\right)} = \frac{1}{\cos\left(\frac{\pi}{2n}\right)}.$$

Because  $C^*$  is a regular  $2n$ -gon, Lemma 2.44 yields  $\delta(C^*) = n \tan\left(\frac{\pi}{2n}\right)$ . And the proof is completed.  $\square$

The formulas of Lemma 2.44 and Lemma 2.45 lead to the values plotted in Figure 2.41. Indeed, they behave like announced in the beginning of this section.

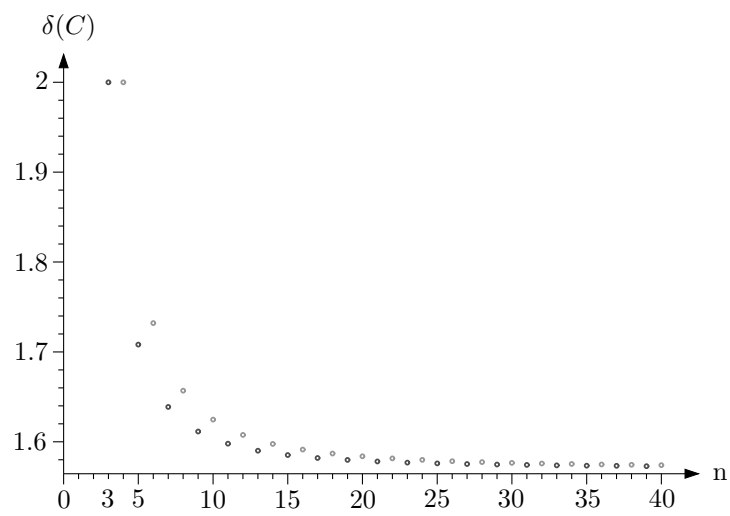


Figure 2.41: The dilation values of regular polygons.





# Chapter 3

## Zindler Curves

In this chapter, we examine closed *curves of constant halving distance*, so-called Zindler-curves. In other words, a closed curve  $C$  in the plane is a *Zindler-curve* iff it satisfies  $h(C) = H(C)$ .

We “discovered” this kind of curves when we were looking for networks of low dilation, cf. [56, 58] and Chapter 5. The intuitive reason why they are useful for constructing such networks lies in the following observation. Theorem 2.12 shows that the dilation of any convex Zindler curve equals  $\delta(C) = |C|/2h$  and it is attained by all its halving pairs. Hence, it is difficult to improve (decrease) the dilation of convex Zindler curves, because local changes decrease  $h$  (while  $|C|$  decreases by a smaller factor) or increase  $|C|$  (while  $h$  remains unchanged), see Figure 3.1.

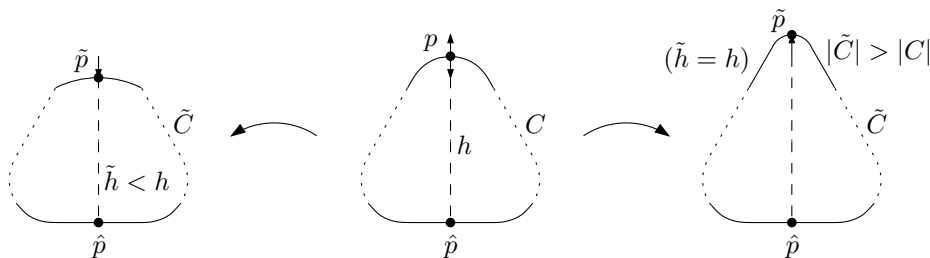


Figure 3.1: Intuitive argument: If one alters a convex Zindler curve only locally, the minimum halving distance decreases or the perimeter increases.

Another way to describe the close relationship between curves of small dilation and Zindler curves appears in Corollary 2.35. Its proof shows that the global dilation minimum of  $\pi/2$  can only be attained by centrally symmetric curves of constant halving distance. Only circles satisfy both conditions. Centrally symmetric curves are well-known. We described their properties related to dilation and halving-distance in Section 2.6. This inevitably raises the question, what kind of curves satisfy only the second condition, and directs our attention to Zindler curves.

At first we thought that circles are the only convex closed curves of constant halving distance. Then, we found some other examples. For the construction in [56, 58] we considered two curves

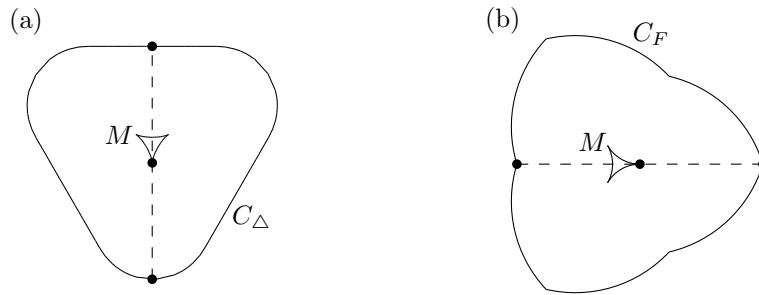


Figure 3.2: The “Rounded Triangle”  $C_\Delta$  and the “Flower”  $C_F$  are Zindler curves.

of constant halving distance, the rounded triangle  $C_\Delta$  and the “flower”  $C_F$ . Both curves are shown in Figure 3.2, and we analyze them in Section 3.2. Although the flower, which consists of six circular arcs, is not convex, it turned out to be better for the dilation of the constructed network.

However, the rounded triangle seems to be the most important example. To prevent misunderstandings we want to mention already that the round parts of the rounded triangle are *not* circular arcs. We prove this in the end of Section 3.2.1. The curve is convex and can be seen as an analogue to the Reuleaux-triangle, the best-known curve of constant breadth, introduced by Reuleaux [165] in 1876, see Figure 3.11, and confer to [115, par. 7], [33]. Günter Rote and Adrian Dumitrescu discovered the rounded triangle independently from us, and after we had presented our joint work [48], we found the curve in an article by Auerbach [10] from 1938.

Besides discovering amazing relations to curves of constant breadth and to bodies floating in an equilibrium in water, which we discuss in Section 3.1.3 and 3.1.4, in that article Auerbach also introduced the term Zindler curve. The name honors Konrad Zindler who was the first to describe these curves in [186] in 1921. We are not the first to rediscover them. In 1934 Salkowski [168, p. 59] constructed an example of a Zindler curve without mentioning Zindler. Astonishingly, his curve is the same as Zindler’s main example. We introduce and analyze it shortly in Section 3.2.3. Regarding the discovery of curves, we share Salkowski’s fate, because the flower  $C_F$  was also mentioned already by Zindler [186, p. 52].

An extensive article covering Zindler-curves, some generalizations and detailed proofs stems from Mampel [145]. In that article he also corrects an earlier proof by Geppert [75]. Furthermore, Zindler curves are mentioned in Chakerian and Groemer’s survey on curves of constant width [33, p. 58] and in Strubecker’s book on differential geometry [176]. Extensions of the concept to higher dimensions were proposed by Hoschek [105] and Wegner [181].

### 3.1 Characterization and Properties

The characterization of Zindler curves we give here can be regarded as known, cf. Mampel [145]. However, we think that our approach based on the derivative vectors results in nice and clear proofs and concentrates on the core of the characterization of Zindler curves.

In [48, 49] we showed that one characterization of convex Zindler curves is that the halving

chords are always tangent to the midpoint curve. This means that the midpoint curve is the *envelope* of the halving chords, cf. for instance [39, p. 292]. Zindler constructed his example curves based on this observation. Others like Mampel [145] considered the envelope of the halving chords and showed that the point where the chords touch their envelope is always the midpoint of the chord. Clearly all these approaches describe the same property, each from a different point of view. We prove this property in Section 3.1.1.

If we do not consider the chords halving the perimeter of  $C$  but the chords which bisect the area of  $C^\circ$ , one can ask an analogous question. Are there convex curves where all those area bisectors have the same length? We call such curves *curves of constant area halving distance*. Zindler [186] examined the envelopes of many chords of a given closed curve, including area bisectors. He knew already that the curves he constructed were both, curves of constant perimeter and curves of constant area halving distance. Later Geppert [75] and Mampel [145] showed that both concepts are basically equivalent. We prove this in Section 3.1.2.

Furthermore, Auerbach [10] discovered that if one turns the diametrical chords of a curve of constant breadth by  $90^\circ$  about their midpoints, the endpoints of the turned chords form a Zindler curve. Mampel [145] noticed and proved that the reverse construction yields all convex curves of constant breadth. We prove this amazing relation with our midpoint approach in Section 3.1.3.

Auerbach's interest in the curves was motivated by another astonishing property. He tried to answer a question of S. Ulam, who asked whether the sphere is the only three-dimensional body of a given density  $q$ ,  $0 < q < 1$ , which for every direction floats in water in an equilibrium with respect to rotation. We describe the connection of this problem to Zindler curves in Section 3.1.4.

### 3.1.1 Constant perimeter halving distance

First, we want to explain the intuition behind the characterization of curves of constant halving distance. We do not call them Zindler curves in this subsection because we want to stress that we only require the curves to have constant halving distance. We will prove later that this is basically equivalent to having constant area halving distance.

In the following, we sometimes consider a parameterization  $c : [0, |C|) \rightarrow C$  of a closed curve  $C$  which has the property that every pair  $(c(t), c(t + |C|/2))$  is a halving pair. We call such parameterizations *halving-pair parameterizations*. Obviously, every arc-length parameterization is a halving-pair parameterization, but they are not the only ones.

Assume we have an arbitrary curve  $C$  in the plane given by a piecewise continuously differentiable parameterization  $c : [0, |C|) \rightarrow C$ . Even, if this is not a halving-pair parameterization, we can define the midpoint curve  $M$  and a transformed centrally symmetric curve  $C^*$  by the parameterizations

$$m(t) := \frac{1}{2}(c(t) + c(t + |C|/2)), \quad c^*(t) := \frac{1}{2}(c(t) - c(t + |C|/2)). \quad (3.1)$$

Both parameterizations are clearly piecewise continuously differentiable. We can subdivide both derivative vectors into components which are parallel to the corresponding chord  $c(t)c(t +$

$|C|/2$ ), or equivalently to the vector  $c^*(t)$ , and components which are orthogonal to  $c^*(t)$ .

$$\begin{aligned}\dot{m}_{\parallel}(t) &:= \left\langle \dot{m}(t), \frac{1}{|c^*(t)|}c^*(t) \right\rangle \frac{1}{|c^*(t)|}c^*(t), & \dot{m}_{\perp}(t) &:= \dot{m}(t) - \dot{m}_{\parallel}(t), \\ \dot{c}_{\parallel}^*(t) &:= \left\langle \dot{c}^*(t), \frac{1}{|c^*(t)|}c^*(t) \right\rangle \frac{1}{|c^*(t)|}c^*(t), & \dot{c}_{\perp}^*(t) &:= \dot{c}^*(t) - \dot{c}_{\parallel}^*(t).\end{aligned}\quad (3.2)$$

Now, every movement of the pair of points  $(c(t), c(t + |C|/2))$  can be decomposed into four types of basic movements which occur if three of the four components disappear and only the remaining one does not equal zero. The four basic movements are displayed in Figure 3.3.

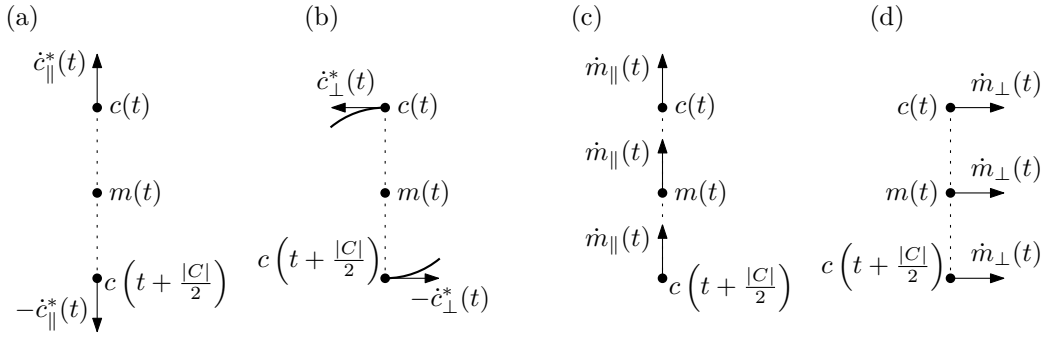


Figure 3.3: The four basic movements of the chord  $c(t)c(t + |C|/2)$ . For halving-pair parameterizations of convex curves of constant halving distance, types (a) and (d) cannot occur.

The component  $\dot{c}_{\parallel}^*(t)$  corresponds to a growing or shrinking chord  $c(t)c(t + |C|/2)$ , see Figure 3.3.a. If  $C$  is a curve of constant halving distance and  $c(t)$  is a halving-pair parameterization, obviously, the length of the chord stays constant, so this component must be zero.

The component  $\dot{c}_{\perp}^*(t)$  is responsible for turning the chord  $c(t)c(t + |C|/2)$ , see Figure 3.3.b.

The movement by  $\dot{m}_{\parallel}(t)$  translates the whole chord parallel to its own direction, see Figure 3.3.c. One could think that such a movement would not be possible if the curve  $C$  is convex. This is indeed true, if it is the only component of the movement, which follows from the statement we prove in Lemma 3.4. However, if there are other components involved,  $\dot{m}_{\parallel}(t)$  does not have to be zero, even if  $C$  is convex, see for example the rounded triangle analyzed in Section 3.2.1.

The last component is  $\dot{m}_{\perp}(t)$ , see Figure 3.3.d. For halving-pair parameterizations of curves of constant halving distance it has to be zero wherever the turning component  $\dot{c}_{\perp}^*(t)$  does not disappear. This is because  $\dot{m}_{\perp} \neq 0$  combined with  $\dot{c}_{\parallel}^* = 0$  and  $\dot{c}_{\perp}^*(t) \neq 0$  would imply

$$\begin{aligned}|\dot{c}(t)|^2 &= |\dot{c}_{\parallel}(t)|^2 + |\dot{c}_{\perp}(t)|^2 = |\dot{m}_{\parallel}(t) + \dot{c}_{\parallel}^*(t)|^2 + |\dot{m}_{\perp}(t) + \dot{c}_{\perp}^*(t)|^2 \\ &= |\dot{m}_{\parallel}(t + |C|/2)|^2 + |\dot{m}_{\perp}(t + |C|/2) - \dot{c}_{\perp}^*(t + |C|/2)|^2 \\ &\neq |\dot{m}_{\parallel}(t + |C|/2)|^2 + |\dot{m}_{\perp}(t + |C|/2) + \dot{c}_{\perp}^*(t + |C|/2)|^2 \\ &= |\dot{c}(t + |C|/2)|^2,\end{aligned}$$

a contradiction to  $|\dot{c}(t)| = |\dot{c}(t + |C|/2)|$ .

In the following we will prove the characterization of curves of constant halving distance more formally. We have used the first argument already in equation (2.15) of the proof of Lemma 2.25. Nevertheless, we want to restate it, slightly generalized, as a lemma.

**Lemma 3.1.** *Let  $c : [0, |C|) \rightarrow C$  be a piecewise continuously differentiable parameterization of the closed curve  $C \in \mathcal{C}$ . It is a halving-pair parameterization if and only if  $\dot{c}^*(t) \perp \dot{m}(t)$  wherever the derivatives exist.*

*Proof.* The linearity and the symmetry of the scalar product yield

$$\begin{aligned} \langle \dot{c}^*(t), \dot{m}(t) \rangle &= \frac{1}{4} \langle \dot{c}(t) - \dot{c}(t + |C|/2), \dot{c}(t) + \dot{c}(t + |C|/2) \rangle \\ &= \frac{1}{4} \left( \langle \dot{c}(t), \dot{c}(t) \rangle + \langle \dot{c}(t), \dot{c}(t + |C|/2) \rangle \right. \\ &\quad \left. - \langle \dot{c}(t), \dot{c}(t + |C|/2) \rangle - \langle \dot{c}(t + |C|/2), \dot{c}(t + |C|/2) \rangle \right) \\ &= \frac{1}{4} \left( |\dot{c}(t)|^2 - |\dot{c}(t + |C|/2)|^2 \right). \end{aligned}$$

Let  $|c([s, t])| := \int_s^t |\dot{c}(\tau)| d\tau$  denote the length of the path traversed by  $c(\tau)$  if the value  $\tau$  rises from  $s$  to  $t$ .

Assume that  $c(t)$  is a halving-pair parameterization. This means  $\forall t : |c([t, t + |C|/2])| = |C|/2$ , hence  $|\dot{c}(t)| = |\dot{c}(t + |C|/2)|$ . By the equation above this implies  $\langle \dot{c}^*(t), \dot{m}(t) \rangle = 0$ .

Assume now that we have  $\dot{c}^*(t) \perp \dot{m}(t)$  wherever the derivatives exist. By the equation above this implies  $|\dot{c}(t)| = |\dot{c}(t + |C|/2)|$ . We can conclude

$$|c([t, t + |C|/2])| \equiv \text{const.}$$

However, as clearly  $|c([0, |C|/2])| + |c([|C|/2, |C|])| = |C|$ , we must have

$$\forall t : |c([t, t + |C|/2])| = |C|/2,$$

and the proof is completed.  $\square$

The next, even easier argument is summarized in the following lemma.

**Lemma 3.2.** *Let  $c : [0, |C|) \rightarrow C$  be a halving-pair parameterization of a closed curve  $C \in \mathcal{C}$ . Then,  $C$  is a curve of constant halving distance if and only if  $\dot{c}^*(t) \perp c^*(t)$  wherever the derivatives exist.*

*Proof.* The curve  $C$  has constant halving distance iff  $|c^*(t)| = \text{const.}$ . Because by definition of  $\mathcal{C}$  the derivative  $\dot{c}^*(t) = \dot{c}(t) - \dot{c}(t + |C|/2)$  exists on the whole interval  $[0, |C|)$  apart from finitely many points, and  $c^*(t)$  is continuous everywhere, this is equivalent to

$$0 = \frac{d}{dt} |c^*(t)|^2 = \frac{d}{dt} \langle c^*(t), c^*(t) \rangle = 2 \langle \dot{c}^*(t), c^*(t) \rangle.$$

wherever both derivatives,  $\dot{c}(t)$  and  $\dot{c}(t + |C|/2)$  exist.  $\square$

The simple arguments from Lemma 3.1 and Lemma 3.2 imply the following nice necessary condition. If  $c : [0, |C|) \rightarrow C$  is a halving-pair parameterization of a curve of constant halving distance, we have

$$\dot{c}^*(t) = 0 \text{ or } \dot{m}(t) \parallel c^*(t). \quad (3.3)$$

wherever the derivatives exist. This means that either the halving chord is only translated due to the movement of its midpoint (case  $\dot{c}^*(t) = 0$ ) or the halving chord lies tangential to the midpoint curve. The second case includes the special case  $\dot{m}(t) = 0$ . Unfortunately, we have to use a slightly more complicated formulation to get a condition which is also sufficient.

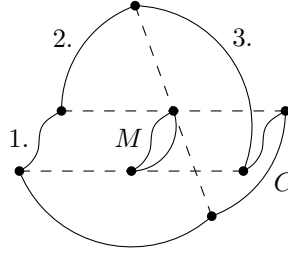


Figure 3.4: The halving chord of a curve of constant halving distance can move in three different ways.

**Theorem 3.3.** *Let  $c : [0, |C|) \rightarrow C$  be a halving-pair parameterization of a closed curve  $C \in \mathcal{C}$ . Then,  $C$  is a curve of constant halving distance if and only if, wherever the derivatives  $\dot{c}(t)$  and  $\dot{c}(t + |C|/2)$  exist, one of the following conditions is satisfied, cf. Figure 3.4:*

1.  $\dot{c}^*(t) = 0$ . (The chord  $c(t)c(t + |C|/2)$  is only translated according to the movement of its midpoint.)
2.  $\dot{m}(t) = 0$  and  $\dot{c}^*(t) \perp c^*(t)$ . (The chord  $c(t)c(t + |C|/2)$  is rotated about its midpoint  $m(t)$ .)
3.  $\dot{c}^*(t) \neq 0$  and  $\dot{m}(t) \neq 0$  and  $\dot{m}(t) \parallel c^*(t)$ . (The chord  $c(t)c(t + |C|/2)$  is tangent to the midpoint curve.)

*Proof.* “ $\Rightarrow$ ”: Let  $c : [0, |C|) \rightarrow C$  be a halving-pair parameterization of a curve  $C$  of constant halving distance, and assume that the derivatives  $\dot{c}(t)$  and  $\dot{c}(t + |C|/2)$  exist. Then, the previous lemmata imply

$$\dot{m}(t) \stackrel{\text{Lem. 3.1}}{\perp} \dot{c}^*(t) \stackrel{\text{Lem. 3.2}}{\perp} c^*(t).$$

This proves that at least one of the conditions is satisfied.

“ $\Leftarrow$ ”: Now, we assume that  $c : [0, |C|) \rightarrow C$  is a halving-pair parameterization of a closed curve  $C$ , such that one of the three conditions is satisfied wherever the derivatives  $\dot{c}(t)$  and  $\dot{c}(t + \frac{|C|}{2})$  exist.

For the first two conditions, we clearly have  $\langle c^*(t), \dot{c}^*(t) \rangle = 0$ . Now we assume that the third condition is satisfied. We have  $\dot{m}(t) \neq 0$ ,  $\dot{c}^*(t) \neq 0$  and  $\dot{m}(t) \parallel c^*(t)$ . We follow the proof of “ $\Rightarrow$ ” in the opposite direction. By Lemma 3.1 we have

$$\dot{c}^*(t) \stackrel{\text{Lem. 3.1}}{\perp} \dot{m}(t) \stackrel{\text{assumption}}{\parallel} c^*(t).$$

Hence, because of  $\dot{m}(t) \neq 0$ , we get  $\dot{c}^*(t) \perp c^*(t)$  also in this case. We have shown  $\dot{c}^*(t) \perp c^*(t)$  wherever  $\dot{c}^*(t)$  exists. Plugging this into Lemma 3.2 implies that  $C$  is a curve of constant halving distance.  $\square$

For convex curves of constant halving distance the characterization is a little easier because translation parts (case 1.) cannot occur. This holds even for a broader class of curves. In the following we will call the set  $pq \setminus \{p, q\}$  the *interior* of the line segment  $pq$ . The simpler characterization holds also for curves of constant halving distance where the interior of every halving chord lies inside the open region  $C^\circ$  bounded by  $C$ . We will call any closed curve where the interiors of the halving chords stay inside  $C^\circ$  a curve *with interior halving chords*.

**Lemma 3.4.** *Let  $c : [0, |C|) \rightarrow C$  be a halving-pair parameterization of a closed curve  $C \in \mathcal{C}$  with interior halving chords. Then, there does not exist any translation part, i.e. there exists no non-empty interval  $(t_1, t_2) \subset [0, |C|)$  such that  $c^*$  is constant on  $(t_1, t_2)$ .*

*In particular this holds for convex curves of constant halving distance.*

*Proof.* Assume that the conditions of the Lemma are satisfied, and that  $c^*(t)$  is constant on  $(t_1, t_2)$ .

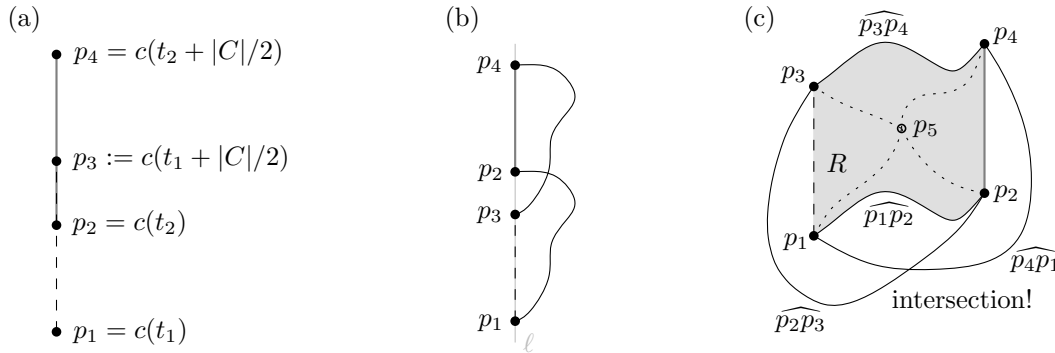


Figure 3.5: If  $c^*(t)$  is constant on  $[t_1, t_2]$ , the interiors of the halving chords cannot all be contained in  $C^\circ$ .

First, we consider the special case where  $p_1 := c(t_1)$ ,  $p_2 := c(t_2)$ ,  $p_3 := c(t_1 + |C|/2)$  and  $p_4 := c(t_2 + |C|/2)$  are collinear. Consider Figure 3.5.a. The halving chords cannot intersect, because in that case an endpoint of one halving chord, a point outside of  $C^\circ$ , would lie on the interior of the other halving chord.

In the remaining special case, where the four points  $p_1, p_2, p_3, p_4$  are collinear but the halving chords  $p_1p_3$  and  $p_2p_4$  do not intersect, we can assume that the points appear on their shared line  $\ell$  in the order  $p_1, p_3, p_2, p_4$ , cf. Figure 3.5.b. This can be reached by possibly switching the orientation of the halving-pair parameterization and by renaming the points appropriately.

Furthermore, we may assume that the paths  $\widehat{p_1p_2} := c([t_1, t_2])$  and  $\widehat{p_3p_4} := c([t_1 + |C|/2, t_2 + |C|/2])$  only intersect with one of the two half-planes induced by  $\ell$ .<sup>1</sup> This can be reached by choosing  $t_2$  to be the first  $t$ -value bigger than  $t_1$  where  $c(t)$  hits  $\ell$ . But then, the path  $\widehat{p_1p_2}$

<sup>1</sup>Then, obviously,  $\widehat{p_1p_2}$  and  $\widehat{p_3p_4}$  are contained in the same half-plane because the halving chord is not turned nor stretched but only translated in  $[t_1, t_2]$ .

encloses  $p_3 = c(t_1 + |C|/2)$  in this half-plane. Hence, there has to be an intersection with  $\widehat{p_3 p_4}$ . This is a contradiction to  $C$  being simple.

We are ready to consider the ordinary case, where the parallel chords  $p_1 p_3$  and  $p_2 p_4$  do not lie on the same line, cf. Figure 3.5.c. Then, the open region  $R$  wiped out by the interiors of the halving chords  $c(\tau)c(\tau + |C|/2)$ ,  $\tau \in (t_1, t_2)$ , is bounded by the halving chords  $p_1 p_3$ ,  $p_2 p_4$  and the paths  $\widehat{p_1 p_2}$ ,  $\widehat{p_3 p_4}$ . Because  $C$  is simple and because the interiors of the halving chords do not intersect with  $C$  by assumption, these four paths and the paths  $\widehat{p_2 p_3} := c([t_2, t_1 + |C|/2])$  and  $\widehat{p_4 p_1} := c([t_2 + |C|/2, t_1])$  do not intersect with each other.

But then, we can regard the six paths and the four points as a simple geometric graph. And we can add an additional node  $p_5$  inside of  $R$  and connect it without intersections with the four previous points  $p_1, p_2, p_3, p_4$ . This would be a simple<sup>2</sup> geometric embedding of  $K_5$ , the complete graph with five vertices. This is a contradiction because it is well-known that such an embedding does not exist, see for instance the solution of exercise 1.3 in [127, p. 16].

It is easy to see that for convex closed curves the interiors of the halving chords lie fully inside of  $C^\circ$ . This is because otherwise such an interior had to intersect with  $C$ . This would imply by convexity that the whole halving chord belongs to  $C$ , one path on  $C$  connecting its two endpoints is the halving chord itself. But then, the other path must have the same length. The curve  $C$  would have to be degenerated to a line segment, a contradiction.  $\square$

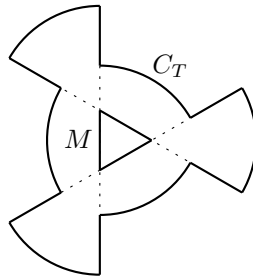


Figure 3.6:  $C_T$  contains translation parts although all halving chords pass through  $\overline{C_T^\circ}$ .

If we drop the intersection condition, there are easy examples of cycles of constant halving distance with translation parts, see for example part “1.” in Figure 3.4. Figure 3.6 shows that it does not suffice that the halving chords are contained in the closure  $\overline{C^\circ}$  to prevent translation parts.

### 3.1.2 Constant area halving distance

Zindler knew already that the halving chords of his curves also bisect the area, and later Geppert [75] and Mampel [145] showed that convex curves of constant (perimeter) halving distance and convex curves of constant area halving distance are the same. In this section we will prove this equivalence by using almost the same approach as in the previous section.

Analogously to halving-pair parameterizations we define area-bisecting parameterizations. We could call them area-halving-pair parameterizations but prefer the shorter name. A parame-

<sup>2</sup>A geometric graph is simple if edges can only intersect at their incident vertices.



terization  $c : [0, |C|) \rightarrow C$  of a closed convex curve  $C$  is an *area-bisecting parameterization* if it traverses  $C$  counter-clockwise and every chord  $c(t)c(t + |C|/2)$  bisects the area of  $C^\circ$ . Any such chord which bisects the area encircled by  $C$  is an *area-halving chord* or *area bisector*. Note that these definitions make sense only if  $C$  is convex.

To define an area-bisecting parameterization more formally, we consider a parameterization<sup>3</sup>  $c : [0, |C|) \rightarrow C$  which traverses  $C$  counter-clockwise. Then, the area right of the chord  $c(s)c(t)$ ,  $s < t$ , is defined by<sup>4</sup>

$$A(c([s, t])) := I(c([s, t]) \oplus c(t)c(s)) = I(c([s, t])) + I(c(t)c(s)) \quad (3.4)$$

where the integral operator  $I$  from the section dealing with Holditch's theorem, Section 2.10, is applied to the concatenation of the part of  $C$  between  $c(s)$  and  $c(t)$  and the chord  $c(t)c(s)$ .

Because of the simplicity of  $C$  all the appearing winding numbers of  $C$  equal 1 or 0. Therefore, Lemma 2.27 shows that the given definition of  $A(c([s, t]))$  is canonical. With this definition a chord  $c(s)c(t)$  is an area-bisector if  $A(c([s, t])) = \frac{1}{2}A(C)$ , which also yields a formal definition of area-bisecting parameterizations, even if  $C$  is not convex.

In Appendix A.2 we show that there always exists a piecewise continuously differentiable area-bisecting parameterization if  $C$  is convex and piecewise continuously differentiable, that is if there exists one arbitrary piecewise continuously differentiable parameterization.

Now, again we start with intuitive arguments based on four different kinds of movements. Assume we have an arbitrary curve  $C$  in the plane given by a piecewise continuously differentiable parameterization  $c : [0, |C|) \rightarrow C$ . As in the previous section we can define a parameterization  $m(t)$  of a midpoint curve and a parameterization  $c^*(t)$  of a symmetrized curve by equation (3.1). And again we decompose the derivative vectors into components  $\dot{m}_{\parallel}(t)$  and  $\dot{c}_{\parallel}^*(t)$  which are parallel to the chord  $c(t)c(t + |C|/2)$  and to the vector  $c^*(t)$ , and into components  $\dot{m}_{\perp}(t)$  and  $\dot{c}_{\perp}^*(t)$  which are orthogonal to  $c^*(t)$ , cf. (3.2).

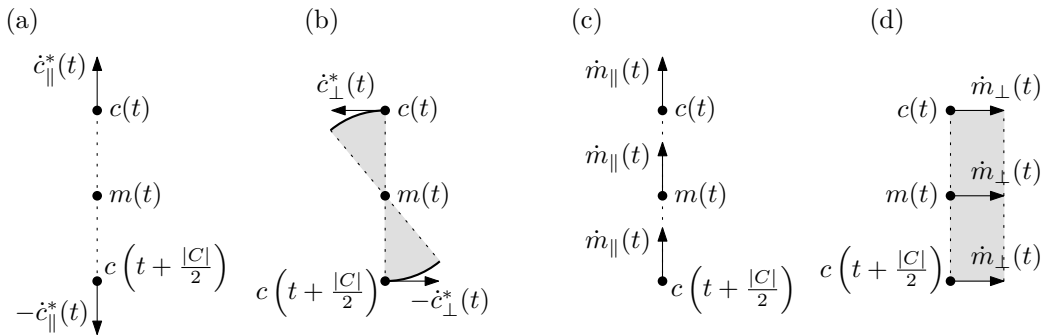


Figure 3.7: The four basic movements of the chord  $c(t)c(t + |C|/2)$ . For area-bisecting parameterizations of curves of constant area-halving distance, types (a) and (d) cannot occur.

The component  $\dot{c}_{\parallel}^*(t)$  corresponds to a growing or shrinking chord  $c(t)c(t + |C|/2)$ , see Figure 3.7.a. If  $C$  is a curve of constant area halving distance and  $c(t)$  is an area-bisecting

<sup>3</sup>The interval  $[0, |C|)$  is not the most natural choice in the area-case, however we use it, because otherwise we would have to introduce different notation in the area-halving case.

<sup>4</sup>Here, we allow the case  $t \in [|C|, 2|C|)$  by extending the parameterization canonically. However,  $s$  and  $t$  must satisfy  $0 \leq t - s \leq |C|$ .

parameterization, again, the length of the chord stays constant, so this component must be zero.

Let us consider the turning component  $\dot{c}_\perp^*(t)$ , see Figure 3.7.b. If the chord rotates about its midpoint, the area swept by it from left to right equals the area swept from right to left. Hence, there is no restriction on the component  $\dot{c}_\perp^*(t)$ .

The movement by  $\dot{m}_\parallel(t)$  translates the whole chord parallel to its own direction, see Figure 3.7.c. Intuitively, such a movement does not change the area to the left nor the area to the right of the chord. Hence, there is no restriction on this component either. As discussed in the beginning of Section 3.1.1, the translation caused by this component does contradict convexity inevitably only if  $\dot{c}_\perp^*(t) = 0$ .

The last component is  $\dot{m}_\perp(t)$ , see Figure 3.7.d. For area-bisecting parameterizations of curves of constant area halving distance it has to be zero, since such a movement decreases the area on one side of the chord and increases the other. This is a contradiction to the assumption that  $c(t)c(t + |C|/2)$  is an area-halving chord for every  $t$ .

This intuitive approach already hints that curves of constant area-halving distance are (almost) the same as curves of constant (perimeter) halving distance. For the latter case, we have proved the most important step of the characterization of such curves in Lemma 3.1, which says that a parameterization  $c : [0, |C|) \rightarrow C$  of a closed curve  $C$  is a halving-pair parameterization iff  $\dot{c}^*(t) \perp \dot{m}(t)$  wherever the derivatives exist. We combined this with the property  $\dot{c}^* \perp c^*$  of parameterization with constant  $|c^*|$  to conclude  $\dot{m} \parallel c^*$ , i.e.  $\dot{m}_\perp = 0$  in the normal case. Already the intuitive thoughts at the beginning of this section show that for curves of constant area-halving distance the main argument is different. In fact, it is simpler. Here, our conclusion  $\dot{m}_\perp(t) = 0$  follows immediately from the area-halving property. We prove this main argument more formally in the following lemma.

**Lemma 3.5.** *Let  $c : [0, |C|) \rightarrow C$  be a piecewise continuously differentiable parameterization of a simple closed curve  $C \in \mathcal{C}$ . It is an area-bisecting parameterization if and only if  $\dot{m}(t) \parallel c^*(t)$  wherever the derivatives  $\dot{c}(t)$  and  $\dot{c}(t + |C|/2)$  exist.*

*Proof.* A sufficient and necessary condition for  $c(t)$  to be an area-bisecting parameterization is

$$\frac{d}{dt}A(c([t, t + |C|/2])) = 0. \quad (3.5)$$

It is obvious that this is a necessary condition. So, assume now that the derivative equals 0 wherever it exists. Then the area right of the chord  $c(t)c(t + |C|/2)$  is the same for every  $t \in [0, |C|)$ . Because of  $A(c([0, |C|/2])) + A(c([|C|/2, |C|])) = A(C)$  this implies  $A(c([t, t + |C|/2])) = A(C)/2$  for every  $t$ ;  $c(t)$  is an area-bisecting parameterization.

We have to show that the conditions stated in the lemma are equivalent to (3.5). This can be done by

$$\frac{d}{dt}A\left(c\left(\left[t, t + \frac{|C|}{2}\right]\right)\right) \stackrel{(3.4)}{=} \frac{d}{dt}\left(I\left(c\left(\left[t, t + \frac{|C|}{2}\right]\right)\right) + I\left(c\left(t + \frac{|C|}{2}\right)c(t)\right)\right)$$

$$\begin{aligned}
& \stackrel{\text{(2.17),}}{\stackrel{\text{Lem. 2.31}}{=}} \frac{d}{dt} \left( \frac{1}{2} \int_t^{t+\frac{|C|}{2}} [c(\tau), \dot{c}(\tau)] d\tau + \frac{1}{2} \left[ c \left( t + \frac{|C|}{2} \right), c(t) \right] \right) \\
& \stackrel{*}{=} \frac{1}{2} \left( \left[ c \left( t + \frac{|C|}{2} \right), \dot{c} \left( t + \frac{|C|}{2} \right) \right] - [c(t), \dot{c}(t)] \right. \\
& \quad \left. + \left[ \dot{c} \left( t + \frac{|C|}{2} \right), c(t) \right] + \left[ c \left( t + \frac{|C|}{2} \right), \dot{c}(t) \right] \right) \\
& \stackrel{[\cdot, \cdot] \text{ lin.}}{\stackrel{\& \text{ antisym.}}{=}} \frac{1}{2} \left( \left[ c \left( t + \frac{|C|}{2} \right), \dot{c}(t) + \dot{c} \left( t + \frac{|C|}{2} \right) \right] \right. \\
& \quad \left. - \left[ c(t), \dot{c}(t) + \dot{c} \left( t + \frac{|C|}{2} \right) \right] \right) \\
& \stackrel{[\cdot, \cdot] \text{ lin.}}{=} -\frac{1}{2} \left[ c(t) - c \left( t + \frac{|C|}{2} \right), \dot{c}(t) + \dot{c} \left( t + \frac{|C|}{2} \right) \right] \\
& \stackrel{(3.1)}{=} -2[c^*(t), \dot{m}(t)] \stackrel{\text{Def. } [\cdot, \cdot]}{=} -2 \langle c^*(t), \mathbf{R}^{90^\circ} \dot{m}(t) \rangle
\end{aligned}$$

The equality marked with a star holds because differentiation and integration cancel out each other, and because the product rule  $(d/dt)[c_1, c_2] = [\dot{c}_1, c_2] + [c_1, \dot{c}_2]$  holds for the operator  $[\cdot, \cdot]$ , which follows immediately from its definition. This shows that  $c(t)$  is an area-bisecting parameterization iff  $c^* \parallel \dot{m}(t)$  wherever the derivatives exist.  $\square$

The next argument is absolutely the same as in the perimeter-halving case.

**Lemma 3.6.** *Let  $c : [0, |C|) \rightarrow C$  be a piecewise continuously differentiable area-bisecting parameterization of a closed curve  $C$ . Then,  $C$  is a curve of constant area-halving distance if and only if  $\dot{c}^*(t) \perp c^*(t)$  wherever the derivatives exist.*

*Proof.* See proof of Lemma 3.2.  $\square$

The statements from Lemma 3.5,  $\dot{m}(t) \parallel c^*(t)$ , and from Lemma 3.6,  $c^*(t) \perp \dot{c}^*(t)$ , show that  $c : [0, |C|) \rightarrow C$  is an area-bisecting parameterization of a curve of constant area-halving distance iff  $\dot{m}(t) \perp \dot{c}^*(t)$ . As  $c^*(t)$  does never disappear for simple curves, we do not have any additional condition. In particular, curves of constant area-halving distance cannot have translation parts.

**Theorem 3.7.** *Let  $c : [0, |C|) \rightarrow C$  be a piecewise continuously differentiable area-bisecting parameterization of a simple closed curve  $C \in \mathcal{C}$ . Then,  $C$  is a curve of constant area halving distance if and only if, wherever the derivatives  $\dot{c}(t)$  and  $\dot{c}(t + |C|/2)$  exist, we have*

$$\dot{m}(t) \perp \dot{c}^*(t).$$

*Proof.* As said before, we only have to combine Lemma 3.5 and Lemma 3.6 with the fact that  $\forall t : c^*(t) \neq 0$  for simple curves.  $\square$

**Corollary 3.8.** *Let  $C \in \mathcal{C}$  be a closed curve in the plane.*

1. If the curve  $C$  is a curve of constant area-halving distance, it is a curve of constant (perimeter) halving distance, and area bisectors and halving chords coincide.
2. If the curve  $C$  is a curve of constant (perimeter) halving distance with interior halving chords, it is a curve of constant area-halving distance, and area bisectors and halving chords coincide.
3. If all the area-halving chords and perimeter-halving chords of a closed curve  $C$  coincide, and for a halving-pair parameterization  $c(t)$  we have  $\dot{c}^*(t) \perp c^*(t)$  wherever  $\dot{m}(t) = 0$ , then  $C$  has constant halving distance.

*Proof.* 1. Let  $c : [0, |C|) \rightarrow C$  be an area-bisecting parameterization of the given curve of constant area-halving distance. It exists by Lemma A.3 in Appendix A.2. By Theorem 3.7 this implies  $\dot{m}(t) \perp \dot{c}^*(t)$ . Then, Lemma 3.1 shows that  $c$  is a halving-pair parameterization. Because of  $|c^*(t)| = \text{const.}$ ,  $C$  is a curve of constant (perimeter) halving distance.

2. Let  $c : [0, |C|) \rightarrow C$  be a halving-pair parameterization of the given convex curve of constant (perimeter) halving distance with interior halving chords. For instance, we can use an arc-length parameterization, which exists by Lemma A.1 in Appendix A.1. By Theorem 3.3 and Lemma 3.4 this implies  $\dot{m}(t) \parallel c^*(t)$ . Then, Lemma 3.5 shows that  $c$  is an area-bisecting parameterization. Because of  $|c^*(t)| = \text{const.}$ ,  $C$  is a curve of constant area-halving distance.

3. Let  $c : [0, |C|) \rightarrow C$  be a halving-pair parameterization of  $C$ . By the assumption it is an area-bisecting parameterization, too. Lemma 3.1 shows that  $\dot{c}^*(t) \perp \dot{m}(t)$ , and Lemma 3.5 implies that  $\dot{m}(t) \parallel c^*(t)$ . Hence for  $t$ -values with  $\dot{m}(t) \neq 0$  we have  $\dot{c}^*(t) \perp c^*(t)$ . Together with the additional assumption for the special case  $\dot{m}(t) = 0$ , the conditions of Lemma 3.2, Theorem 3.3 or Lemma 3.6 are satisfied and we can apply each of them to conclude that  $C$  is a curve of constant halving distance.  $\square$

This corollary shows the correct relation between curves of constant halving distance and curves of constant area-halving distance. For curves with interior halving chords, in particular for convex curves, both concepts are the same. The curves analyzed by Zindler [186] are convex. However, in this thesis we defined any curve of constant halving distance to be a Zindler curve.

The example in Figure 3.4 on page 86 shows that – due to translation parts – there exist non-convex Zindler curves which do not have constant area-halving distance.

Geppert [75, p. 118] claimed that any curve where area bisectors and halving pairs coincide is a Zindler curve. However, the relation proved in part 3. of the corollary above is best possible. Any centrally symmetric curve which is not a circle shows that there are (even convex) curves with coinciding area and perimeter bisectors which are not Zindler curves.

### 3.1.3 Constant breadth

Auerbach [10] was the first to observe the following interesting duality between Zindler curves and curves of constant breadth.

If one takes the halving chords of a Zindler curve and rotates each of them by  $90^\circ$  about its midpoint, the curve described by the endpoints of these turned chords is a curve of constant

breadth, if it is convex. Conversely, if one rotates each diametral chord of a convex curve of constant breadth by  $90^\circ$  about its midpoint, the curve described by the endpoints of the rotated chords is a Zindler curve. To prove this, again we can use the same approach as in the previous sections.

The famous curves of constant breadth, cf. Chakerian and Groemer's survey [33], satisfy the defining condition  $w = D$ . The best-known example, the Reuleaux-triangle, is shown in Figure 3.11 on page 97. It was introduced by Reuleaux [165] in 1876. It can be constructed based on an equilateral triangle by replacing each of the three line segments by a circular arc centered at the opposite vertex.

Analogously to halving-pair parameterizations and area-bisecting parameterizations, we want to define extremal parameterizations. To this end, we need some additional notation. For any set  $S \subset \mathbb{R}^2$ , a point  $p \in S$  is an *extreme point* of  $S$  in direction  $v \in \mathbb{S}^1$  iff

$$\langle p, v \rangle = \max\{\langle q, v \rangle \mid q \in S\}.$$

A convex curve  $C \subset \mathbb{R}^2$  is *strictly convex* if for every  $v \in \mathbb{S}^1$  it has a unique extreme point. It is easy to see, that this is equivalent to saying that no part of  $C$  is a line segment<sup>5</sup>.

An extremal parameterization can be defined only for strictly convex curves. However, this is not a problem, because every curve of constant breadth is strictly convex.

**Remark 3.9.** *Let  $C \subset \mathbb{R}^2$  be a convex curve of constant breadth. Then,  $C$  is strictly convex.*

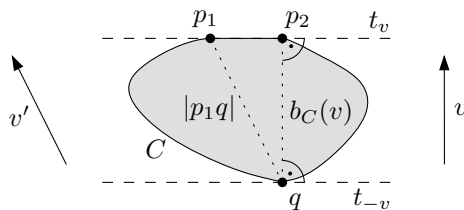


Figure 3.8: Proving that any convex curve of constant breadth is strictly convex.

*Proof.* The main arguments are the same as in the proof of Lemma 2.6.1. Consider Figure 3.8. Assume that  $C$  is a curve of constant breadth which is not strictly convex. Then, there exist two extreme points  $p_1 \neq p_2$  for a direction  $v \in \mathbb{S}^1$ . Let  $q$  be an extreme point of direction  $-v$ . The points  $p_1$  and  $p_2$  lie on a tangent  $t_v$  which is orthogonal to  $v$ . And the point  $q$  lies on the other tangent  $t_{-v}$  which is orthogonal to  $v$ . The distance of the two tangents equals

$$b_C(v) = |t_v t_{-v}| = \langle p_1 - q, v \rangle = \langle p_2 - q, v \rangle.$$

Because of  $p_1 \neq p_2$  at least one of the distances  $|p_1 q|$  and  $|p_2 q|$  must be bigger than  $b_C(v)$ . We assume  $|p_1 q| > b_C(v)$ . Let  $v' \in \mathbb{S}^1$  be the direction of  $p_1 - q$ . Then, we can conclude  $b_C(v') \geq |p_1 q| > b_C(v)$ , contradicting that  $C$  is a curve of constant breadth.  $\square$

<sup>5</sup>If there are two extreme points  $p, q$  for  $v \in \mathbb{S}^1$  the line segment  $pq$  has to be part of  $C$ . If there is a line segment  $pq$  part of  $C$ , then the corresponding line has to be a tangent, hence,  $p$  and  $q$  are extreme points in the same direction orthogonal to  $pq$ .

After this short remark, we finally define extremal parameterizations. Let  $C$  be a closed, strictly convex curve  $C \subset \mathbb{R}^2$ . An *extremal parameterization* of  $C$  is a parameterization  $c : [0, |C|) \rightarrow C$  such that for every  $t$  the point  $c(t)$  is the extreme point in direction  $(\cos \frac{2\pi t}{|C|}, \sin \frac{2\pi t}{|C|})$ . Note that we do not require  $c$  to be injective, because for curves like the Reuleaux-triangle there exist points which are extremal for several directions. Hence, the extremal parameterization is not a nice parameterization in the sense of Section 2.1.

Of course, it would be more natural to define extremal parameterizations based on the interval  $[0, 2\pi)$ , but the approach chosen here unifies the notation. We do not have to redefine the midpoint curve, nor  $c^*(t)$ .

In Appendix A.3 we prove the existence of piecewise continuously differentiable extremal parameterizations. However, the proof requires the curve  $C$  to satisfy two additional conditions.

The first one is that there exists a nice parameterization which is even twice piecewise continuously differentiable. The second derivatives are necessary because the extremal parameterization depends on the direction of the tangent, which is given by the first derivative. Hence, the first derivative of any extremal parameterization depends also on the second derivatives of  $C$ .

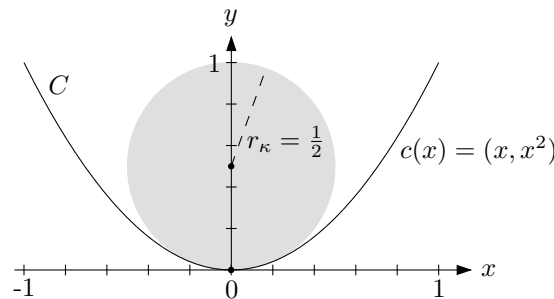


Figure 3.9: The radius of curvature of the parabola  $C$  in 0 equals  $r_\kappa(C, 0) = \frac{1}{2}$ , the curvature equals  $\kappa(C, 0) = 2$ .

The second condition is that the curvature never equals zero. The *curvature*  $\kappa(C, p)$  of a curve  $C$  in a point  $p$  can be defined by

$$\kappa(C, p) := \frac{1}{|\dot{c}(t)|^3} \langle \ddot{c}(t), \mathbb{R}^{90^\circ} \dot{c}(t) \rangle. \quad (3.6)$$

for any parameterization of  $C$  which is twice differentiable in  $p = c(t)$ . Its sign depends on the orientation of the parameterization. If  $c(t)$  traverses a convex curve  $C$  counter-clockwise, we have  $\kappa(C, p) \geq 0$ . The absolute value of  $\kappa(C, p)$  is independent from the parameterization. It is the reciprocal of the *radius of curvature*  $r_\kappa(C, p)$ . Intuitively spoken, this is the radius of the circle through  $p$  which best approximates  $C$  in the vicinity of  $p$ , see Figure 3.9 for an example and [38, pp. 354-360] or [182] for details.

The condition on the curvature is not a real restriction in the situation of this section, because it is satisfied by every curve of constant breadth. This is easy to explain, see Figure 3.10. Assume we had  $\kappa(C, p) = 0$ . Let  $qp$  be a diametral chord. Such a chord exists orthogonal to every supporting line through  $p$  by the arguments from Remark 3.9. The disappearing curvature implies that every circle through  $p$  whose center is on the ray emanating from  $p$

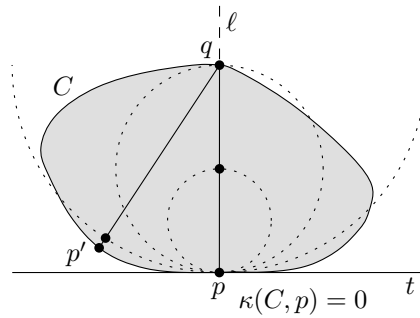


Figure 3.10: Showing with a proof by contradiction that a convex curve  $C$  of constant breadth can at no point have curvature  $\kappa(C, p) = 0$ .

in the direction of  $q$  lies locally inside of  $C$ . Hence, the circle around  $q$  with radius  $|qp| = D(C) = w(C)$  lies locally inside of  $C$ . We can rotate  $pq$  by a small angle about  $q$  and expand it slightly, and the resulting chord  $qp'$  is still contained in  $C$ . But then, the breadth of  $C$  in the direction  $v \in \mathbb{S}^1$  of  $q' - p$  satisfies  $b_C(v) \geq |pq'| > |pq| = D(C)$ , a contradiction.

After these introducing comments regarding the definition and existence of an extremal parameterization, we now assume that we have given a piecewise continuously differentiable parameterization (which does not have to be injective)  $c : [0, |C|) \rightarrow C$ . We want to find the decisive properties which characterize extremal parameterizations of curves of constant breadth.

Again, we start with intuitive arguments based on the four different kinds of movements. The parameterization  $c : [0, |C|) \rightarrow C$  induces a parameterization  $m(t)$  of a midpoint curve and a parameterization  $c^*(t)$  of a symmetrized curve by equation (3.1). They have the derivative components  $\dot{m}_{\parallel}(t)$  and  $\dot{c}_{\parallel}^*(t)$  which are parallel to the chord  $c(t)c(t + |C|/2)$  and to the vector  $c^*(t)$ , and the components  $\dot{m}_{\perp}(t)$  and  $\dot{c}_{\perp}^*(t)$  which are orthogonal to  $c^*(t)$ , cf. (3.2).

The first argument for the characterization of curves of constant breadth is quite easy. Let  $c : [0, |C|) \rightarrow C$  be an extremal parameterization of such a curve  $C$ . Then, if the derivative  $\dot{c}(t)$  exists, it either equals 0, or it is orthogonal to  $\alpha := 2\pi t/|C|$ . This is because, if the derivative exists and does not disappear, it points into the direction of the unique tangent through  $c(t)$ . By the definition of extreme points, the line  $\ell$  through  $c(t)$  which is orthogonal to  $\alpha$  is a tangent of  $C$ , hence  $\dot{c}(t) \perp \alpha$ .

The next argument comes from Lemma 2.6.1. It states that each direction of maximum breadth is a direction of maximum length, and the maxima are equal. For curves of constant breadth, every direction is a direction of maximum breadth. Hence, we know that  $b_C(\alpha) = l_C(\alpha)$  for every direction  $\alpha \in [0, 2\pi)$ . As the whole curve  $C$  is enclosed by the two tangents  $t_1, t_2$  which are orthogonal to  $\alpha$ , this can only be the case if there exists a pair of points  $(p, q) \in C \times C$  of direction  $\alpha$ , where  $p \in t_1$  and  $q \in t_2$ . But, by Remark 3.9 we know that there exists only one point on each of the tangents  $t_1$  and  $t_2$ , namely  $c(\alpha|C|/2\pi)$  and  $c(\alpha|C|/2\pi + |C|/2)$ . This shows that the vector  $c(t) - c(t + |C|/2)$  has direction  $\alpha = 2\pi t/|C|$  and that  $c(t)c(t + |C|/2)$  is a diametral chord of direction  $\alpha$  for every  $t$ .

Combining both arguments yields  $\dot{c}(t) \perp c^*(t)$ .

As the component  $\dot{c}_{\parallel}^*(t)$  must equal zero for any extremal parameterization of curves of constant breadth, because it is responsible for the growth of the diametral chord, we conclude that  $\dot{m}_{\parallel}$  must disappear, too. Otherwise we had  $\dot{c}_{\parallel} \neq 0$  in contradiction to  $\dot{c}(t) \perp c^*(t)$ .

Hence, for extremal parameterizations of curves of constant breadth only the orthogonal translation due to  $\dot{m}_{\perp}(t)$  and the turning of the diametral chord due to  $\dot{c}_{\perp}^*(t)$  (and combinations of both basic movements) are possible. We summarize and prove the result more formally in the following lemma.

**Lemma 3.10.** *Let  $C$  be a convex closed curve  $C \in \mathcal{C}$ , and let  $c : [0, |C|) \rightarrow C$  be a piecewise continuously differentiable parameterization.*

1. *If  $c$  is an extremal parameterization of a curve of constant breadth, we have  $\dot{m}(t) \perp c^*(t) \perp \dot{c}^*(t)$  wherever the derivatives exist, and  $2|c^*(t)| \equiv D(C) = w(C)$ .*
2. *If  $\dot{m}(t) \perp c^*(t) \perp \dot{c}^*(t)$  is satisfied wherever the derivatives exist, then  $C$  is a curve of constant breadth, and we have  $2|c^*(t)| \equiv D(C) = w(C)$ .*

*Proof.* If the derivative  $\dot{c}(t)$  exists and does not disappear, it points towards the direction of the only supporting line of  $C$  through  $c(t)$ .

1. If  $c$  is an extremal parameterization of a convex curve of constant breadth,  $c(t)$  is extremal in direction  $\alpha := (2\pi t)/|C|$ , and  $c(t + |C|/2)$  is extremal in direction  $\alpha + \pi$ . The arguments of Remark 3.9 show that  $c(t + |C|/2)c(t)$  is a diametral chord in direction  $\alpha$ . Hence,  $b_C(\alpha) = |c(t) - c(t + |C|/2)| = 2|c^*(t)|$  and  $c^*(t) \parallel \alpha$ .

By the remark at the beginning of this proof, the definition of extremal parameterizations implies  $\dot{c}(t) \perp \alpha \perp \dot{c}(t + |C|/2)$  wherever the derivatives exist. Hence, we have

$$\dot{c}(t) \perp c^*(t) \perp \dot{c}\left(t + \frac{|C|}{2}\right).$$

Note that these conditions are also satisfied if  $\dot{c}(t) = 0$  and/or  $\dot{c}(t + |C|/2) = 0$ . Because of  $\dot{m}(t) = \frac{1}{2}(\dot{c}(t) + \dot{c}(t + |C|/2))$ , we can conclude  $\dot{m}(t) \perp c^*(t)$ .

As in the proofs of Lemma 3.2 and Lemma 3.6, we can prove  $c^*(t) \perp c^*(t)$ .

2. Now, assume we have  $\dot{m}(t) \perp c^*(t) \perp \dot{c}^*(t)$  wherever the derivatives exist.

As already stated in (2.14) the definitions of  $m(t)$  and  $c^*(t)$  in (3.1) imply

$$c(t) = m(t) + c^*(t) \quad \text{and} \quad c\left(t + \frac{|C|}{2}\right) = m(t) - c^*(t).$$

Hence, from the assumption we derive  $\dot{c}(t) \perp c^*(t) \perp \dot{c}(t + |C|/2)$ . If  $\dot{c}(t) \neq 0$ , this combined with the convexity of  $C$  implies that there is a supporting line of  $C$  through  $c(t)$  which is orthogonal to  $c^*(t)$ . With more complicated arguments we prove this statement for every  $t \in [0, |C|)$  in the end of this proof.

This shows that for every  $t$  there are supporting lines of  $C$  through  $c(t)$  and through  $c(t + |C|/2)$  which are orthogonal to  $c^*(t)$ . Thus, the breadth of  $C$  in the direction of  $c^*(t)$  equals  $|c(t) - c(t + |C|/2)| = 2|c^*(t)|$ .

As in the proofs of Lemma 3.2 and Lemma 3.6, from  $c^*(t) \perp c^*(t)$  we can conclude that  $|c^*(t)|$  is constant, which completes the proof.



We still have to show that even in the case  $\dot{c}(t) = 0$ , there exists a supporting line of  $C$  through  $c(t)$  which is orthogonal to  $c^*(t)$ .

To this end, we define  $\alpha(t)$  to be the direction of  $\dot{c}(t)$  if the derivative exists and does not disappear. The remaining case we denote by  $\alpha(t) = \emptyset$ . We may assume that  $c$  traverses  $C$  counter-clockwise, because otherwise we can use  $\tilde{c}(t) := c(|C| - t)$ . Hence due to the convexity of  $C$ , we can choose a monotonously increasing representation of  $\alpha(t)$  with values in an interval  $[a, a + 2\pi)$ . Now, we define

$$\begin{aligned} \alpha_-(t) &:= \sup \{ \alpha(\tau) \mid \tau \leq t \wedge \alpha(\tau) \neq \emptyset \} \\ \text{and } \alpha_+(t) &:= \inf \{ \alpha(\tau) \mid \tau \geq t \wedge \alpha(\tau) \neq \emptyset \} \end{aligned}$$

Then, due to convexity for every  $\beta \in [\alpha_-(t), \alpha_+(t)]$  there is a supporting line of  $C$  through  $c(t)$  in direction  $\beta$ .

By arguments analogous to the proof of Lemma 2.21.2 the direction of  $c^*(t)$  is also monotonously increasing. And by our arguments for the case  $\dot{c}(t) \neq 0$ , there exist values  $t_- \leq t$  and  $t_+ \geq t$  such that  $c^*(t_-) \perp \alpha_-$  and  $c^*(t_+) \perp \alpha_+$ . Because the direction of  $c^*(t)$  lies in between the directions of  $c^*(t_1)$  and  $c^*(t_2)$ , it is therefore orthogonal to a direction in  $[\alpha_-, \alpha_+]$ . This shows that there exists a supporting line of  $C$  through  $c(t)$  which is orthogonal to  $c^*(t)$ .  $\square$

This leads to the *duality* between curves of constant breadth and Zindler curves stated in the following corollary and visualized in Figure 3.11. The dual of the Reuleaux triangle shown there, is the flower  $C_F$ , which we analyze in Section 3.2.2.

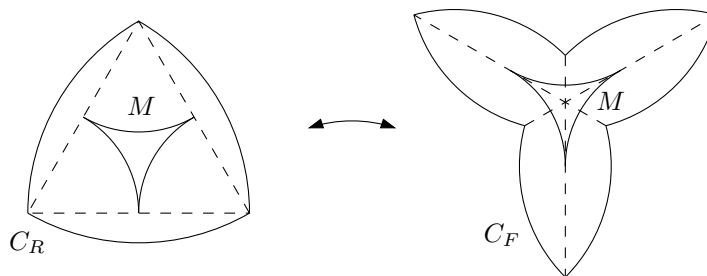


Figure 3.11: The *Reuleaux-triangle* is the best-known curve of constant breadth. Its dual is the flower  $C_F$ .

**Corollary 3.11.** 1. Let  $C \subset \mathbb{R}^2$  be a convex curve of constant breadth given by a piecewise twice continuously differentiable parameterization. If one rotates every diametral chord by  $90^\circ$  about its midpoint, the curve formed by the endpoints of the turned chords is a Zindler curve of halving distance  $D(C)$ .

2. Let  $C \in \mathcal{C}$  be a Zindler curve with interior halving chords<sup>6</sup>. We rotate every halving chord by  $90^\circ$  about its midpoint. If the curve formed by the endpoints of the turned chords is convex, it is a curve of constant breadth. And its diameter equals  $H(C)$ .

<sup>6</sup>Remember that in particular every convex curve has interior (halving) chords.

*Proof.* 1. We have discussed in the beginning of this subsection that the curvature of the given curve of constant breadth  $C$  does not disappear at any point  $p \in C$ . Hence, Lemma A.5 from Appendix A.3 shows that there exists a piecewise continuously differentiable extremal parameterization  $c : [0, |C|) \rightarrow C$ .

Lemma 3.10 gives  $\dot{m}(t) \perp c^*(t) \perp \dot{c}^*(t)$  wherever the derivatives exist. Now, if we turn every diametral chord  $c(t)c(t+|C|/2)$  by  $90^\circ$  about its midpoint, we get a parameterization  $\tilde{c} : [0, |C|) \rightarrow \tilde{C}$  of a new closed curve  $\tilde{C}$  which satisfies

$$\dot{\tilde{m}}(t) \parallel \tilde{c}^*(t) \perp \dot{\tilde{c}}^*(t)$$

because  $\dot{\tilde{m}}(t) = \dot{m}(t)$ ,  $\tilde{c}^*(t) = R^{90^\circ} c^*(t)$  and  $\dot{\tilde{c}}^*(t) = R^{90^\circ} \dot{c}^*(t)$ . By Theorem 3.3 this suffices to prove that  $\tilde{C}$  is a Zindler curve of halving distance  $2|c^*(t)| = D(C)$ .

2. Let  $c : [0, |C|) \rightarrow C$  be a halving-pair parameterization of a given Zindler curve with interior halving chords. Then, Theorem 3.3 and Lemma 3.4 show  $\dot{m}(t) \parallel c^*(t) \perp \dot{c}^*(t)$  wherever the derivatives exist. If we turn every halving chord  $c(t)c(t+|C|/2)$  by  $90^\circ$  about its midpoint, we get a parameterization  $\tilde{c} : [0, |C|) \rightarrow \tilde{C}$  of a new closed curve  $\tilde{C}$  which satisfies

$$\dot{\tilde{m}}(t) \perp \tilde{c}^*(t) \perp \dot{\tilde{c}}^*(t)$$

because  $\dot{\tilde{m}}(t) = \dot{m}(t)$ ,  $\tilde{c}^*(t) = R^{90^\circ} c^*(t)$  and  $\dot{\tilde{c}}^*(t) = R^{90^\circ} \dot{c}^*(t)$ . If  $\tilde{C}$  is convex, by Lemma 3.10 this suffices to prove that  $\tilde{C}$  is a curve of constant breadth with diameter  $2|c^*(t)| = H(C)$ .

□

### 3.1.4 Floating equilibrium

As mentioned before, Auerbach [10] was interested in Zindler curves because he wanted to answer a question by S. Ulam concerning bodies floating in water.

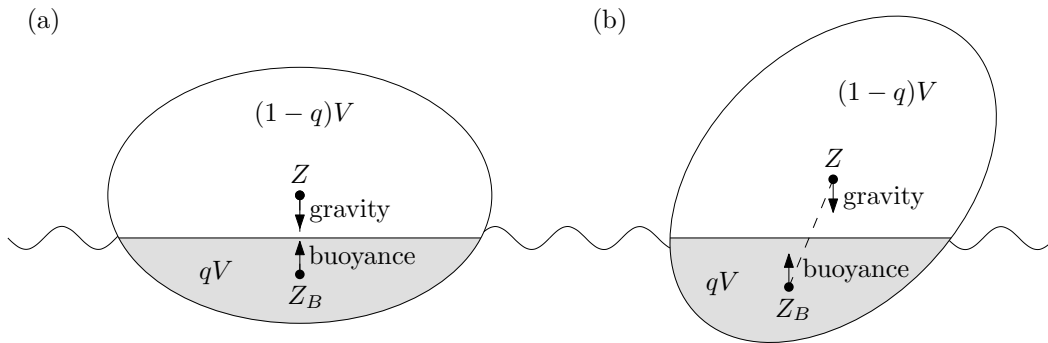


Figure 3.12: An ellipsoid of density  $q = 1/3$  floats in equilibrium only for few directions (two-dimensional cross-section).

Consider Figure 3.12. Assume we let a three dimensional body of volume  $V$  and of a certain uniform density  $q$ ,  $0 < q < 1$ , float in water. Because the density of water equals 1, this means that by *Archimedes' principle* a part of volume  $qV$  will be below the waterline and  $(1-q)V$  will be above.

Whether the body is in an equilibrium with respect to rotation or not depends on the positions of two particular *centers of gravity*, also called *centers of mass* or *centroids*. The first one is the centroid  $Z$  of the whole ellipsoid. The second one is the center of mass  $Z_B$  of the part which lies below the waterline.

The buoyancy pulls  $Z_B$  upward in a direction perpendicular to the waterline. And gravity pushes  $Z$  downward in the opposite direction. Thus, if the line segment  $Z_BZ$  is perpendicular to the waterline, the two forces cancel out each other, and the body is in an equilibrium. In every other position, the forces will result in a rotation.

It is easy to see that the sphere floats in an equilibrium for every direction and for every density  $q$ . Ulam's question is whether for any density  $q$  there exists a different body which is in a floating equilibrium for every direction. This question is still unanswered.

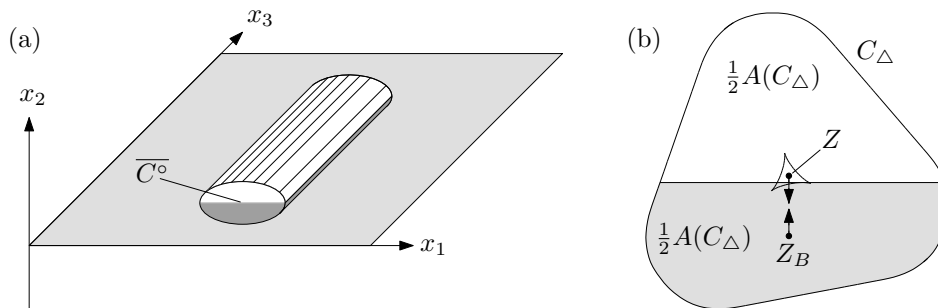


Figure 3.13: (a) An elliptic cylinder of density  $1/2$  floating in water. (b) A rounded triangle of density  $1/2$  floats in an equilibrium for every direction, because it is a Zindler curve.

Surprisingly, Auerbach gave a positive answer to the analogous question for two dimensions and density  $1/2$ . Consider Figure 3.13.a. For a convex cycle  $C$  in the plane, we consider a three-dimensional cylinder of density  $q$  whose cross section is the region  $\overline{C^\circ}$  bounded by  $C$ . More formally, the cylinder is defined as  $\overline{C^\circ} \times [0, 1]$ , if the length of the log equals 1.

To decide whether the cylinder is in an equilibrium with respect to rotation around its main axis (movement orthogonal to the third coordinate axis), it suffices to consider  $C$ . Analogous to the three-dimensional case, for every direction we can consider the two-dimensional centroid  $Z$  of  $\overline{C^\circ}$  and the centroid  $Z_B$  of the area below the waterline. Here, the waterline is a line which divides  $\overline{C^\circ}$  in the lower part of area  $qA(C)$  and the upper part of area  $(1 - q)A$ .

We say that  $C$  has the *equilibrium property* for density  $q$  if the segment  $Z_BZ$  is orthogonal to the waterline for every direction. Auerbach proved the following statement, which is exemplified in Figure 3.13.b.

**Theorem 3.12.** (Auerbach [10]) *A convex closed curve  $C$  in the plane has the equilibrium property for density  $1/2$  if and only if it is a Zindler curve.*

We do not want to repeat the proof here, but we want to mention an implication of Auerbach's work he was not (and could not be) aware of. He wrote that he did not know if there exists any curve with equilibrium property for any density  $q \neq 1/2$  besides the circle, see [10, p. 122]. However, his proof shows that for such a curve  $C$  all the chords which divide  $\overline{C^\circ}$  in two parts of area  $qA(C)$  and  $(1 - q)A(C)$  would have to have the same length, see the very beginning of

§3 in [10, p. 128]. This means that the curve would be what Mampel [145] calls a generalized Zindler curve. But he proved in 1969, 31 years after Auerbach's article, that closed Zindler curves can only exist for  $q = 1/2$ . Hence, Auerbach's question is answered. For density  $q \neq 1/2$  the circle is the only cycle with equilibrium property.

## 3.2 Example curves

### 3.2.1 Rounded triangle

The rounded triangle  $C_\Delta$  shown in Figure 3.14 is probably the most important Zindler curve. It was also analyzed by Auerbach [10, pp. 140f.].

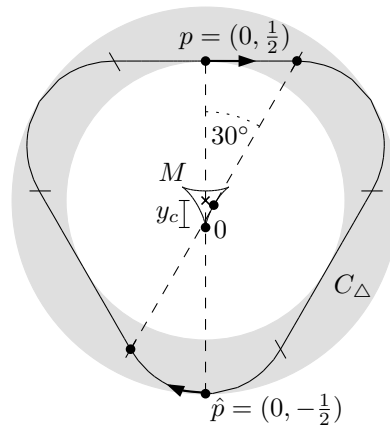


Figure 3.14: The construction of the rounded triangle  $C_\Delta$ .

We construct it by starting with a pair of points  $p := (0, \frac{1}{2})$  and  $\hat{p} := (0, -\frac{1}{2})$ . Next, we move  $p$  to the right along a horizontal line. Simultaneously,  $\hat{p}$  moves to the left such that the distance  $|p\hat{p}| = 1$  is preserved and both points move with equal speed. These conditions lead to a differential equation which we solve after the description of the construction.

We move  $p$  and  $\hat{p}$  like this until the connecting line segment  $p\hat{p}$  forms an angle of  $30^\circ$  with the  $y$ -axis. Next, we swap the roles of  $p$  and  $\hat{p}$ . Now,  $\hat{p}$  moves along a line with the direction of its last movement, and  $p$  moves with equal speed on the unique curve which guarantees  $|p\hat{p}| \equiv 1$ , until  $p\hat{p}$  has rotated with another  $60^\circ$ . Again, we swap the roles of  $p$  and  $\hat{p}$  for the next  $60^\circ$  and so forth. In this way we end up with six pieces of equal length (three straight line segments and three curved pieces) to build the rounded triangle  $C_\Delta$  shown in Figure 3.14.a. Note again that the rounded pieces are not parts of circles. This can be verified later, when we have a closed form for a parameterization.

Such a parameterization of  $C_\Delta$  can be found by two different approaches, by solving the differential equation or by considering the midpoint curve.

First, we solve the differential equation. Because of the symmetry, it suffices to give a parameterization of the first half rounded piece. As the curve  $C_\Delta$  contains three curved pieces, it consists of six halves like the one described in the following. Together with the straight line

segments of the same length they build the whole rounded triangle.

The piece examined here starts at  $c(0) := (0, -\frac{1}{2})$  and it is determined by the two conditions

$$\begin{aligned} |p\hat{p}| &= \sqrt{(x(t) - t)^2 + (y(t) - \frac{1}{2})^2} \equiv 1 \\ \text{and } |\dot{c}(t)| &= \sqrt{x'(t)^2 + y'(t)^2} \equiv 1. \end{aligned} \quad (3.7)$$

Solving the first one for  $y$  yields

$$\begin{aligned} (y - \frac{1}{2})^2 &= 1 - (x - t)^2 \Rightarrow y - \frac{1}{2} = \sqrt{1 - (x - t)^2} \\ &\Leftrightarrow y = \sqrt{1 - (x - t)^2} + \frac{1}{2}. \end{aligned}$$

We take the derivative with respect to  $t$ . By combining this with the second equality from (3.7), which we solve for  $y'(t)$ , we get

$$-\frac{(x(t) - t)(x'(t) - 1)}{\sqrt{1 - (x(t) - t)^2}} = y'(t) = \sqrt{1 - x'(t)^2}.$$

By squaring we get the quadratic equation

$$\begin{aligned} (x - t)^2 (x' - 1)^2 &= (1 - (x - t)^2) (1 - x'^2) \\ \Leftrightarrow (x - t)^2 \left( (x' - 1)^2 + (1 - x'^2) \right) &= 1 - x'^2 \\ \Leftrightarrow (x - t)^2 2(1 - x') - (1 + x')(1 - x') &= 0 \\ \Leftrightarrow (1 - x') \left( 2(x - t)^2 - (1 + x') \right) &= 0. \end{aligned}$$

As the second possible solution  $x'(t) \equiv 1$  does not make any sense in this context, we get

$$x'(t) = 2(x(t) - t)^2 - 1. \quad (3.8)$$

This differential equation with the constraint  $x(0) = 0$  yields

$$x(t) = t - \frac{e^{4t} - 1}{e^{4t} + 1} \quad \text{and} \quad y(t) = -2\frac{e^{2t}}{e^{4t} + 1} + \frac{1}{2}. \quad (3.9)$$

The first of the twelve pieces ends at the  $t$ -value  $t_1$  when the halving chord has reached an angle of  $+60^\circ$ , i.e. an angle of  $30^\circ$  with the  $y$ -axis. By Theorem 3.3 we know that this means  $\dot{m}(t_1) = |\dot{m}(t_1)|(\cos 60^\circ, \sin 60^\circ)$ . But  $\dot{m}(t_1)$  is the arithmetic mean of the two unit vectors  $\dot{c}(t_1)$  and  $\dot{c}(t_1 + |C|/2)$ . As  $\dot{c}(t_1 + |C|/2) = (1, 0) = (\cos 0^\circ, \sin 0^\circ)$ , we conclude  $\dot{c}(t_1) = (\cos 120^\circ, \sin 120^\circ)$ , in particular  $x'(t_1) = \cos 120^\circ = -\frac{1}{2}$ . By applying (3.8), (3.9), and by substituting  $z := e^{4t_1}$ , we get

$$\begin{aligned} -\frac{1}{2} &= x'(t_1) \stackrel{(3.8)}{=} 2(x(t_1) - t_1)^2 - 1 \stackrel{(3.9)}{=} 2\left(\frac{e^{4t_1} - 1}{e^{4t_1} + 1}\right)^2 - 1 \\ &= \frac{2(z - 1)^2 - (z + 1)^2}{(z + 1)^2} = \frac{z^2 - 6z + 1}{z^2 + 2z + 1} \\ \Leftrightarrow -z^2 - 2z - 1 &= 2z^2 - 12z + 2 \Leftrightarrow 3z^2 - 10z + 3 = 0 \\ \Leftrightarrow z^2 - \frac{10}{3}z + 1 &= 0 \end{aligned}$$

which has the solution  $z = \frac{5}{3} \pm \sqrt{\left(\frac{5}{3}\right)^2 - 1} = \frac{5}{3} \pm \frac{4}{3}$ . As we are looking for a positive solution  $t_1$ , we get  $z = 3$  and  $t_1 = \ln(3)/4$ . The whole closed curve consists of twelve parts of this length. Hence, its perimeter equals

$$|C_\Delta| = 12 \frac{\ln 3}{4} = 3 \ln 3 \approx 3.2958. \quad (3.10)$$

Auerbach [10, p. 141] obtained the same result with different methods. By Theorem 2.12 this results in

$$\delta(C_\Delta) \stackrel{\text{Thm. 2.12}}{=} \frac{|C_\Delta|}{2h(C_\Delta)} = \frac{3}{2} \ln 3 \approx 1.6479.$$

Another approach for analyzing the rounded triangle is to consider its midpoint curve. As we will discuss now, it is built from six congruent pieces that are arcs of a tractrix.

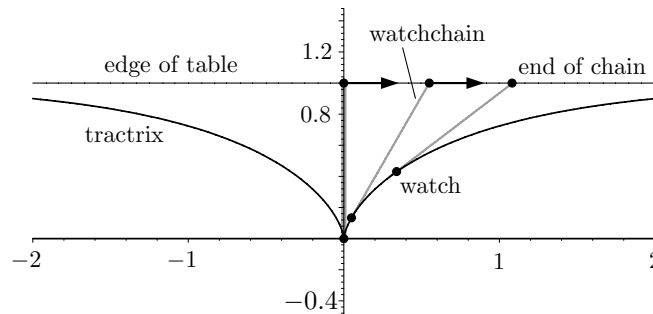


Figure 3.15: The tractrix, the curve of a watch on a table towed with its watchchain (the curve is symmetric about the  $y$ -axis).

The tractrix is illustrated in Figure 3.15. It was first studied by Huygens and Leibniz in 1692, see for instance Yates' [185, p. 221] and Lockwood's [144, p. 124] collections of curves. The following explanation stems from Leibniz.

A watch is placed on a table, say at the origin  $(0,0)$  and the end of its watchchain of length 1 is pulled along the horizontal edge of the table starting at  $(0,1)$ , either to the left or to the right. As the watch is towed in the direction of the chain, the chain is always tangent to the path of the watch, the tractrix.

From the definition it is clear that the midpoint curve  $M_\Delta$  of the cycle  $C_\Delta$  scaled by 2 consists of such tractrix pieces. This happens plotted in Figure 3.16. The reason for  $2M_\Delta$  to consist of tractrix pieces is that by definition, by Theorem 3.3 and by Lemma 3.4 the halving chords of  $C_\Delta$  are always tangent to the midpoint curve, always one of the points of these pairs is moving on a straight line, and its distance to the midpoint curve stays  $\frac{1}{2}$ .

This is a special case of a more general relation between Zindler curves and tractrix curves. As Theorem 3.3 and Lemma 3.4 apply to every Zindler curve with interior halving chords, the halving chords are always tangent to the midpoint curve for every member of this class of curves. Hence, each midpoint curve of such a Zindler curve can be regarded as a kind of tractrix in the sense that it describes the movement of an object which is towed and/or pushed by a stick of length  $h/2$  whose other endpoint moves on the curve  $C$ . Mampel [145] noticed this fact and it motivated him to examine the class of generalized tractrices more deeply.

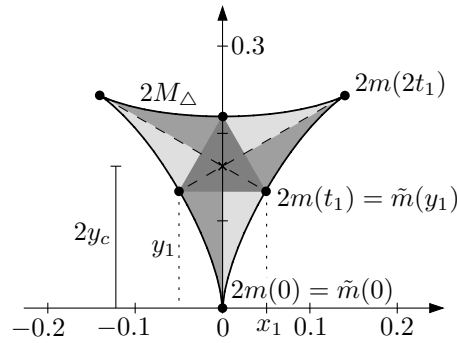


Figure 3.16: We can calculate the area of  $2M_\Delta$  by adding six times the area of the curved bright grey triangle and the area of the equilateral triangle in the center.

For our analysis of the rounded triangle  $C_\Delta$  it suffices to consider the ordinary tractrix. There are several known parameterizations, and we can use them to calculate the area  $A(M_\Delta)$ . Then, we only have to plug the result into the corollary of Holditch's theorem, Corollary 2.30, to get the area of  $C_\Delta$ .

Because we want to apply the known tractrix parameterizations without the annoying factor  $1/2$ , we calculate the area of the curve  $2M_\Delta$ . First we examine the area of the curved bright grey triangle in Figure 3.16. It is the area between the tractrix curve  $2m(t)$  restricted to the interval  $[0, t_1]$ , and the  $y$ -axis. For the necessary integration we use a different parameterization of the tractrix, depending on the  $y$ -coordinate. The following parameterization can be found in every book on curves, e.g. [185, p. 222], [144, p. 123].

$$\tilde{m}(y) := (\operatorname{arcsech}(1 - y) - \sqrt{1 - (1 - y)^2}, y)$$

First, we want to figure out at which parameter-value  $y_1$  the point  $2m(t_1)$  is reached. By construction this is when the derivative vector  $\dot{\tilde{m}}(y)$  points to the direction  $(\cos 60^\circ, \sin 60^\circ)$ . As the  $y$ -value of the derivative always equals 1, the  $x$ -value must satisfy

$$\frac{d}{dy} \left( \operatorname{arcsech}(1 - y) - \sqrt{2y - y^2} \right) \Big|_{y=y_1} = \tilde{m}'_x(y_1) \stackrel{!}{=} \frac{\cos 60^\circ}{\sin 60^\circ} = \frac{1}{\sqrt{3}}.$$

As

$$\frac{d}{d\tau} \operatorname{arcsech}(\tau) \Big|_{\tau=t} = -\frac{1}{t\sqrt{1-t^2}},$$

we get

$$\begin{aligned} \tilde{m}'_x(y) &= \frac{1}{(1-y)\sqrt{1-(1-y)^2}} - \frac{2-2y}{2\sqrt{2y-y^2}} \\ &= \frac{1}{(1-y)\sqrt{2y-y^2}} - \frac{(1-y)^2}{(1-y)\sqrt{2y-y^2}} \\ &= \frac{2y-y^2}{(1-y)\sqrt{2y-y^2}} = \frac{\sqrt{2y-y^2}}{1-y}. \end{aligned} \tag{3.11}$$

Regarding  $y_1$ , this implies

$$\begin{aligned} \frac{1}{\sqrt{3}} &= \frac{\sqrt{2y_1 - y_1^2}}{1 - y_1} \Rightarrow (1 - y_1)^2 = 3(2y_1 - y_1^2) \\ \Rightarrow y_1^2 - 2y_1 + \frac{1}{4} &= 0 \Rightarrow y_1 = 1 \pm \frac{\sqrt{3}}{2}. \end{aligned}$$

Because we are looking for a solution in the interval  $[0, 1]$ , we conclude

$$y_1 = 1 - \frac{\sqrt{3}}{2}. \quad (3.12)$$

As a side effect, this enables us to calculate the length of  $M_\Delta$ , which will be helpful for comparing the rounded triangle  $C_\Delta$  to Zindler's example curve  $C_Z$ .

$$\begin{aligned} |M_\Delta| &= \frac{1}{2}|2M_\Delta| = \frac{1}{2}6 \int_0^{y_1} \sqrt{1 + \tilde{m}_x'^2(y)} dy & (3.13) \\ &\stackrel{(3.11)}{=} 3 \int_0^{1 - \frac{\sqrt{3}}{2}} \sqrt{1 + \frac{2y - y^2}{(1 - y)^2}} dy = 3 \int_0^{1 - \frac{\sqrt{3}}{2}} \frac{1}{1 - y} dy \\ &\stackrel{t=1-y}{=} 3 \int_{\frac{\sqrt{3}}{2}}^1 \frac{1}{t} dt = -3 \ln\left(\frac{\sqrt{3}}{2}\right) \end{aligned}$$

We get back to calculating  $A(2M_\Delta)$ . Next, we integrate  $\tilde{m}_x$  and get

$$\int_0^{y_1} \tilde{m}_x(\tau) d\tau = \left[ -(1 - \tau) \operatorname{arcsech}(1 - \tau) + \arctan \sqrt{\frac{1}{(1 - \tau)^2} - 1} + \frac{1}{2}(1 - \tau) \sqrt{2\tau - \tau^2} - \frac{1}{2} \arcsin(\tau - 1) \right]_0^{y_1}.$$

Hence, the area of the bright grey curved triangle equals

$$\begin{aligned} &-\frac{\sqrt{3}}{2} \underbrace{\operatorname{arcsech} \frac{\sqrt{3}}{2}}_{=\ln(3)/2} + \underbrace{\arctan \frac{1}{\sqrt{3}}}_{=\pi/6} + \frac{\sqrt{3}}{8} - \frac{1}{2} \underbrace{\arcsin\left(-\frac{\sqrt{3}}{2}\right)}_{=-\pi/3} \\ &+ \underbrace{\operatorname{arcsech}(1)}_{=0} - \underbrace{\arctan(0)}_{=0} - 0 + \frac{1}{2} \underbrace{\arcsin(-1)}_{=-\pi/4} \\ &= -\frac{\sqrt{3} \ln 3}{4} + \frac{\pi}{6} + \frac{\sqrt{3}}{8} + \frac{\pi}{6} - \frac{\pi}{4} \\ &= +\frac{\pi}{12} + \frac{\sqrt{3}}{8} - \frac{\sqrt{3} \ln 3}{4} \end{aligned}$$

It remains to calculate the area of the dark grey, equilateral triangle in Figure 3.16. But this is easy. The side-length of the triangle equals

$$2\tilde{m}_x(y_1) = 2 \underbrace{\operatorname{arcsech} \frac{\sqrt{3}}{2}}_{=\ln(3)/2} - 2 \underbrace{\sqrt{1 - \left(\frac{\sqrt{3}}{2}\right)^2}}_{=1/2} = \ln(3) - 1.$$



As the area of an equilateral triangle of side-length one equals  $\sqrt{3}/4$ , the area of the dark grey triangle is  $(\ln(3) - 1)^2 \sqrt{3}/4$ . As said before, the area of  $2M_\Delta$  equals six times the area of the light grey curved triangle plus the area of the dark grey equilateral triangle. This yields

$$\begin{aligned} A(M_\Delta) &= \frac{1}{4}A(2M_\Delta) = \frac{1}{4} \left( 6 \left( \frac{\pi}{12} + \frac{\sqrt{3}}{8} - \frac{\sqrt{3} \ln 3}{4} \right) + (\ln(3) - 1)^2 \frac{\sqrt{3}}{4} \right) \\ &= \frac{\pi}{8} + \frac{\sqrt{3}}{16} (\ln^2(3) - 8 \ln(3) + 4) \approx 0.004942 \end{aligned}$$

As the midpoint curve is traversed twice counter-clockwise when the rounded triangle is traversed once clockwise, Corollary 2.30, which resulted from applying Holditch's theorem to the halving pair transformation, yields

$$\begin{aligned} A(C_\Delta) &= A(C_\Delta^*) - 2A(M_\Delta) = \frac{\pi}{4} - 2 \left( \frac{\pi}{8} + \frac{\sqrt{3}}{16} (\ln^2(3) - 8 \ln(3) + 4) \right) \\ &= \frac{\sqrt{3}}{8} (8 \ln(3) - \ln^2(3) - 4) \approx 0.7755. \end{aligned} \quad (3.14)$$

Again, this confirms Auerbach's result [10, p. 141]. We conjecture – in accordance with Auerbach [10, p. 138] – that the rounded triangle is the convex Zindler curve which attains smallest possible area for a given halving distance  $h$ . By Corollary 2.30 this is equivalent to the statement that its midpoint curve attains the maximum area amongst these curves. It seems that it is not possible to increase the area of the midpoint curve  $M_\Delta$  without giving up the convexity of the original curve. However, we have no proof so far. Auerbach also conjectured that the rounded triangle maximizes the perimeter amongst Zindler curves. In the light of Lemma 2.25 this is related but not necessarily equivalent to maximizing the perimeter of the midpoint curve.

**Open Problem 4.** *Does the rounded triangle  $C_\Delta$  minimize  $A/h^2$  amongst convex Zindler curves? Does it maximize  $|C|/h$ ?*

Next, we want to calculate the inradius  $r(C_\Delta)$  and the circumradius  $R(C_\Delta)$  of the rounded triangle. We need these values for calculating the benefit of  $C_\Delta$  for the design of networks of small dilation in Section 5.2.4. From the construction it follows

$$r(C_\Delta) = \frac{1}{2} - y_c, \quad R(C_\Delta) = \frac{1}{2} + y_c,$$

where  $y_c$  denotes the distance between the center  $c$  of the midpoint curve  $M_\Delta$  and the lower intersection of  $M_\Delta$  and the  $y$ -axis, see Figure 3.14. The analysis of  $M_\Delta$  shows on the other hand that  $2y_c$  equals  $y_1$  plus one third of the height of the equilateral triangle of side length  $2x_1$ , see Figure 3.16. The height of this equilateral triangle equals  $\sqrt{3}x_1$ , and  $x_1$  is given by

$$\begin{aligned} x_1 &:= \tilde{m}_x(y_1) = \operatorname{arcsech}(1 - y_1) - \sqrt{1 - (1 - y_1)^2} \\ &\stackrel{(3.12)}{=} \operatorname{arcsech} \left( \frac{\sqrt{3}}{2} \right) - \frac{1}{2} \operatorname{arcsech}(x) \stackrel{\operatorname{arcsech}(x) = \ln \left( \frac{1}{x} + \sqrt{\frac{1}{x^2} - 1} \right)}{=} \frac{\ln(3) - 1}{2}. \end{aligned} \quad (3.15)$$

This yields

$$\begin{aligned} 2y_c &= y_1 + \frac{1}{3}\sqrt{3}x_1 \stackrel{(3.12), (3.15)}{=} 1 - \frac{\sqrt{3}}{2} + \frac{1}{\sqrt{3}} \frac{\ln(3) - 1}{2} \\ &= 1 + \frac{1}{\sqrt{3}} \left( \frac{\ln 3}{2} - 2 \right) \end{aligned}$$

and finally

$$\begin{aligned} r(C_\Delta) &= \frac{1}{2} - y_c = \frac{1}{\sqrt{3}} \left( 1 - \frac{\ln 3}{4} \right) \approx 0.4188 \\ R(C_\Delta) &= \frac{1}{2} + y_c = 1 - \frac{1}{\sqrt{3}} \left( 1 - \frac{\ln 3}{4} \right) \approx 0.5812 \end{aligned} \tag{3.16}$$

In the end, we want to prove that the rounded pieces of  $C_\Delta$  are not circular arcs. We concentrate on the arc  $c(|C|/2, |C|/2 + t_1)$  starting at  $\hat{p}$  in Figure 3.14. The derivative vector turns by  $60^\circ = \frac{\pi}{3}$  during the traversal of this arc. Hence, if it was a circular arc, the radius would have to satisfy

$$\frac{\pi}{3} \tilde{r} = t_1 = \frac{\ln 3}{4} \Rightarrow \tilde{r} = \frac{3 \ln 3}{4\pi}.$$

The midpoint of the circle had to be

$$\tilde{m} = \left( 0, -\frac{1}{2} + \frac{3 \ln 3}{4\pi} \right).$$

But then, the  $y$ -coordinate of  $c(|C|/2 + t_1)$  would be

$$\tilde{m}_y + \tilde{r} \sin\left(\frac{7}{6}\pi\right) = -\frac{1}{2} + \frac{3 \ln 3}{4\pi} \underbrace{\left(1 + \sin\left(\frac{7}{6}\pi\right)\right)}_{=-\frac{1}{2}} = \frac{1}{2} \left(-1 + \frac{3 \ln 3}{4\pi}\right).$$

On the other hand, because  $c(t_1) = (t_1, 1/2)$  it had to equal

$$\frac{1}{2} + 1 \cdot \underbrace{\sin\left(\frac{4}{3}\pi\right)}_{=-\frac{\sqrt{3}}{2}} = \frac{1 - \sqrt{3}}{2}.$$

It is easy to see that both values do not equal. Hence, the rounded parts of  $C_\Delta$  are not circular arcs.

Analogously to the construction of the rounded triangle we can also build rounded  $(2n + 1)$ -gons for every  $n \in \mathbb{N}$ . Within the construction at the beginning of this sub-section, we simply have to swap the roles of  $p$  and  $\hat{p}$  each time the chord  $p\hat{p}$  has turned by another  $90^\circ/(2n + 1)$ . Figure 3.17 shows the *rounded pentagon* constructed this way. The midpoint curves of all these curves consist of tractrix pieces and have  $2n + 1$  corners.

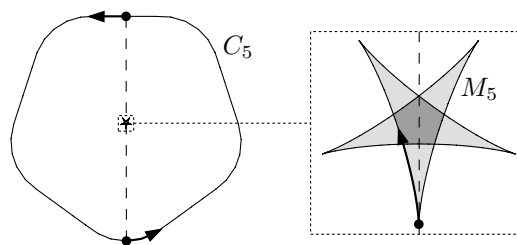


Figure 3.17: Analogously to the rounded triangle, we can build a rounded  $(2n + 1)$ -gon for every  $n \in \mathbb{N}$ . This figure shows a rounded pentagon and its midpoint curve.

### 3.2.2 Flower

In this subsection we construct and analyze another important Zindler curve, the *flower*  $C_F$ . It appears first in Zindler's article [186, p. 52]. In the introduction of this chapter we have mentioned that it consists of six circular arcs. Also, we have mentioned before that it is the dual of the Reuleaux-triangle, see Figure 3.11. We used it in [56, 58] to construct a grid graph of small dilation. This is explained in Chapter 5.

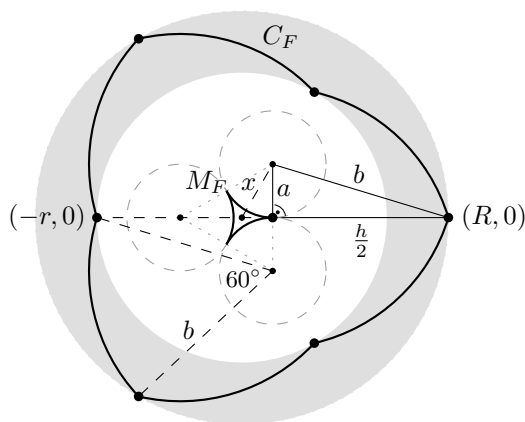


Figure 3.18: The construction of the “flower”  $C_F$ .

The construction of  $C_F$  is quite simple, see Figure 3.18. It is determined by its halving distance  $h$  and its midpoint curve  $M_F$  which consists of three concave circular arcs.

To construct  $M_F$ , we draw three circles of the same radius  $a$  *kissing* each other, i.e., each pair touches each other but does not intersect. Then, the centers of the circles build an equilateral triangle. We choose the position of the circles so that the center of the equilateral triangle is the origin  $0$  and one of its corners points towards the negative  $x$ -direction. The midpoint curve  $M_F$  is the boundary of the face built by the circles containing  $0$ .

Because of Theorem 3.3 and Lemma 3.4 there is only one way to get a Zindler curve of halving distance  $h$  with midpoint curve  $M_F$ . We move a line segment of length  $h$ , the halving chord, so that its midpoint stays on  $M_F$  and the chord is always tangent to the midpoint curve. Then, the endpoints of the chord traverse the curve  $C_F$  which consists of six circular arcs,

each of radius  $b = \sqrt{a^2 + h^2/4}$  and angle  $60^\circ$  like shown in Figure 3.18. Hence, the length of  $C_F$  is given by

$$|C_F| = 2\pi b = \pi\sqrt{4a^2 + h^2} \quad (3.17)$$

Because the center of any equilateral triangle divides any of the three heights in the ratio  $2 : 1$ , it is also easy to calculate the inradius  $r$  and the circumradius  $R$ , cf. Figure 3.18. The height of the equilateral triangle formed by the three circle centers equals  $\sqrt{3}a$  because its side-length is  $2a$ . We get

$$r = \frac{h}{2} - \frac{1}{3}\sqrt{3}a = \frac{h}{2} - \frac{a}{\sqrt{3}} \quad \text{and} \quad R = \frac{h}{2} + \frac{1}{3}\sqrt{3}a = \frac{h}{2} + \frac{a}{\sqrt{3}}. \quad (3.18)$$

Additionally, we want to calculate the distance  $x$  between any of the three corners of  $M_F$  and the origin  $0$ , because we need it in Section 5.2.4. Figure 3.18 and simple trigonometry yield

$$x = \frac{2}{\sqrt{3}}a \quad (3.19)$$

Although the flower  $C_F$  is not convex, we can show that for  $a \leq \left(\frac{\sqrt{3}}{2} - \frac{1}{3}\right)h \approx 0.5327h$  its dilation is also attained by a halving pair. This can be proved by remembering the proof of Theorem 2.12. It shows that a local detour maximum can only appear at a halving pair or at a pair of points where at least at one of the points  $C$  is not strictly convex, that is where  $C$  locally is a line segment or it allows no outer tangent.

If the dilation of  $C_F$  is attained by a halving pair, its dilation equals

$$\delta_1 := \frac{|C_F|}{2h} \stackrel{(3.17)}{=} \frac{2\pi b}{2h} = \frac{\pi\sqrt{4a^2 + h^2}}{2h} = \frac{\pi}{2}\sqrt{4\left(\frac{a}{h}\right)^2 + 1} \quad (3.20)$$

The other case can only occur if one of the three non-convex corners is involved. Further analysis shows that the dilation of  $C$  is either attained by a halving pair or between two of the three non-convex corners. Their detour equals

$$\delta_2 := \frac{\frac{2\pi}{3}b}{2r \sin(60^\circ)} = \frac{2\pi}{3\sqrt{3}} \frac{b}{r}.$$

We have  $\delta_1 \geq \delta_2$  iff

$$\begin{aligned} \frac{2\pi b}{2h} \geq \frac{2\pi}{3\sqrt{3}} \frac{b}{r} &\Leftrightarrow 2h \leq 3\sqrt{3}r = 3\sqrt{3}\left(\frac{h}{2} - \frac{a}{\sqrt{3}}\right) \\ \Leftrightarrow \left(\frac{3\sqrt{3}}{2} - 2\right)h &\geq 3a \Leftrightarrow a \leq \left(\frac{\sqrt{3}}{2} - \frac{2}{3}\right)h \end{aligned}$$

This proves  $\delta(C_F) = \delta_1$  for  $a \leq \left(\frac{\sqrt{3}}{2} - \frac{2}{3}\right)h$ .

In the end of this subsection we want to prove that the flower  $C_F$  shows the tightness of the stability result in Lemma 2.39 apart from the coefficient of  $\sqrt{\varepsilon}$ .

**Remark 3.13.** We consider the flower  $C_F$  for  $a \leq \left(\frac{\sqrt{3}}{2} - \frac{2}{3}\right)h$ . Let  $\varepsilon$  be the real value satisfying  $\delta(C_F) = (1 + \varepsilon)\frac{\pi}{2}$ . Note that  $\varepsilon \searrow 0$  for  $a \searrow 0$ . Then,  $C_F$  cannot be enclosed in any  $(1 + \frac{2\sqrt{2}}{\sqrt{3}}\sqrt{\varepsilon})$ -annulus.

*Proof.* We assume  $h = 1$ . As shown above, we have

$$\delta(C_F) = \delta_1 \stackrel{(3.20)}{=} \frac{\pi}{2} \sqrt{4a^2 + 1}$$

This translates to

$$\sqrt{4a^2 + 1} = (1 + \varepsilon) \Rightarrow a = \sqrt{\frac{(1 + \varepsilon)^2 - 1}{4}} = \frac{\sqrt{\varepsilon^2 + 2\varepsilon}}{2} \quad (3.21)$$

We want to get a lower bound to  $R/r$  in terms of  $\varepsilon$ .

$$\begin{aligned} \frac{R}{r} &\stackrel{(3.18)}{=} \frac{\frac{1}{2} + \frac{a}{\sqrt{3}}}{\frac{1}{2} - \frac{a}{\sqrt{3}}} = \frac{\sqrt{3} + 2a}{\sqrt{3} - 2a} \stackrel{*}{=} 1 + \frac{4a}{\sqrt{3} - 2a} \\ &\stackrel{(3.21)}{=} 1 + \frac{2\sqrt{\varepsilon^2 + 2\varepsilon}}{\sqrt{3} - \sqrt{\varepsilon^2 + 2\varepsilon}} \geq 1 + \frac{2\sqrt{2}}{\sqrt{3}} \sqrt{\varepsilon}. \end{aligned}$$

The equality marked with ‘\*’ holds because  $(\sqrt{3} + x)/(\sqrt{3} - x) = 1 + 2x/(\sqrt{3} - x)$ . This completes the proof.  $\square$

### 3.2.3 Zindler’s example

As mentioned before, Zindler [186, Section 7] discovered some convex curves of constant halving distance already in 1921. He restricted his analysis to curves whose midpoint curves have three cusps like the one of the rounded triangle. We want to present his main example curve in this section. It was rediscovered by Salkowski [168] in 1934.

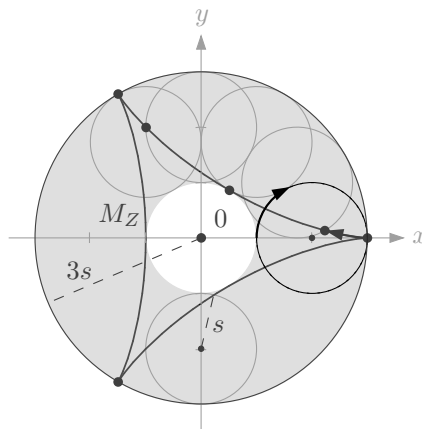


Figure 3.19: The construction of Steiner’s hypocycloid, the deltoid, which is the midpoint curve of Zindler’s example curve.

Its midpoint curve is *Steiner’s hypocycloid* also called *deltoid*, cf. [38, p. 331], [144, p. 73], [188, pp. 293f.], [182]. It is the path of a point on a circle of radius  $s$  which rolls inside a bigger circle of radius  $3s$ , see Figure 3.19.

We will denote this curve by  $M_Z$ , because it is the midpoint curve of *Zindler’s example*  $C_Z$ . Let  $\theta$  be the angle of the line segment connecting the origin  $0$ , the center of the bigger

circle, with the center of the smaller circle. Furthermore, let  $\varphi$  be the angle of the line segment connecting the center of the smaller circle with the point on its boundary which traverses  $M_Z$ . The start position is determined by  $\theta = 0$  and  $\varphi = 0$ . Because the smaller circle is rolling inside of the bigger one, we always have  $\varphi = -2\theta$ . This leads to the following parameterization.

$$m(\theta) = 2s \begin{pmatrix} \cos \theta \\ \sin \theta \end{pmatrix} + s \begin{pmatrix} \cos \varphi \\ \sin \varphi \end{pmatrix} = 2s \begin{pmatrix} \cos \theta \\ \sin \theta \end{pmatrix} + s \begin{pmatrix} \cos 2\theta \\ -\sin 2\theta \end{pmatrix} \quad (3.22)$$

As before, the Zindler curve of halving distance  $h$  with midpoint curve  $M_Z$  is built by moving a chord of length  $h$  in such a way that its midpoint stays on  $M_Z$  and it is always tangent to  $M_Z$ , see Figure 3.20.

If  $h$  is too small, the resulting Zindler curve  $C_Z$  is not convex. To be more precise, the curve  $C_Z$  is convex iff  $h \geq 48s$ . Zindler proved this in [186], basically by calculating for which  $h$ -value one has

$$\forall \theta \in [0, 4\pi) : \left\langle \ddot{c}(\theta), \mathbf{R}^{90^\circ} \dot{c}(\theta) \right\rangle \leq 0. \quad (3.23)$$

In other words, he checked for which  $h$ -value the derivative vector of the resulting parameterization always turns clockwise<sup>7</sup>. Note that this is the correct convexity condition because the resulting parameterization

$$c : [0, 4\pi) \rightarrow C_Z, \quad c(\theta) := m(\theta) + \frac{h}{2|\dot{m}|(\theta)}\dot{m}(\theta) \quad (3.24)$$

traverses  $C_Z$  clockwise. Zindler proved a more general convexity condition for any sufficiently

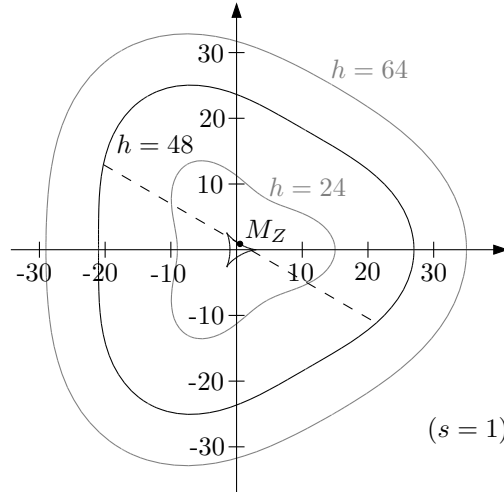


Figure 3.20: Some Zindler curves whose midpoint curve is the deltoid  $M_Z$ . The curve for  $h = 48s$  is the smallest convex one.

differentiable closed curve. His condition, see (26) in [186], depends on  $h(\alpha)$ , its first and

<sup>7</sup>Actually, Zindler considered the radius of curvature, but its sign depends only on the scalar product examined here.

second order derivative, and on the radius of curvature of  $M$  and its first order derivative. Here, we want to prove only the convexity condition for  $C_Z$ . It turns out that  $C_Z$  is convex iff  $h \geq 48s$ . This shows that the curve  $C_Z$  satisfying  $h = 48s$  is the most interesting one. Like the rounded triangle  $C_\Delta$  it is the smallest convex curve amongst all Zindler curves with the given midpoint curve, cf. Figure 3.20.

**Lemma 3.14.** *Zindler's example curve  $C_Z$  is convex iff  $h \geq 48s$ .*

*Proof.* To get a formula for  $c(\theta)$  depending only on  $\theta$ ,  $s$  and  $h$ , we calculate the derivative of  $m(\theta)$  from (3.22).

$$\begin{aligned} \dot{m}(\theta) &= 2s \begin{pmatrix} -\sin \theta \\ \cos \theta \end{pmatrix} + 2s \begin{pmatrix} -\sin 2\theta \\ -\cos 2\theta \end{pmatrix} \\ &\stackrel{\substack{\sin x + \sin y = 2 \sin \frac{x+y}{2} \cos \frac{x-y}{2}, \\ \cos x - \cos y = -2 \sin \frac{x+y}{2} \sin \frac{x-y}{2}}}{=} -4s \sin \left( \frac{3\theta}{2} \right) \begin{pmatrix} \cos \left( -\frac{\theta}{2} \right) \\ \sin \left( -\frac{\theta}{2} \right) \end{pmatrix} \end{aligned} \quad (3.25)$$

This implies  $\dot{m}(\theta)/|\dot{m}(\theta)| = (\cos(-\frac{\theta}{2}), \sin(-\frac{\theta}{2}))$ . By plugging this and the formula for  $m(\theta)$  from (3.22) into (3.24) we get

$$c(\theta) = 2s \begin{pmatrix} \cos \theta \\ \sin \theta \end{pmatrix} + s \begin{pmatrix} \cos 2\theta \\ -\sin 2\theta \end{pmatrix} + \frac{h}{2} \begin{pmatrix} \cos \left( -\frac{\theta}{2} \right) \\ \sin \left( -\frac{\theta}{2} \right) \end{pmatrix} \quad (3.26)$$

We can easily calculate the first order and the second order derivative.

$$\begin{aligned} \dot{c}(\theta) &= 2s \begin{pmatrix} -\sin \theta \\ \cos \theta \end{pmatrix} + 2s \begin{pmatrix} -\sin 2\theta \\ -\cos 2\theta \end{pmatrix} - \frac{h}{4} \begin{pmatrix} -\sin \left( -\frac{\theta}{2} \right) \\ \cos \left( -\frac{\theta}{2} \right) \end{pmatrix} \\ &\stackrel{\text{as above}}{=} 4s \sin \left( \frac{3\theta}{2} \right) \begin{pmatrix} -\cos \frac{\theta}{2} \\ \sin \frac{\theta}{2} \end{pmatrix} - \frac{h}{4} \begin{pmatrix} \sin \frac{\theta}{2} \\ \cos \frac{\theta}{2} \end{pmatrix} \end{aligned}$$

$$\begin{aligned} \ddot{c}(\theta) &= 2s \begin{pmatrix} -\cos \theta \\ -\sin \theta \end{pmatrix} + 4s \begin{pmatrix} -\cos 2\theta \\ \sin 2\theta \end{pmatrix} + \frac{h}{8} \begin{pmatrix} -\cos \left( -\frac{\theta}{2} \right) \\ -\sin \left( -\frac{\theta}{2} \right) \end{pmatrix} \\ &= 2s \begin{pmatrix} -\cos \theta + \cos 2\theta \\ -\sin \theta - \sin 2\theta \end{pmatrix} + 6s \begin{pmatrix} -\cos 2\theta \\ \sin 2\theta \end{pmatrix} + \frac{h}{8} \begin{pmatrix} -\cos \frac{\theta}{2} \\ \sin \frac{\theta}{2} \end{pmatrix} \\ &= -4s \sin \left( \frac{3\theta}{2} \right) \begin{pmatrix} \sin \frac{\theta}{2} \\ \cos \frac{\theta}{2} \end{pmatrix} + 6s \begin{pmatrix} -\cos 2\theta \\ \sin 2\theta \end{pmatrix} + \frac{h}{8} \begin{pmatrix} -\cos \frac{\theta}{2} \\ \sin \frac{\theta}{2} \end{pmatrix} \end{aligned}$$

We plug the formulas into the convexity condition (3.23). This shows that  $C_Z$  is convex iff

every  $\theta$  satisfies

$$\begin{aligned}
0 &\geq \langle \ddot{c}(\theta), \mathbf{R}^{90^\circ} \dot{c}(\theta) \rangle \\
&= 16s^2 \sin^2\left(\frac{3\theta}{2}\right) - \frac{h^2}{32} - 24s^2 \sin\left(\frac{3\theta}{2}\right) \underbrace{\left(-\sin\frac{\theta}{2} \cos 2\theta + \cos\frac{\theta}{2} \sin 2\theta\right)}_{\sin\frac{3\theta}{2}} \\
&\quad - \frac{3}{2}hs \underbrace{\left(\cos\frac{\theta}{2} \cos 2\theta + \sin\frac{\theta}{2} \sin 2\theta\right)}_{\cos\frac{3\theta}{2}} \\
&= -8s^2 \sin^2\frac{3\theta}{2} - \frac{h^2}{32} - \frac{3}{2}hs \cos\frac{3\theta}{2} \\
&= 8s^2 \cos^2\frac{3\theta}{2} - \frac{3}{2}hs \cos\frac{3\theta}{2} - \frac{h^2}{32} - 8s^2 \\
&= 2 \underbrace{\left(4s^2 \cos^2\frac{3\theta}{2} - \frac{3}{4}hs \cos\frac{3\theta}{2} + \frac{9}{256}h^2\right)}_{(2s \cos\frac{3\theta}{2} - \frac{3}{16}h)^2} - \frac{13}{128}h^2 - 8s^2.
\end{aligned}$$

Obviously the part in brackets on the right-hand side attains its maximum where  $\cos\frac{3\theta}{2} = -1$ . Hence the condition is fulfilled for every  $\theta$  iff

$$\begin{aligned}
0 &\geq 2 \left(4s^2 + \frac{3}{4}hs + \frac{9}{256}h^2\right) - \frac{13}{128}h^2 - 8s^2 \\
\Leftrightarrow 0 &\geq \frac{3}{2}hs - \frac{h^2}{32} \Leftrightarrow h \geq 48s.
\end{aligned}$$

This completes the proof of the lemma.  $\square$

Figure 3.20 might raise the conjecture that Zindler's example curve  $C_Z$  for  $h = 48s$  equals the rounded triangle  $C_\Delta$ . We disprove this by considering the length of the deltoid  $M_Z$ . It equals

$$\begin{aligned}
|M_Z| &= \int_0^{2\pi} |\dot{m}(\theta)| d\theta \stackrel{(3.25)}{=} \int_0^{2\pi} \left|4s \sin\frac{3\theta}{2}\right| d\theta \tag{3.27} \\
&= 3 \int_0^{\frac{2}{3}\pi} 4s \sin\frac{3\theta}{2} d\theta \stackrel{\alpha=\frac{3}{2}\theta}{=} 3 \int_0^\pi 4s \sin(\alpha) \frac{2}{3} d\alpha \\
&= 8s \int_0^\pi \sin(\alpha) d\alpha = 8s [-\cos\alpha]_0^\pi = 16s.
\end{aligned}$$

This means that for  $h = 48s$  and  $s = 1$  the length of the midpoint curve would equal 16. Scaling everything down to  $h = 1$  yields

$$\frac{|M_Z|}{h} = \frac{1}{3} \approx 0.3333 \neq 0.4315 \approx -3 \ln\left(\frac{\sqrt{3}}{2}\right) \stackrel{(3.13)}{=} \frac{M_\Delta}{h}.$$

This shows that indeed the two curves  $C_\Delta$  and  $C_Z$  are different.



Our conjecture from Open Problem 4, that the rounded triangle minimizes the area amongst convex Zindler curves, motivates us to calculate the area of Zindler's example for  $h = 48s$ . The area of the deltoid is known to equal  $A(M_Z) = 2\pi s^2$ , see for instance [144, p. 58], [182].

To be able to compare  $A(C_Z)$  easily to  $A(C_\Delta)$ , we set  $h = 1$  and  $s = 1/48$ . Like in the two previous examples, the midpoint curve is traversed twice clockwise while the Zindler curve is traversed once counter-clockwise. With the notation of Corollary 2.30, this results in  $I(M_Z) = -2A(M_Z)$ . The area formula from this corollary of Holditch's theorem yields

$$A(C_Z) \stackrel{\text{Cor. 2.30}}{=} A(C_Z^*) - 2A(M_Z) = \frac{\pi}{4} - \frac{4\pi}{48^2} \approx 0.7799 > 0.7755 \stackrel{(3.14)}{\approx} A(C_\Delta).$$

Hence, Zindler's curve  $C_Z$  is not a counter example to our conjecture that the rounded triangle  $C_\Delta$  minimizes the area amongst convex Zindler curves.

In the end of this subsection we briefly want to mention a natural generalization of  $C_Z$  which was observed already by Zindler. The same way one can build rounded  $(2n + 1)$ -gons analogously to the rounded triangle, one can build Zindler curves from hypocycloids with  $(2n + 1)$  corners for every  $n \in \mathbb{N}$ . To construct such a midpoint curve one simply has to consider a small circle of radius  $s$  rolling inside of a bigger circle of radius  $(2n + 1)s$ .



# Chapter 4

## Halving Distance

In the previous chapter we considered Zindler curves, closed curves of constant halving distance. In Chapter 2 we applied some known inequalities from convex geometry and some inequalities involving the minimum halving distance  $h$  to prove lower bounds to the dilation of closed curves. This motivates us to take a closer look at the relation between halving distance and other important quantities of closed convex curves, before we finally try to apply our knowledge to the main problem of this thesis, to embed any given finite point set into a graph of small dilation.




In this chapter we list inequalities relating the minimum and maximum halving distance  $h$  and  $H$  of a convex closed curve  $C \subset \mathbb{R}^2$  to other geometric quantities of  $C$ , namely width  $w$ , diameter  $D$ , perimeter  $|C|$ , inradius  $r$ , circumradius  $R$ , and area  $A$ . We try to find tight inequalities, and characterize their *extremal sets*, the sets attaining equality. Some of the relations are known, for others we prove new inequalities.

A notion very closely related to the halving distance analyzed here is the *area halving distance*, the length of a chord bisecting the area of a compact convex set in  $\mathbb{R}^2$ . We have seen in Section 3.1.2 that convex cycles of constant halving distance also have constant area halving distance and vice versa. With Klein, Miori and Segura Gomis [96] we recently examined the relation of minimum and maximum *area* halving distance to the 6 basic quantities of convex geometry listed above. But as area halving distance is not related directly to dilation, those results are not included in this thesis.

### 4.1 Overview

The table in this section gives an overview of the results. Below each inequality, symbols represent the corresponding extremal sets. The symbol ‘ $\triangle_E$ ’ denotes an equilateral triangle, ‘ $\triangle_I$ ’ symbolizes an isosceles triangle where the third angle equals  $2\varphi$  and  $\varphi$  solves  $2\sin^3\varphi + \sin\varphi = 1$ , cf. Section 4.3, and ‘—’ represents a line segment.

New results with a more involved proof are marked with a grey background. Most other results are either very easy to prove, or they follow easily from known inequalities. All of them are explained in Section 4.2. Only the inequalities not marked with a grey background and bounding  $H$  from below, are the known ones with more difficult proofs. We review (and

	$H \leq$	$H \geq$	$h \leq$	$h \geq$
$w$	none see — (Sect. 4.2)	$H \geq w$ $\mathcal{CB}, \mathcal{ZC}, \triangle_E, ?$ (Sect. 4.6)	$h \leq w$ $\supseteq \mathcal{CS}, \mathcal{ZC}$ (Sect. 4.2)	$h > \frac{1}{2}w$  (Sect. 4.7)
$D$	$H \leq D$ $\supseteq \mathcal{CS}, \mathcal{CB}$ (Sect. 4.2)	$H \geq 0.843...D$ $\triangle_I$ (Sect. 4.3)	$h \leq D$ $\bigcirc$ (Sect. 4.2)	none see — (Sect. 4.2)
$ C $	$H \leq \frac{1}{2} C $ — (Sect. 4.2)	$[H \geq 0.268... C ]$ not tight (Sect. 4.5)	$h \leq \frac{1}{\pi} C $ $\bigcirc$ (Sect. 4.2)	none see — (Sect. 4.2)
$r$	none see — (Sect. 4.2)	$H \geq 2r$ $\bigcirc, ?$ (Sect. 4.6)	$[h \leq 3r]$ not tight (Sect. 4.2)	$h > r$  (Sect. 4.8)
$R$	$H \leq 2R$ $\supseteq \{\bigcirc\}$ (Sect. 4.2)	$H \geq \frac{3}{2}R$ $\triangle_E$ (Sect. 4.4)	$h \leq 2R$ $\bigcirc$ (Sect. 4.2)	none see — (Sect. 4.2)
$A$	none see — (Sect. 4.2)	$H^2 \geq \frac{4}{\pi}A$ $\bigcirc$ (Sect. 4.9)	$[h^2 \leq \sqrt{3}A]$ not tight (Sect. 4.10)	none see  (Sect. 4.10)

in one case slightly correct) these or give a shorter proof based on the results from Chapter 2. For some relations we do not know the tight inequality. In these cases the best known bound is written in square brackets.

The letters “ $\mathcal{CS}$ ” denote the centrally symmetric curves, “ $\mathcal{CB}$ ” the curves of constant breadth, and “ $\mathcal{ZC}$ ” the Zindler curves, the curves of constant halving distance. Note that all three types of curves include the circle.

The symbol “ $\supseteq$ ” denotes that the enumerated sets are extremal sets, but there are more. For example all the sets symmetric with respect to their diameter satisfy  $H = D$  but are not necessarily centrally symmetric nor of constant breadth. And all the sets symmetric with respect to their shortest chord satisfy  $h = w$  while, obviously, they do not have to be centrally symmetric nor of constant halving distance.

## 4.2 Basic results

By definition it is clear that  $H \leq D$  holds. Equality is attained if and only if a diameter is a halving chord. This is the case for every centrally symmetric curve. It also holds for curves of constant breadth, because we show in Section 4.6 that  $w \leq H$ . Hence  $w = D$  implies  $w = H = D$ . Still, there are more curves satisfying  $H = D$  like all the curves symmetric with respect to their diameter.

Plugging  $H \leq D$  into the trivial tight inequalities  $D \leq |C|/2$  and  $D \leq 2R$  yields  $H \leq |C|/2$  and  $H \leq 2R$ .

Clearly, the equality  $D = |C|/2$  is attained if and only if  $C$  is degenerated to a line segment. In these cases, we also have  $H = D$ . This shows that  $H = |C|/2$  is attained if and only if  $C$  is degenerated to a line segment.

The equality  $D = 2R$  is attained if and only if  $C$  touches the circumcircle in a pair of *diametric points*. Those are points whose connecting line segment is a diameter of the circumcircle. Therefore  $H = 2R$  holds if and only if such a pair of points exists and the connecting chord is a halving chord. Clearly, this holds for every circle but also for many other curves like the ones which are symmetric with respect to a line segment connecting such a diametric pair.

By definition it is clear that  $h \leq w$ . Equality  $h = w$  is attained by a closed curve  $C$  if and only if a  $w$ -chord  $|pq|$  (remember this means  $|pq| = l(v) = w$ ) is a halving chord. This is the case for every centrally symmetric curve. Also, equality holds for every curve of constant halving distance, since in Section 4.6 we prove  $w \leq H$ . Hence  $H = h$  implies  $h = w$ . Still,  $h = w$  is satisfied by many more curves like the ones symmetric with respect to a  $w$ -chord.

Plugging  $h \leq w$  into the known inequalities  $w \leq D$  (trivial),  $w \leq |C|/\pi$  (see Corollary 2.9),  $w \leq 3r$  (see [115, 68., p. 177–180], [184, 6-2, p. 215–217]) and  $w \leq 2R$  (trivial) yields  $h \leq D$ ,  $h \leq |C|/\pi$ ,  $h \leq 3r$  and  $h \leq 2R$ .

Paul Goodey has pointed out to us that the inequality  $h \leq |C|/\pi$  was first conjectured by Herda [101] in 1971 and confirmed by Ault [11], Chakerian [31], Goodey [77], Witsenhausen [183] and others, see [102]. It is amazing that this inequality has found so much attention, although it follows so easily from the known inequality  $w \leq |C|/\pi$  or Cauchy's surface area formula.

The curves satisfying  $w = D$  are the well-known curves of constant breadth. The equality  $w = |C|/\pi$  is attained only by these curves of constant breadth, see Corollary 2.9. Therefore, obviously,  $h = D$  and  $h = |C|/\pi$  are attained if and only if  $C$  is a curve of constant breadth satisfying  $h = w$ . Clearly the circle satisfies this condition. And our dilation formula for convex curves in Theorem 2.12 and Cauchy's surface area formula, Lemma 2.7, prove that it is the only set, because they imply

$$\delta(C) \stackrel{\text{Th. 2.12}}{=} \frac{|C|}{2h} \stackrel{h=w, \text{Lem. 2.7}}{=} \frac{\pi w}{2w} = \frac{\pi}{2}.$$

By Corollary 2.35 only circles attain this dilation value.

The inequality  $h \leq 3r$  cannot be tight. Yaglom and Boltyanski prove in [115, 68., p. 177–180], [184, 6-2, p. 215–217], that  $w = 3r$  is only attained by equilateral triangles. Their proof can be extended to a stability result saying that any convex cycle where  $w/r$  is close to 3 has to be close<sup>1</sup> to being an equilateral triangle. Now, if there was a sequence of convex cycles such that  $h(C_i)/r(C_i) \rightarrow 3$ , it would also satisfy  $w(C_i)/r(C_i) \rightarrow 3$ . We can scale each cycle  $C_i$  so that  $r(C_i) = 1$ . Hence, by the stability result, the cycles of the sequence must get arbitrarily close to an equilateral triangle of inradius 1. But then, the continuity of  $h$  and  $r$  implies that for big numbers  $i \in \mathbb{N}$ , the ratio  $h(C_i)/r(C_i)$  must be close to the ratio  $h(\Delta_E)/r(\Delta_E) = \frac{3}{4}/\frac{1}{2\sqrt{3}} = 3\sqrt{3}/2 \approx 2.5981$  of an equilateral triangle  $\Delta_E$ . This contradicts  $h(C_i)/r(C_i) \rightarrow 3$ . For more details on Hausdorff distance and the continuity of  $h$  and  $r$  see Section 4.11.

**Open Problem 5.** *What is the supremum of  $h/r$ ?*

<sup>1</sup>Here “close” means that the Hausdorff distance of the two cycles is small, cf. Section 4.11.

Clearly, only a circle attains  $w = 2R$ . Because circles satisfy  $h = w$ , also  $h = 2R$  is attained if and only if  $C$  is a circle.

Furthermore, at all cells marked with “none, see —” in the table of Section 4.1 a convex closed curve degenerated to a line segment shows that there cannot be any inequality for the corresponding pair of quantities.

### 4.3 Maximum halving distance $H$ and diameter $D$

Known results with more involved proofs are lower bounds to the maximum halving distance  $H$  in terms of the diameter  $D$ , the circumradius  $R$  and area  $A$ . The one concerning the diameter was given by Radziszewski [163] in 1954. Because the original proof is in French, and it seems to include a small miscalculation, we present here a translated, corrected and slightly simplified version.

**Theorem 4.1.** (Radziszewski [163]) *Let  $C \subset \mathbb{R}^2$  be a convex closed curve. Then  $H \geq \eta D$ , where  $\eta$  is the constant defined as*

$$\eta := \frac{\sqrt{x_0^2 - 4x_0 + 3}}{2x_0}, \quad x_0 = \frac{1}{6} \left( 54 + 6\sqrt{87} \right)^{\frac{1}{3}} - \frac{1}{\left( 54 + 6\sqrt{87} \right)^{\frac{1}{3}}}. \quad (4.1)$$

Approximately we have  $\eta \approx 0.843046$ , which is a little different from the approximation  $\eta \approx 0.829$  Radziszewski calculated. Equality in this bound is attained only by the isosceles triangle described in Lemma 4.3.

The proof of this theorem is based on some lemmata.

**Corollary 4.2.** (Radziszewski [163, Lemma 1]) *We consider an isosceles triangle  $\triangle(A, B, C)$  where  $|AB| = 2a \geq |AC| = |BC|$ , see Figure 4.1. Then the maximum halving distance is attained by the halving chord  $AF$  where  $F$  is the point on  $BC$  such that  $|CF| = a$ .*

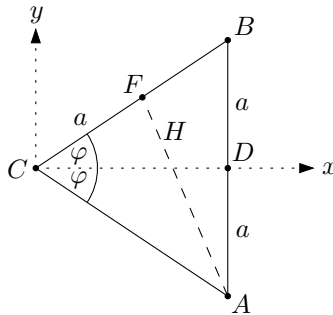


Figure 4.1: Maximum halving distance  $H$  of an isosceles triangle.

*Proof.* We do not have to follow Radziszewski’s proof because the statement is a corollary of Lemma 2.42 as by the law of sines  $|AB| \geq |AC| = |BC|$  implies  $\gamma \geq \beta = \alpha$  for the interior angles in  $C$ ,  $B$  and  $A$  respectively.  $\square$

**Lemma 4.3.** (cf. Radziszewski [163, Lemma 2]) *Amongst the isosceles triangles  $\triangle(A, B, C)$  with  $|AB| = 2a \geq |AC| = |BC|$ , which have diameter  $D = 2a$ , there is exactly one where the maximum halving distance  $H$  attains a minimum.*

Let  $\gamma = 2\varphi$  denote the interior angle in  $C$ . Then, this particular triangle satisfies

$$\varphi = \arcsin x_0 \approx 36.1396^\circ \quad \text{and} \quad H = 2a\eta = \eta D \approx 0.843046D, \quad (4.2)$$

where  $x_0$  and  $\eta$  are defined as in (4.1).

*Proof.* We consider the set of isosceles triangles  $\triangle(A, B, C)$  with  $|AB| = 2a \geq |AC| = |BC|$  like shown in Figure 4.1. We assume that  $C$  lies at the origin  $0 = (0, 0)$ , the midpoint<sup>2</sup>  $D$  lies on the positive  $x$ -axis, and  $AB$  is vertical such that  $B$  has the positive  $y$ -coordinate  $a$ .

We can conclude  $A = (a \cot \varphi, -a)$ ,  $B = (a \cot \varphi, a)$ ,  $D = (a \cot \varphi, 0)$  and  $F = (a \cos \varphi, a \sin \varphi)$ . By Corollary 4.2 we know

$$H^2(\varphi) = |AF|^2 = a^2 \left( (\cot \varphi - \cos \varphi)^2 + (1 + \sin \varphi)^2 \right). \quad (4.3)$$

We substitute  $\sin \varphi = x$  which by basic trigonometry results in  $\cos \varphi = \sqrt{1 - x^2}$  and  $\cot \varphi = \sqrt{1 - x^2}/x$ . We get

$$\begin{aligned} H^2(x) &= a^2 \left( \left( \frac{\sqrt{1 - x^2}}{x} - \sqrt{1 - x^2} \right)^2 + (1 + x)^2 \right) \\ &= a^2 \left( (1 - x^2) \left( \frac{1 - x}{x} \right)^2 + (1 + x)^2 \right) \\ &= a^2 \left( \frac{(1 - x^2)(1 - x)^2}{x^2} + \frac{(1 + x)^2 x^2}{x^2} \right) \\ &= a^2 \left( \frac{1 - 2x + x^2 - x^2 + 2x^3 - x^4}{x^2} + \frac{x^2 + 2x^3 + x^4}{x^2} \right) \\ &= a^2 \frac{4x^3 + x^2 - 2x + 1}{x^2}. \end{aligned} \quad (4.4)$$

The derivative equals

$$\begin{aligned} \frac{dH^2(x)}{dx} &= a^2 \frac{(12x^2 + 2x - 2)x^2 - (4x^3 + x^2 - 2x + 1)2x}{x^4} \\ &= a^2 \frac{12x^4 + 2x^3 - 2x^2 - 8x^4 - 2x^3 + 4x^2 - 2x}{x^4} \\ &= a^2 \frac{4x^3 + 2x - 2}{x^3} = 2a^2 \frac{2x^3 + x - 1}{x^3} \end{aligned} \quad (4.5)$$

Clearly, the numerator of the derivative is strictly increasing in  $x$ , it is negative for  $x = 0$ , equals zero at the only real-valued root of  $2x^3 + x - 1$  and is positive for all bigger  $x$ -values. The sign of the derivative equals the sign of  $2x^3 + x - 1$ . Therefore,  $H^2(x)$  attains its global minimum at the root  $x_0$  of  $2x^3 + x - 1$  whose closed form is given in (4.1).

---

<sup>2</sup>We follow Radziszewski's notation although this causes the letter  $D$  to denote both, the midpoint of  $AB$  and the diameter of  $AB$ . However, this ambiguity should not cause any problems.

Finally, we can simplify the formula for  $H^2(x_0)$  a little bit by taking advantage of  $2x_0^3 + x_0 - 1 = 0$ :

$$\begin{aligned}
 H^2(x_0) &\stackrel{(4.4)}{=} a^2 \frac{4x_0^3 + x_0^2 - 2x_0 + 1}{x_0^2} \\
 &\stackrel{4x_0^3 + 2x_0 - 2 = 0}{=} a^2 \frac{x_0^2 - 4x_0 + 3}{x_0^2}
 \end{aligned}$$

This completes the proof of Lemma 4.3.  $\square$

We have proved the inequality  $H \geq \eta D$  for a small class of convex cycles. The next steps show that it holds for every convex closed curve.

**Lemma 4.4.** (Radziszewski [163, Lemma 3]) *Let  $\triangle(A_0, B_0, C_0)$  be the isosceles triangle of minimum  $H$  described in Lemma 4.3, see Figure 4.2.a. We draw two circular arcs with radius  $|A_0F_0| = H$  around  $A_0$  and  $B_0$ . These arcs intersect each other in a point  $S$  close to  $C_0$ , and they intersect  $A_0B_0$  in the points  $L$  and  $K$  respectively.*

*We consider another triangle  $\triangle(A_0, B_0, C)$  also of diameter  $D = 2a$  such that the edge  $A_0C$  intersects the arc  $\widehat{KS}$  in a point  $P$  and  $B_0C$  intersects  $\widehat{LS}$  in a point  $R$ . If there is more than one intersection of  $A_0C$  ( $B_0C$ ) with  $\widehat{KS}$  ( $\widehat{LS}$ ) then  $P$  ( $R$ ) denotes the point closer to  $K$  ( $L$ ) on  $\widehat{KS}$  ( $\widehat{LS}$ ).*

*Then, the polygonal chain  $PCR$  is not longer than  $2a$ . Equality is attained only for  $C = C_0$ .*

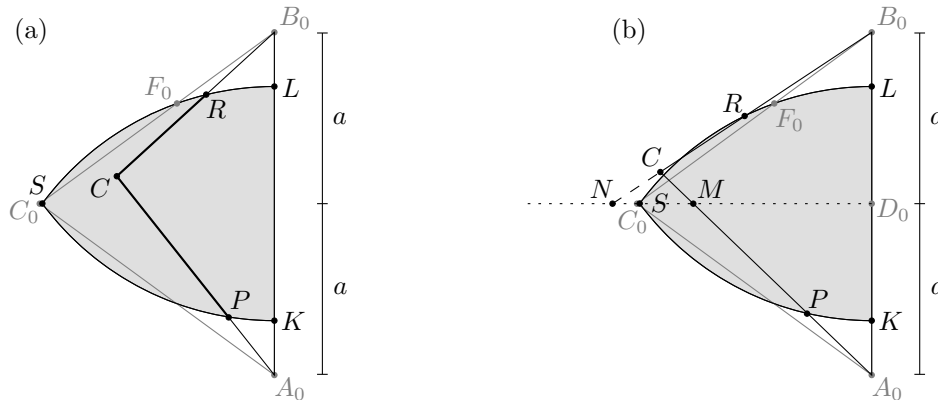


Figure 4.2: The construction in Lemma 4.4.

*Proof.* First we show that the lemma holds for *isosceles* triangles. Consider the degenerate isosceles triangle  $\triangle(A_0, B_0, C)$  where  $C$  is the midpoint of  $A_0B_0$ . Then, obviously, we have  $|PC| + |CR| < 2a$  in this case. Now move  $C$  horizontally and continuously to the left. Then  $|PC| + |CR|$  changes continuously, too. Note that if we have  $|PC| + |CR| = 2a$ , then  $R$  is the halving partner of  $A_0$  in  $\triangle(A_0, B_0, C)$ .

If there was an isosceles triangle where  $|PC| + |CR| > 2a$ , then by continuity we can find such an isosceles triangle  $\triangle(A_0, B_0, C)$ , whose diameter is still  $A_0B_0$ , and where  $|PC| + |CR|$  is arbitrarily close to  $2a$ , hence the halving partner  $F$  of  $A_0$  in  $\triangle(A_0, B_0, C)$  is arbitrarily close



to  $R$ . Because of  $|PC| + |CR| > 2a$  and due to symmetry the point  $F$  must lie on  $RC$ . As at least a small part of  $RC$  has to intersect with the lune  $KSL$ , we therefore find an isosceles triangle such that  $F$  is contained in the lune  $KSL$ , hence  $H = |AF| < |AF_0|$ , a contradiction to Lemma 4.3. Closer analysis of  $H$ , for instance as a function of  $\varphi$ , shows that the triangle  $\triangle(A_0, B_0, C_0)$  is the only isosceles triangle attaining  $|PC| + |CR| = 2a$ .

Now we consider the general case (not isosceles), see Figure 4.2.b. We assume that  $C$  lies on the same side of line( $C_0, D_0$ ) as  $B_0$ , where  $D_0$  denotes the midpoint of  $A_0B_0$ . Let  $M$  be the intersection of  $A_0C$  with line( $C_0, D_0$ ). Then, we conclude from what we have shown above and by considering the isosceles triangle  $\triangle(A_0, B_0, M)$  that  $|PM| \leq a$ , and that equality is attained only for  $M = C_0$ . Let  $N$  be the intersection of line( $B_0, C$ ) with line( $D_0, C_0$ ). Then we have  $|NC| > |MC|$  because of the law of sines and  $\angle MNC = 90^\circ - \angle CB_0A_0 < 90^\circ - \angle CA_0B_0 = \angle NMC$ . Here  $\angle MNC$ , sometimes also written as  $\angle(M, N, C)$ , denotes the angle  $\angle(M - N, C - N)$  in point  $N$ . We have shown  $|RN| > |RC| + |CM|$ . But we know  $|RN| \leq a$  because of the isosceles triangle  $\triangle(A_0, B_0, N)$ . Plugging everything together shows  $|PC| + |CR| = |PM| + |MC| + |CR| \leq 2a$ , and equality is attained only for the isosceles triangle from Lemma 4.3.  $\square$

We are now able to prove the theorem.

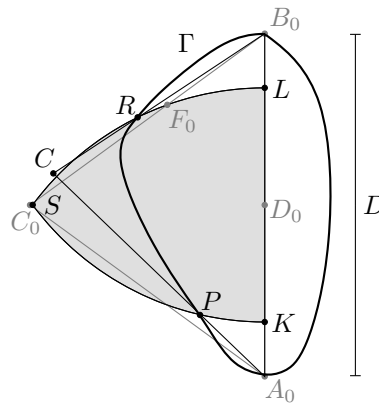


Figure 4.3: Proving Theorem 4.1.

*Proof.* (of Theorem 4.1) Let  $\Gamma \subset \mathbb{R}^2$  be a closed convex curve, and let  $A_0B_0$  be a diameter of  $\Gamma$ . Consider Figure 4.3. We draw the isosceles triangle  $\triangle(A_0, B_0, C_0)$  of minimum  $H$  from Lemma 4.3 at that side of  $A_0B_0$  which contains the longer path (or one of the two paths of equal length) on  $\Gamma$  from  $A_0$  to  $B_0$ .

If  $\Gamma$  intersects only with one of the arcs  $\widehat{KS}$  or  $\widehat{LS}$  defined like above, it is easy to show that not both, the halving partner from  $A_0$  and the one from  $B_0$ , can lie inside the lune  $KSL$ , hence  $H > \eta D$ . The same implication is trivial, if  $\Gamma$  does not intersect at all with the lune  $KSL$ .

If  $\Gamma$  intersects with both arcs  $\widehat{KS}$  and  $\widehat{LS}$ , then if  $P$  ( $R$  resp.) is the intersection closest to  $A_0$  ( $B_0$ ) on  $\Gamma$ , the path  $\Gamma_R^P$  on  $\Gamma$  from  $P$  to  $R$  not visiting  $A_0$  satisfies  $|\Gamma_R^P| \leq 2a$ . This follows if we consider the triangle  $\triangle(A_0, B_0, C)$  where  $C$  is the intersection of line( $A_0, P$ )

and  $\text{line}(B_0, R)$ . Because the convexity of  $\Gamma$  implies  $|\Gamma_R^P| \leq |PC| + |CR|$ . And applying Lemma 4.4 to  $\triangle(A_0, B_0, C)$  yields  $|PC| + |CR| \leq 2a$ , hence  $|\Gamma_R^P| \leq 2a$ . If we assume  $|\Gamma_P^{A_0}| \leq |\Gamma_{B_0}^R|$ , this shows that the halving partner  $F$  of  $A_0$  in  $\Gamma$  lies in the part  $\Gamma_{B_0}^R$  outside the lune  $KSL$ . Hence  $H(\Gamma) \geq |A_0F| \geq |A_0F_0| \geq \eta D$ .

The proof also shows that equality can be attained only if  $|\Gamma_R^P| = |PC| + |CR| = 2a$ , and if  $\Gamma$  contains the segment  $A_0B_0$ . This means that  $\Gamma$  is a triangle, and because of  $|PC| + |CR| = 2a$  and Lemma 4.4 it has to be the triangle from Lemma 4.3.  $\square$

This immediately yields an inequality between maximum halving distance  $H$  and perimeter  $|C|$ .

**Corollary 4.5.** *Let  $C \subset \mathbb{R}^2$  be a closed curve in the plane. Then, its maximum halving distance  $H$  is bounded by  $H > \frac{2}{\pi}|C| \approx 0.2683|C|$ . This inequality is not tight.*

*Proof.* We combine the well-known inequality  $D \geq |C|/\pi$  from Corollary 2.9 with  $H \geq \eta D$  from Theorem 4.1. The corollary also states that only sets of constant breadth attain the equality  $D = |C|/\pi$ . On the other hand the equality  $H = \eta D$  is only attained by the particular isosceles triangle defined in Theorem 4.1 which clearly is not a set of constant breadth. Continuity arguments then show that  $H$  cannot become arbitrarily close to  $\eta|C|/\pi$ , see Section 4.11.  $\square$

## 4.4 Maximum halving distance $H$ and circumradius $R$

Another known tight inequality was introduced by Eggleston [64]. However, in that article he gives a full proof only for the analogous inequality between the circumradius  $R$  and maximum area halving distance, the maximum length of an area bisector. In the end he states that similar arguments can be used for the chords halving the perimeter. Here we give a full proof. The arguments turned out to be not as similar as expected. Only the basic ideas are similar. Both proofs use the inequality  $H \geq \eta D$  from Theorem 4.1 to restrict the cases which have to be considered, and both proofs consider the triangle of three points touching the circumcircle.

**Theorem 4.6.** (Eggleston [64]) *Let  $C \subset \mathbb{R}^2$  be a closed convex curve in the plane. Then the maximum halving distance  $H$  is bounded from below by*

$$H \geq \frac{3}{2}R.$$

*Proof.* It is well-known that there are either two points  $p, q \in C$  on the circumcircle such that  $pq$  is a diameter of the circle, or there exist at least three points  $p_1, p_2, p_3 \in C$  on the circumcircle which form an acute triangle (e.g. see [184, 6-1], [115, A67]). We first consider the second case displayed in Figure 4.4.

We want to prove that either  $H \geq 3R/2$  follows immediately from the inequality  $H \geq \eta D$  in Theorem 4.1 or the halving partner of each of the three points  $p_1, p_2$  and  $p_3$  is located on the arc of  $C$  between the other two points.

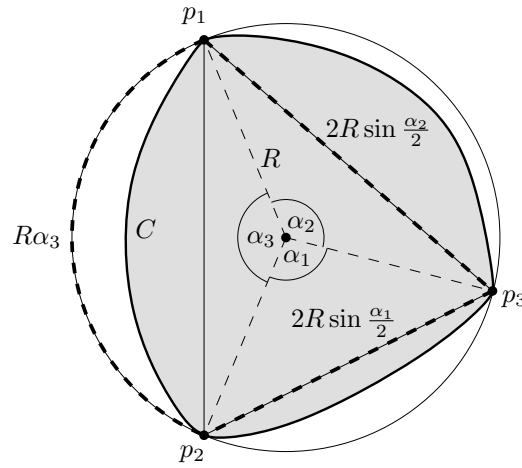


Figure 4.4: Proving Theorem 4.6 for the case that  $C$  touches the circumcircle in three points forming an acute triangle.

Let  $\alpha_i$ ,  $i \in \{1, 2, 3\}$ , denote the angle between the points in  $\{p_1, p_2, p_3\} \setminus \{p_i\}$  as seen from the circumcircle's center. We define  $\bar{\alpha} := \max(\alpha_1, \alpha_2, \alpha_3)$ . If  $\bar{\alpha}$  is big enough, we have

$$H \stackrel{\text{Theor. 4.1}}{\geq} \eta D \geq \eta \max(|p_1 p_2|, |p_2 p_3|, |p_1 p_3|) \geq \frac{3}{2} R. \quad (4.6)$$

The last inequality holds iff

$$2R \sin(\bar{\alpha}/2) = \max(|p_1 p_2|, |p_2 p_3|, |p_1 p_3|) \geq 3R/2\eta$$

which is equivalent to  $\bar{\alpha} \geq \tilde{\alpha}$  where

$$\tilde{\alpha} := 2 \arcsin \frac{3}{4\eta} \approx 2.1931. \quad (4.7)$$

The case, where there are two points  $p, q \in C$  on the circumcircle such that  $pq$  is a diameter of the circle turns out to be the special case where  $\bar{\alpha} = \pi/2$ . Hence  $\bar{\alpha} \geq \tilde{\alpha}$  holds and the proof for this case is completed, too.

We still have to consider the case  $\bar{\alpha} < \tilde{\alpha}$ . And we want to show that the halving partner of every point from  $\{p_1, p_2, p_3\}$  lies on the arc of  $C$  between the other two points. Without loss of generality we consider the halving partner  $\hat{p}_1$  of  $p_1$ . Consider again Figure 4.4. We will show that  $p_1$  cannot lie on  $C_{p_1}^{p_2}$ , even if  $|p_1 p_2|$  is the longest side of the triangle  $\triangle(p_1, p_2, p_3)$ , i.e.  $\bar{\alpha} = \alpha_3$ . If we had

$$\alpha_3 \leq 2 \sin \frac{\alpha_1}{2} + 2 \sin \frac{\alpha_2}{2} \quad (4.8)$$

we could conclude

$$|C_{p_1}^{p_2}| \leq R\alpha_3 \leq R \left( 2 \sin \frac{\alpha_1}{2} + 2 \sin \frac{\alpha_2}{2} \right) \leq |C_{p_2}^{p_3}| + |C_{p_1}^{p_3}|.$$

And this inequality means that  $p_1$ 's halving partner  $\hat{p}_1$  cannot lie on  $p_1 p_2$ . Thus, it remains

to show only the inequality (4.8). Its right-hand side equals

$$\begin{aligned} 2 \sin \frac{\alpha_1}{2} + 2 \sin \frac{\alpha_2}{2} &= 2 \left( \sin \frac{\alpha_1}{2} + \sin \frac{2\pi - \alpha_3 - \alpha_1}{2} \right) \\ &\stackrel{\sin(\pi-x)=\sin(x)}{=} 2 \left( \sin \frac{\alpha_1}{2} + \sin \frac{\alpha_3 + \alpha_1}{2} \right) \\ &\stackrel{\sin x + \sin y = 2 \cos \frac{x-y}{2} \sin \frac{x+y}{2}}{=} 4 \cos \frac{\alpha_3}{4} \sin \left( \frac{\alpha_1}{2} + \frac{\alpha_3}{4} \right). \end{aligned}$$

By symmetry we can assume that  $\alpha_1 \geq \alpha_2 = 2\pi - \alpha_1 - \alpha_3$  which implies  $\alpha_1 \geq \pi - \alpha_3/2$  and

$$\frac{\alpha_1}{2} + \frac{\alpha_3}{4} \geq \frac{\pi}{2} - \frac{\alpha_3}{4} + \frac{\alpha_3}{4} = \frac{\pi}{2}.$$

Hence, the right-hand side of (4.8) is monotonously decreasing in  $\alpha_1$  for given  $\alpha_3$ . Under our assumption  $\alpha_1 \leq \bar{\alpha} = \alpha_3$ , it attains the minimum for  $\alpha_1 = \alpha_3$ . Hence, it suffices to show

$$\begin{aligned} \alpha_3 &\leq 2 \sin \frac{\alpha_3}{2} + 2 \sin \frac{2\pi - 2\alpha_3}{2} = 2 \sin \frac{\alpha_3}{2} + 2 \sin \alpha_3 \\ &\stackrel{\sin(2x)=2 \sin x \cos x}{=} 2 \sin \frac{\alpha_3}{2} + 4 \sin \frac{\alpha_3}{2} \cos \frac{\alpha_3}{2} \end{aligned}$$

This is equivalent to

$$\frac{\alpha_3}{2 \sin \frac{\alpha_3}{2}} \leq 1 + 2 \cos \frac{\alpha_3}{2}$$

where the left hand side is increasing and the right-hand side is decreasing for  $\alpha_3 \in [0, \pi]$ . Because of this and  $\alpha_3 = \bar{\alpha} < \tilde{\alpha}$  it suffices to show that the inequality holds for  $\tilde{\alpha}$ . This can be verified easily.

Now we know that the halving partner  $\hat{p}_1$  of  $p_1$  cannot lie on  $C_{p_1}^{p_2}$  if  $\alpha_3 = \bar{\alpha}$ . But then,  $\hat{p}_1$  cannot lie on  $C_{p_1}^{p_2}$  in any case, since this would only decrease the possible length of  $|C_{p_1}^{p_2}|$  and increase the lower bound on  $|C_{p_2}^{p_3}| + |C_{p_1}^{p_3}|$ . Hence,  $p_1$  cannot lie on  $C_{p_1}^{p_2}$  in any case. These arguments can be applied to any point of  $\{p_1, p_2, p_3\}$  and any of the adjacent arcs of  $C$ . Thus, for  $\bar{\alpha} < \tilde{\alpha}$  the halving partner of any of the points  $\{p_1, p_2, p_3\}$  lies on the arc of  $C$  connecting the other two points.

This means that the maximum height of the triangle  $\Delta(p_1, p_2, p_3)$  is a lower bound to the maximum halving distance  $H$ . As the interior angle of the triangle  $\Delta(p_1, p_2, p_3)$  in  $p_i$  equals  $\theta_i := \alpha_i/2$  for  $i \in \{1, 2, 3\}$  due to generalized Thales' theorem, the following lemma concludes the proof of Theorem 4.6.  $\square$

**Lemma 4.7.** *Let  $p_1, p_2, p_3$  be three distinct points on the unit circle. And let  $h_i$  denote the height of the triangle  $\Delta(p_1, p_2, p_3)$  through  $p_i$ , and let  $\theta_i$  be the interior angle in  $p_i$ ,  $i \in \{1, 2, 3\}$ . If  $\max(\theta_1, \theta_2, \theta_3) < \tilde{\alpha}/2 \approx 1.0965$  (definition of  $\tilde{\alpha}$  in (4.7) on page 123). Then  $\max(h_1, h_2, h_3) \geq 3/2$  and equality is attained only by equilateral triangles.*

*Proof.* Consider Figure 4.5. Without loss of generality we assume that  $\theta_1 \geq \theta_2 \geq \theta_3$ . By the generalized Thales' theorem we have  $|p_2 p_3| = 2 \sin \theta_1$ . This implies

$$h_2 = 2 \sin \theta_1 \sin \theta_3 \quad \text{and} \quad h_3 = 2 \sin \theta_1 \sin \theta_2 = 2 \sin \theta_1 \sin(\pi - \theta_1 - \theta_3)$$

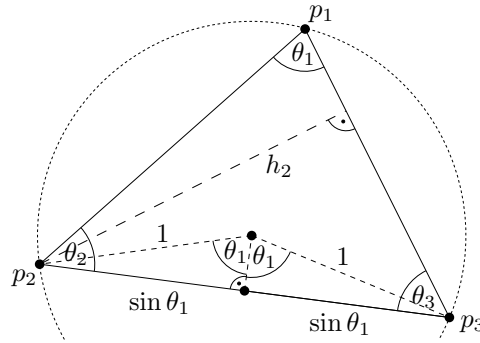


Figure 4.5: Proving that the maximum height of a triangle in the unit circle is  $\geq 3/2$ .

We have  $\theta_1 = \max(\theta_1, \theta_2, \theta_3) < \tilde{\alpha}/2 < \pi/2$  and  $\pi - \theta_1 - \theta_3 = \theta_2 < \pi/2$ . Hence for given  $\theta_1$  the height  $h_2$  is strictly increasing in  $\theta_3$  and the height  $h_3$  is strictly decreasing in  $\theta_3$ . As for  $\theta_3 = 0$  we have  $h_2 = 0 \leq h_3$ , we minimize  $\max(h_2, h_3)$  by finding the unique value  $\theta_3$  where  $h_2 = h_3$ . This happens for  $\theta_3 = \theta_2 = (\pi - \theta_1)/2$ . Hence, we have to minimize the function

$$f(\theta_1) := 2 \sin \theta_1 \sin \frac{\pi - \theta_1}{2} = 2 \sin \theta_1 \cos \frac{\theta_1}{2} \quad \text{where } \theta_1 \in [\pi/3, \tilde{\alpha}/2].$$

The following lemma yields that  $f(\theta_1)$  is increasing within this interval. Hence, there is a unique minimum of value  $3/2$  at  $\theta_1 = \pi/3$ . This also shows that the minimum of the maximum height is attained only by equilateral triangles.  $\square$

**Lemma 4.8.** *The function  $f(x) := 2 \sin x \cos \frac{x}{2}$  is strictly increasing for  $x \in [\pi/3, \tilde{\alpha}/2]$  (definition of  $\tilde{\alpha}$  in (4.7) on page 123).*

*Proof.* We show that the derivative is positive in the considered interval.

$$\begin{aligned} f'(x) &= 2 \cos x \cos \frac{x}{2} - \sin x \sin \frac{x}{2} \\ &\stackrel{\text{add. theor.}}{=} 2 \left( \cos^2 \frac{x}{2} - \sin^2 \frac{x}{2} \right) \cos \frac{x}{2} - \left( 2 \sin \frac{x}{2} \cos \frac{x}{2} \right) \sin \frac{x}{2} \\ &= 2 \cos^3 \frac{x}{2} - 2 \sin^2 \frac{x}{2} \cos \frac{x}{2} - 2 \sin^2 \frac{x}{2} \cos \frac{x}{2} \\ &\stackrel{\sin^2 x = 1 - \cos^2 x}{=} 2 \cos^3 \frac{x}{2} - 4 \left( 1 - \cos^2 \frac{x}{2} \right) \cos \frac{x}{2} \\ &= 6 \cos^3 \frac{x}{2} - 4 \cos \frac{x}{2} \end{aligned}$$

We substitute  $y = \cos(x/2)$ .

$$f'(x) = 6y^3 - 4y = 2y(3y^2 - 2)$$

This is obviously positive if  $y > \sqrt{2/3}$ . Since  $0 < \pi/6 < \tilde{\alpha}/4 < \pi/4$ ,  $\cos(x/2)$  is decreasing in the considered interval. Hence, the minimum value of  $y = \cos(x/2)$  equals  $\cos(\tilde{\alpha}/4) \approx 0.8534 > 0.8165 \approx \sqrt{2/3}$ .  $\square$

## 4.5 Maximum halving distance $H$ and perimeter $|C|$

The inequality  $H \geq 3R/2$  from Theorem 4.6 immediately implies

$$H \geq \frac{3}{4\pi}|C| \approx 0.2387|C|$$

if combined with the simple inequality  $|C| \leq 2\pi R$ . However this inequality is not tight.

Combining  $H \geq \eta D$  from Theorem 4.1 with the known inequality  $|C| \leq \pi D$  from Corollary 2.9 yields the better lower bound like shown in Corollary 4.5:

$$H \geq \frac{\eta}{\pi}|C| \approx 0.2683|C|$$

We also proved that this inequality is not tight.

If our conjecture from Section 2.8 held, which states that the length of the halving pair transformation is bounded by  $|C^*| \geq \sqrt{3}|C|/2$ , this would immediately imply a better lower bound on  $H/|C|$ . Since Lemma 2.21.4 tells us  $H(C) = H(C^*)$ , and the centrally symmetric curve  $C^*$  satisfies  $H(C^*) = D(C^*)$  by Lemma 2.13.1, and since we can use  $|C^*| \leq \pi D(C^*)$  from Corollary 2.9, we would get

$$H \stackrel{\text{Lem. 2.21.4}}{=} H(C^*) \stackrel{\text{Lem. 2.13.1}}{=} D(C^*) \stackrel{\text{Cor. 2.9}}{\geq} \frac{|C^*|}{\pi} \stackrel{\text{conjecture}}{\geq} \frac{\sqrt{3}}{2\pi}|C| \approx 0.2757|C|.$$

However, even this inequality  $H \geq \sqrt{3}|C|/2\pi$  would not be tight since  $|C^*| = \pi D(C^*)$  is attained only if  $C^*$  is a circle (see Corollary 2.9), which is equivalent to  $C$  being a Zindler curve. The equality  $|C^*| = \sqrt{3}|C|/2$  would be attained only by an equilateral triangle which is not a Zindler curve, and continuity arguments would show that  $|C|/|C^*| \geq \sqrt{3}/2$  is not tight, cf. Section 4.11.

**Open Problem 6.** *What is the infimum of  $H/|C|$ ?*

## 4.6 Maximum halving distance $H$ and width $w$

**Lemma 4.9.** *Let  $C \subset \mathbb{R}^2$  be a convex closed curve. Then  $H \geq w$ .*

*Proof.* We used an analogous idea to show that the maximum area-halving distance  $H_A$  satisfies  $H_A \geq w$  in the joint work [96] with Klein, Miori and Segura Gomis.

Since both  $H$  and  $w$  depend continuously on  $C$ , and  $C$  can be approximated by polygons, see Section 4.11, it suffices to prove the lemma for polygons. We want to show that there exists a direction  $v \in [0, 2\pi)$  and two points  $p, q \in C$  such that  $p$  ( $q$  resp.) is extremal in direction  $v$  ( $v + \pi$  resp.) and  $pq$  is a halving chord.

By the following lemma there exist continuous functions  $p_+ : [0, 1] \rightarrow C$ ,  $p_- : [0, 1] \rightarrow C$  and  $v : [0, 1] \rightarrow [0, 2\pi]$  such that  $p_+(t)$  ( $p_-(t)$  resp.) is extremal in direction  $v(t)$  ( $v(t) + \pi$  resp.) for every  $t \in [0, 1]$ , and the function  $v$  is non-decreasing, starting in  $v(0) = 0$  and ending in  $v(1) = 2\pi$ . Let  $t_\pi \in [0, 1]$  satisfy  $v(t_\pi) = \pi$ . W.l.o.g. we assume that there exists only one extremal point in direction 0 and only one extremal point in direction  $\pi$ . This can be achieved by turning  $C$ , and it implies  $p_+(t_\pi) = p_-(0)$  and  $p_-(t_\pi) = p_+(0)$ .

We consider the length of the part of  $C$  which one uses when moving from  $p_+(t)$  to  $p_-(t)$  counter-clockwise. This length  $s(t) := |C_{p_+(t)}^{p_-(t)}|$  is continuous with respect to  $t$  and we have

$$s(0) + s(|C|/2) = |C_{p_+(0)}^{p_-(0)}| + |C_{p_+(t_\pi)}^{p_-(t_\pi)}| = |C_{p_+(0)}^{p_-(0)}| + |C_{p_-(0)}^{p_+(0)}| = |C|.$$

Hence, by the intermediate value theorem there exists a value  $t \in [0, t_\pi]$  such that  $s(t) = (s(0) + s(t_\pi))/2 = |C|/2$ . The corresponding points  $p_+(t)$  and  $p_-(t)$  form a halving pair. This implies

$$H \geq |p_+(t)p_-(t)| = b(v(t)) \geq w$$

which concludes the proof of the inequality.  $\square$

Taking into account the trivial inequalities  $D \geq H$  and  $w \geq h$ , we now know

$$D \geq H \geq w \geq h \tag{4.9}$$

For curves of constant breadth ( $D = w$ ) this implies  $H = w$ . The same is true for Zindler curves ( $H = h$ ). Furthermore the equilateral triangle satisfies  $H = w$ .

**Open Problem 7.** *Are there convex cycles besides Zindler curves, curves of constant breadth and equilateral triangles attaining  $H = w$ ?*

In the proof we applied the following rather technical lemma. Note that we could get an alternative proof by applying the extremal parameterization from Section 3.1.3 and Appendix A.3, and by proving that the cycles admitting such an extremal parameterization are dense in the class of convex cycles.

**Lemma 4.10.** *Let  $C \subset \mathbb{R}^2$  be a convex polygon, and define  $L := 2\pi + 2|C|$ . Then, there exist continuous functions  $p_+ : [0, L] \rightarrow C$ ,  $p_- : [0, L] \rightarrow C$  and  $v : [0, L] \rightarrow [0, 2\pi]$  such that  $p_+(t)$  ( $p_-(t)$  resp.) is extremal in direction  $v(t)$  ( $v(t) + \pi$  resp.) for every  $t \in [0, L]$ , and the function  $v$  is non-decreasing, starting in  $v(0) = 0$  and ending in  $v(L) = 2\pi$ .*

*Proof.* We define the functions inductively. We may assume that there exist only one extremal point in direction 0 and only one extremal point in direction  $\pi$ . The induction hypothesis is that we have the desired functions  $p_+$ ,  $p_-$  and  $v$  defined up to a value  $\tau \in [0, L]$  where

$$v(\tau) + |C_{p_+(0)}^{p_+(\tau)}| + |C_{p_-(0)}^{p_-(\tau)}| = \tau. \tag{4.10}$$

Let  $\hat{v}$  be the maximal value in  $[v(\tau), 2\pi]$  such that  $p_+(\tau)$  is still extremal in direction  $\hat{v}$  and  $p_-(\tau)$  is still extremal in direction  $\hat{v} + \pi$ .

Consider Figure 4.6.a. If  $\hat{v} > v(\tau)$ , we can simply extend the existing functions to the interval  $[\tau, \tau + \hat{v} - v(\tau)]$  by defining

$$p_+(t) := p_+(\tau), \quad p_-(t) := p_-(\tau), \quad \text{and} \quad v(t) := v(\tau) + t - \tau.$$

It can easily be verified that the extended functions satisfy the desired conditions of the lemma and (4.10) up to  $\tau + \hat{v} - v(\tau)$ .

If  $\hat{v} = v(\tau)$ , there exists a small  $\varepsilon > 0$  such that  $p_+(\tau)$  is not extremal for the directions in  $(v(\tau), v(\tau) + \varepsilon]$ , or  $p_-(\tau)$  is not extremal for the directions in  $(v(\tau) + \pi, v(\tau) + \pi + \varepsilon]$ .

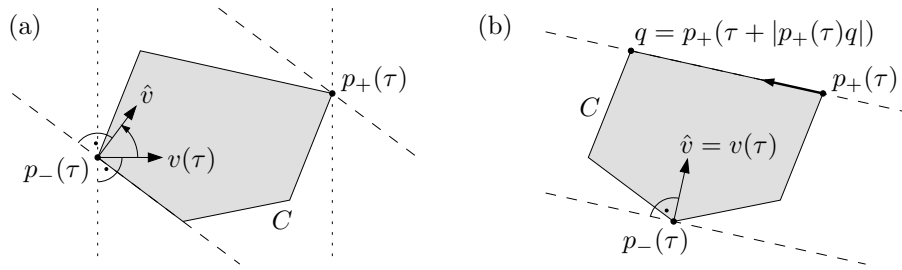


Figure 4.6: Two cases while constructing extreme points which move continuously around a polygon  $C$ .

We assume the first case. The second case can be treated analogously. If both cases apply simultaneously, we treat it like the first case. The next induction step will then deal with  $p_-$ .

In the considered case,  $p_+(\tau)$  must be a vertex adjacent to an edge of  $C$  which is orthogonal to  $v(\tau)$ , like shown in Figure 4.6.b. Let  $q$  be the other vertex of this edge. We extend the functions to the interval  $[\tau, \tau + |p_+(\tau)q|]$  by

$$p_+(t) := \frac{\tau + |p_+(\tau)q| - t}{|p_+(\tau)q|} p_+(\tau) + \frac{(t - \tau)}{|p_+(\tau)q|} q,$$

$$p_-(t) := p_-(\tau), \quad \text{and} \quad v(t) := v(\tau).$$

It can easily be verified that the extended functions satisfy the desired conditions of the lemma and (4.10) up to  $\tau + |p_+(\tau)q|$ .

By this induction we can extend the functions up to  $L$  which gives the desired result.  $\square$

Luckily, the inequality  $H \geq w$  immediately implies a tight inequality between  $H$  and  $r$ .

**Corollary 4.11.** *Let  $C \subset \mathbb{R}^2$  be a convex closed curve. Then  $H \geq 2r$ . This inequality is tight because circles attain equality.*

*Proof.* If we combine  $H \geq w$  from Lemma 4.9 with the known tight inequality  $w \geq 2r$ , we get  $H \geq 2r$ . The inequality  $w \geq 2r$  is trivial because clearly the width  $w$  of  $C$  cannot be smaller than the width of the incircle contained in  $C$ . And the width of the incircle equals  $2r$ .  $\square$

Clearly, the equality  $w = 2r$  holds for a convex curve if and only if its incircle touches its boundary at two points which are symmetric with respect to the incircle's center. Therefore,  $H = 2r$  can only hold in a situation like this. Still, additional arguments would be needed to show that the circle is the only convex set attaining  $H = 2r$ .

**Open Problem 8.** *Are there other convex cycles besides circles attaining  $H = 2r$ ?*

## 4.7 Minimum halving distance $h$ and width $w$

One can prove  $h \geq w/2$  like we did in Section 7.2 of [49]. There, we showed  $A \leq Dh$  and combined this new result with the known inequality  $A \geq Dw/2$ .

Here we present a different, direct approach based on similar ideas.



**Lemma 4.12.** *If  $C$  is a convex closed curve in  $\mathbb{R}^2$ , then for every direction  $v \in \mathbb{S}^1$  we have  $h(v) > l(v)/2$ . This inequality cannot be improved.*

*Proof.* Consider Figure 4.7. We may assume that  $v$  is vertical. Let  $p\hat{p}$  be the halving chord with direction  $v$ ,  $p$  on top and  $\hat{p}$  at the bottom. And let  $q\tilde{q}$  be the longest vertical chord,  $q$  on top and  $\tilde{q}$  at the bottom, with length  $l(v) := |q\tilde{q}|$ . Without loss of generality,  $q\tilde{q}$  lies to the left of  $p\hat{p}$ .

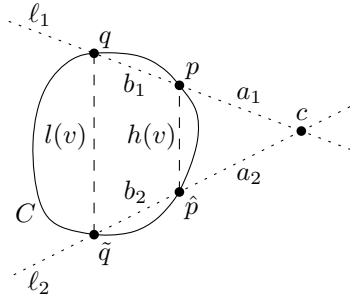


Figure 4.7: Proving  $h(v) \geq l(v)/2$ . (The figure is unrealistic because  $p\hat{p}$  is not a halving chord of the displayed curve  $C$ .)

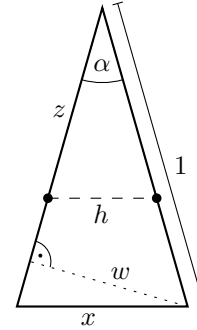


Figure 4.8: In a thin isosceles triangle  $h/w \searrow 1/2$  if  $\alpha \rightarrow 0$ .

We connect  $p$  and  $q$  with a line  $\ell_1 := \text{line}(p, q)$  and  $\hat{p}$  and  $\tilde{q}$  with a line  $\ell_2 := \text{line}(\hat{p}, \tilde{q})$ . If  $l(v) \leq h(v)$ , we are done. If  $l(v) > h(v)$ , the lines  $\ell_1$  and  $\ell_2$  intersect right of  $p\hat{p}$ . Let  $c$  be the intersection point,  $a_1 := |cp|$ ,  $a_2 := |c\hat{p}|$ ,  $b_1 := |pq|$ ,  $b_2 := |\hat{p}\tilde{q}|$ . Then, because  $p\hat{p}$  is a halving chord and by convexity, we have  $b_1 + l(v) + b_2 \leq a_1 + a_2$ . Because the triangles  $\Delta(c, p, \hat{p})$  and  $\Delta(c, q, \tilde{q})$  are similar, we know  $h(v)/(a_1 + a_2) = l(v)/(a_1 + b_1 + a_2 + b_2)$ . Hence

$$\begin{aligned} h(v) &= l(v) \frac{a_1 + a_2}{a_1 + a_2 + b_1 + b_2} \\ &\geq l(v) \frac{b_1 + b_2 + l(v)}{b_1 + b_2 + l(v) + b_1 + b_2} > \frac{1}{2} l(v). \end{aligned}$$

The first inequality becomes an equality if and only if  $C$  is the triangle  $\Delta(c, q, \tilde{q})$ . The second inequality cannot become an equality, but the two numbers can become arbitrarily close if  $l(v)$  is small compared to  $b_1 + b_2$ . This happens if the triangle is very thin and  $q\tilde{q}$  is its shortest side. □

**Corollary 4.13.** *If  $C$  is a convex closed curve in  $\mathbb{R}^2$ , then we have  $h > w/2$ . This inequality cannot be improved.*

*Proof.* The main statement  $h > w/2$  follows immediately from Lemma 4.12 and the definitions of  $h$  and  $w$ .

In order to see that the inequality cannot be improved, we consider a thin isosceles triangle like in Figure 4.8. If  $h$  denotes the minimum halving distance, by Lemma 2.42.2 we have

$2z = 1 + x/2 = 1 + \sin(\alpha/2)$ , thus

$$h \stackrel{\text{similarity of triangles}}{=} \frac{z}{1} x = \frac{1 + \sin\left(\frac{\alpha}{2}\right)}{2} 2 \sin\left(\frac{\alpha}{2}\right) = \left(1 + \sin\left(\frac{\alpha}{2}\right)\right) \sin\left(\frac{\alpha}{2}\right).$$

On the other hand, the width is given by  $w = \sin \alpha = 2 \sin(\alpha/2) \cos(\alpha/2)$ , therefore  $h/w = (1 + \sin(\alpha/2))/(2 \cos(\alpha/2)) \searrow 1/2$  for  $\alpha \rightarrow 0$ .  $\square$

## 4.8 Minimum halving distance $h$ and inradius $r$

Corollary 4.13 further implies the following corollary.

**Corollary 4.14.** *If  $C \subset \mathbb{R}^2$  is a convex closed curve, then  $h > r$ . This bound is tight.*

*Proof.* We only have to combine  $h > w/2$  from Corollary 4.13 with the known inequality  $r \leq w/2$ . The latter inequality is trivial because if  $C$  contains a circular disk with radius  $r$  then the width of  $C$  is bigger than the width of the disk, which obviously equals  $2r$ .

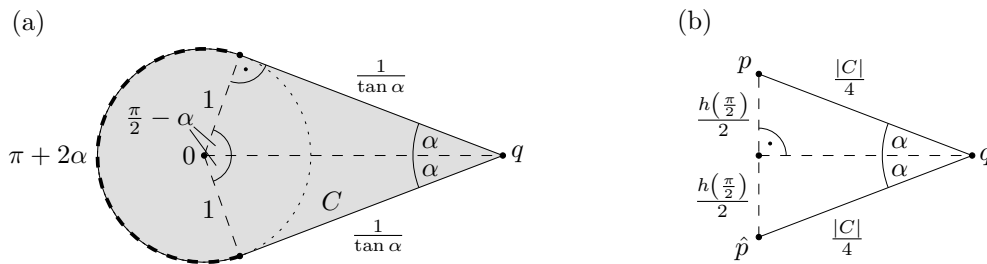


Figure 4.9: The closed curve  $C$  surrounding the grey region attains  $h/r \searrow 1$  for  $\alpha \searrow 0$ , i.e.  $q_x \nearrow \infty$ .

Now consider the convex closed curve  $C$  of Figure 4.9.a. Its region is the convex hull of a unit circle centered at the origin and a point  $q = (q_x, 0)$ ,  $q_x \geq 1$ . The inradius obviously equals  $r = 1$ . Let  $\alpha$  denote half the interior angle of  $C$  in  $q$ . Basic trigonometry yields

$$|C| = 2\pi - 2\left(\frac{\pi}{2} - \alpha\right) + \frac{2}{\tan \alpha} = \pi + 2\alpha + \frac{2}{\tan \alpha}. \quad (4.11)$$

For small  $\alpha$ ,  $q_x$  gets big and the vertical halving chord  $p\hat{p}$  of  $C$  is located in the triangular part of  $C$ . Remember that  $h(\pi/2)$  denotes the length of this halving chord. By Lemma 2.41 we can conclude that  $h = h(\pi/2)$  holds in this situation, but we only need the trivial inequality  $h \leq h(\pi/2)$ .

Consider Figure 4.9.b. Because  $p\hat{p}$  is a halving chord and by the symmetry about the  $x$ -axis we get

$$\frac{h(\pi/2)}{\frac{|C|}{4}} = \sin \alpha. \quad (4.12)$$

Plugging everything together yields

$$\begin{aligned} h/r &= h \leq h \left(\frac{\pi}{2}\right) \stackrel{(4.12)}{=} \frac{|C|}{2} \sin \alpha \\ \stackrel{(4.11)}{=} \frac{\pi + 2\alpha + \frac{2}{\tan \alpha}}{2} \sin \alpha &= \left(\frac{\pi}{2} + \alpha\right) \sin \alpha + \cos \alpha \xrightarrow{\alpha \rightarrow 0} 1. \end{aligned}$$

□

## 4.9 Maximum halving distance $H$ and area $A$

In this section we will show that the circle minimizes the ratio  $H^2/A$ . This was proved by Goodey [78] in 1982. Here, we can give a very short proof by applying results from Chapter 2.

**Lemma 4.15.** *Let  $C \subset \mathbb{R}^2$  be a convex close curve. Then  $H^2 \geq (4/\pi)A$ . Equality is attained if and only if  $C$  is a circle.*

*Proof.* First, we assume that  $C$  is piecewise continuously differentiable. By Corollary 2.30 and Lemma 2.21.4 we know that the curve  $C^*$  resulting from the halving pair transformation satisfies  $A(C^*) \geq A(C)$  and  $H(C^*) = H(C)$ . For the centrally symmetric curve  $C^*$  however, the circumradius is clearly given by  $R(C^*) = H(C^*)/2$ , as mentioned already in equation (2.6), and obviously  $A(C^*) \leq \pi R^2(C^*)$  holds. Plugging everything together yields

$$H^2 = H^2(C^*) = (2R(C^*))^2 = 4R^2(C^*) \geq \frac{4}{\pi}A(C^*) \geq \frac{4}{\pi}A.$$

Clearly,  $A(C^*) = \pi R^2(C^*)$  holds only if  $C^*$  is a circle. This means that  $C$  is a Zindler curve. Furthermore by Corollary 2.30 the equality  $A(C^*) = A(C)$  holds only if  $C$  is centrally symmetric, which implies  $C = C^*$  apart from translation. Hence  $H^2 = 4A/\pi$  holds only for circles.

Due to continuity of  $H$  and  $A$  the result can be extended to arbitrary convex cycles by approximating them with polygons, see Section 4.11. □

## 4.10 Minimum halving distance $h$ and area $A$

Although the only inequality  $h^2 \leq \sqrt{3}A$  we can show between minimum halving distance  $h$  and area  $A$  follows easily from known results, although this inequality is not tight, and although it is easy to see that there cannot be any lower bound to  $h^2/A$ , we decided to dedicate a whole section to these questions, because we want to mention related work by other authors and we would like to state some conjectures.

First, we prove the announced results.

**Lemma 4.16.** *Let  $C$  be an arbitrary convex closed curve in the plane. Then, its minimum halving distance  $h$  and its area  $A$  satisfy*

$$h^2 \leq \sqrt{3}A.$$

*This bound is not tight.*

*On the other hand, the ratio  $h^2/A$  can become arbitrarily close to 0.*

*Proof.* Plugging  $h \leq w$  into the known inequality  $w^2 \leq \sqrt{3}A$  (see [158], [184, 6-4, pp. 221f.], [115, 70., p. 183]) yields  $h^2 \leq \sqrt{3}A$ .

The equality  $w^2 = \sqrt{3}A$  is attained only by equilateral triangles (see references above) and their minimum halving distance  $h$  is strictly smaller than their width  $w$ . This implies by continuity arguments that the inequality  $h^2 \leq \sqrt{3}A$  cannot be tight, see Section 4.11.

A rectangle with a short side of length  $h$  and a long side of length  $A/h$  shows that the minimum halving distance  $h$  can get arbitrarily small for any given area value  $A$ .  $\square$

**Open Problem 9.** *What is the supremum of  $h^2/A$ ?*

In [40] Croft et al. published a question by Santaló, who asked whether the supremum of  $h^2/A$  equals  $4/\pi$ . This would mean that circles attain the maximum. Although Santaló's question is formulated for the chords bisecting the area, i.e. it asks for the supremum of  $h_A^2/A$  where  $h_A$  denotes the minimum length of any chord bisecting the area, the negative answer for both concepts can be based on the same curves.

The Zindler curves satisfy  $h^2 = H^2 = h_A^2 = H_A^2 = 4A(C^*)/\pi$  since their halving pair transformation  $C^*$  is a circle with radius  $h/2$ . Corollary 2.30 from Section 2.10 shows  $A(C) = A(C^*) + I(M)$ . Remember that  $I(M)$  denotes the negative area of the midpoint curve where each encircled region is counted with the multiplicity of the corresponding winding number. If the curve  $C$  is not a circle, we have  $I(M) < 0$ , and we can deduce

$$A(C) \stackrel{\text{Cor. 2.30}}{=} A(C^*) + I(M) < A(C^*) = \frac{\pi}{4}h^2 = \frac{\pi}{4}h_A^2.$$

Hence, every Zindler curve which is not a circle proves a negative answer to Santaló's question both for  $h$  and for  $h_A$ . Goodey's surveying write-up [76] shows that this consequence is known.

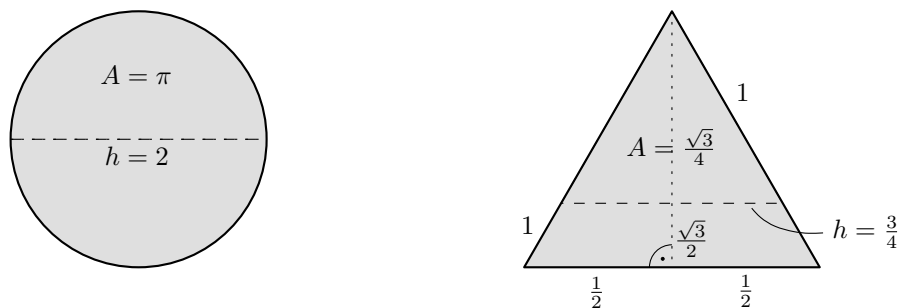


Figure 4.10: The equilateral triangle has a bigger ratio  $h^2/A = (3\sqrt{3})/4 \approx 1.30$  than the circle ( $4/\pi \approx 1.27$ ).

It is easy to prove that the equilateral triangle attains  $h^2/A = (\frac{3}{4})^2/\frac{\sqrt{3}}{4} = \frac{3\sqrt{3}}{4} \approx 1.30$ , see Figure 4.10. This is a value bigger than  $4/\pi \approx 1.27$  and even bigger than the result  $\approx 1.29$  of the rounded triangle  $C_\Delta$  from Section 3.2.1, which we conjecture to maximize the ratio  $h^2/A$  amongst the Zindler-curves. Although we have no proof so far, we would not be surprised if the equilateral triangle attained the global maximum.

## 4.11 Continuity and approximation arguments

In this section we want to discuss briefly the continuity arguments which are used throughout the chapter.

To compare two compact, convex sets  $X, Y \subset \mathbb{R}^2$ , we can use the *Hausdorff distance*

$$d_H(X, Y) := \max \left( \sup_{p \in X} \inf_{q \in Y} |pq|, \sup_{q \in Y} \inf_{p \in X} |pq| \right)$$

or the *Eggleston-distance* introduced by Eggleston [63, p. 60],

$$d_E(X, Y) := \sup_{p \in X} \inf_{q \in Y} |pq| + \sup_{q \in Y} \inf_{p \in X} |pq|.$$

It is well-known and straight forward to show that both equations define metrics. For  $d_E$  we refer to Eggleston [63, p. 60], for  $d_H$  this can be proved analogously. Furthermore, from the definitions follows

$$d_H(X, Y) \leq d_E(X, Y) \leq 2d_H(X, Y),$$

the two metrics are equivalent.

Now let  $\mathcal{X}$  denote the set of compact, convex sets in  $\mathbb{R}^2$ . A sequence of sets  $X_i \in \mathcal{X}$ ,  $i \in \mathbb{N}$ , *converges* to a set  $X \in \mathcal{X}$ , iff  $d_H(X_i, X) \rightarrow 0$ . We denote this by  $X_i \rightarrow X$ . A function  $f : \mathcal{X} \rightarrow \mathbb{R}$  is *continuous* iff  $f(X_i) \rightarrow f(X)$  for every converging sequence  $X_i \rightarrow X$ . As in metric spaces sequence convergence is equivalent to convergence, see for instance [7, 0.15.4)], this is equivalent to

$$\forall X \in \mathcal{X} : \forall \varepsilon > 0 : \exists \delta > 0 : \forall Y \in \mathcal{X} : \\ d_H(X, Y) < \delta \Rightarrow |f(X) - f(Y)| < \varepsilon.$$

It is known that every compact convex set  $X \in \mathcal{X}$  can be approximated by polygons, i.e. there exist polygons  $P_i$ ,  $i \in \mathbb{N}$ , such that  $P_i \rightarrow X$ . Proofs can be found for instance in [63, pp. 68f.] and [22, pp. 35f.].

The convex bodies in  $\mathcal{X}$  can also be approximated by smooth bodies, i.e., the sets  $\{x \in \mathbb{R}^2 \mid \varphi(x) \leq 1\}$  for analytic functions  $\varphi(x)$  are dense in  $\mathcal{X}$ . This result was first proved by Minkowski [150], see also Bonnesen and Fenchel [22, pp. 36f.]. An overview of approximations of convex bodies can be found in Gruber's survey [89].

It is sufficient to prove inequalities between continuous quantities of convex sets for polygons. Because of continuity and because every set  $X \in \mathcal{X}$  can be approximated by polygons, this immediately proves the inequality for every convex set  $X \in \mathcal{X}$ .

The probably most important result from convex geometry in this context, which is also important for some argumentation in this chapter, is the *Blaschke selection theorem*. Blaschke [19] proved it in 1916, and it appears in almost every textbook of convex geometry and in Gruber's survey [90].

**Theorem 4.17.** (*Blaschke [19]*) *Let  $\mathcal{Y} \subset \mathcal{X}$  be an infinite set of uniformly bounded convex sets. This means, there exists a radius  $\rho$  such that every  $X \in \mathcal{Y}$  is contained in  $B_\rho(0)$ . Then, there exists a sequence of sets  $X_i \in \mathcal{Y}$  and a set  $X \in \mathcal{X}$  such that  $X_i \rightarrow X$ .*

In this chapter, the theorem is useful to prove that certain inequalities between two continuous, translation invariant, scalable, non-negative quantities  $a(\cdot)$ ,  $b(\cdot)$  are not tight. We call the quantity  $a(\cdot)$  scalable, iff  $\forall s \in \mathbb{R} : \forall X \in \mathcal{X} : a(sX) = sa(X)$ . Additionally, we assume that  $b(\cdot)$  is bounding, i.e.  $\exists \rho \in \mathbb{R} : \forall X \in \mathcal{X} : R(X) \leq \rho b(X)$ . For example, the diameter  $D$  is bounding but the minimum halving distance  $h$  is not.

The situation is that two known inequalities  $a(X) \leq \rho_1 c(X)$  and  $c(X) \leq \rho_2 b(X)$  imply  $a(X) \leq \rho_1 \rho_2 b(X)$  for constants  $\rho_1, \rho_2 > 0$ . And we know that there is no common extremal set of both known inequalities, i.e., there is no set which attains equality for both inequalities.

Then, we can use a proof by contradiction to show that the derived inequality  $a(X) \leq \rho_1 \rho_2 b(X)$  is not tight (apart from possible degenerate cases with  $a(X) = b(X) = 0$ ). If it was tight, there would exist a sequence of sets  $X_i \in \mathcal{X}$  such that  $a(X_i)/b(X_i) \rightarrow \rho_1 \rho_2$ . By scaling, we can achieve  $b(X_i) = 1$  for every  $X_i$ . Because  $b(\cdot)$  is bounding, by translation we can achieve that all the sets  $X_i$  are contained in the same  $B_\rho(0)$ .

Then, by the Blaschke selection theorem, the sequence converges to a set  $X \in \mathcal{X}$ . As  $X$  cannot be extremal for both known inequalities, we have  $a(X) < \rho_1 c(X)$  or  $c(X) < \rho_2 b(X)$ , hence  $a(X) < \rho_1 \rho_2 b(X)$ . However, as both,  $a(\cdot)$  and  $b(\cdot)$  are continuous, we conclude  $b(X) = \lim b(X_i) = 1$  and  $a(X) = \lim a(X_i) = \rho_1 \rho_2$ , a contradiction.

Because of these applications, we are interested in proving the continuity of the quantities considered in this chapter.

**Lemma 4.18.** *Width  $w$ , diameter  $D$ , perimeter  $|C|$ , inradius  $r$ , circumradius  $R$  and area  $A$  are continuous on  $(\mathcal{X}, d_H)$ .*

*Proof.* Note that as before, we identify any convex set  $X \in \mathcal{X}$  with its boundary curve  $C = \partial X$ .

It is easy to prove that the  $v$ -breadth  $b_C(v)$  is continuous for every fixed  $v \in \mathbb{S}^1$ . To this end, we first prove the continuity of the *support function* defined by

$$s_C : \mathbb{S}^1 \rightarrow \mathbb{R}, \quad s_C(v) := \max_{z \in C} \langle z, v \rangle. \quad (4.13)$$

Let  $\varepsilon > 0$  be a given constant, and let  $v \in \mathbb{S}^1$  be a given direction. We consider an extreme point  $p \in C$  in direction  $v$ , i.e.  $\langle p, v \rangle = s_C(v)$ . Every boundary curve  $C_\delta$  of a set  $X_\delta \in \mathcal{X}$  satisfying  $d_H(X, X_\delta) < \delta := \varepsilon$  contains a point  $p' \in C_\delta$  such that  $|pp'| < \delta$ . This implies

$$|\langle p' - p, v \rangle| < \delta \quad (4.14)$$

and

$$s_{C_\delta}(v) \stackrel{\text{Def.}}{\geq} \langle p', v \rangle \stackrel{(4.14)}{>} \langle p, v \rangle - \delta = s_C(v) - \delta.$$

This argument is symmetric between  $C$  and  $C_\delta$ . Thus, we also have

$$s_C(v) > s_{C_\delta}(v) - \delta.$$

Combining both statements with  $\delta = \varepsilon$  yields

$$|s_C(v) - s_{C_\delta}(v)| < \varepsilon,$$

which completes the proof of the continuity of the support function.

Due to  $b_C(v) = s_C(v) - s_C(-v)$ , this immediately implies the continuity of any  $v$ -breadth, the continuity of the width  $w$  and the diameter  $D$ . By Cauchy's surface area formula, Lemma 2.7, it also proves the continuity of the perimeter  $|C|$ . The continuity of the inradius  $r$  and the circumradius  $R$  can be proved with similar arguments. For the continuity of the area we refer to Eggleston [63, pp. 72f.] and Bonnesen and Fenchel [22, p. 38].  $\square$

Of course, we also want to prove the continuity of  $h$  and  $H$ . As every boundary curve  $C = \partial X$  of a set  $X \in \mathcal{X}$  is rectifiable, we can define halving distance for every  $X \in \mathcal{X}$ . Only the special case where  $X$  is degenerated to a line segment  $pq$  needs special attention, because then  $C = \partial X$  is not simple. In this case, we choose the natural definition, that  $h_C(v) := 0$  for every  $v \in \mathbb{S}^1$  apart from the direction  $w \in \mathbb{S}^1$  of the segment  $pq$ , where we define  $h_C(w) := h_C(-w) := |pq|$ .

**Lemma 4.19.** *Minimum and maximum halving distance,  $h$  and  $H$ , are continuous on  $\mathcal{X}$ .*

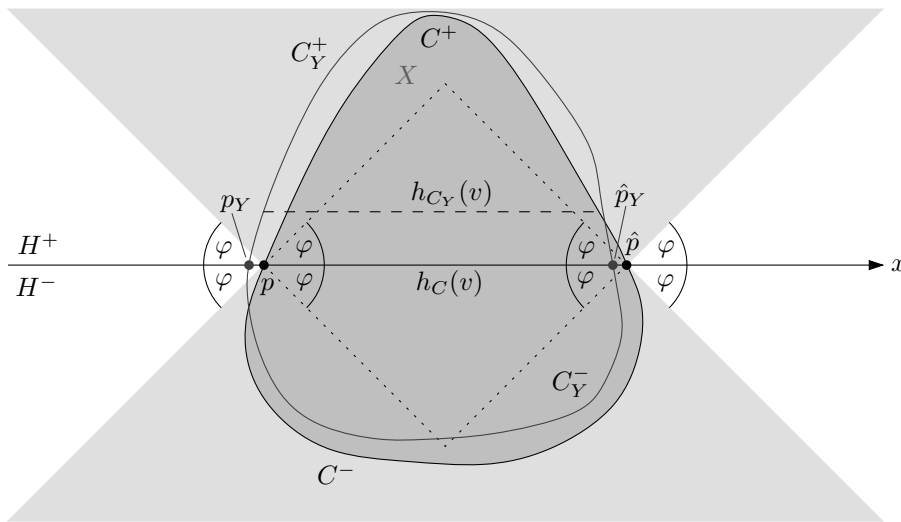


Figure 4.11: Proving that  $h_C(v)$  is continuous at a non-degenerate convex cycle  $C$ .

*Proof.* First, we consider the case where the set  $X \in \mathcal{X}$  is not degenerated to a line segment, see Figure 4.11. We prove that the halving distance  $h_C(v)$  is continuous for a given arbitrary direction  $v \in \mathbb{S}$ . This immediately implies the continuity of  $h$  and  $H$ .

Let  $\varepsilon > 0$  be a given constant, and let  $C := \partial X$  be the boundary curve of  $X$ . We may assume that  $v = (1, 0)$ , and that the halving pair  $(p, \hat{p})$  with direction  $v$  lies on the  $x$ -axis. By  $C^+$  we denote the part of  $C$  which lies in the half-plane with positive  $y$ -coordinate  $H^+$ , and  $C^-$  is the other part in the complementary half-plane  $H^-$ .

Because  $X$  is not degenerated to a segment, it must contain a rhombus with apices  $p$  and  $\hat{p}$  and some apex angle  $2\varphi > 0$ . And it is contained in the light grey region shown in Figure 4.11. Let  $Y \in \mathcal{X}$  be a convex set satisfying  $d_H(X, Y) < \delta$ . We define  $C_Y := \partial Y$ ,  $C_Y^+ := C_Y \cap H_+$ ,  $C_Y^- := C_Y \cap H_-$ .

We prove  $|C_Y^+| \rightarrow |C^+|$  and  $|C_Y^-| \rightarrow |C^-|$  for  $\delta \rightarrow 0$ . Because of the rhombus contained in  $X$  and the convexity of  $Y$ ,  $C_Y$  must intersect with the  $x$ -axis exactly twice for a sufficiently

small  $\delta$ . One intersection point,  $p_Y$ , is closer to  $p$ , and the other one,  $\hat{p}_Y$ , is closer to  $\hat{p}$ . At first glance one could assume that  $d_H(Y \cap H^+, X \cap H^+) < \delta$ . However, this does not have to hold, as for instance the point  $q \in X$  closest to  $p_Y$  could lie a little below the  $x$ -axis, guaranteeing  $d_H(Y, X) < \delta$  but not  $d_H(Y \cap H^+, X \cap H^+) < \delta$ . Still, easy but technical angle

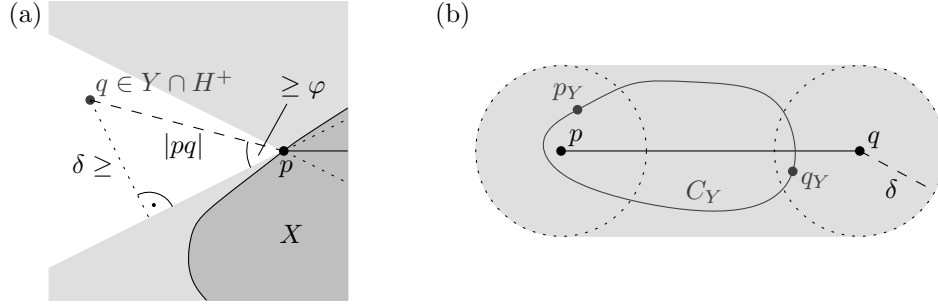


Figure 4.12: (a) Angle analysis in the normal case. (b) Proving continuity of  $H(C)$  and  $h(C)$  at a line segment  $C = pq$ .

arguments sketched in Figure 4.12.a yield

$$d_H(Y \cap H^+, X \cap H^+) < \frac{\delta}{\sin \varphi}, \quad d_H(Y \cap H^-, X \cap H^-) < \frac{\delta}{\sin \varphi},$$

$$|p_Y p| < \frac{\delta}{\sin \varphi} \quad \text{and} \quad |\hat{p}_Y \hat{p}| < \frac{\delta}{\sin \varphi}.$$

Due to the continuity of the perimeter, this yields

$$\begin{aligned} |C_Y^+| &= |\partial(Y \cap H^+)| - |p_Y \hat{p}_Y| \\ &\quad \downarrow \qquad \qquad \downarrow \\ &|\partial(X \cap H^+)| - |p \hat{p}| = |C^+| \quad \text{for } \delta \rightarrow 0 \end{aligned}$$

and, analogously,  $|C_Y^-| \rightarrow |C^-| = |C|/2$ . Furthermore, we have  $|C_Y| \rightarrow |C|$ . For the given  $\varepsilon > 0$ , we choose  $\delta > 0$  so small that we can conclude  $\delta/\sin \varphi < \varepsilon/4$ ,  $\| |C_Y^+| - |C^+| \| < \varepsilon/4$  and  $\| |C_Y^-| - |C^-| \| < \varepsilon/4$ . Hence, we have to move  $p_Y$  and  $\hat{p}_Y$  only by a summed distance of less than  $\varepsilon/2$  on  $C_Y$  to reach a horizontal halving pair. Because of  $|p_Y p| < \delta/\sin \varphi$  and  $|\hat{p}_Y \hat{p}| < \delta/\sin \varphi$ , this yields

$$|h_{C_Y}(v) - h_C(v)| < 2 \frac{\delta}{\sin \varphi} + \frac{\varepsilon}{2} \leq \varepsilon.$$

This proves the continuity of  $h_C(v)$  for non-degenerate  $C$ .

Now, let  $X$  be degenerated to a single point  $p$ , then  $h_C(v) = 0$  for every  $v \in \mathbb{S}^1$ . And every  $Y \in \mathcal{X}$  satisfying  $d_H(X, Y) < \delta$  is contained in  $B_\delta(p)$ . Hence, for every direction  $v \in \mathbb{S}^1$  we have  $h_{C_Y}(v) \leq b_{C_Y}(v) \leq 2\delta$ . This proves the continuity of  $h_C(v)$  for  $X = \{p\}$ .

Finally, let  $X$  be degenerated to a line segment  $pq$  as shown in Figure 4.12.b. Unfortunately, in this case  $h_C(v)$  is not continuous if  $v \in \mathbb{S}^1$  denotes the direction  $v$  of  $pq$ , because in this case the segment can be approximated by slightly turned segments  $Y_i$  of the same length, which all satisfy  $h_{C_{Y_i}}(v) = 0$ , while  $h_C(v) = |pq| > 0$ .



However, nevertheless, minimum and maximum halving distance,  $h(C)$  and  $H(C)$ , are continuous in a set  $X$  degenerated to a line segment  $pq$ . We have  $h(C) = 0$ , and every set  $Y \in \mathcal{X}$  satisfying  $d_H(X, Y) < \delta$  yields  $h(C_Y) < w(C_Y) < 2\delta$ , which proves the continuity of  $h(C)$  in this case. On the other hand, we have  $H(C) = |pq|$ , and every set  $Y \in \mathcal{X}$  satisfying  $d_H(X, Y) < \delta$  has to contain a point  $p_Y \in B_\delta(p)$  and a point  $q_Y \in B_\delta(q)$ . The length of the shorter path connecting them on  $C_Y$  is  $\geq |p_Y q_Y| \geq |pq| - 2\delta$ . Hence, as  $|C_Y| \leq 2\pi\delta + 2|pq|$ , the length of the longer path connecting  $p_y$  and  $q_y$  on  $C_Y$  is  $\leq |pq| + 2\pi\delta + 2\delta$ . Thus, by moving the two points by a summed distance  $\leq (\pi + 2)\delta$  on  $C_Y$  we reach a halving pair. This proves

$$|pq| + 2\delta \geq D(C_Y) \geq H(C_Y) \geq |p_Y q_Y| - (\pi + 2)\delta \geq |pq| - (\pi + 4)\delta.$$

Maximum halving distance  $H(C)$  is continuous also in this case. □



# Chapter 5

## Point Sets

### 5.1 Embedding point sets with small geometric dilation

We have discussed in detail the dilation of cycles in Chapter 2 and properties of Zindler curves in Chapter 3. The results of both chapters will help us now to deal with the main question of this thesis.

Given a finite point set  $S \subset \mathbb{R}^2$ , we want to find a finite, simple, geometric graph  $G$  of small geometric dilation which *embeds*  $S$ . This means that every point  $p \in S$  lies either on an edge or on a vertex of  $G$ . Note that, as before, we do not restrict our consideration to straight edges, but we allow arbitrary piecewise continuously differentiable edges.

It seems to be very difficult to determine the best (=smallest) possible dilation value for any graph which embeds a given finite point set  $S$ . Remember that we call the best possible value, or, more precisely, the infimum of these values, the (*geometric*) *dilation* of the finite point set  $S$ . In equation (1.3) from the introduction we defined this as

$$\delta(S) := \inf_{G \text{ simple, finite, } S \subset G} \delta(G). \quad (5.1)$$

#### 5.1.1 Optimal embeddings for particular point sets

As an example, we want to mention the known best embedding for three points  $\{a, b, c\} \subset \mathbb{R}^2$ , see Figure 5.1. Ebbers-Baumann et al. [60] proved that it is either a Steiner-tree with  $120^\circ$ -angles or a curve built of two line segments and a part of a logarithmic spiral.

The example shows that finding the graph of smallest dilation which embeds a given finite point set is not easy, even for point sets of size 3. It turns more complicated for a growing number of points. In [56, 58] we answered the question for every set  $S_n$  of  $n$  points spaced evenly on a circle. The result is shown in Figure 5.2. We give a full proof of  $\delta(S_5) = \frac{\pi}{2}$  in Section 5.3.1.

However, we are far from being able to describe a general construction algorithm which returns for a given finite point set  $S \subset \mathbb{R}^2$  a graph of smallest dilation embedding  $S$ . It is not even clear if there exists such a graph for every point set, i.e., if the infimum is attained by a graph.

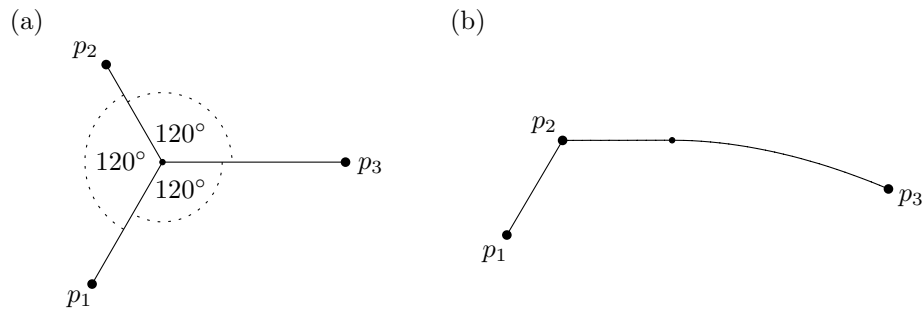


Figure 5.1: The dilation-optimal embedding of three points is either (a) a Steiner-tree with  $120^\circ$ -angles or (b) a curve built of two line segments and a part of a logarithmic spiral.

**Open Problem 10.** *Given an arbitrary finite point set  $S \subset \mathbb{R}^2$ , is there always a geometric graph  $G_S$  of smallest dilation embedding  $S$ ? How can we construct  $G_S$ ? Or how can we compute  $\delta(S)$ ?*

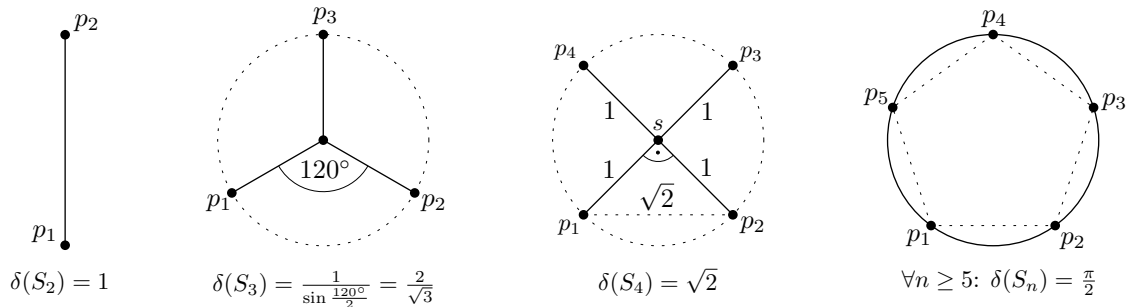


Figure 5.2: The optimal embeddings of the point sets  $S_n$ , which contain  $n$  points placed evenly on a circle.

### 5.1.2 Bounding the worst-case dilation

As seen in the previous subsection, so far, optimal embeddings are only known for few special cases. Therefore, it is an interesting question, which dilation value we can guarantee for any finite point set. In the introduction we defined this value as

$$\Delta := \sup_{S \subset \mathbb{R}^2, |S| < \infty} \delta(S) \stackrel{(5.1)}{=} \sup_{S \subset \mathbb{R}^2, |S| < \infty} \inf_{G \text{ simple, finite, } S \subset G} \delta(G). \tag{5.2}$$

### 5.1.3 Dilation attained by mutually visible points

Before we try to give first approximations to the value  $\Delta$ , we transfer a well-known argument to the situation of arbitrary geometric graphs. This argument was used before by Ebberts-Baumann et al. [61, Lemma 4] to approximate the dilation of polygonal curves. Agarwal et

al. [3, 2] reused it to compute the dilation of such paths exactly. And I applied it to compute the dilation of polygons in my diploma thesis [92, Lemma 3.1].

Apart from the exceptional case which we considered already for closed curves in Lemma 2.1, there always exist two mutually visible points  $p, q \in G$  attaining maximum detour. Two points  $p$  and  $q$  are called *mutually visible*, if the line segment  $pq$  does not intersect with  $G$  apart from its endpoints.

**Lemma 5.1.** *Let  $G$  be a geometric graph in the plane satisfying  $\delta(G) > 1$ . Then one of the following statements holds.*

1. *The dilation of  $G$  is the limit of detour values of a sequence of pairs  $(p_n, q_n)_{n \in \mathbb{N}} \subset G \times G$ , so that  $(p_n)_{n \in \mathbb{N}}$  and  $(q_n)_{n \in \mathbb{N}}$  approach the same point  $p \in G$  from different sides.*
2. *The dilation of  $G$  is attained by a pair of mutually visible points  $p, q \in G$ .*

*Proof.* The proof of Lemma 2.1 can be extended easily to the kind of graphs we consider in this chapter. Hence, we know that either case 1. holds or we have a pair of points  $p, q \in G$  satisfying  $\delta(G) = \delta_G(p, q)$ .

We choose the two points  $p$  and  $q$  so that the distance  $|pq|$  is minimal amongst all the pairs attaining maximum detour. Such a pair exists because in any case we have a sequence of pairs with maximum detour whose distances approach the infimum. By compactness arguments, there is a subsequence converging to the desired pair.

We use a proof by contradiction and assume that  $p$  and  $q$  are not mutually visible, see Figure 5.3.

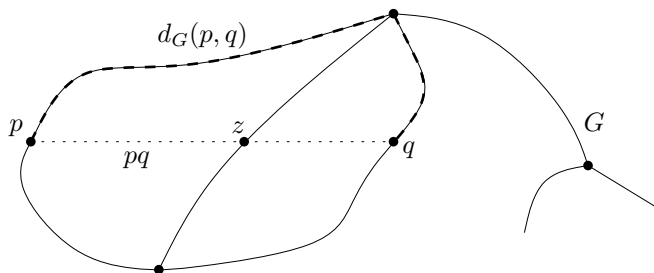


Figure 5.3: If two points  $p, q$ , which attain maximum detour, are not mutually visible, we can find another pair,  $(p, z)$  or  $(z, q)$ , of maximum detour and smaller distance.

Then, there exists a point  $z$ ,  $z \neq p$ ,  $z \neq q$ , on the line segment  $pq$  which lies on an edge of the graph  $G$ . Because the three points are collinear and appear in the order  $p, z, q$  on  $pq$ , we have  $|pq| = |pz| + |zq|$ . The triangle inequality for the shortest-path metric yields  $d_G(p, q) \leq d_G(p, z) + d_G(z, q)$ . Plugging this together results in

$$\begin{aligned} \delta_G(p, q) &= \frac{d_G(p, q)}{|pq|} \stackrel{\Delta\text{-inequ.}}{\leq} \frac{d_G(p, z) + d_G(z, q)}{|pz| + |zq|} \\ &\stackrel{*}{\leq} \max\left(\frac{d_G(p, z)}{|pz|}, \frac{d_G(z, q)}{|zq|}\right) = \max(\delta_G(p, z), \delta_G(z, q)). \end{aligned}$$

The inequality marked with a star is analogous to the one used in the end of the proof of Theorem 2.12. It holds because of the following observation. If we have  $a_i/b_i \leq c$  for positive values  $a_i, b_i$  and for every  $i \in \{1, \dots, n\}$ <sup>1</sup>, we can conclude  $(\sum a_i)/(\sum b_i) \leq c$ . This can be seen easily by multiplying all the inequalities by its denominators.

We have shown that the pair  $(p, z)$  or the pair  $(z, q)$  have the same (maximum) detour as  $(p, q)$ . As  $|pz| < |pq| > |zq|$ , this is a contradiction, because  $pq$  has the smallest distance amongst the pairs attaining maximum detour. Hence,  $p$  and  $q$  must be mutually visible.  $\square$

## 5.2 Upper bounds

### 5.2.1 Rectangular grid

Now we are able to give upper bounds to the dilation constant  $\Delta$ . To this end, we have to embed any finite point set  $S$ . A first idea could be to draw horizontal and vertical lines through every given point, and remove the parts which are outside of the bounding box  $R(S)$ . This construction is shown in Figure 5.4.a.

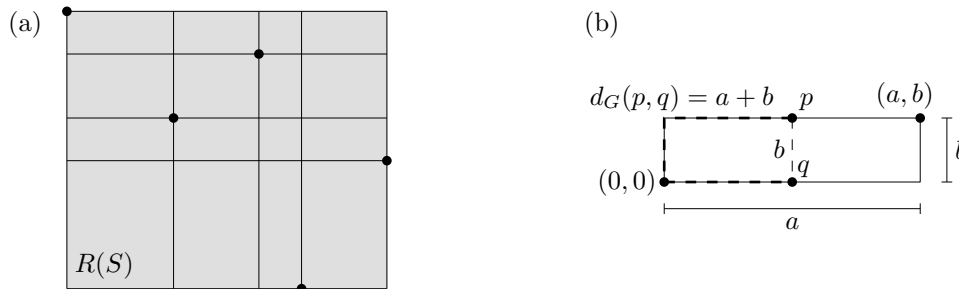


Figure 5.4: Embedding a point set  $S$  by the rectangular grid induced by  $S$  is not a very good idea.

As we discussed briefly in Section 1.3.5 of the introduction, this is optimal concerning the  $L_1$ -dilation; see for instance the articles by Gudmundsson et al. [98] and by Benkert et al. [16] dealing with minimum Manhattan networks.

However, for our problem the induced rectilinear grid is not very helpful. Even for only two points, the resulting dilation can become arbitrarily big. See Figure 5.4.b for an example. The dilation of the rectangle induced by the point set  $S := \{(0,0), (a,b)\}$ ,  $a, b > 0$ , equals  $(a + b)/\min(a, b)$ . This follows directly from Theorem 2.12. For instance if  $a \equiv 1$  and  $b \searrow 0$  this dilation value becomes arbitrarily big.

### 5.2.2 Square grid

Obviously, the dilation  $(a + b)/\min(a, b)$  of a rectangle attains its minimum 2 for  $a = b$ . Therefore we would prefer to embed the given point set  $S$  by a *square grid* like the one shown in Figure 5.5.a.

<sup>1</sup>In this proof, we only need the case  $n = 2$ .

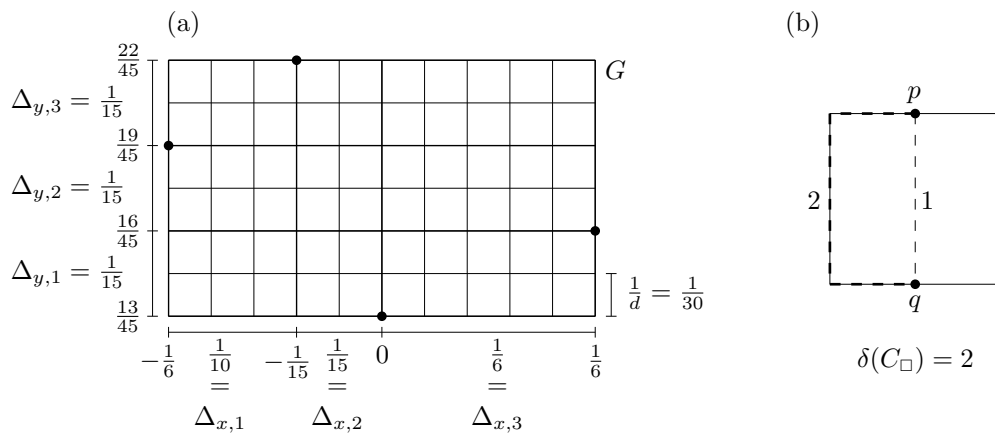


Figure 5.5: By embedding a point set  $S$  into a square grid  $G$  we show  $\delta(S) \leq 2$ , because any square satisfies  $\delta(C_\square) = 2$ .

Because of the formula in Lemma 2.1 the dilation limit of pairs of points  $(p_n, q_n)$  which approach the same point  $p$  from different sides, cannot be bigger than  $1/\sin(90^\circ/2) = \sqrt{2}$  in the case of a square grid.

In the remaining case of Lemma 5.1, the dilation is attained by a mutually visible pair of points. This means, the two points lie on the boundary of a common square. Hence, their detour is not bigger than the dilation of the square, which equals 2 by Lemma 2.44, cf. Figure 5.5.b. This proves that the dilation of the square grid equals 2.

However, can we embed any finite point set  $S$  by a square grid? This is clearly possible if all the coordinates are integers. And it is not difficult either to find a fitting square grid if all the coordinates are rationals, cf. Figure 5.5.a.

Let  $S$  be the given finite point set of size  $n$ . And let  $x_1 < x_2 < \dots < x_l$ ,  $l \leq n$ ,  $y_1 < y_2 < \dots < y_m$ ,  $m \leq n$ , denote the sorted  $x$ -coordinates ( $y$ -coordinate resp.) of the given points such that each value appears only once. We define

$$\begin{aligned} \Delta_{x,i} &:= x_{i+1} - x_i \quad \text{for } i \in \{1, \dots, l-1\} \\ \text{and } \Delta_{y,j} &:= y_{j+1} - y_j \quad \text{for } j \in \{1, \dots, m-1\}. \end{aligned}$$

Then, we can choose the side length of the squares as  $1/d$ , where  $d$  denotes the least common denominator  $d := \text{lcd}(\Delta_{x,1}, \dots, \Delta_{x,l-1}, \Delta_{y,1}, \dots, \Delta_{y,m-1})$  of the coordinate distances. Clearly, there exists a square grid of square size  $1/d$  such that every point from  $S$  lies on a vertex of the grid.

In the remaining case, where not all the coordinates of the given points are rationals, there are situations where the given finite point set cannot be embedded into a square grid. For instance, this is the case for the point set  $S := \{(0, 0), (1, 1), (\pi, \pi)\}$  because  $\Delta_{x,1} = 1$  is rational but  $\Delta_{x,2} = \pi - 1$  is irrational, and the square size must be a divisor of both values.

However, by applying a result from number theory we can show that one can embed any finite point set into a slightly perturbed square grid whose dilation is arbitrarily close to 2. We published this general approximation argument first in [56, 58], and we will repeat it in

Section 5.2.5. It can be used for any *regular grid*, i.e. an infinite geometric graph which can be constructed by repeating the same parallelogram cell. Here, however, we restrict our consideration to rectangular cells. Not only the square grid but also the hexagonal grid and the improved hexagonal grids, which we analyze in the following subsections, belong to this category. Komorowski examined the graph-theoretic dilation of grids with a rectangular cell, which he called “Grundzellengraphen” (basic cell graphs), in Section 3.3.3 of his German diploma thesis [132].

By the approximation argument we have completed the proof of a first upper bound to the dilation of any finite point set,  $\Delta \leq 2$ .

### 5.2.3 Hexagonal grid

From Section 2.13.2 we know that the dilation of regular  $2k$ -gons decreases if  $k$  increases, cf. Figure 2.41. As, obviously, the equilateral triangle, the square and the hexagon are the only regular polygons which admit a tessellation of the plane, cf. for instance [91, p. 58], the next natural idea is to use a *hexagonal grid*, see Figure 5.6.a.

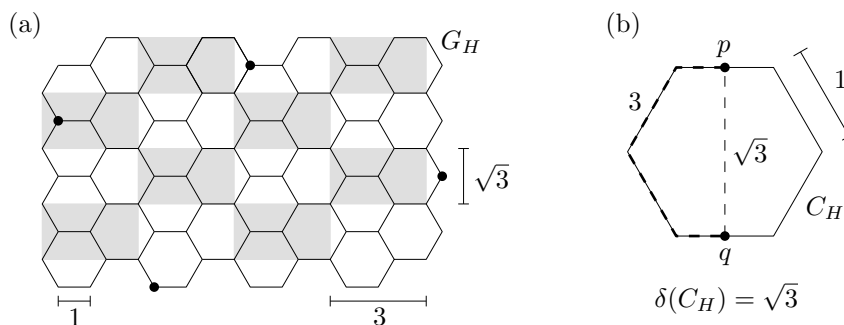


Figure 5.6: By embedding a point set  $S$  into a hexagonal grid  $G_H$ , we show  $\delta(S) \leq \sqrt{3}$ , because any hexagon  $C_H$  satisfies  $\delta(C_H) = \sqrt{3}$ .

The same arguments as for the square grid show that the geometric dilation of the hexagonal grid equals the dilation of the hexagon, which is  $\sqrt{3} \approx 1.732$  by Lemma 2.44, cf. Figure 5.6.b. We have to be a little careful when we prune the hexagonal grid to get a finite graph for the embedding. A bad pruning can cause increased detour values at the boundary. However, if we proceed like in Figure 5.6.a, the dilation remains  $\sqrt{3}$ .

We consider the grid of hexagons with side length 1 where two sides of each hexagon have a horizontal direction. This time finding an embedding for a given point set  $S$  is easy, if all the  $y$ -coordinate distances  $\Delta_{y,j}$  are rationals and all the  $x$ -coordinate distances  $\Delta_{x,i}$  are rationals multiplied by  $\sqrt{3}$  or vice versa. This is the case, because the underlying rectangular cell of the hexagonal grid has the horizontal side length 3 and the vertical side length  $\sqrt{3}$ , cf. Figure 5.6.a. To be slightly more general, we can easily use the hexagonal grid to embed  $S$ , if there exists a constant  $c \in \mathbb{R}$  such that  $\{\Delta_{x,1}, \dots, \Delta_{x,l-1}\} \subset \sqrt{3}c\mathbb{Q}$  and  $\{\Delta_{y,1}, \dots, \Delta_{y,m-1}\} \subset c\mathbb{Q}$ .

Again, we can use the approximation argument from Section 5.2.5 to embed any arbitrary finite point set  $S$  in a scaled and slightly perturbed hexagonal grid. And this results in the better upper bound  $\Delta \leq \sqrt{3} \approx 1.732$ .



### 5.2.4 Improved hexagonal grid

How can we improve the dilation of the hexagonal grid? In the hexagon, the dilation  $\sqrt{3}$  is attained only by pairs of points which lie on the midpoints of opposite edges. Hence, a natural idea would be to smooth the corners of the hexagon a little bit in order to decrease its perimeter and thereby also the detour of the critical midpoint pairs, while the detour values in the corners should not exceed them, either.

In this way, we can try to reach a cycle which is closer to a circle. However, there would appear holes in the grid. The dilation of these holes has to be small, too.

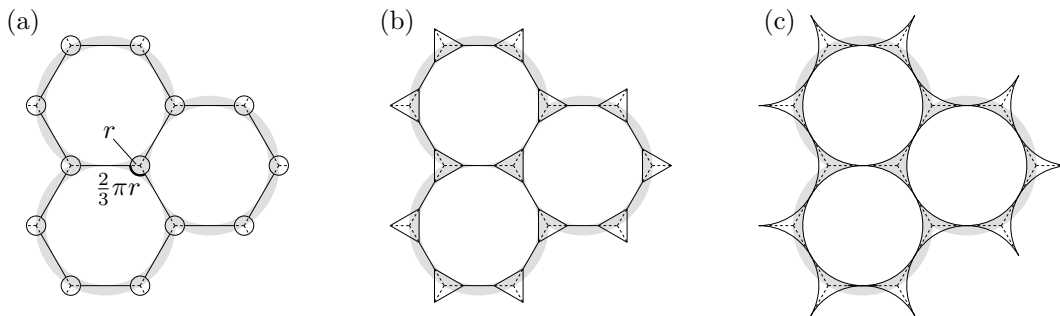


Figure 5.7: Adding circular, triangular or concave triangular holes to the hexagonal grid does not improve its dilation.

We have tried several shapes for these holes. Circles would have the best possible dilation  $\pi/2$ , but they do not help for any radius  $r$ , because they increase the length of the hexagon in the considered corner from  $2r$  to  $\frac{2}{3}\pi r \approx 2.094r$ , see Figure 5.7.a.

The other extreme would be to use triangles, see Figure 5.7.b, or even the concave kind of triangle displayed in Figure 5.7.c. They decrease the dilation of the hexagon, but their own dilation is too big. The equilateral triangle  $\triangle_E$  has dilation  $\delta(\triangle_E) = 2$ , cf. Lemma 2.42 or Lemma 2.45, and the dilation of the concave version is even infinite, because the interior angle in the corners equals  $0^\circ$ .

Clearly, one has to find a happy medium between those extremal configurations. The two best candidates we discovered are the rounded triangle  $C_\Delta$  from Section 3.2.1 and the flower  $C_F$  from Section 3.2.2.

The rounded triangle  $C_\Delta$  is a promising candidate, because it is a convex Zindler curve. Like explained in the introduction of Chapter 3, any local change of such a curve increases its dilation. However, it turns out that using  $C_\Delta$  for the holes like shown in Figure 5.8.a does not decrease the dilation of the whole grid to  $\delta(C_\Delta) = 1.6479$  but only to  $\delta(G_\Delta) \approx 1.6967$ .

The reason is that, depending on the scaling factor  $\varsigma$  of the rounded triangle, the dilation of the hexagonal cycle equals

$$\delta(H_\Delta) \stackrel{*}{=} \frac{|H_\Delta|}{2H(H_\Delta)} = \frac{6 + 6\varsigma \left( \frac{|C_\Delta|}{3} - 2R(C_\Delta) \right)}{2 \min(\sqrt{3}, 2 - 2\varsigma r(C_\Delta))}$$

The inequality ‘ $\geq$ ’ in the step marked with a star holds because the dilation of  $C_\Delta$  is at least the maximum dilation of its halving pairs. The other inequality ‘ $\leq$ ’ would have to be

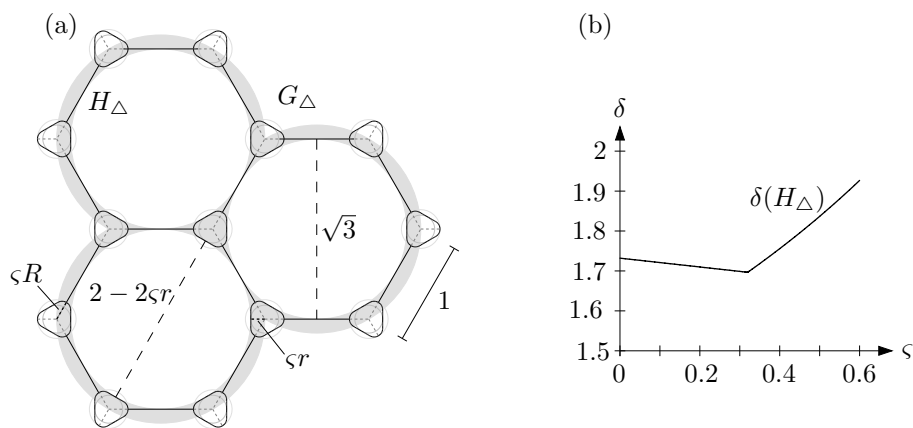


Figure 5.8: Using the rounded triangle  $C_\Delta$  as a “hole” in the hexagonal grid, improves the dilation from  $\sqrt{3} \approx 1.7321$  to  $\approx 1.6967$ .

proven with additional arguments. We cannot apply Theorem 2.12 directly, because  $H_\Delta$  is not convex. However, it turns out that for reasonable values of  $\zeta$  indeed the equality holds. We do not go into detail here, because we do not plan to use the grid  $G_\Delta$  anyway.

Finally, after applying the closed forms for  $|C_\Delta|$ ,  $r(C_\Delta)$  and  $R(C_\Delta)$  from (3.10) and (3.16) it is not difficult to prove that  $\delta(H_\Delta)$  attains its minimum  $\approx 1.6967$  for the scaling factor  $\zeta_{\text{opt}} \approx 0.3199$ , see the plot in Figure 5.8.b. This is where the two values which appear inside of the minimum in the denominator are equal, i.e., where the rounded triangle touches the incircle of the hexagon. We skip the existing but a little complicated and not very helpful closed forms for  $\delta(G_\Delta)$  and  $\zeta_{\text{opt}}$ .

The flower  $C_F$  is preferable, although the variant we will use has a slightly bigger dilation  $\delta(C_F) \approx 1.6778 > 1.6479 \approx \delta(C_\Delta)$ . The flower is better for decreasing the dilation of the hexagonal cycles. In Section 3.2.2 we defined the cycle  $C_F$  in dependence of the two values  $a$  and  $h$ . It is even more intuitive to consider the two parameters

$$\alpha := \frac{a}{h}$$

and  $h$  instead, because in this setting  $\alpha$  defines the shape of  $C_F$  completely and  $h$  is only a scaling factor.

We want to find the values of  $\alpha$  and  $h$  which minimize the dilation of the resulting grid  $G_F$ . However, to get a closed form for the optimal parameters and for  $\delta(G_F)$ , we would have to deal with too complicated formulas. As this dilation value is only a non-tight upper bound to  $\Delta$ , we are satisfied with a very good approximation, which we achieved by Maple analysis. In the following, we describe the main arguments.

Remember the notation from Section 3.2.2, especially Figure 3.18. By inserting flowers in the hexagonal grid like shown in Figure 5.9, in each of the six corners we replace parts of length  $2R(C_F)$  by two circular arcs, each such pair of total length  $|C_F|/3$ . For a reasonable choice of  $\alpha$ , this shortens the hexagonal cycle  $H_F$ . Its length becomes

$$|H_F| = 6 + 6 \left( \frac{|C_F|}{3} - 2R(C_F) \right) \quad (5.3)$$

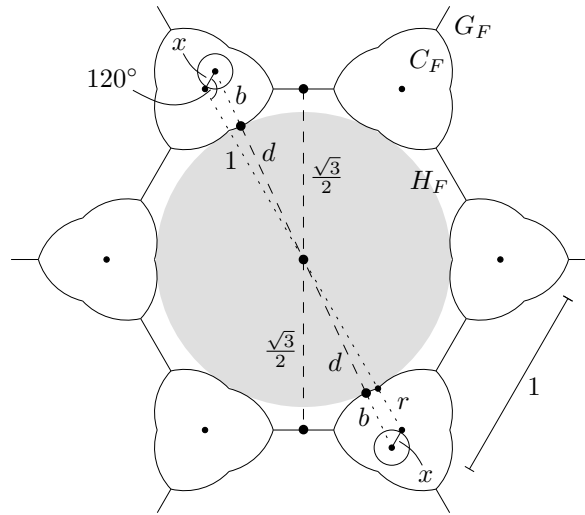


Figure 5.9: The flower  $C_F$  decreases the dilation of the hexagonal grid to  $\approx 1.6778$ . Here, the flowers are bigger than optimal, in order to illustrate the notation.

Hence, in order to decrease the dilation  $|H_F|/2\sqrt{3}$  of the old halving pairs of distance  $\sqrt{3}$ , we would want to make the flowers as big as possible. However, we have to keep in mind that making the flower-cycles too big decreases the inradius of the hexagonal cycles like shown in Figure 5.9. The inradius equals their minimum halving distance due to their central symmetry, see (2.6) in Section 2.6. This influence increases the dilation. Intuitively, one would guess that the optimum is achieved for a scaling value  $h$  where the flowers touch but do not intersect with the inradius of the hexagon. Indeed, this turns out to be true for reasonable  $\alpha$ -values.

To achieve an exact formula, we have to calculate the smallest distance  $2d$  of halving pairs situated on opposite flowers. Figure 5.9 illustrates that there exists a triangle of side-lengths  $1$ ,  $x$  and  $b + d$  with an interior angle of  $120^\circ$ . The law of cosine yields

$$(b + d)^2 = 1^2 + x^2 - 2x \cos(120^\circ).$$

Because of  $\cos(120^\circ) = -\frac{1}{2}$ ,  $x = \frac{2}{\sqrt{3}}a$  by (3.19), and  $b = \sqrt{a^2 + h^2/4}$ , we conclude

$$\begin{aligned} d &= \sqrt{x^2 + x + 1} - b \stackrel{(3.19), \text{Def. } b}{=} \sqrt{\frac{4}{3}a^2 + \frac{2}{\sqrt{3}}a + 1} - \sqrt{a^2 + \frac{h^2}{4}} \\ &\stackrel{\alpha = \frac{a}{h}}{=} \sqrt{\frac{4}{3}\alpha^2 h^2 + \frac{2}{\sqrt{3}}\alpha h + 1} - h\sqrt{\alpha^2 + \frac{1}{4}}. \end{aligned} \quad (5.4)$$

The dilation of the hexagonal cycle equals

$$\delta(H_F) \stackrel{*}{=} \frac{|H_F|}{2h(C_F)} \stackrel{(5.3)}{=} \frac{6 \left(1 + \frac{|C_F|}{3} - 2R(C_F)\right)}{2 \min(\sqrt{3}, 2d)}. \quad (5.5)$$

By the equations (3.17) for  $|C_F|$ , (3.18) for  $R(C_F)$  and (5.4) for  $d$ , we can get a formula which depends only on  $\alpha$  and  $h$ .

In the step marked with a star, the direction  $\geq$  is clear, because the dilation of  $H_F$  is at least the maximum dilation of its halving pairs. Unfortunately, again, for the other direction we cannot use Theorem 2.12, because  $H_F$  is not convex. We do not want to prove the other direction, as this would lead to quite nasty angle arguments. However, Maple analysis shows that the equality holds for reasonable values of  $\alpha$  and  $h$ , in particular for the optimal parameters.

By Lemma 5.1, the dilation of the grid  $G_F$  is attained by pairs of mutually visible points, as, clearly, the angles between arcs ending in the same point are bigger than  $90^\circ$  for a reasonable choice of  $C_F$ . Thus, the dilation of the sequences  $(p_n, q_n)$  dealt with in part 1. of Lemma 5.1 is always smaller than  $1/\sin(\frac{90^\circ}{2}) = \sqrt{2}$ , and does not have any effect. Therefore, we have

$$\delta(G_F) = \max(\delta(C_F), \delta(H_F)).$$

We have discussed that (5.5) results in a formula for  $\delta(H_F)$  which depends only on  $\alpha$  and  $h$ . On the other hand, by (3.20) we know

$$\delta(C_F) = \frac{\pi}{2} \sqrt{4\alpha^2 + 1}.$$

All this results in a closed form for  $\delta(G_F)$  which depends only on  $\alpha$  and  $h$ . We approximated the unique minimum with Maple-analysis. The results are

$$h_{\text{opt}} \approx 0.3188, \quad \alpha_{\text{opt}} \approx 0.1877, \quad a_{\text{opt}} \approx 0.0598, \quad \delta(G_F) \approx 1.6778.$$

The digits given here are sure to be correct. We rounded the approximation result, which involved three more digits.

The grid  $G_F$  is not best possible. One could smooth the concave corners of  $C_F$  a little, which lowers both the dilation of  $C_F$  and the dilation of  $H_F$ . However, the possible improvements are so small that we do not try to pursue this further optimization.

### 5.2.5 Embedding any point set

We have constructed several regular grids of small dilation, the square grid of dilation 2, the hexagonal grid of dilation  $\sqrt{3} \approx 1.732$ , and the improved hexagonal grids of dilation  $\delta(G_\Delta) \approx 1.6967$  and  $\delta(G_F) \approx 1.6778$ .

Like described before, by scaling the square grid appropriately, we can use it to embed any point set  $S$  where all the coordinate distances  $\Delta_{x,1}, \dots, \Delta_{x,l-1}, \Delta_{y,1}, \dots, \Delta_{y,m-1}$  are rational.

Analogously, by scaling we can use the hexagonal grid and its improved variants to embed any point set  $S$  where there exists a constant  $c \in \mathbb{R}$  such that  $\{\Delta_{x,1}, \dots, \Delta_{x,l-1}\} \subset \sqrt{3}c\mathbb{Q}$  and  $\{\Delta_{y,1}, \dots, \Delta_{y,m-1}\} \subset c\mathbb{Q}$ .

Now, let us assume that we have an arbitrary finite point set  $S \subset \mathbb{R}$ . As  $\mathbb{Q}$  is dense in  $\mathbb{R}$ , of course, for every  $\varepsilon > 0$ , we can use a scaled version of these grids, such that every point  $p_i \in S$  has a grid vertex  $q_i$  in its  $\varepsilon$ -ball, i.e.  $|p_i q_i| < \varepsilon$ . In this situation we want to perturb the grid so that  $q_i = p_i$ , that is we would like to move each point  $q_i$  to  $p_i$ . Obviously, we also have to modify the edges which are incident to  $q_i$ . However, this perturbation can increase the dilation arbitrarily, it can even cause self-intersections, as the scaling factor  $\varsigma$  of the grid might

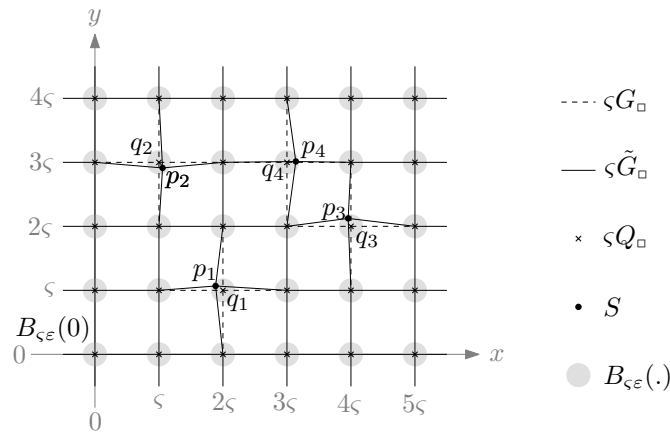


Figure 5.10: If we find for any given finite point set  $S \subset \mathbb{R}^2$  and for every  $\varepsilon > 0$  a scaling factor  $\varsigma \in \mathbb{R}$  such that<sup>3</sup>  $S \subset \varsigma Q_{\square} + B_{\varsigma \varepsilon}(0)$ , then we can embed  $S$  with dilation arbitrarily close to  $\delta(G_{\square}) = 2$ .

be so small that even the given small value  $\varepsilon > 0$  is big compared to  $\varsigma$ . This shows that it is not enough to have  $|p_i q_i| < \varepsilon$ .

We need a stronger result guaranteeing that the distances  $p_i q_i$  are small relatively to the scaled grid  $\varsigma G$ . Written more formally, we need the statement

$$\forall \varepsilon > 0 : \exists \varsigma > 0 : \forall p_i \in S : \exists q_i \in \varsigma Q : |p_i q_i| \leq \varsigma \varepsilon \quad (5.6)$$

where  $Q = d_x \mathbb{Z} \times d_y \mathbb{Z} \subset G$  denotes the vertices of a rectangular grid which lie on edges of  $G$  in such a way that small perturbations of these edges result in small changes of  $\delta(G)$ . For example for the square grid  $G_{\square}$  from Figure 5.10 one can use  $Q_{\square} := \mathbb{Z} \times \mathbb{Z}$ , and for the improved hexagonal grid  $G_F$  from Figure 5.11 we can take  $Q_F := 3\mathbb{Z} \times \sqrt{3}\mathbb{Z}$ .

In order to prove (5.6), we follow the idea we introduced in [56, 58]. It uses the following well-known approximation result by Dirichlet, see for instance Chapter 2 of Matoušek's book on discrete geometry [147].

**Theorem 5.2.** (*Dirichlet*) *Let  $\rho_1, \dots, \rho_m$  be real numbers, and let  $\tilde{\varepsilon} > 0$  be an arbitrary small constant. Then, there exist numbers  $k \in \mathbb{N}$  and  $z_1, \dots, z_m \in \mathbb{Z}$  satisfying*

$$\forall j \in \{1, \dots, m\} : |\rho_j k - z_j| \leq \frac{1}{k^{\frac{1}{m}}} < \tilde{\varepsilon}.$$

With this theorem we can prove the statement (5.6), which we reformulate as a lemma. As mentioned before, one can easily generalize the result to arbitrary regular grids whose basis cell is a parallelogram instead of a rectangle, i.e.  $Q = \mathbb{Z}v + \mathbb{Z}w$  for linearly independent vectors  $v, w \in \mathbb{R}^2$ . However, we formulate only the rectangular case here, because this covers all the grids considered in this thesis.

**Lemma 5.3.** *Given  $n$  points  $p_1, \dots, p_n$  in the plane,  $p_i = (x_i, y_i)$ , and the vertex set  $Q := d_x \mathbb{Z} \times d_y \mathbb{Z}$  of a rectangular grid of horizontal side length  $d_x > 0$  and vertical side length  $d_y > 0$ .*

<sup>3</sup>The Minkowski sum  $\varsigma Q_{\square} + B_{\varsigma \varepsilon}(0)$  contains a  $\varsigma \varepsilon$ -disk around each grid point from  $\varsigma Q_{\square}$ .

Then, for any given small error tolerance  $\varepsilon > 0$ , we can find a scaling factor  $\varsigma > 0$  of  $Q$ , such that every given point  $p_i$  has a “neighbor”  $q_i$  in the scaled vertex set  $\varsigma Q$  satisfying  $|p_i q_i| < \varsigma \varepsilon$ .

*Proof.* Let  $p_1, \dots, p_n$  be arbitrary points satisfying the preconditions of the lemma, let  $d_x > 0$  and  $d_y > 0$  be arbitrary grid parameters, and let  $\varepsilon > 0$  be an arbitrary error tolerance value. Note that this is the error tolerance of the lemma we want to prove, while  $\tilde{\varepsilon}$  denotes the tolerance of Dirichlet’s Theorem, which we apply.

We define the values

$$\rho_j := \begin{cases} \frac{x_j}{d_x} & \text{for } j \in \{1, \dots, n\} \\ \frac{y_{j-n}}{d_y} & \text{for } j \in \{n+1, \dots, 2n\} \end{cases} \quad \text{and} \quad \tilde{\varepsilon} := \min \left( \frac{\varepsilon}{\sqrt{2}d_x}, \frac{\varepsilon}{\sqrt{2}d_y} \right).$$

We apply Dirichlet’s approximation result from Theorem 5.2 to  $\rho_1, \dots, \rho_{2n}$ ,  $m = 2n$ , and  $\tilde{\varepsilon}$ . We get a natural number  $k$  and integers  $z_1, \dots, z_{2n}$  satisfying

$$\forall j \in \{1, \dots, 2n\} : \quad |\rho_j k - z_j| \leq \frac{1}{k^{2n}} < \tilde{\varepsilon}.$$

Next, we define

$$\begin{aligned} \varsigma &:= \frac{1}{k}, \quad a_i := z_i, \quad b_i := z_{n+i} \\ &\text{and } q_i := (\varsigma d_x a_i, \varsigma d_y b_i) \text{ for every } i \in \{1, \dots, n\}. \end{aligned}$$

This results in

$$\forall i : \quad \left| \underbrace{\frac{x_i}{d_x}}_{\rho_i} \underbrace{\frac{1}{\varsigma}}_k - \underbrace{a_i}_{z_i} \right| < \underbrace{\frac{\varepsilon}{\sqrt{2}d_x}}_{\geq \tilde{\varepsilon}} \quad \wedge \quad \left| \underbrace{\frac{y_i}{d_y}}_{\rho_{n+i}} \underbrace{\frac{1}{\varsigma}}_k - \underbrace{b_i}_{z_{n+i}} \right| < \underbrace{\frac{\varepsilon}{\sqrt{2}d_y}}_{\geq \tilde{\varepsilon}}$$

which implies

$$\forall i : \quad |x_i - \varsigma d_x a_i| < \frac{\varsigma \varepsilon}{\sqrt{2}} \quad \wedge \quad |y_i - \varsigma d_y b_i| < \frac{\varsigma \varepsilon}{\sqrt{2}}$$

And we can conclude

$$|p_i q_i| = \sqrt{(x_i - \varsigma d_x a_i)^2 + (y_i - \varsigma d_y b_i)^2} < \varsigma \varepsilon.$$

This completes the proof of the lemma.  $\square$

Now, we summarize the results by reviewing the application of the hexagonal grid with flower holes  $G_F$ . Consider Figure 5.11. Let  $S = \{p_1, \dots, p_n\} \subset \mathbb{R}^2$  be an arbitrary finite point set. And let  $\varepsilon > 0$  be a given small constant. We want to use the grid points  $Q_F := 3\mathbb{Z} \times \sqrt{3}\mathbb{Z} \subset G_F$  to embed  $S$ . By Lemma 5.3 we find a scaling value  $\varsigma$  and grid points  $q_1, \dots, q_n \subset \varsigma Q_F$ , such that  $|p_i q_i| < \varsigma \varepsilon$  for every  $i$ . This means, that by perturbing  $G_F$  slightly, we can embed  $S$  in the perturbed and scaled version  $\varsigma \tilde{G}_F$ .

Note that the necessary local changes of  $G_F$  involve only moving some points from the grid by a distance smaller than  $\varepsilon$ . As we can choose the constant  $\varepsilon > 0$  arbitrarily small, we can reach a dilation arbitrarily close to  $\delta(G_F)$ . Analogous arguments can be used for any other regular grid like  $G_\square$ ,  $G_H$  and  $G_\Delta$ .

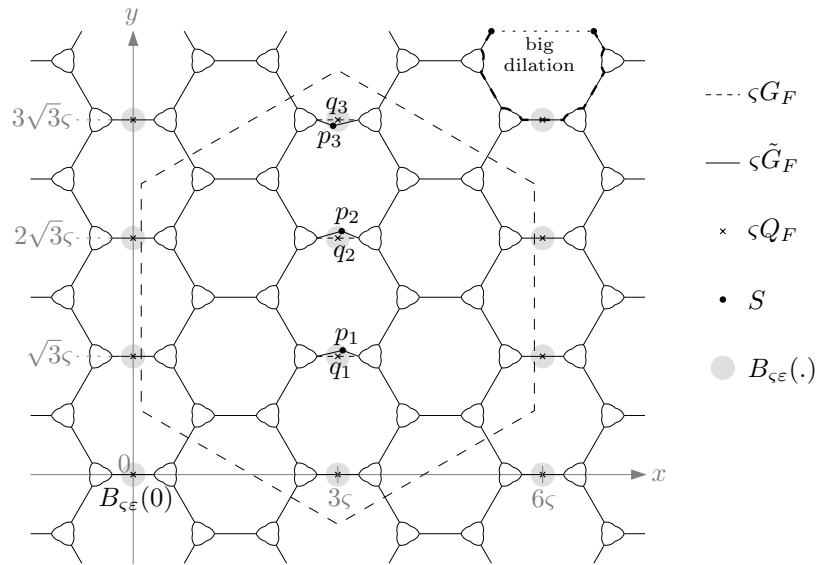


Figure 5.11: For every finite point set  $S \subset \mathbb{R}^2$  we can find a value  $\zeta \in \mathbb{R}$  and a slightly perturbed variant  $\tilde{G}_F$  of  $G_F$  of dilation arbitrary close to  $\delta(G_F)$ , such that the scaled graph  $\zeta\tilde{G}_F$  embeds  $S$ . Because pruning the grid in a rectangular shape can increase its dilation, we use a hexagonal shape, like the dashed one shown here.

There is only one additional question, we have to address. By the arguments above, we have found a slightly perturbed, scaled version of  $G_F$  which embeds  $S$  and whose dilation is arbitrarily close to  $\delta(G_F)$ . However, this is an infinite graph. We want to embed  $S$  in a finite graph. To this end, we have to prune  $\zeta\tilde{G}_F$  without increasing its dilation. This has to be done carefully. If we prune the graph in a rectangular way, we might increase its dilation as shown in the top right part of Figure 5.11. However, we can always cut the edges along a big enough hexagonal shape, like the dashed one in the same figure, without increasing the dilation.

We have proved the upper bound

$$\Delta \leq \delta(G_F) < 1.6779.$$

### 5.3 Lower bounds

Next, we want to prove lower bounds to  $\Delta$ . Obviously, there is the trivial lower bound  $\Delta \geq 1$ , but after all the work we have done in the previous chapter, even proving a non-trivial lower bound is not difficult anymore.

#### 5.3.1 A first lower bound

Actually, we have mentioned first lower bounds already. In Section 5.1.1 we talked about the dilation  $\delta(S_n)$  of the vertex set of a regular  $n$ -gon, cf. Figure 5.2.

The biggest dilation is  $\delta(S_n) = \pi/2$  for  $n \geq 5$ . By the definition of  $\Delta$  this implies

$$\Delta \geq \frac{\pi}{2}.$$

Because of this implication, we want to give a proof for  $\delta(S_5) \geq \frac{\pi}{2}$ . Remember that we have proved the lower bound  $\delta(C) \geq \frac{\pi}{2}$  for any closed curve  $C \in \mathcal{C}$  in Corollary 2.8. Hence, if we could find such a cycle with the property  $\delta(C) \leq \delta(G)$  in any graph  $G$  embedding  $S_5$ , we would have proven  $\delta(S_5) \geq \frac{\pi}{2}$ . However, clearly, we need additional arguments for graphs without cycles.

**Theorem 5.4.** *Let  $S_n$  denote the vertex set of a regular  $n$ -gon on the unit circle. Then, we have  $\Delta(S_n) = \pi/2 \approx 1,5708$  for each  $n \geq 5$ .*

*Proof.* In Corollary 2.35 we have proved, that any circle  $C_o$  has dilation  $\delta(C_o) = \pi/2$ . Because the unit circle embeds any point set  $S_n$ , we conclude

$$\delta(S_n) \leq \delta(C_o) \stackrel{\text{Cor. 2.35}}{=} \frac{\pi}{2}.$$

In order to prove  $\delta(S_n) \geq \pi/2$ , we will show that neither a graph with cycles nor a tree containing the given point set can attain a dilation smaller than  $\pi/2$ .

To prove the first part, let  $G$  be an arbitrary geometric graph that contains a bounded face. Then, there exists at least one cycle in  $G$ . Let  $C$  be a shortest cycle in  $G$ . Then, for any two points,  $p$  and  $q$  of  $C$ , a shortest path  $\xi_G(p, q)$  from  $p$  to  $q$  in  $G$  is a subset of  $C$ . Otherwise we could find a smaller cycle by replacing the shortest path  $C_p^q$  on  $C$  by  $\xi_G(p, q)$ . This implies  $\delta_G(p, q) = \delta_C(p, q)$  for all  $p, q \in C$ . We get

$$\delta(G) \geq \delta(C) \stackrel{\text{Cor. 2.8}}{\geq} \frac{\pi}{2}.$$

It remains to show, that no graph without cycles, i.e. a tree, can provide a smaller dilation for embedding the vertex set  $S_n$  of a regular  $n$ -gon with  $n \geq 5$ . Assume that the graph  $G$  is a tree which contains  $S_n$ , and that  $\delta(G) < \pi/2$  holds. Then, if  $p, q$  are two neighboring points of  $S_n$ , the unique shortest path  $\xi(p, q)$  in  $G$  connecting them is of length at most  $\delta(G) \cdot |pq|$ , where

$$|pq| = 2 \sin\left(\frac{\pi}{n}\right) \leq 2 \sin\left(\frac{\pi}{5}\right), \quad (5.7)$$

see Figure 5.12. Therefore this shortest path  $\xi(p, q)$  must be contained in the ellipse  $E(p, q) := \{z \mid |pz| + |zq| \leq \frac{\pi}{2}|pq|\}$ , i.e. an ellipse with foci  $p, q$  and a major axis of length  $\frac{\pi}{2}|pq|$ .

In this ellipse  $E(p, q)$ , per definition, the sum of distances from each point on the boundary of  $E(p, q)$  to the foci,  $p$  and  $q$ , equals

$$|pq| \cdot \frac{\pi}{2} \stackrel{(5.7)}{\leq} \sin\left(\frac{\pi}{5}\right) \cdot \pi = 1,846\dots$$

On the other hand, because both  $p$  and  $q$  lie on the unit circle, the sum of their distances from the circle's center equals 2. Hence, no ellipse  $E(p, q)$  can contain the unit circle's center.



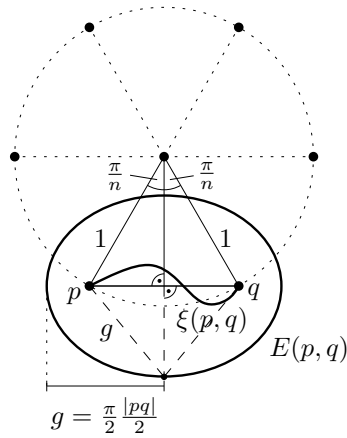


Figure 5.12: The path  $\xi(p, q)$  between neighboring points is contained in their ellipse  $E(p, q)$ .

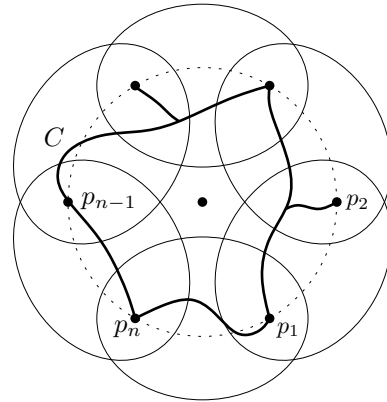


Figure 5.13: All paths together,  $C := \xi(p_1, p_2) \oplus \dots \oplus \xi(p_{n-1}, p_n) \oplus \xi(p_n, p_1)$ , form a cycle.

Now let us consider the arrangement of all ellipses  $E(p_i, p_{i+1})$  of neighboring points, as depicted in Figure 5.13, and assume that the points are labelled  $p_1, p_2, \dots, p_n$  in counterclockwise order. The concatenation

$$C = \xi(p_1, p_2) \oplus \xi(p_2, p_3) \oplus \dots \oplus \xi(p_{n-1}, p_n) \oplus \xi(p_n, p_1)$$

is a (possibly non-simple) closed path in  $G$  that is contained in, and visits, all ellipses associated with these pairs of points. The cycle  $C$  encircles the center of the unit circle and is, thus, not contractible, contradicting the fact that  $G$  is a tree.

This proves  $\delta(G) \geq \frac{\pi}{2}$  if  $G$  is a tree. And the proof of Theorem 5.4 is completed.  $\square$

### 5.3.2 Motivation for improved lower bound

The lower bound  $\Delta \geq \pi/2$  is a nice result, and we even know some point sets  $(S_n, n \geq 5)$  attaining this dilation value. However, already when we first published this result in 2003 [56], we did not expect that the equality  $\Delta = \pi/2$  holds.

This is because Corollary 2.35 tells us that circles are the only cycles attaining a dilation of  $\pi/2$ . Every different cycle has bigger dilation. And it seems one cannot embed more complex point sets with finite graphs which satisfy the condition that every bounded face is a circular disk, cf. Figure 5.14. Moreover, if two circles touch each other, the dilation gets infinitely big in this point, because of Lemma 2.1.2 and because the interior angle between the tangents equals  $\alpha = 0$ , cf. Figure 5.14.

However, even if we succeed in formalizing this idea to get a proof for  $\delta(G) > \pi/2$  for every graph  $G$  which embeds a given finite point set  $S$ , this would still not prove  $\delta(S) > \pi/2$ , as there might be a sequence  $(G_n)_{n \in \mathbb{N}}$  of graphs embedding  $S$  such that  $\delta(G_n) \searrow \pi/2$ .

Hence, in order to prove  $\Delta > \pi/2$ , we need another argument. We will apply the stability result from Lemma 2.39, which says that every cycle of dilation close to  $\pi/2$  has to be

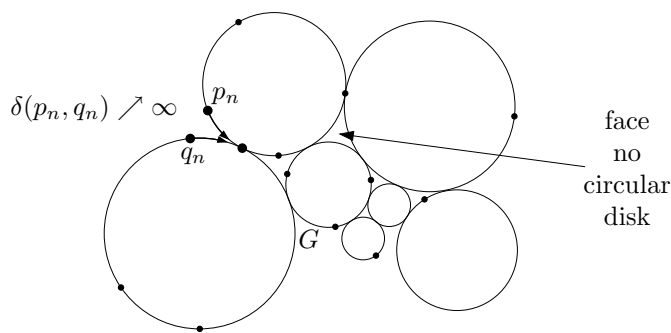


Figure 5.14: For more complicated point sets, there does not seem to be any embedding graph, which consists only of circular faces. Where two circles touch each other, the dilation gets infinitely big.

contained in a thin annulus. Hence, if we want to embed a more complicated finite point set  $S \subset \mathbb{R}^2$  with dilation close to  $\pi/2$ , all the appearing faces would have to be almost circular disks. And even this does not seem to be possible by the intuition shown in Figure 5.14.

### 5.3.3 Disk-packing result

How can we formalize this intuition? Fortunately, there exists an appropriate disk-packing result by Kuperberg et al. [134] which says that no packing of circular disks of maximum radius 1 can cover a square of side length 4, even if we enlarge each disk by the factor  $\tilde{\Lambda} := 1.00001$  around its center. A *(disk) packing* is a set of disks such that two disks may touch but not overlap. Note that the enlarged disks, however, are allowed to overlap.

For a disk packing  $\mathcal{D}$  and a constant  $\lambda > 0$  we call the set of disks resulting from scaling every given disk by the factor  $\lambda$  around its center the  $\lambda$ -*enlargement* of  $\mathcal{D}$ . More formally it is defined by

$$\mathcal{D}^\lambda := \left\{ \overline{B_{\lambda r}(p)} \mid \overline{B_r(p)} \in \mathcal{D} \right\}. \quad (5.8)$$

With this notation, we formulate the disk-packing result as a theorem.

**Theorem 5.5.** [134] *Let  $\mathcal{D}$  be a (finite or infinite) packing in the plane of circular disks with radius at most 1. For the constant  $\tilde{\Lambda} = 1.00001$  consider the  $\tilde{\Lambda}$ -enlargement  $\mathcal{D}^{\tilde{\Lambda}}$  of  $\mathcal{D}$ . Then,  $\mathcal{D}^{\tilde{\Lambda}}$  covers no square of side length 4.*

It was a splendid idea from Adrian Dumitrescu to apply this disk packing result to our problem. Combined with the stability result and after solving some additional technical problems, indeed, this leads to an improved lower bound to  $\Delta$ . We will prove this bound in Section 5.3.4. We presented the first version in [50, 49].

Unfortunately, there is a flaw in the proof of Theorem 5.5 in [134]. Using the terminology of [134], in the case  $\beta/80 < r \leq \frac{1}{8}$  it might occur that by the construction of the paper, we do not have  $R_{n+1} \subset R_n$ , although this assumption is crucial for the proof. Therefore, we give a corrected and more detailed version of the proof in Appendix B.

Moreover, this appendix also contains some ideas how the result can probably be improved to a value  $\tilde{\Lambda}$  significantly bigger than 1.00001. For this reason, we state our main result in dependence on the value  $\tilde{\Lambda}$ , and we state the search for an improved disk packing bound as an open problem.

More generally, in this disk-packing context we can ask for a constant  $\Lambda$  which is similar to the constant  $\Delta$  in our main problem. To this end, we define for any disk packing  $\mathcal{D}$  the maximum radius  $r(\mathcal{D}) := \sup\{r(D), D \in \mathcal{D}\}$ . Then, we can define the *cover factor* of a disk packing  $\mathcal{D}$  with respect to a set  $R \subseteq \mathbb{R}^2$  by

$$\lambda_R(\mathcal{D}) := \inf \left\{ c \in [0, \infty) \mid R \subseteq \bigcup \mathcal{D}^c \right\}. \tag{5.9}$$

With this definition, the cover factor of a set  $R \subset \mathbb{R}^2$  is

$$\lambda(R) := \inf_{\substack{\mathcal{D} \text{ disk packing,} \\ r(\mathcal{D}) \leq 1}} \lambda_R(\mathcal{D}). \tag{5.10}$$

Another variant can be defined by allowing only finite disk packings. We denote the corresponding value by  $\lambda_{\text{fin}}(R)$ . Obviously, considering this value does only make sense for a bounded set  $R$ . Then, we can define the following two interesting cover factor constants.

$$\Lambda := \lambda(\mathbb{R}^2) \quad \text{and} \quad \Lambda_{\text{fin}} := \sup_{R \subset \mathbb{R}^2 \text{ compact}} \lambda_{\text{fin}}(R). \tag{5.11}$$

Kuperberg et al. [134] call the value  $\Lambda - 1$  the *Bárány number* of circular disks with radius  $\leq 1$ , because Imre Bárány raised these kind of questions by presenting a problem at [13].

Note that Theorem 5.5 states  $\lambda_{\text{fin}}(R_{\square}) \geq \lambda(R_{\square}) \geq 1.00001$ , where  $R_{\square}$  denotes a square of side length 4. As, clearly,  $\lambda(\mathbb{R}^2) \geq \lambda(R_{\square})$ , Theorem 5.5 implies  $\Lambda \geq 1.00001$  and  $\Lambda_{\text{fin}} \geq 1.00001$ .

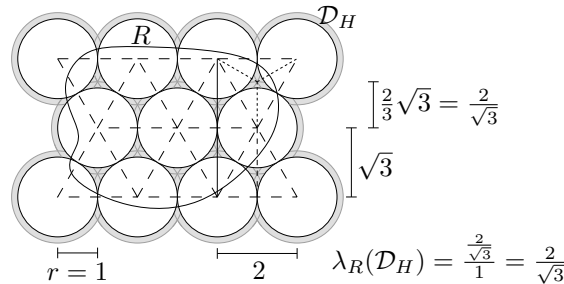


Figure 5.15: The hexagonal disk packing  $\mathcal{D}_H$  attains a cover factor of  $\lambda_R(\mathcal{D}_H) = 2/\sqrt{3}$ .

On the other hand, we can always apply a hexagonal disk packing like shown in Figure 5.15. This proves  $\Lambda, \Lambda_{\text{fin}} \leq 2/\sqrt{3} \approx 1.1547$ . A better upper bound is achieved by the Apollonian packing, which we present in Section 5.3.6.

**Open Problem 11.** *Prove  $\Lambda \geq \underline{\Lambda}$  or  $\Lambda_{\text{fin}} \geq \underline{\Lambda}_{\text{fin}}$ , for better lower bounds  $\underline{\Lambda}, \underline{\Lambda}_{\text{fin}} > 1.00001!$  Which better upper bounds can be proved?*

It seems that there exist no articles besides [134] dealing exactly with these kind of questions. The known problem from disk packing most closely related is probably the problem of *simultaneously packing and covering*, see for instance Zong [187]. The variant considering disks

in the plane asks for a packing of unit disks such that its  $\lambda$ -enlargement covers the whole plane for a factor  $\lambda > 0$  which is as small as possible. The simultaneous packing and covering constant of disks in the plane is

$$\gamma := \inf_{\substack{\mathcal{D} \text{ disk packing,} \\ D \in \mathcal{D} \Rightarrow r(D)=1}} \lambda_{\mathbb{R}^2}(\mathcal{D}).$$

If we replace “ $r(D) = 1$ ” by “ $r(D) \leq 1$ ” we have the definition of the cover factor  $\lambda(\mathbb{R}^2)$ . This shows the close relation between the two concepts.

The other known problems from circle and sphere packing do not have close relations to cover factor questions. The literature is mostly concerned with maximizing a kind of density, the quotient between the measure of the union of the disks divided by the measure of the whole space. An overview of these results can be found in a survey by Fejes Tóth and Kuperberg [71].

### 5.3.4 Improved lower bound

In this section we combine the stability result from Lemma 2.39, which said that cycles of small dilation are contained in a thin annulus, with the disk-packing result to achieve an improved lower bound to the dilation constant  $\Delta$ . Because we believe that the theorem holds for values  $\tilde{\Lambda}$  which are significantly bigger than 1.00001, we formulate the improved lower bound in dependence of  $\tilde{\Lambda}$ .

**Theorem 5.6.** *Suppose Theorem 5.5 is true for a factor  $\tilde{\Lambda}$  with  $\tilde{\Lambda} \leq 1.03$ , i.e.  $\lambda(R_{\square}) \geq \tilde{\Lambda}$ . Then, the minimum geometric dilation  $\Delta$  which is necessary to embed any finite point set in the plane satisfies*

$$\Delta \geq \underline{\Delta}(\tilde{\Lambda}) := \left( 1 + \left( \frac{\tilde{\Lambda} - 1}{3} \right)^2 \right) \frac{\pi}{2}.$$

As Theorem 5.5 holds for  $\tilde{\Lambda} = 1.00001$ , this results in  $\Delta \geq (1 + (10^{-10})/9)\pi/2 > (1 + 10^{-11})\pi/2$ .

*Proof.* We first give an overview of the proof, and present the details afterwards. Consider the set

$$P := \{ (x, y) \mid x, y \in \{-9, -8, \dots, 9\} \}$$

of grid points with integer coordinates in the square  $Q_1 := [-9, 9]^2 \subset \mathbb{R}^2$ , see Figure 5.16.a. We use a proof by contradiction and assume that there exists a planar connected graph  $G$  that embeds  $P$  and satisfies  $\delta(G) < \underline{\Delta}(\tilde{\Lambda})$ .

The idea of the proof is to show that if  $G$  attains such a low dilation, it contains a collection  $\mathcal{M}$  of cycles with disjoint interiors which cover the smaller square  $Q_2 := [-8, 8]^2$ . We choose  $\mathcal{M}$  in such a way that the dilation of every cycle  $C \in \mathcal{M}$  is bounded by  $\delta(C) \leq \delta(G) < \underline{\Delta}(\tilde{\Lambda})$ . The function  $\underline{\Delta}(\tilde{\Lambda})$  is defined so that we can easily apply the stability result, Lemma 2.39, to this situation. In particular,  $\tilde{\Lambda} \leq 1.03$  guarantees  $\underline{\Delta}(\tilde{\Lambda}) \leq 1.0001\pi/2$ . We derive that every  $C \in \mathcal{M}$  has to be contained in a  $\tilde{\Lambda}$ -annulus. This is shown in Figure 5.16.b. However, to allow a good visualization we had to use a bigger dilation  $\delta(G)$  and a bigger cover factor  $\tilde{\Lambda}$  in the figure.

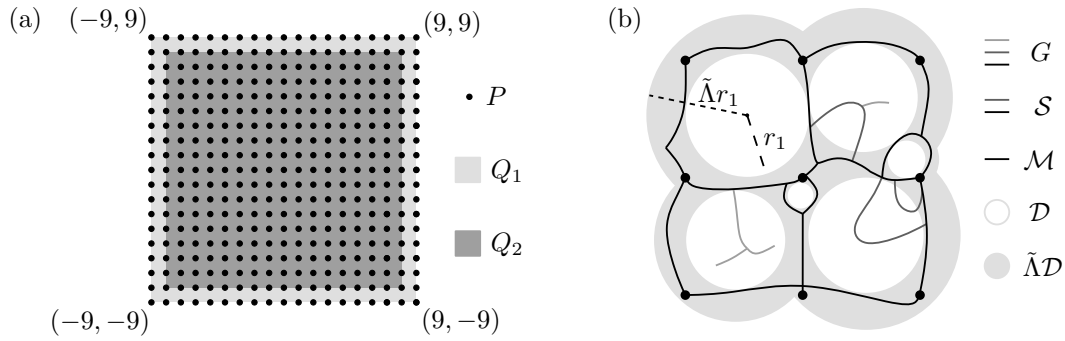


Figure 5.16: (a) The point set  $P$  and the square  $Q_2$  which has to be covered by an embedding graph of low dilation. (b) The cycles of  $\mathcal{M}$  induce a disk packing  $\mathcal{D}$  whose  $\tilde{\Lambda}$ -enlargement covers  $Q_2$ .

As by Claim 1 the length of each cycle  $C \in \mathcal{M}$  is bounded by  $8\pi$ , the inner disks of these annuli have a radius  $r \leq 4$ . This is a contradiction to Theorem 5.5 (situation scaled by 4) because the inner disks of the annuli of maximum radius 4 are disjoint and their  $\tilde{\Lambda}$ -enlargements cover  $Q_2$ , a square of side length 16.

We would like to use the cycles bounding the faces of  $G$  for  $\mathcal{M}$ . Indeed,  $\delta(G) < \underline{\Delta}(\tilde{\Lambda}) < 2$  implies that they cover  $Q_2$ , see Claim 1 below. However, their dilation could be bigger than the dilation  $\delta(G)$  of the graph, cf. Figure 5.18.b. There could be shortcuts in the exterior of  $C$ , i.e., a shortest path between  $p, q \in C$  does not necessarily use  $C$ . Hence, we could have  $\delta(C) > \delta(G)$ , which would prevent us from applying Lemma 2.39.

Therefore, we have to find a different class of disjoint cycles covering  $Q_2$  which do not allow shortcuts. The idea is to consider for every point  $x$  in  $Q_2$  a shortest cycle of  $G$  such that  $x$  is contained in the open region bounded by the cycle. We denote the set of those cycles by  $\mathcal{S}$ . The cycles from  $\mathcal{S}$  are *non-crossing*, that is, their interiors<sup>4</sup> are either disjoint or one contains the other, see Claim 4. If we define  $\mathcal{M}$  to contain only the cycles of  $\mathcal{S}$  which are maximal with respect to inclusion of their interiors, it provides all the properties we need.

We now present the proof in detail.

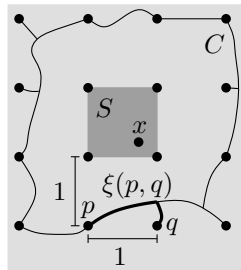


Figure 5.17: Every point  $x \in Q_2$  is encircled by a cycle of length  $\leq 12\delta(G)$ .

<sup>4</sup>Remember that the *interior*  $C^\circ$  of a cycle  $C$  is the open region which is bounded by  $C$ .

**Claim 1.** Every point  $x \in Q_2$  is enclosed by a cycle  $C$  of  $G$  of length at most  $8\pi$ .

*Proof.* We consider an arbitrary point  $x \in Q_2$  and a grid square  $S$ , which contains  $x$ , like shown in Figure 5.17. For every pair  $p, q$  of neighboring grid points of  $P$  let  $\xi(p, q)$  be a shortest path in  $G$  connecting  $p$  and  $q$ . The length of each such path  $\xi(p, q)$  is bounded by  $|\xi(p, q)| \leq \delta_G(p, q) \cdot 1 < 2$ . Consider the closed curve  $C$  obtained by concatenating the 12 shortest paths between adjacent grid points on the boundary of the  $3 \times 3$  square around  $S$ . None of the shortest paths can enter  $S$  because this would require a length bigger than 2. Therefore  $C$  encloses but does not enter  $S$ , thus it also encloses  $x \in S$ . The total length of  $C$  is bounded by  $|C| \leq 12 \cdot \delta(G) \leq 12\Delta(\tilde{\Lambda}) \leq 12 \cdot 1.0001(\pi/2) < 8\pi$ .  $\square$

For any point  $x \in Q_2$ , let  $C(x)$  denote a *shortest cycle* in  $G$  such that  $x$  is contained in its closed region  $\overline{C^\circ}$ . If the shortest cycle is not unique, we pick the one which encloses the smallest area. It follows from Claim 4 below that this defines the shortest cycle  $C(x)$  uniquely, but this fact is not essential for the proof. Obviously,  $C(x)$  is a simple cycle. Let  $R(x)$  denote the open region  $C^\circ$  enclosed by  $C(x)$ .

**Claim 2.** For every  $x \in Q_2$  we have:

1. No shortest path of  $G$  can cross  $R(x)$ .
2. Between two points  $p, q$  on  $C(x)$ , there is always a shortest path on  $C(x)$  itself.

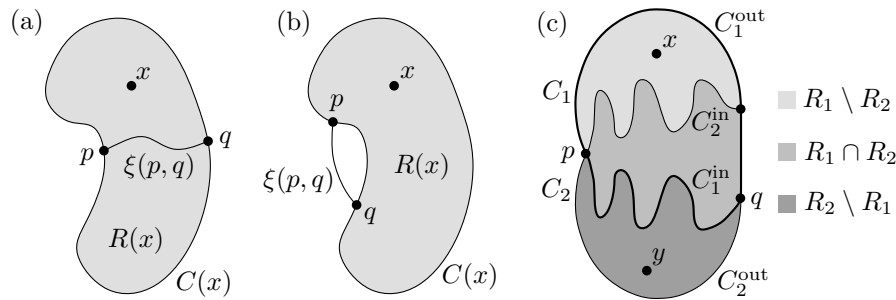


Figure 5.18: Impossible situations: (a) a shortest path  $\xi(p, q)$  crossing  $R(x)$  or (b) being a shortcut; (c) two crossing shortest cycles.

*Proof.* 1. Since every subpath of a shortest path is a shortest path, it suffices to consider a path  $\xi(p, q)$  between two points  $p, q$  on  $C(x)$  whose interior is completely contained in  $R(x)$ , see Figure 5.18.a. This path could replace one of the two arcs of  $C(x)$  between  $p$  and  $q$  and yield a better cycle enclosing  $x$ , contradicting the definition of  $C(x)$ .

2. We have already excluded shortest paths which intersect  $R(x)$ . We now exclude any path  $\xi(p, q)$  between two points  $p, q$  on  $C(x)$  which is strictly shorter than each of the two arcs of  $C(x)$  between  $p$  and  $q$ , see Figure 5.18.b. If such a path existed, again, we could replace one of the arcs from  $C$  connecting  $p$  and  $q$  by  $\xi(p, q)$  and receive a shorter cycle encircling  $x$ , a contradiction.  $\square$

As an immediate consequence of Claim 2.2, we get:

**Claim 3.** *The dilation of every cycle  $C(x)$  is at most the dilation  $\delta(G)$  of the whole graph  $G$ .*

This allows us to apply Lemma 2.39 to every cycle  $C(x)$ . However, to obtain a packing, we still have to select a subset of cycles with disjoint interiors. To this end we prove the following claim.

**Claim 4.** *For arbitrary points  $x, y \in Q_2$ , the cycles  $C(x)$  and  $C(y)$  are non-crossing, i.e.,  $R(x) \cap R(y) = \emptyset \vee R(x) \subseteq R(y) \vee R(x) \subseteq R(y)$ .*

*Proof.* We use a proof by contradiction, see Figure 5.18.c. Assume that the interiors  $R_1$  and  $R_2$  of the shortest cycles  $C_1 := C(x)$  and  $C_2 := C(y)$  overlap, but none is fully contained inside the other. This implies that their union  $R_1 \cup R_2$  is a bounded open connected set. Its boundary  $\partial(R_1 \cup R_2)$  contains a simple cycle  $C$  enclosing  $R_1 \cup R_2$ .

By the assumptions we know that there is a part  $C_1^{\text{in}}$  of  $C_1$  which connects two points  $p, q \in C_2$  and is, apart from its endpoints, completely contained in  $R_2$ . Let  $C_1^{\text{out}}$  denote the other path on  $C_1$  connecting  $p$  and  $q$ . By Claim 2.2, at least one of the paths  $C_1^{\text{in}}$  or  $C_1^{\text{out}}$  must be a shortest path. By Claim 2.1,  $C_1^{\text{in}}$  cannot be a shortest path, since it intersects  $R_2$ . Hence, only  $C_1^{\text{out}}$  is a shortest path, implying  $|C_1^{\text{out}}| < |C_1|/2$ .

Analogously, we can split  $C_2$  into two paths  $C_2^{\text{in}}$  and  $C_2^{\text{out}}$  such that  $C_2^{\text{in}}$  is contained in  $R_1$ , apart from its endpoints, and  $|C_2^{\text{out}}| < |C_2|/2$ .

The boundary cycle  $C$  consists of parts of  $C_1$  and parts of  $C_2$ . It cannot contain any part of  $C_1^{\text{in}}$  or  $C_2^{\text{in}}$  because it intersects neither with  $R_1$  nor with  $R_2$ . Hence, we have

$$|C| \leq |C_1^{\text{out}}| + |C_2^{\text{out}}| < \frac{|C_1| + |C_2|}{2} \leq \max\{|C_1|, |C_2|\}.$$

Since  $C$  encloses  $x \in R_1$  and  $y \in R_2$ , this contradicts the choice of  $C_1 = C(x)$  or  $C_2 = C(y)$ . This proves Claim 4.  $\square$

Let  $\mathcal{S}$  be the set of shortest cycles  $\mathcal{S} := \{C(x) \mid x \in Q_2\}$ , and let  $\mathcal{M} \subset \mathcal{S}$  be the set of *maximal shortest cycles* with respect to inclusion of their interiors.

By Claim 3, the dilation of every cycle  $C \in \mathcal{M} \subseteq \mathcal{S}$  satisfies  $\delta(C) \leq \delta(G) \leq \underline{\Delta}(\tilde{\Lambda})$ . Therefore, like described in the beginning of this proof, we can apply Lemma 2.39 to every  $C \in \mathcal{M}$ . It shows that  $C$  is contained in a  $\tilde{\Lambda}$ -annulus, i.e. there exists a disk  $D_C$  such that  $D_C \subset C^\circ \subset \tilde{\Lambda}D_C$ .

As the disks  $D_C$  are disjoint by construction and by Claim 4, they build a packing  $\mathcal{D}$ . The same claim shows that the cycles of  $\mathcal{M}$  cover  $Q_2$ , hence the  $\tilde{\Lambda}$ -enlargement  $\mathcal{D}^\Lambda$  does the same.

Claim 1 proves that the inradius of any  $C \in \mathcal{M}$  satisfies  $r(C) \leq 4$ , implying  $r(D_C) \leq 4$ . The  $\tilde{\Lambda}$ -enlargements of these disks cover  $Q_2$ , a square of side length 16. This is a contradiction to the assumption on  $\tilde{\Lambda}$ . Hence, we have proved that the dilation of any graph  $G$  which embeds  $P$  cannot be smaller than  $\underline{\Delta}(\tilde{\Lambda})$ .  $\square$

Theorem 5.6 establishes a strong link between the disk-packing questions from the previous section and the dilation problems of this chapter. It shows that a lower bound  $\tilde{\Lambda}$  to the cover factor  $\lambda(R_\square)$  implies a lower bound to the dilation constant  $\Delta$ . Any improvement of the lower bound to  $\lambda(R_\square)$  immediately implies an improved lower bound to  $\Delta$ .

Although the step from  $\pi/2$  to  $(1+10^{-10})\pi/2$  does not look like a big improvement, we regard the improved lower bound as a very important statement, because it shows that  $\Delta > \pi/2$ . Still, we believe that the value of  $\Delta$  is not close to  $\pi/2$  and that new ideas are needed to prove better lower bounds. Overall, the gap between the best known lower and upper bound remains a challenging problem.

**Open Problem 12.** *How can one prove better upper and lower bounds to the dilation constant  $\Delta$ ? Can we even determine the correct value of  $\Delta$ ?*

### 5.3.5 Reverse link between disk packing and dilation

Knowing the argumentation of our lower bound to dilation, Theorem 5.6, one may ask, whether one can find a reverse statement. Can one construct from a disk packing with small cover factor a graph of small dilation? We published this question in the conclusions of [50, 49]. Here, we shortly discuss some related ideas.

To this end let  $\mathcal{D}$  denote a disk packing with a small cover factor, say  $\lambda := \lambda_{R_\square}(\mathcal{D})$ . A natural idea would be to extend each disk  $D \in \mathcal{D}$  to a face  $F$  of a graph, such that  $D \subset F \subset \lambda D$ . Let  $C := \partial F$  denote the cycle on the boundary of  $F$ . If  $C$  is convex, we can apply the reverse stability result from Lemma 2.40. It says that the dilation of a *convex* closed curve contained in an  $\eta$ -annulus is bounded by

$$\delta(C) \leq \frac{\pi}{2} \frac{\eta}{1 - \frac{\pi}{4}(\eta - 1)}.$$

The lemma indeed shows that any convex cycle contained in a thin annulus attains small dilation, as the value  $\frac{\eta}{1 - \frac{\pi}{4}(\eta - 1)}$  approaches 1 for  $\eta \searrow 1$ .

However, it is not possible to construct a graph from every disk packing  $\mathcal{D}$  with small cover factor  $\lambda$  in such a way that each disk  $D \in \mathcal{D}$  is extended to a *convex* face  $F_D$  satisfying  $D \subset F_D \subset \lambda D$ . The packing from Figure 5.19 is a counter example. It covers a disk with radius slightly bigger than  $\lambda r(D_1)$ . The boundary of the face belonging to the big disk  $D_1$  would have to pass through all the annuli of the small disks surrounding it. Hence, the boundary cycle  $C_1 := \partial F_{D_1}$  cannot be convex.

And this missing convexity does not only prevent us from applying Lemma 2.40. It actually increases the dilation of  $C_1$  intolerably. This can be seen the easiest way, if neighboring small annuli hardly overlap, and if the number  $n$  of the small disks tends to infinity. The part of  $C_1$  inside of one small annulus, replaces an arc of length  $\approx 2\pi\lambda r(D_1)/n$  by an arc of length almost  $\frac{\pi}{2} (2\pi\lambda r(D_1)/n)$ . Hence,

$$\delta(C_1) \geq \frac{|C_1|}{2h(C_1)} \geq \frac{|C_1|}{4\lambda r(D_1)} \approx \frac{n\frac{\pi}{2}(2\pi\lambda r(D_1)/n)}{4\lambda r(D_1)} = \frac{\pi^2}{4} \approx 2.4674.$$

If, on the other hand, we try to improve the dilation of  $C_1$ , the cycles belonging to the small disks have to leave their  $\lambda$ -annuli, and this cannot be done without increasing their dilation significantly.

Because of these thoughts we believe that building graphs of small dilation is in some sense more difficult than building good<sup>5</sup> disk packings, as a graph of small dilation induces a good disk packing, but the reverse statement does not seem to be true.

<sup>5</sup>We regard a disk packing to be *good*, if it has a small cover factor.



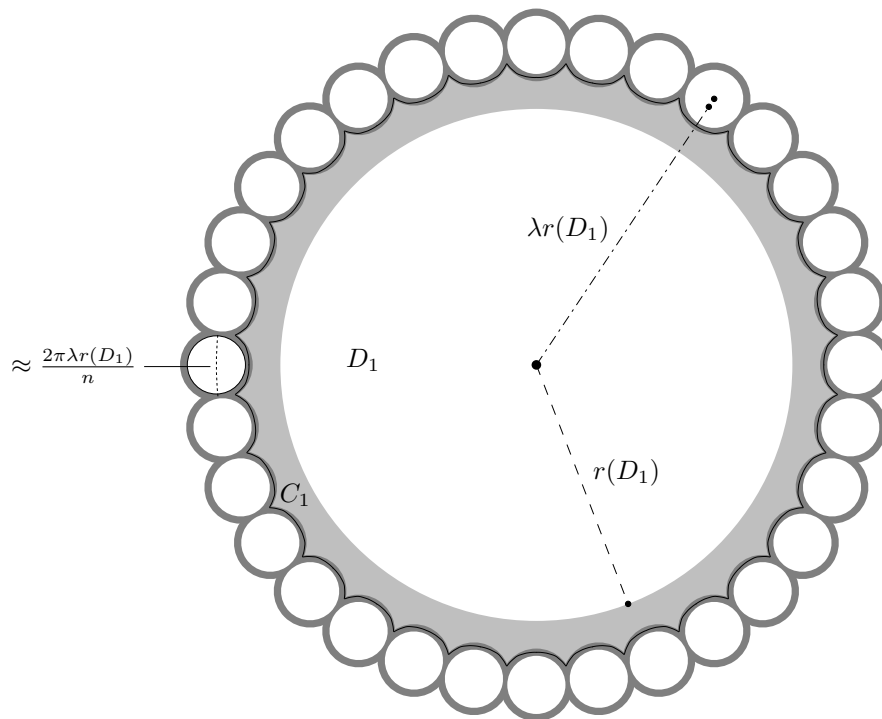


Figure 5.19: A disk packing with small cover factor  $\lambda$  which does not induce a graph of small dilation.

### 5.3.6 Apollonian packing

If we look for graphs of small dilation or for good disk packings, on both tracks we will inevitably meet the Apollonian packing, a fascinating fractal structure.

Remember the improved grids from Section 5.2.4. We lowered the dilation of the hexagonal grid by inserting new cycles in the corners of the hexagons. It is a natural idea to iterate this approach by inserting new cycles in the corners of the improved grid, and so on. Actually, we have tried to do so, and the dilation can be reduced a little, but we were not able to reach a really important improvement.

The analogous idea comes to mind, if we try to find a good disk packing. Obviously, we can reduce the cover factor of the hexagonal packing by inserting new disks in the holes of the original packing. If we insert in each hole the biggest possible disk, we have done the first iteration step towards the *Apollonian packing*  $\mathcal{D}_A$ . This infinite packing is reached, if we proceed by always inserting the biggest possible disks in the existing holes, see Figure 5.20.

Most commonly the Apollonian packing is not described based on the hexagonal packing, as we do here, but does refer to the analogous packing inside of the circumcircle of three congruent and mutually tangent circles of the starting configuration. But of course, the packing inside of the first hole build from these three congruent circles is equal in both cases. This part is often called *Apollonian gasket*.

The name honors *Apollonius of Perga*, a Greek mathematician of great influence whose origi-

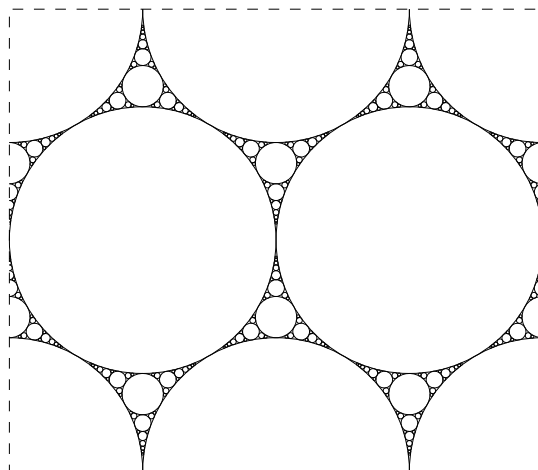


Figure 5.20: The Apollonian packing results if we start with a hexagonal packing and always insert the biggest possible disks in the existing holes.

nal works, unfortunately, are lost. Boyer devotes a whole chapter of his history of mathematics [26] to Apollonius, who is supposed to have lived from 262 to 190 B.C. One of his most important achievements was to describe all possible circles which are tangent to three given circles. This problem is called *Apollonius' problem*, see for instance Weisstein [182].

In the situation considered here, the three given circles are mutually tangent. This simplifies the solution. There are only two circles which are tangent to all three given circles, the circumcircle and the incircle. Their radius  $r_4$  can be derived from the three given radii  $r_1$ ,  $r_2$  and  $r_3$  by *Soddy's formula* also called *Descartes circle theorem* or *Descartes equation* which in its easiest form considers the reciprocals of the radii, the *curvatures* or *bends*  $b_1, \dots, b_4$  of the circles.

$$\begin{aligned}
 2(b_1^2 + b_2^2 + b_3^2 + b_4^2) &= (b_1 + b_2 + b_3 + b_4)^2 & (5.12) \\
 \Leftrightarrow b_4 &= b_1 + b_2 + b_3 \pm 2\sqrt{b_1b_2 + b_2b_3 + b_1b_3} \\
 \Leftrightarrow r_4 &= \frac{r_1r_2r_3}{r_1r_2 + r_2r_3 + r_1r_3 \pm 2\sqrt{r_1r_2r_3(r_1 + r_2 + r_3)}}
 \end{aligned}$$

The Nobel laureate Frederick Soddy rediscovered these dependencies of four circles touching each other and described it in the well-known poem “The kiss precise” [175] in 1936. Descartes had mentioned their relationship already in a letter to Elisabeth of Bohemia in 1643.

These formulas help to analyze the marvellous structure of the Apollonian packing. Some of the miracles which appear in the sequences of disks it contains are analyzed enthusiastically by Aharonov and Stephenson [4]. The fractal properties of the Apollonian packing are described for instance in Mandelbrot's famous book “The fractal geometry of nature” [146] and by Falconer [69]. From this point of view one of the most challenging tasks is to calculate the Hausdorff dimension of the residual set, the set of points which is not covered by any disk. First approximations were given for instance by Hirst [103] and Boyd [25]. A recent estimate of  $\approx 1.305688$  stems from McMullen [148].

Furthermore, the Apollonian packing includes interesting number theoretical structures. In a

series of articles Graham, Lagarias, Mallows, Wilks and Yan [79, 80, 81, 82] and Eriksson and Lagarias [68] examine Apollonian packings where the bends of all the circles are integers. This is possible if one does not start the iteration with unit circles but with different configurations of three mutually tangent circles.

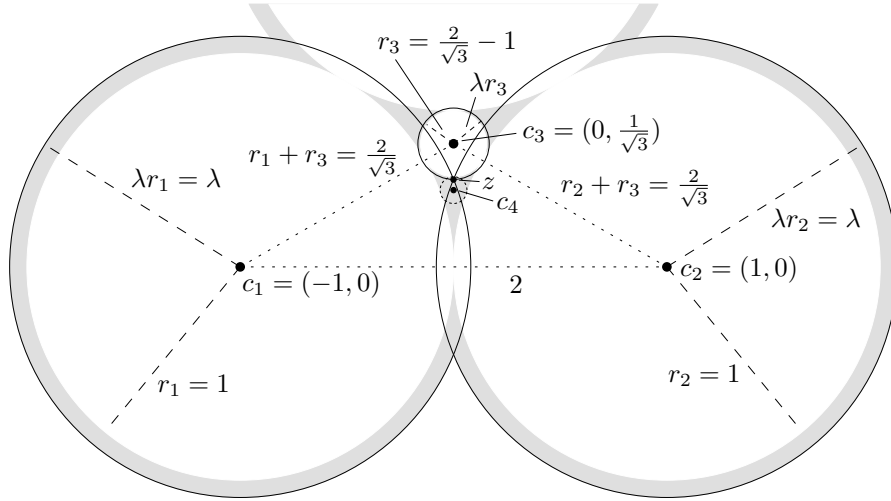


Figure 5.21: The enlarged circles of the first iteration  $\mathcal{D}_{A1}$  of the Apollonian packing meet in the point  $z \neq c_4$ .

As a kind of appetizer, we now calculate the cover factor of the first iteration  $\mathcal{D}_{A1}$  of the Apollonian packing, that is the stage where a disk has been added into each hole of the hexagonal packing, see Figure 5.21. By symmetry it suffices to calculate the cover factor which is needed to cover one of the remaining holes. Each hole is enclosed by two unit disks  $D_1, D_2$  and one disk  $D_3$  with radius  $r_3 = \frac{2}{\sqrt{3}} - 1$ . Let the centers of these disks be located at  $c_1 = (-1, 0)$ ,  $c_2 = (1, 0)$  and  $c_3 = (0, 1/\sqrt{3})$ .

Now, we enlarge the three disks by a factor  $\lambda$ , where  $\lambda$  increases, starting from  $\lambda = 1$ . Clearly, the hole is covered, when all three enlarged circles meet in a single point  $z$ . Because the situation is symmetric about the  $y$ -axis, we know that  $z$  has to be located on this axis. If  $y$  denotes the  $y$ -coordinate of  $z$ , we have  $z = (0, y)$ .

When all three enlarged circles meet in  $z$ , we must have  $|zc_1| = \lambda r_1$  and  $|zc_3| = \lambda r_3$ . This results in

$$\sqrt{1 + y^2} = |zc_1| = \lambda r_1 = \lambda \quad \wedge \quad \frac{1}{\sqrt{3}} - y = |zc_3| = \lambda r_3 = \lambda \left( \frac{2}{\sqrt{3}} - 1 \right).$$

This leads to a quadratic equation for  $y$  whose solution is

$$y = \frac{3 + \sqrt{3} - \sqrt{22\sqrt{3} - 36}}{8} \approx 0.4101$$

$$\text{and } \lambda = \frac{1}{8} \sqrt{40 + 2(1 - \sqrt{3})\sqrt{36 + 30\sqrt{3} + 28\sqrt{3}}} \approx 1.0808.$$

This is a better upper bound to  $\lambda_{\mathbb{R}^2}(\mathcal{D}_A)$  and thereby to  $\Lambda$ .

Note that the point  $z$  is not the center  $c_4$  of the disk added in the next iteration of the Apollonian packing, cf. Figure 5.21. This might raise the conjecture, that the Apollonian packing is not the best disk packing in terms of its cover factor.

Naturally, at this point the following questions arise.

**Open Problem 13.** *What is the cover factor  $\lambda_{\mathbb{R}^2}(\mathcal{D}_A)$  of the Apollonian packing  $\mathcal{D}_A$ ? Is the Apollonian packing the best option, i.e., do we have  $\Lambda = \lambda_{\mathbb{R}^2}(\mathcal{D}_A)$ ?*

Here, we do not continue to investigate these questions, as they do not belong to the main topics of this thesis, dilation and halving distance. However, this seems to be a very interesting problem for further research.

# Appendix A

## Existence and Differentiability of Certain Parameterizations

This chapter is an appendix to Chapter 3. There, we assume that for a closed curve  $C \in \mathcal{C}$ , there exist an arc-length parameterization, an area-bisecting parameterization and a breadth-parameterization. Furthermore we assume that these parameterizations are piecewise continuously differentiable.

Because we have not found any proofs for the area-bisecting parameterization nor the breadth-parameterization, although the chances do not seem too low that they have been written down before somewhere, we prove their existence and differentiability here.

### A.1 Arc-length parameterization

The existence and differentiability of the arc-length parameterization is known, see for instance Remark 2 in Do Carmo's well-known textbook [46, p. 21]. However, as it is not difficult, we want to review the proof.

**Lemma A.1.** *Let  $C \in \mathcal{C}$  be a closed curve in the plane. Then, there exists an arc-length parameterization  $\bar{c} : [0, |C|) \rightarrow C$  of  $C$ . It is nice, in particular it is piecewise continuously differentiable.*

*Proof.* By the assumptions of the lemma there exists a nice parameterization  $c : [a, b) \rightarrow C$  of  $C$ , in particular  $c$  is piecewise continuously differentiable and  $\dot{c}(t) \neq 0$  wherever the derivative exists. Hence, the corresponding length-function

$$\ell : [a, b) \rightarrow [0, |C|), \quad \ell(\tau) := \int_a^\tau |\dot{c}(t)| dt$$

is well-defined, monotonic and piecewise continuously differentiable. Furthermore, we have  $\ell'(\tau) = |\dot{c}(\tau)| > 0$  wherever the derivative exists. We consider the inverse function

$$f : [0, |C|) \rightarrow [a, b], \quad f(t) := \ell^{-1}(t).$$

By basic analysis, see for instance Section 3.2 in [38], we know that  $f$  is monotonic, and that the derivative of  $f$  equals

$$f'(t) = \frac{1}{\ell'(f(t))} = \frac{1}{|\dot{c}(f(t))|}$$

wherever  $\ell'(f(t)) \neq 0$ . Hence, the function  $f$  and finally the parameterization

$$\bar{c} : [0, |C|) \rightarrow C, \quad \bar{c}(t) := c(f(t)),$$

are well-defined and piecewise continuously differentiable. This follows by the chain rule. The same rule for one-sided derivatives shows that the one-sided derivatives of  $\bar{c}$  exist and do not disappear (of course with the exception of the left derivative in 0 and the right derivative in  $|C|$ ). It is straight forward to check that  $\bar{c}(t)$  is an arc-length parameterization.  $\square$

## A.2 Area-bisecting parameterization

In this section we prove that for any closed curve  $C \in \mathcal{C}$  we always have a piecewise continuously differentiable area-bisecting parameterization.

Let us briefly review the definition of an area-bisecting parameterization. It is a parameterization  $c : [0, |C|) \rightarrow C$  of the curve  $C$  which traverses the curve counter-clockwise and satisfies

$$\forall t \in [0, |C|) : A(c([t, t + |C|/2])) = A(C)/2.$$

This is the formal way of saying that every chord  $c(t)c(t + |C|/2)$  is an area-bisector. The area right of the chord  $c(s)c(t)$  is defined in (3.4) as

$$A(c([s, t])) := I(c([s, t]) \oplus c(t)c(s)) = I(c([s, t])) + I(c(t)c(s)),$$

that is the area bounded by the curve  $c([s, t])$  and the line segment  $c(t)c(s)$ . The integral operator  $I$  is defined in Section 2.10 as

$$I(c([s, t])) := \frac{1}{2} \int_s^t [c(\tau), \dot{c}(\tau)] d\tau.$$

The definition of  $A(c([s, t]))$  is natural because of Lemma 2.27, and because the appearing winding numbers equal 0 or 1 due to the simplicity of  $C$ .

For proving the existence of a piecewise continuously differentiable area-bisecting parameterization we need the following auxiliary lemma.

**Lemma A.2.** *Let  $c : [0, |C|) \rightarrow C$  be a nice parameterization of  $C \in \mathcal{C}$  which traverses  $C$  counter-clockwise. Let  $s$  and  $t$  be real values satisfying  $0 \leq s \leq t < 2|C|$ ,  $t - s \leq |C|$  and  $A(C) > A(c([s, t])) > 0^1$ . Then, the right-sided derivative  $\dot{c}(t+)$  satisfies*

$$\left\langle \dot{c}(t+), \mathbf{R}^{90^\circ}(c(t) - c(s)) \right\rangle > 0.$$

---

<sup>1</sup>We extend the parameterization canonically to parameter values  $t \in [|C|, 2|C|)$  by defining  $c(t) := c(t - |C|)$ .

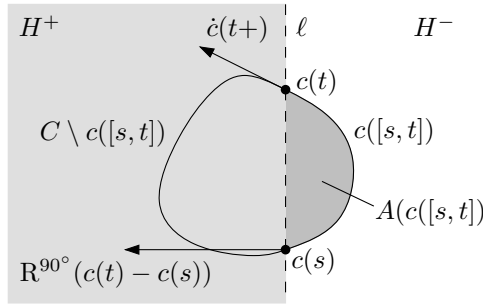


Figure A.1: The right-sided derivative satisfies  $\langle \dot{c}(t+), \mathbf{R}^{90^\circ}(c(t) - c(s)) \rangle > 0$  wherever  $0 < A(c([s, t]) < A(C)$ .

*Proof.* Consider Figure A.1. Let  $\ell$  be the line through  $c(s)$  and  $c(t)$ . Because of the convexity we know that  $c([s, t])$  must stay in one closed half-plane bounded by  $\ell$ , and  $C \setminus c([s, t])$  must lie in the other closed half-plane. Because  $c$  traverses  $C$  counter-clockwise, we can make this statement more precise. Let the two half-planes be denoted by

$$H^+ := \left\{ p \mid \left\langle p - c(t), \mathbf{R}^{90^\circ}(c(t) - c(s)) \right\rangle > 0 \right\}$$

$$\text{and } H^- := \left\{ p \mid \left\langle p - c(t), \mathbf{R}^{90^\circ}(c(t) - c(s)) \right\rangle < 0 \right\}.$$

Then, we have

$$c([s, t]) \subset \overline{H^-} \quad \text{and} \quad C \setminus c([s, t]) \subset \overline{H^+}.$$

This shows  $\langle \dot{c}(t+), \mathbf{R}^{90^\circ}(c(t) - c(s)) \rangle \geq 0$ , because for any small  $\varepsilon > 0$  we have  $c(t + \varepsilon) \in \overline{H^+}$ .

However, we cannot have  $\langle \dot{c}(t+), \mathbf{R}^{90^\circ}(c(t) - c(s)) \rangle = 0$ , because that means  $\dot{c}(t+) \parallel (c(t) - c(s))$ . But then, because of convexity,  $\ell$  had to be a tangent of  $C$ . Either  $c([s, t])$  or  $C \setminus c([s, t])$  would have to be degenerated to a line segment. This is a contradiction to the area-assumption.  $\square$

This helps us to prove the desired existence and differentiability result.

**Lemma A.3.** *Let  $C \subset \mathcal{C}$  be a convex closed curve in the plane. Then, there exists an area-bisecting parameterization  $\tilde{c} : [0, |C|) \rightarrow C$  of  $C$ . It is piecewise continuously differentiable.*

*Proof.* By the assumption of the lemma, and by Lemma A.1 there exists a nice arc-length parameterization  $\bar{c} : [0, |C|) \rightarrow C$  of  $C$ . As  $A(\bar{c}([0, \tau]))$  is continuous in  $\tau$ ,  $A(\bar{c}([0, 0])) = 0$  and  $A(\bar{c}([0, |C|])) = A(C)$ , there exists a  $\tau_{\frac{1}{2}} \in [0, |C|)$  such that

$$A(\bar{c}([0, \tau_{\frac{1}{2}}])) = A(C)/2.$$

In other words,  $\bar{c}(0)\bar{c}(\tau_{\frac{1}{2}})$  is an area-bisector.

The first half of the area-bisecting parameterization  $\tilde{c}$  we want to build, is the same as the given parameterization. We only scale it to achieve  $\tilde{c}(|C|/2) = \bar{c}(\tau_{\frac{1}{2}})$ :

$$\forall t \in \left[ 0, \frac{|C|}{2} \right] : \tilde{c}(t) := \bar{c} \left( \frac{\tau_{\frac{1}{2}}}{|C|} t \right).$$

Hence obviously, the first part is also a nice parameterization.

The definition of the second half of  $\tilde{c}$  has to guarantee that for every  $t \in [|C|/2, |C|)$  the chord  $\tilde{c}(t - |C|/2)\tilde{c}(t)$  is an area-bisector. Written down formally, this means for every  $t \in [|C|/2, |C|)$

$$c(t) := c(\tau) \quad \text{where} \quad A \left( \bar{c} \left( \left[ \frac{2\tau_{\frac{1}{2}}}{|C|} \left( t - \frac{|C|}{2} \right), \tau \right] \right) \right) = \frac{A(C)}{2}.$$

Here it is not as easy to prove the existence and differentiability of  $\tau(t)$  as it was to prove the same for  $f(t)$  in the proof of Lemma A.1, because it is not the inverse of a known function. Instead we have to apply the implicit function theorem, see e.g. Section 3.1 in [39]. To this end, we define

$$F : \left[ \frac{|C|}{2}, |C| \right) \times \left[ \frac{|C|}{2}, |C| \right) \rightarrow \mathbb{R},$$

$$F(t, \tau) := A \left( \bar{c} \left( \left[ \frac{2\tau_{\frac{1}{2}}}{|C|} \left( t - \frac{|C|}{2} \right), \tau \right] \right) \right) - \frac{A(C)}{2}.$$

Hence, the function  $\tau(t)$  we are looking for solves  $F(t, \tau(t)) = 0$ . By the definition of  $\tau_{\frac{1}{2}}$  we know that  $F(|C|/2, |C|/2) = 0$ . This means that we have a start-value  $\tau(|C|/2) = |C|/2$ . The implicit function theorem, slightly generalized to one-sided derivatives, shows that we can uniquely extend the known solution as long as

$$\frac{d}{dt}F(t+, \tau) < 0 \quad \text{and} \quad \frac{d}{d\tau}F(t, \tau+) > 0. \tag{A.1}$$

Then, the one-sided derivative of the solution  $\tau(t)$  satisfies

$$\tau'(t+) = \frac{-\frac{d}{dt}F(t+, \tau)}{\frac{d}{d\tau}F(t, \tau+)} > 0.$$

Furthermore, if both (two-sided) partial derivatives of  $F$  exist in  $(t, \tau(t))$ , the theorem of implicit functions implies that the solution  $\tau$  is differentiable in  $t$ .

Hence, if we prove (A.1) for all values  $(t, \tau)$  such that  $F(t, \tau) = 0$ , then, the definition

$$\forall t \in \left[ \frac{|C|}{2}, |C| \right) : \tilde{c}(t) := \bar{c}(\tau(t))$$

would result in a nice area-bisecting parameterization of  $C$ .

We complete the proof by showing that (A.1) follows from Lemma A.2. Let  $(t, \tau) \in [|C|/2, |C|)^2$  satisfy  $F(t, \tau) = 0$ . We define  $s := (\tau_{\frac{1}{2}}2/|C|)(t - |C|/2)$ . From the assumption follows



that  $\bar{c}(s)\bar{c}(\tau)$  is an area bisector. And we can conclude

$$\begin{aligned}
 \frac{d}{d\tau}F(t, \tau+) &= \frac{d}{d\tau}A(\bar{c}([s, \tau+])) \\
 &= \frac{d}{d\tau}(I(\bar{c}([s, \tau+])) + I(\bar{c}(\tau+)\bar{c}(s))) \\
 &\stackrel{(2.17), \text{Lem. 2.31}}{=} \frac{d}{d\tau}\left(\frac{1}{2}\int_s^{\tau+} [\bar{c}(x), \dot{\bar{c}}(x)]dx + \frac{1}{2}[\bar{c}(\tau+), \bar{c}(s)]\right) \\
 &= \frac{1}{2}([\bar{c}(\tau), \dot{\bar{c}}(\tau+)] + [\dot{\bar{c}}(\tau+), \bar{c}(s)]) \\
 &\stackrel{\text{lin. \& anti-sym. of } [\cdot, \cdot]}{=} \frac{1}{2}[\bar{c}(\tau) - \bar{c}(s), \dot{\bar{c}}(\tau+)] \\
 &\stackrel{\text{Def. of } [\cdot, \cdot]}{=} \frac{1}{2}\langle \mathbb{R}^{90^\circ}(\bar{c}(\tau) - \bar{c}(s)), \dot{\bar{c}}(\tau+) \rangle \stackrel{\text{Lem. A.2}}{>} 0.
 \end{aligned}$$

The second condition in (A.1) follows analogously, if we apply  $A(\bar{c}([s, t])) = A(C) - A(\bar{c}([t, s + |C|]))$ . □

### A.3 Extremal parameterization

In this section we prove that for any twice piecewise continuously differentiable, closed, convex curve  $C \in \mathcal{C}$  whose curvature never disappears, there exists a piecewise continuously differentiable extremal parameterization.

Unfortunately, we need the existence of the second derivatives, because the first derivative gives the direction of the corresponding tangent, and for a differentiable extremal parameterization we need the derivative of this direction.

The first step of the proof is to show that we may assume that  $C$  is given by an arc-length parameterization. To this end, we show that given a twice continuously differentiable parameterization whose curvature does never disappear the construction of Lemma A.1 results in an arc-length parameterization with the same properties.

In particular the curvature remains the same for every point  $p \in C$ . And this is why it makes sense to denote it by  $\kappa(C, p)$  independently from the parameterization.

**Lemma A.4.** *Let  $c : [a, b] \rightarrow C$  be a piecewise twice continuously differentiable curve such that  $\dot{c}(t) \neq 0$  and  $\kappa(C, p) \neq 0$  for every  $p \in C$ , in particular  $\ddot{c}(t) \neq 0$  wherever the derivative exists. Then, the arc-length parameterization constructed in the proof of Lemma A.1 has the same properties and the same curvature.*

*Proof.* Let  $c(\tau)$  be twice continuously differentiable on the open interval  $(a_{i-1}, a_i)$ . It remains to show that the arc-length parameterization  $\bar{c}(t) = c(f(t))$  from Lemma A.1 is twice continuously differentiable on  $(\ell(a_{-1}), \ell(a_i))$ , and that its curvature equals the one from  $c$ .

We know already that

$$\dot{\bar{c}}(\tau) = f'(\tau)\dot{c}(f(\tau)) = \frac{1}{|\dot{c}(f(\tau))|}\dot{c}(f(\tau)). \tag{A.2}$$

We only have to calculate the second derivative. To this end, from

$$f'(\tau) = \frac{1}{|\dot{c}(f(\tau))|} = \sqrt{\langle \dot{c}(f(\tau)), \dot{c}(f(\tau)) \rangle}^{-\frac{1}{2}}$$

we conclude

$$\begin{aligned} f''(\tau) &= -\frac{1}{2} \sqrt{\langle \dot{c}(f(\tau)), \dot{c}(f(\tau)) \rangle}^{-\frac{3}{2}} 2 \langle \ddot{c}(f(\tau)), \dot{c}(f(\tau)) \rangle f'(\tau) \\ &= -\frac{\langle \ddot{c}(f(\tau)), \dot{c}(f(\tau)) \rangle}{|\dot{c}(f(\tau))|^4}. \end{aligned}$$

We can use this to derive a formula for the second derivative from (A.2).

$$\begin{aligned} \ddot{c}(\tau) &= f''(\tau) \dot{c}(f(\tau)) + (f'(\tau))^2 \ddot{c}(f(\tau)) \\ &= -\frac{\langle \ddot{c}, \dot{c} \rangle}{|\dot{c}|^4} \dot{c} + \frac{1}{|\dot{c}|^2} \ddot{c} \end{aligned}$$

Because of  $|\dot{c}| \neq 0$ , this shows that the second derivative exists on the whole interval. The curvature calculated from the new arc-length parameterization  $\bar{c}$  equals by its definition

$$\begin{aligned} \kappa_{\bar{c}}(C, p) &\stackrel{(3.6)}{=} \frac{1}{|\dot{\bar{c}}|^3} \langle \ddot{\bar{c}}, \mathbf{R}^{90^\circ} \dot{\bar{c}} \rangle \stackrel{|\dot{\bar{c}}|=1}{=} \langle \ddot{\bar{c}}, \mathbf{R}^{90^\circ} \dot{\bar{c}} \rangle \\ &= -\langle \ddot{\bar{c}}, \dot{\bar{c}} \rangle \underbrace{\langle \dot{\bar{c}}, \mathbf{R}^{90^\circ} \dot{\bar{c}} \rangle}_0 + \langle \ddot{\bar{c}}, \mathbf{R}^{90^\circ} \dot{\bar{c}} \rangle \\ &\stackrel{|\dot{\bar{c}}|=1}{=} \frac{1}{|\dot{\bar{c}}|^3} \langle \ddot{\bar{c}}, \mathbf{R}^{90^\circ} \dot{\bar{c}} \rangle \stackrel{(3.6)}{=} \kappa_c(C, p) \neq 0 \end{aligned}$$

This also implies  $\ddot{\bar{c}} \neq 0$ . □

**Lemma A.5.** *Let  $c$  be a nice, twice piecewise continuously differentiable parameterization  $c : [a, b) \rightarrow C$  of a closed, strictly convex curve  $C \in \mathcal{C}$ , such that  $\kappa(C, p) \neq 0$  for every  $p \in C$ . Then, there exists a piecewise continuously differentiable extremal parameterization  $\tilde{c} : [0, |C|) \rightarrow C$ .*

*Proof.* Because of Lemma A.4 we may assume that the given parameterization is an arc-length parameterization  $\bar{c} : [0, |C|) \rightarrow C$ . Furthermore, we may assume that  $\bar{c}(\tau)$  traverses  $C$  counter-clockwise, as otherwise we can consider  $c(|C| - \tau)$  instead.

If we identify  $\tau = 0$  with  $\tau = |C|$ , we have piecewise continuous one-sided derivatives

$$\dot{\bar{c}}(\tau+) \in \mathbb{S}^1 \quad \text{and} \quad \dot{\bar{c}}(\tau-) \in \mathbb{S}^1 \quad \text{for every } t \in [0, |C|).$$

We want to apply an inverse of

$$\gamma : \mathbb{R} \rightarrow \mathbb{S}^1, \quad \gamma(\alpha) := (\cos \alpha, \sin \alpha)$$

to the derivative vectors of  $\bar{c}(t)$  in order to get their angle-value depending on  $t$ . We define

$$\alpha_+(\tau) := \gamma^{-1}(\dot{\bar{c}}(\tau+)) \quad \text{and} \quad \alpha_-(\tau) := \gamma^{-1}(\dot{\bar{c}}(\tau-))$$

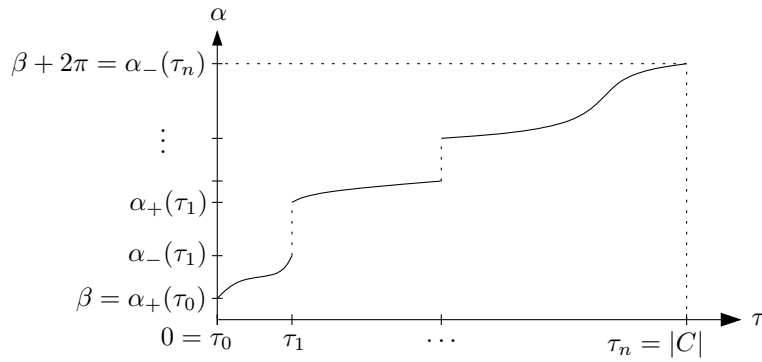


Figure A.2: The angle-value  $\alpha$  of the supporting line(s) through  $c(\tau)$ .

Consider the example in Figure A.2. Because  $c(\tau)$  traverses  $C$  counter-clockwise, and  $C$  is strictly convex, we can choose  $\gamma^{-1}$  so that both functions are strictly increasing, and the image of both functions lies in the same interval  $[\beta, \beta + 2\pi)$ .

Let  $0 = \tau_0 < \tau_1 < \dots < \tau_n = |C|$  be the partition such that  $c(\tau)$  is twice continuously differentiable on each interval  $(\tau_{i-1}, \tau_i)$ , and the first derivatives and the curvature do not disappear. Then, clearly, we have  $\alpha_-(\tau) = \alpha_+(\tau)$  for every  $\tau \in (\tau_{i-1}, \tau_i)$ , and the function is continuous on the open interval. For these values we define  $\alpha(\tau) := \alpha_-(\tau) = \alpha_+(\tau)$ . However, there can be jumps,  $\alpha_-(\tau_i) < \alpha_+(\tau_i)$ , at the values  $\tau_i, i \in \{0, \dots, n\}$ .

As  $C$  is convex, for every  $\tau$  and every  $\alpha \in [\alpha_-(\tau), \alpha_+(\tau)]$  there exists a supporting line of  $C$  through  $c(\tau)$  with direction  $\alpha$ . But this means, that  $c(\tau)$  is an extreme point in direction  $\alpha - \pi/2$ . Because  $C$  is strictly convex, the intervals  $[\alpha_-(\tau), \alpha_+(\tau)], \tau \in [a, b)$ , are a disjunctive cover of  $[\beta, \beta + 2\pi)$ .

Obviously, to construct the desired extremal parameterization, we need a kind of inverse of  $\alpha(\tau)$ . Let  $\tau(\alpha)$  denote the unique  $\tau$ -value such that  $\alpha \in [\alpha_-(\tau), \alpha_+(\tau)]$ . It is easy to see that  $\tau : [\beta, \beta + 2\pi) \rightarrow [0, |C|)$  is non-decreasing and continuous. It is constant on each interval  $[\alpha_-(\tau_i), \alpha_+(\tau_i)]$  and strictly increasing on each interval  $[\alpha_+(\tau_{i-1}), \alpha_-(\tau_i)]$ . It remains to prove that it is continuously differentiable on  $(\alpha_+(\tau_{i-1}), \alpha_-(\tau_i))$ .

On such an interval, we can simply define  $\tau(\alpha) := \dot{c}^{-1}(\gamma(\alpha))$  because  $\alpha(t) = \gamma^{-1}(\dot{c}(t))$  is well-defined, continuous, and strictly monotonously increasing on  $(\tau_{i-1}, \tau_i)$  with values in  $(\alpha_+(\tau_{i-1}), \alpha_-(\tau_i))$ . We write the defining equation in two different ways:

$$\tau(\alpha) := \dot{c}^{-1}(\gamma(\alpha)) = \begin{cases} \dot{c}_x^{-1}(\cos \alpha) & (\alpha \notin \{k\pi | k \in \mathbb{Z}\}) \\ \dot{c}_y^{-1}(\sin \alpha) & (\alpha \notin \{k\pi + \frac{\pi}{2} | k \in \mathbb{Z}\}) \end{cases}$$

One might suspect problems with these definitions, because in general there are two solutions for  $\dot{c}_x^{-1}$  (above and below the  $x$ -axis), and two solutions for  $\dot{c}_y^{-1}$  (left and right of the  $y$ -axis). However, as  $\tau(\alpha)$  has to be non-decreasing and continuous, it will not be a problem to decide which solution is meant.

And we only need to consider the inverse in a small interval to show that its derivative exists and is continuous in  $\alpha$ . We do not consider the first version in the case  $\alpha = k\pi$ , because then,  $\dot{c}$  is not monotonic in an interval around the corresponding  $\tau$ -value. Analogous reasons prevent

us from using the second version if  $\alpha = k\pi + \frac{\pi}{2}$ . But clearly, in every case, we can choose one of the two versions which is monotonic in a small interval around the analyzed  $\tau(\alpha)$ -value. Hence, we can apply the formula for the derivative of the inverse function, and get

$$\tau'(\alpha) = \begin{cases} \frac{1}{\tilde{c}_x(\tau(\alpha))}(-\sin \alpha) & (\alpha \notin \{k\pi | k \in \mathbb{Z}\}) \\ \frac{1}{\tilde{c}_y(\tau(\alpha))}(\cos \alpha) & (\alpha \notin \{k\pi + \frac{\pi}{2} | k \in \mathbb{Z}\}) \end{cases} .$$

As we are considering  $\alpha$ -values in an interval  $(\alpha_+(\tau_{i-1}), \alpha_-(\tau_i))$ , the derivative  $\dot{c}(\tau)$  exists on the corresponding interval  $(\tau_{i-1}, \tau_i)$ , and it does not disappear, because its curvature does not disappear. Hence, if  $\alpha \notin \{k\frac{\pi}{2} | k \in \mathbb{Z}\}$ , we can choose one of the two options depending on whether  $\tilde{c}_x(\tau(\alpha)) \neq 0$  or  $\tilde{c}_y(\tau(\alpha)) \neq 0$ . If  $\alpha = k\pi$  for a  $k \in \mathbb{Z}$ , we have to use the second option. But then,  $\tilde{c} \perp \dot{\tilde{c}}$  guarantees that  $\tilde{c}_y \neq 0$ , as  $\tilde{c}$  points in  $x$ -direction. Analogous arguments hold for  $\alpha = k\pi + \frac{\pi}{2}$ ,  $k \in \mathbb{Z}$ , where we choose the first option. Thus,  $\tau'(\alpha)$  is continuously differentiable on  $(\alpha_+(\tau_{i-1}), \alpha_-(\tau_i))$ , and the derivative does not disappear.

This makes it easy to get the desired extremal parameterization. We define

$$\tilde{c}(t) := \bar{c} \left( \tau \left( \frac{2\pi t}{|C|} + \frac{\pi}{2} \right) \right).$$

This implies the following formula for the derivative.

$$\dot{\tilde{c}}(t) := \dot{\bar{c}} \left( \tau \left( \frac{2\pi t}{|C|} + \frac{\pi}{2} \right) \right) \tau' \left( \frac{2\pi t}{|C|} + \frac{\pi}{2} \right) \frac{2\pi}{|C|}$$

We have shown that  $\tau'(\alpha)$  is continuous and does not disappear on any interval  $(\alpha_+(\tau_{i-1}), \alpha_-(\tau_i))$ . And we know that  $\dot{\tilde{c}}(\tau)$  is continuous on the corresponding interval  $(\tau_{i-1}, \tau_i)$  and does not disappear. Hence, we have shown the same for  $\dot{\tilde{c}}(t)$  on any interval  $(\alpha_+(\tau_{i-1})|C|/2\pi, \alpha_-(\tau_{i-1})|C|/2\pi)$ .

And it is easy to see that  $\tilde{c}(t)$  is an extremal parameterization as by definition of  $\tau$  the derivative  $\dot{\tilde{c}}(\tau(\frac{2\pi t}{|C|} + \frac{\pi}{2}))$  points in direction  $\frac{2\pi t}{|C|} + \frac{\pi}{2}$ . This means that  $\dot{\tilde{c}}(t)$  points in direction  $\frac{2\pi t}{|C|} + \frac{\pi}{2}$ . Hence,  $\tilde{c}(t)$  is extremal in direction  $2\pi t/|C|$ .  $\square$

# Appendix B

## A Proof of the Disk-Packing Result

In Chapter 5 we proved a new lower bound to the dilation constant  $\Delta$ . To this end, we have applied Theorem 5.5, a disk-packing result from Kuperberg et al. [134]. Because there is an overlooked special case in the original proof of this disk-packing result, here we give a detailed, corrected version which follows in parts a suggestion by Günter Rote. Some arguments of the original proof had to be altered but the idea and the skeleton of the proof remain the same.

**Theorem 5.5.** Let  $\mathcal{D}$  be a (finite or infinite) packing in the plane of circular disks with radius at most 1. For the constant  $\tilde{\Lambda} = 1.00001$  consider the  $\tilde{\Lambda}$ -enlargement  $\mathcal{D}^{\tilde{\Lambda}}$  of  $\mathcal{D}$ . Then,  $\mathcal{D}^{\tilde{\Lambda}}$  covers no square of side length 4.

In order to prove this statement, we first introduce some notation.

Recall that for a given disk  $D = \overline{B_r(c)} := \{p \in \mathbb{R}^2 \mid |pc| \leq r\}$  and a factor  $\lambda > 0$  we define the  $\lambda$ -enlargement of  $D$  by  $D^\lambda := \overline{B_{\lambda r}(c)}$ . The center of any disk  $D$  will be denoted by  $c(D)$  and its radius by  $r(D)$ . The  $\lambda$ -enlargement of a set of disks  $\mathcal{D}$  is defined as  $\mathcal{D}^\lambda := \{D^\lambda \mid D \in \mathcal{D}\}$ . We say that a disk  $D$  bites into a region  $R \subset \mathbb{R}^2$ , if  $D^\lambda \cap R \neq \emptyset$ . Note that every disk which intersects with  $R$  bites into  $R$ , but not vice versa.

### B.1 Idea of the proof

The general idea of the proof is the same as in the original article. We assume that there is a packing  $\mathcal{D}$  of disks with radius at most 1 whose  $\tilde{\Lambda}$ -enlargement  $\mathcal{D}^{\tilde{\Lambda}}$  covers a square  $R_\square$  of side length 4. Inductively we construct compact regions  $R_1 \supset R_2 \supset R_3 \supset \dots$ , and corresponding values  $r_n \in \mathbb{R}$ ,  $n \in \mathbb{N}$ , such that  $R_1 \subset R_\square$ , and for every  $n \in \mathbb{N}$  we have  $R_n \neq \emptyset$  and no disk  $D \in \mathcal{D}$  with radius  $r(D) > r_n$  bites into  $R_n$ . Furthermore,  $r_n \searrow 0$  will hold for  $n \rightarrow \infty$ .

We choose a sequence of points  $p_n \in R_n \subset R_1$ . Because  $R_1 = R_\square$  is compact, there exists a converging subsequence  $\tilde{p}_n \rightarrow p$ . Let  $\tilde{r}_n$  and  $\tilde{R}_n$  denote the corresponding subsequences of radii and regions. The limit point  $p$  of  $\tilde{p}_n$  belongs to every  $\tilde{R}_n$  because we have  $\tilde{p}_j \in \tilde{R}_n$  for every  $j \geq n$ , and  $\tilde{R}_n$  is closed. Thus, the point  $p \in R_\square$  is not bitten by any disk  $D \in \mathcal{D}$  with radius  $r(D) > r_n$ . And this statement holds for every  $n$ . Because of  $r_n \rightarrow 0$  this implies that  $p \in R_\square$  is not bitten by any  $D \in \mathcal{D}$ . It is not covered by any  $D^{\tilde{\Lambda}}$ ,  $D \in \mathcal{D}$ , a contradiction.

To facilitate notation, we define  $\varepsilon := 0.00001$ , so that  $\tilde{\Lambda} = 1 + \varepsilon$ .

There are two types of regions. The first case is a *circular region* (replacing the square-type region in the original proof). It is a closed disk  $R_n := \overline{B_r(c)}$  where  $r_n := \frac{1}{2}r$ . This means, a circular region  $R_n$  is a disk with radius  $r$  such that no disk  $D \in \mathcal{D}$  with radius  $r(D) > r/2$  bites into  $R$ .

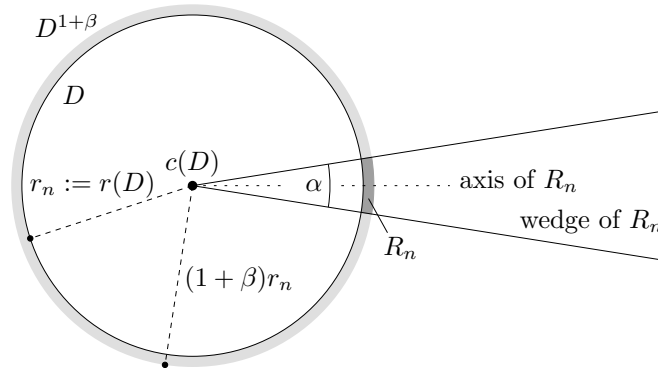


Figure B.1: A crescent-type region  $R_n$  of the disk  $D$ .

The second case is a crescent-type region, see Figure B.1. As in the original paper, a crescent is determined by two constants, the angle  $\alpha \in [0, \pi]$  and the factor  $\beta \in (0, \infty)$ . We follow the original definition of  $\beta$ ,  $\beta := \frac{1}{16}$ , and we increase  $\alpha$  slightly by defining  $\alpha := \frac{\pi}{10} = 18^\circ$ .

A *crescent* of a disk  $D \in \mathcal{D}$  is the intersection of a wedge of angle  $\alpha$  and corner point  $c(D)$  with the  $\beta$ -annulus  $\overline{D^{(1+\beta)}} \setminus D$ . The beam emanating from  $c(D)$  and halving the wedge is called its *axis*. For every crescent  $R_n$ , we choose the corresponding radius  $r_n$  as the radius of the disk  $D$ .

## B.2 Inductive construction

We explained above that, in order to prove Theorem 5.5, it suffices to construct a sequence of certain regions  $R_n$  and corresponding radii  $r_n$ . In the next section we will show that, indeed, we can construct such regions inductively.

### B.2.1 Induction Base

The first region  $R_1$  is circular, see Figure B.2. Its center is the center of the square  $R_\square$ , and its radius equals 2. This ensures  $R_1 \subset R_\square$ . Formally, we can write

$$R_1 := \overline{B_2(c(R_\square))},$$

where  $c(R_\square)$  is the center of  $R_\square$ .

Furthermore, we choose  $r_1 := 1$ . As the radius of every disk  $D \in \mathcal{D}$  is bounded by  $r(D) \leq 1$ , no disk  $D \in \mathcal{D}$  with radius  $r(D) > 1 = r_1$  bites into  $R_1$ . These definitions also ensure that  $r_1$  is half the radius of  $R_1$ . Hence,  $R_1$  and  $r_1$  fulfill all the desired properties.

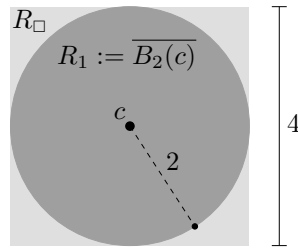


Figure B.2: The definition of the first region  $R_1$  inside of  $R_\square$ .

### B.2.2 Induction Step: $R_n$ crescent

Let now  $R_n$  be a crescent of a disk  $D_n \in \mathcal{D}$  with radius  $r(D_n) = r_n$ , such that no disk  $D \in \mathcal{D}$  with radius  $r > r_n$  bites into  $R_n$ . For simplicity we assume that  $D_n$  is a unit disk centered at the origin, i.e.  $c_n := c(D_n) = (0, 0)$  and  $r_n = 1$ .

Consider Figure B.3. Like in the original proof, let  $I$  denote the intersection of  $R_n$  with  $D^{1+\gamma}$ , where  $\gamma := \frac{\beta}{16} = \frac{1}{256}$ . The idea of this induction step is sketched in the following, see Figures B.3 and B.4.

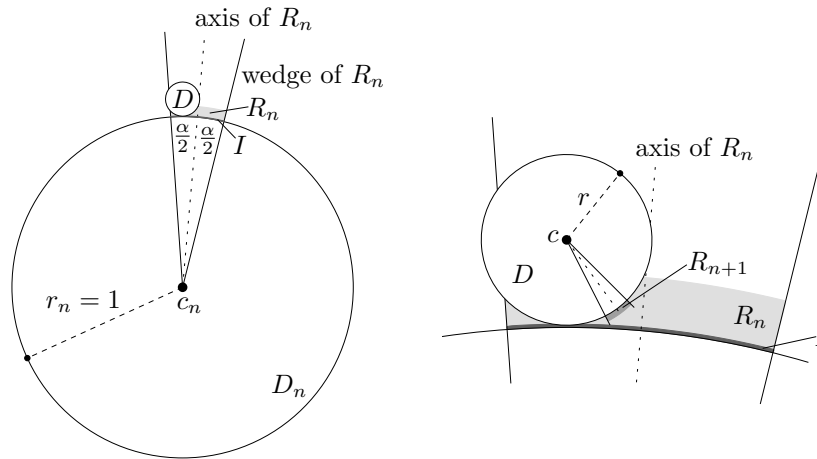


Figure B.3: Construction of  $R_{n+1}$  if a medium size disk  $D$  intersects with  $I$ .

If there exists a disk  $D$  intersecting with  $I$ , it is very close to the disk  $D_n$ .

If, furthermore,  $D$  is not too big and not too small, as shown in Figure B.3, we can find a crescent of  $D$  inside of  $R_n$  which is not bitten by  $D_n$  and which cannot be bitten by any other disk  $\tilde{D} \in \mathcal{D}$  with radius  $\tilde{r}$ ,  $r(D) < \tilde{r} \leq 1$ , because  $D$  and  $D_n$  do not admit such a disk  $\tilde{D}$ .

If there do not exist such medium size disks intersecting  $I$ , we only have quite big disks and very small disks of  $\mathcal{D}$  intersecting  $I$ . The big disks leave some space for a circular region  $R_{n+1}$  inside of  $I$ , as shown in Figure B.4. This is a valid circular region, because only small disks can bite into it.

In the following subsections, we state these arguments more precisely, and we prove them in

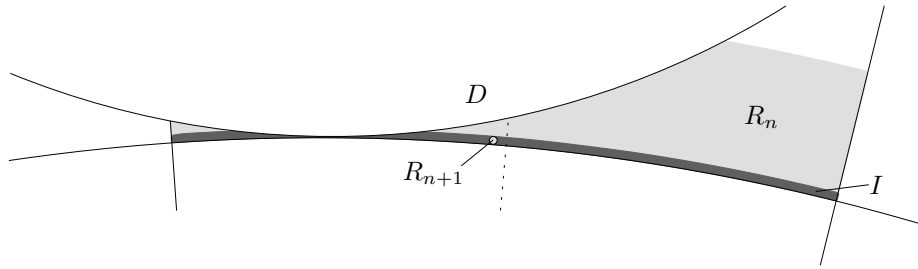


Figure B.4: Construction of  $R_{n+1}$  if no medium size disk intersects with  $I$ .

detail.

### B.2.2.1 Medium size disk intersecting $I$

We treat the most important and probably most difficult case first. In this case, there exists a disk  $D$  intersecting  $I$ , whose center  $c := c(D)$  lies in the wedge of  $R_n$  and whose radius  $r$  satisfies  $1/1280 \leq r \leq 1/8$ . We will explain later, why the additional condition on  $c$  is necessary. Furthermore, by symmetry we may assume that  $c$  lies in the left half of the wedge of  $R_n$  or on its axis. For simplicity we assume that  $c$  lies on the positive  $y$ -axis.

We want to find a crescent of  $D$  which cannot be bitten by any other disk  $\tilde{D} \in \mathcal{D}$  with radius  $\tilde{r} > r$ . For each point  $p \in \mathbb{R}^2 \setminus \{c\}$  we denote the smaller of the two angles between the segment  $c_n c$  and the segment  $pc$  by

$$\alpha_D(p) := \angle(c_n, c, p) = \angle(c_n - c, p - c).$$

We will show that

$$R_{n+1} := \overline{D^{1+\beta} \setminus D} \cap \left\{ p \in \mathbb{R}^2 \mid p_x \geq 0 \wedge \alpha_D(p) \in \left[ \frac{3}{20}\pi, \frac{5}{20}\pi \right] = [27^\circ, 45^\circ] \right\}$$

is a valid crescent, i.e.  $R_{n+1} \subset R_n$  and there is no disk  $\tilde{D} \in \mathcal{D}$  with radius  $\tilde{r} > r$  biting into  $R_{n+1}$ . Note that by this definition the crescent  $R_{n+1}$  lies to the right of  $cc_n$ , it is located in the bigger of the two parts of  $R_n$  divided by  $cc_n$ .

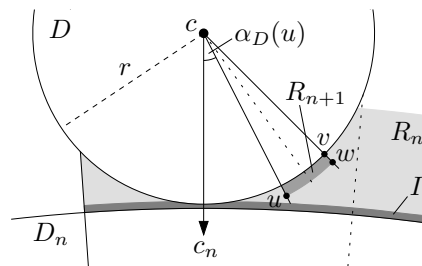


Figure B.5: The corner points  $u$ ,  $v$  and  $w$  of the crescent  $R_{n+1}$ .

First, we show that  $R_{n+1}$  is fully contained in  $R_n$ . This is necessary for our argumentation, and it also guarantees that no disk  $\tilde{D} \in \mathcal{D}$  with radius  $r(\tilde{D}) > r(D_n) = 1$  bites into  $R_{n+1}$ . We



follow the arguments of the original paper, cf. Figure B.5. Let  $u$  be the point of  $R_{n+1}$  which is closest to  $c_n$ , let  $v$  be the point of  $R_{n+1}$  which is farthest from  $c_n$ , and let  $w$  be the point of  $R_{n+1}$  which maximizes the distance to  $c$  and  $\alpha_D(w)$ . In order to show that  $R_{n+1} \subset R_n$  it suffices to prove

$$|uc_n| \geq r_n = 1, \quad |vc_n| \leq (1 + \beta)r_n = 1 + \beta \quad \text{and} \quad \angle(w, c_n, c) \leq \alpha/2.$$

Instead of  $|uc_n| \geq r_n = 1$  we even prove  $|uc_n| > (1 + \varepsilon)r_n = 1 + \varepsilon$ , because this also shows that  $D_n$  does not bite into  $R_{n+1}$ . By the law of cosines, we have

$$\begin{aligned} |uc_n|^2 &= |uc|^2 + |cc_n|^2 - 2|uc||cc_n| \cos \angle(c_n, c, u) \\ &\geq (1 + \beta)^2 \left(\frac{1}{1280}\right)^2 + \left(1 + \frac{1}{1280}\right)^2 \\ &\quad - 2 \cdot (1 + \beta) \frac{1}{1280} \cdot \left(1 + \gamma + \frac{1}{1280}\right) \cos \frac{3}{20}\pi \\ &= 1.0000776\dots \end{aligned}$$

The inequality holds because  $|uc_n|$  is minimized if  $r$  is minimal, i.e.  $r = 1/1280$ , and because of  $\angle(c_n, c, u) = (3/20)\pi$ ,  $|uc| = (1 + \beta)r$  and  $1 + r \leq |cc_n| \leq 1 + \gamma + r$ . We conclude  $|uc_n| > 1.0000388\dots > 1.00001 = (1 + \varepsilon)$ , which we wanted to show.

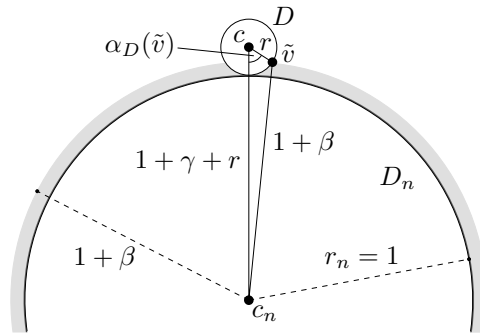


Figure B.6: The angle  $\alpha_D(\tilde{v})$  is minimal if  $D$  hardly intersects  $I$  and  $r = 1/8$ .

Consider Figure B.6. In order to prove that  $|vc_n| < (1 + \beta)$  we show that the right intersection point  $\tilde{v}$  of the circles  $\partial D$  and  $\partial D_n^{1+\beta}$  has a corresponding angle  $\alpha_D(\tilde{v}) > \frac{5}{20}\pi$ . The angle  $\alpha_D(\tilde{v})$  is smallest, if  $D$  hardly intersects  $I$ , and  $r$  is as big as possible. Again, we apply the law of cosines and get

$$\begin{aligned} \alpha_D(\tilde{v}) &\geq \arccos \left( \frac{r^2 + (1 + \gamma + r)^2 - (1 + \beta)^2}{2r(1 + \gamma + r)} \right) \\ &\geq \arccos \left( \frac{\left(\frac{1}{8}\right)^2 + \left(1 + \gamma + \frac{1}{8}\right)^2 - (1 + \beta)^2}{2\frac{1}{8}\left(1 + \gamma + \frac{1}{8}\right)} \right) \\ &= 0.9630871\dots > 0.7853981\dots = \frac{5}{20}\pi \end{aligned}$$

The angle  $\angle(c, c_n, w)$  is maximal if  $r$  is as big as possible, and if the disk  $D_n$  touches  $D$ . By

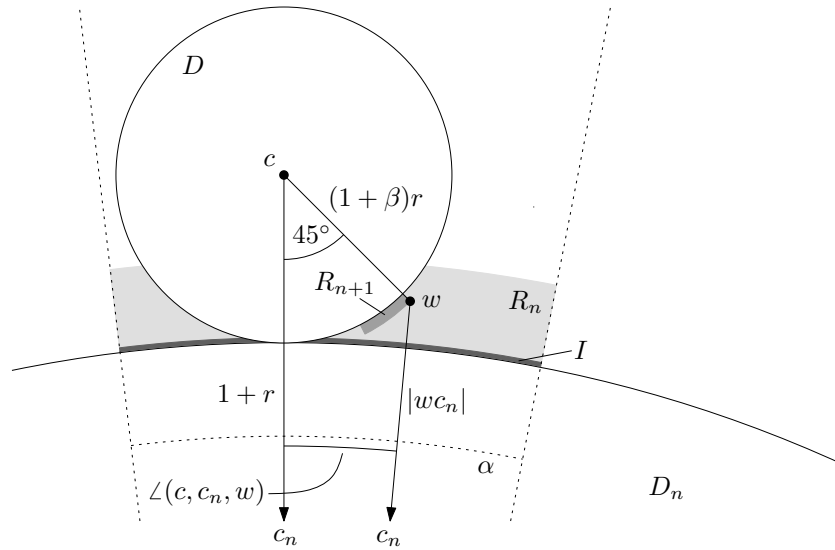


Figure B.7: The maximal angle  $\angle(c, c_n, w)$  is attained if  $D$  touches  $D_n$ , and if  $r = 1/8$ .

first applying the law of sines and then the law of cosines, we get

$$\begin{aligned}
 \angle(c, c_n, w) &= \arcsin\left(\frac{|cw|}{|c_n w|} \sin \frac{5}{20}\pi\right) \\
 &= \arcsin\left(\frac{|cw|}{\sqrt{|cw|^2 + |cc_n|^2 - 2|cw||cc_n| \cos \frac{5}{20}\pi}} \sin \frac{5}{20}\pi\right) \\
 &\leq \arcsin\left(\frac{\frac{1+\beta}{8} \sin \frac{5}{20}\pi}{\sqrt{\left(\frac{1+\beta}{8}\right)^2 + \left(1 + \frac{1}{8}\right)^2 - 2\frac{1+\beta}{8}\left(1 + \frac{1}{8}\right) \cos \frac{5}{20}\pi}}\right) \\
 &= 0.0908305\dots < 0.1570796\dots = \alpha/2.
 \end{aligned}$$

At this point we know that  $R_{n+1}$  is contained in  $R_n$  which implies that no disk  $\tilde{D} \in \mathcal{D}$  with radius  $r(\tilde{D}) > r_n = 1$  bites into  $R_{n+1}$ .

Figure B.8 shows why it is essential to consider only disks  $D$  in this case whose center  $c$  lies inside the wedge of  $R_n$ . Otherwise  $R_{n+1}$  might not be contained in  $R_n$ . This is the flaw of the original proof. There, the crescent begins at an angle  $\alpha_D(p) = 2\alpha = \pi/8 < (3/20)\pi$ . Hence, indeed, the same problem occurs.

In addition to  $R_{n+1} \subset R_n$ , we also showed that  $D_n$  does not bite into  $R_{n+1}$ . It remains to show that no other disk  $\tilde{D} \in \mathcal{D} \setminus \{D_n\}$  with radius  $r(\tilde{D}) \in (r(D), 1]$  bites into  $R_{n+1}$ .

This might be considered obvious by some readers, and actually the original article spends only one sentence on this topic, but we want to be careful in order not to overlook anything. We will prove that the angle  $\alpha_D(p)$  of any point  $p \in D^{1+\beta}$  bitten by  $\tilde{D}$  is either smaller than  $\frac{3}{20}\pi$  or bigger than  $\frac{5}{20}\pi$ . We use the notation  $\tilde{c} := c(\tilde{D})$  and  $\tilde{r} := r(\tilde{D})$ .

<sup>1</sup>In order to show the situation clearly, the  $\varepsilon$ -value used in the figure is significantly bigger than 0.00001.

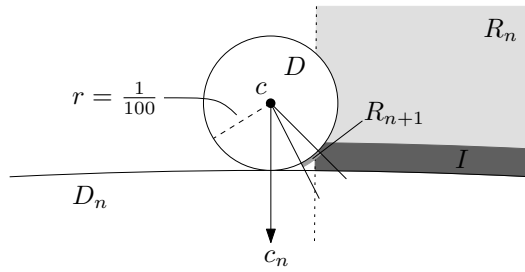


Figure B.8: If we do not require  $c$  to lie inside the wedge of  $R_n$ , we cannot guarantee  $R_{n+1} \subset R_n$ .

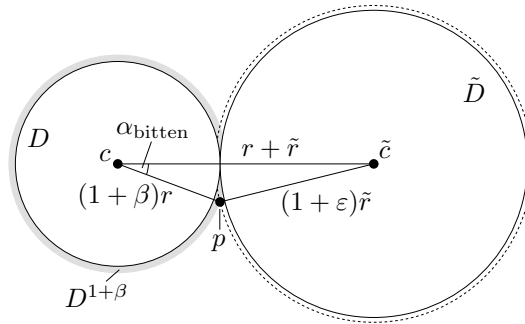


Figure B.9: The definition of  $\alpha_{\text{bitten}}(r, \tilde{r})$ .<sup>1</sup>

As a first step, we derive an upper bound for the angle  $\angle(p, c, \tilde{c})$ , where  $p$  is a point from  $D^{1+\beta}$  bitten by  $\tilde{D}$  like shown in Figure B.9. Clearly, this angle is biggest, if the two disks touch. As it will be useful also in some other cases, we introduce a name for this angle. We call it  $\alpha_{\text{bitten}}$ . A simple application of the law of cosines yields

$$\alpha_{\text{bitten}}(r, \tilde{r}) = \arccos \left( \frac{(r + \tilde{r})^2 + (r(1 + \beta))^2 - (\tilde{r}(1 + \varepsilon))^2}{2(r + \tilde{r})(r(1 + \beta))} \right). \quad (\text{B.1})$$

It is maximal if  $r$  is minimal, and if  $\tilde{r}$  is maximal, i.e.  $r = 1/1280$  and  $\tilde{r} = 1$ . This yields

$$\begin{aligned} \angle(\tilde{c}, c, p) &\leq \alpha_{\text{bitten}}^{\max} := \alpha_{\text{bitten}} \left( \frac{1}{1280}, 1 \right) \\ &= 0.3785916\dots < 0.4712388\dots = \frac{3}{20}\pi \end{aligned} \quad (\text{B.2})$$

This shows that any point  $p \in D^{1+\beta}$  bitten by a disk  $\tilde{D} \in \mathcal{D} \setminus \{D_n\}$  with radius  $\tilde{r} > r$ , whose center  $\tilde{c}$  lies left of  $c$  and  $c_n$ , satisfies  $\alpha_D(p) < \frac{3}{20}\pi$ . The disk  $\tilde{D}$  does not bite into  $R_{n+1}$ .

What can we say, if  $\tilde{c}$  lies to the right of  $c$  and  $c_n$ ? If the angle  $\angle(\tilde{c}, c_n, c)$  is less than  $\alpha/2$ , we know that  $|\tilde{c}c_n| > 1 + \gamma + \tilde{r}$ , because otherwise  $\tilde{D}$  would intersect with  $I$ , contradicting that  $D$  is the largest disk from  $\mathcal{D}$  intersecting  $I$ . Hence, in this case, the angle  $\angle(c_n, c, \tilde{c})$  is minimal if<sup>2</sup>  $\tilde{r} = r = 1/8$ , if  $\tilde{D}$  hardly bites into  $D^{1+\beta}$ , if  $D$  hardly intersects  $I$ , and if  $\tilde{D}$  almost

<sup>2</sup>Of course we consider only disks  $\tilde{D}$  with radius  $\tilde{r} > r$ , but  $\tilde{r}$  may be arbitrarily close to  $r$ .

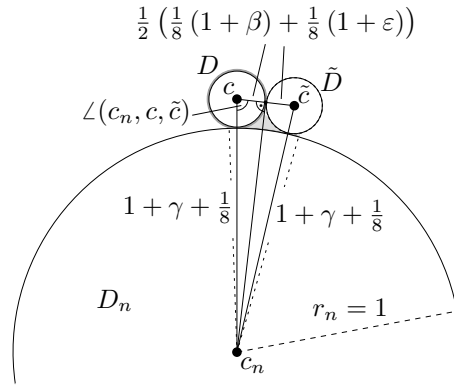


Figure B.10: The angle  $\angle(c_n, c, \tilde{c})$  is minimal if  $\tilde{r} = r = 1/8$ ,  $\tilde{D}$  hardly bites into  $D^{1+\beta}$  and both touch  $I$ .

intersects  $I$ . As shown in Figure B.10, basic trigonometry yields

$$\angle(c_n, c, \tilde{c}) \geq \arccos\left(\frac{\frac{1}{2}\left(\frac{1}{8}(1+\beta) + \frac{1}{8}(1+\epsilon)\right)}{1 + \gamma + \frac{1}{8}}\right) = 1.4563593\dots$$

Because of (B.2), this shows that the angle  $\alpha_D(p)$  of any  $p \in D^{1+\beta}$  bitten by such a  $\tilde{D}$  satisfies

$$\alpha_D(p) \geq 1.4563593\dots - 0.3785916\dots = 1.0777676\dots > 0.7853981\dots = \frac{5}{20}\pi.$$

The disk  $\tilde{D}$  cannot bite into  $R_{n+1}$ .

Finally, we have to consider a disk  $\tilde{D} \in \mathcal{D} \setminus \{D_n\}$  with radius  $\tilde{r} > r$  which lies to the right of  $c$  and  $c_n$  but not in the wedge of  $R_n$ . Can it bite into  $R_{n+1}$ ? In order to answer this question,

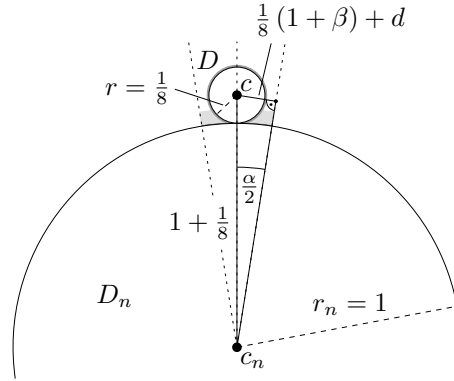


Figure B.11: The minimum distance  $d$  between the disk  $D^{1+\beta}$  and the right border of  $R_n$ .

we first prove a lower bound to the distance between  $D^{1+\beta}$  and the right border line of  $R_n$ 's wedge. Consider Figure B.11. This distance is minimal if  $D$  touches  $D_n$ , if its center  $c$  lies on the axis of  $R_n$ , and if its radius  $r$  is maximal, i.e.  $r = 1/8$ . Then, the distance equals

$$d = \left(1 + \frac{1}{8}\right) \sin \frac{\alpha}{2} - \frac{1}{8}(1 + \beta) = 0.0431762\dots$$

Therefore, the disk  $\tilde{D}$  can only bite into  $D^{1+\beta}$  if its radius  $\tilde{r}$  satisfies

$$(1 + \varepsilon)\tilde{r} \geq d$$

$$\Leftrightarrow \tilde{r} \geq \frac{d}{1 + \varepsilon} = 0.0431758\dots =: \tilde{r}_{\min}$$

The current sub-case is more difficult than the one before, because, if  $\tilde{c}$  lies outside the wedge of  $R_n$ , the disk  $\tilde{D}$  may touch  $D_n$ , whereas the disks centered inside the wedge are not allowed to intersect with  $D_n^{1+\gamma}$ , as this would make them intersect with  $I$ . Hence, the lower bound to  $\angle(c_n, c, \tilde{c})$  is not as good in the current case.

For given values of  $r$  and  $\tilde{r}$  the angle is minimal, if  $D$  hardly intersects  $I$ , and if  $\tilde{D}$  touches  $D_n$ . We can always reach this situation by first turning  $\tilde{D}$  around  $c$  clockwise until it touches  $D_n$ . This reduces  $\angle(c_n, c, \tilde{c})$ . Then, we move  $D$  away from  $c_n$  until it only touches  $I$ . If  $|cc_n| \geq |\tilde{c}c_n|$  this can be done without any problems, the disk  $\tilde{D}$  cannot block such a movement of  $D$ . If  $|cc_n| < |\tilde{c}c_n|$ , we might have to rotate  $\tilde{D}$  slightly around  $c_n$ , but in this case such a movement only reduces  $\angle(c_n, c, \tilde{c})$  some more, as we will discuss next. After these movements we have reached a situation where  $D$  hardly intersects  $I$ ,  $\tilde{D}$  touches  $D_n$  and still  $\tilde{D}$  bites into  $D^{1+\beta}$  but does not intersect  $D$ .

This determines two side lengths of the triangle  $\triangle(c_n, c, \tilde{c})$ , namely  $|cc_n| = (1 + \gamma) + r$  and  $|\tilde{c}c_n| = 1 + \tilde{r}$ . The third side length is bounded by  $r + \tilde{r} \leq |c\tilde{c}| \leq r(1 + \beta) + \tilde{r}(1 + \varepsilon)$ , as  $D$  and  $\tilde{D}$  may not overlap and  $\tilde{D}$  has to bite into  $D^{1+\beta}$ .

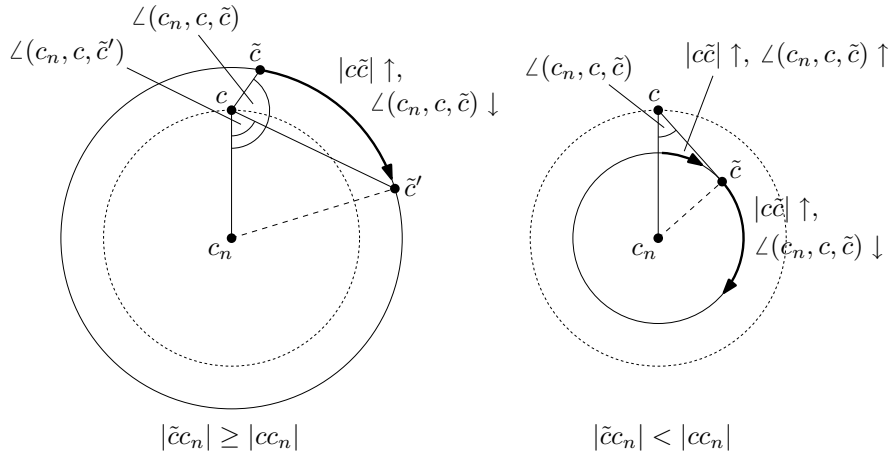


Figure B.12: Let  $|\tilde{c}c_n|$  and  $|cc_n|$  be fixed. If  $|\tilde{c}c_n| \geq |cc_n|$ , the angle  $\angle(c_n, c, \tilde{c})$  is monotonously decreasing in  $|c\tilde{c}|$ . If  $|\tilde{c}c_n| < |cc_n|$ ,  $\angle(c_n, c, \tilde{c})$  is increasing until  $c\tilde{c}$  is tangential to the circle with radius  $|\tilde{c}c_n|$  centered at  $c_n$ . From then on it is decreasing in  $|c\tilde{c}|$ .

Consider Figure B.12. If  $|c_n c| \leq |c_n \tilde{c}|$  holds, the angle  $\angle(c_n, c, \tilde{c})$  becomes minimal if  $|c\tilde{c}|$  is maximal. If  $|c_n c| > |c_n \tilde{c}|$ , the angle  $\angle(c_n, c, \tilde{c})$  is first monotonously increasing with increasing  $|c\tilde{c}|$ . Then, when  $c\tilde{c}$  is tangential to the circle with radius  $|c_n \tilde{c}|$  centered at  $c_n$ , it attains a maximum. And afterwards it is decreasing in  $|c\tilde{c}|$ . Hence, in both cases the minimum of  $\angle(c_n, c, \tilde{c})$  is attained for minimal or for maximal  $|c\tilde{c}|$ , i.e. for  $|c\tilde{c}| = r + \tilde{r}$  or for  $|c\tilde{c}| = r(1 + \beta) + \tilde{r}(1 + \varepsilon)$ .

The law of cosines yields

$$\angle(c_n, c, \tilde{c}) \geq \min \left( \arccos \left( \frac{(r + \tilde{r})^2 + (1 + \gamma + r)^2 - (1 + \tilde{r})^2}{2(r + \tilde{r})(1 + \gamma + r)} \right), \arccos \left( \frac{(r(1 + \beta) + \tilde{r}(1 + \varepsilon))^2 + (1 + \gamma + r)^2 - (1 + \tilde{r})^2}{2(r(1 + \beta) + \tilde{r}(1 + \varepsilon))(1 + \gamma + r)} \right) \right).$$

We want to find the minimum of the function on the right-hand side where  $r \in [\frac{1}{1280}, \frac{1}{8}]$  and  $\tilde{r} \in [\max(r, \tilde{r}_{\min}), 1]$ . Further analysis shows that the minimum is attained for  $\tilde{r} = r = 1/8$ , see the plots in Figure B.13. This yields

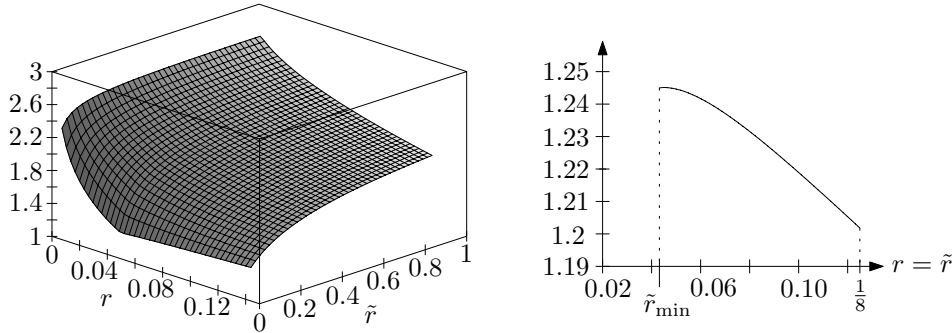


Figure B.13: Plots of the lower bounds to  $\angle(c_n, c, \tilde{c})$ . On the left border of the first plot the function is decreasing in  $r$ . It looks as if it was increasing because the border line is not parallel to the  $r$ -axis, it lies in the plane  $r = \tilde{r}$ .

$$\angle(c_n, c, \tilde{c}) \geq 1.201814\dots$$

Analogously to the previous case where  $\tilde{c}$  was inside the wedge of  $R_n$ , we can conclude due to (B.2) that the angle  $\alpha_D(p)$  of any  $p \in D^{1+\beta}$  bitten by a disk  $\tilde{D} \in \mathcal{D} \setminus \{D_n\}$  with radius  $\tilde{r} > r$  centered outside  $R_n$ 's wedge satisfies

$$\alpha_D(p) \geq 1.201814\dots - 0.3785916\dots = 0.823222\dots > 0.7853981\dots = \frac{5}{20}\pi.$$

The disk  $\tilde{D}$  cannot bite into  $R_{n+1}$ .

Overall, we have proved that  $R_{n+1}$  is not bitten by any disk  $\tilde{D} \in \mathcal{D}$  with radius  $\tilde{r} > r$ . The proof of this sub-case is completed.

### B.2.2.2 No medium size disk intersecting $I$

In the remaining sub-case there does not exist any disk  $D \in \mathcal{D}$  intersecting  $I$  whose radius  $r$  is bounded by  $1/1280 \leq r \leq 1/8$  and whose center lies in the wedge of  $R_n$ . We will show that in this case one can find a valid circular region  $R_{n+1}$  inside  $R_n$ .

<sup>4</sup>This sketch uses bigger values for the constants  $\gamma$ ,  $\alpha'$  and  $\varepsilon$  in order to clarify the idea.

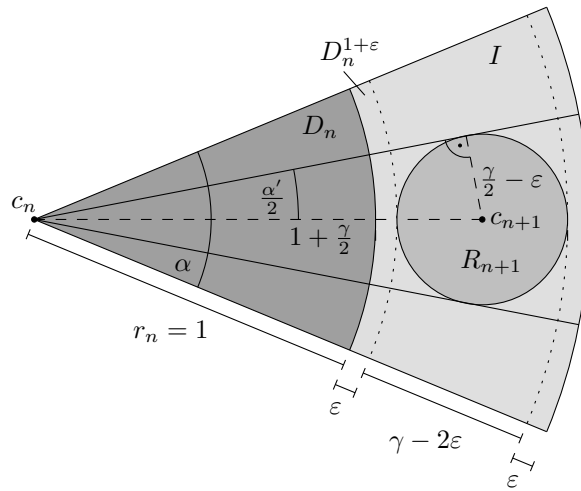


Figure B.14: Choosing a valid circular region  $R_{n+1}$  inside a wedge of interior angle  $\alpha'$ , if no big disk from  $\mathcal{D}$  bites into the wedge and  $I$ .<sup>4</sup>

A first step is to prove that it suffices to find a certain wedge of  $I$  which is not intersected by any disk  $D \in \mathcal{D}$  with radius  $r > 1/8$ . Consider Figure B.14. If we can place a disk  $R_{n+1}$  with radius  $r_{n+1} := \gamma/2 - \varepsilon$  like shown there inside  $I$ , it is not bitten by  $D_n$  nor by any disk  $D \in \mathcal{D}$  of radius  $r > 1/8$ . Furthermore, we consider the wedge built by the tangents of  $R_{n+1}$  through  $c_n$ . The interior angle of this wedge in  $c_n$  equals

$$\alpha' = 2 \arcsin \left( \frac{\frac{\gamma}{2} - \varepsilon}{1 + \frac{\gamma}{2}} \right) = 0.0038786\dots$$

If no big disk  $D \in \mathcal{D} \setminus \{D_n\}$  with radius  $r > 1/8$  intersects this wedge and  $I$ , then, there are only disks  $\tilde{D} \in \mathcal{D}$  with radius  $\tilde{r} < 1/1280$  biting into  $R_{n+1}$ . This means that

$$\tilde{r} < \frac{1}{1280} = 0.0007812\dots < 0.0009715\dots = \frac{\frac{\gamma}{2} - \varepsilon}{2} = \frac{r_n}{2}.$$

Hence,  $R_{n+1}$  is a valid circular region.

Therefore, in the current sub-case we only have to find a wedge of interior angle  $\alpha'$  in  $c_n$  such that its intersection with  $D_n^{1+\gamma}$  lies fully inside  $I$ , and such that no disk  $D \in \mathcal{D} \setminus \{D_n\}$  with radius  $r > 1/8$  intersects with this wedge and  $I$ .

There are two types of disks which can prevent us from finding such a wedge because they intersect with  $I$ . First, there can be a disk with radius  $r \leq 1$  whose center is outside of  $R_n$ 's wedge but which cuts into  $I$ . Such a disk  $D \in \mathcal{D}$  intersects with a maximal piece of  $I$ , if it is centered on the border line of  $R_n$ 's wedge, if  $r = 1$ , and if it touches  $D_n$ . Consider Figure B.15. The maximal angle  $\angle(c, c_n, p)$  of a point  $p \in I \cap D$  for such a disk  $D$  equals

$$\alpha_{\text{inters.}}^{\max} := \arccos \left( \frac{1^2 + 2^2 - (1 + \gamma)^2}{2 \cdot 1 \cdot 2} \right) = 0.0625712\dots$$

<sup>4</sup>This sketch uses bigger values for the constants  $\gamma, \beta$  and  $\alpha$  in order to clarify the idea.

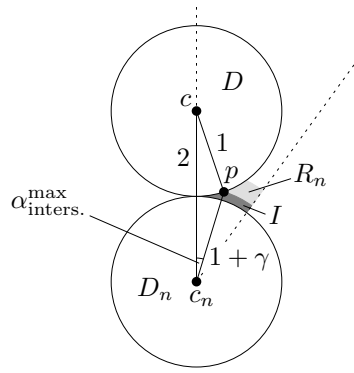


Figure B.15: The maximal angle  $\angle(c, c_n, p)$  of a point  $p \in I$  intersected by a disk  $D \in \mathcal{D}$  with radius  $r = r_n = 1$  and center  $c$  outside  $R_n$ 's wedge.<sup>6</sup>

This angle can be intersected by disks from both sides of  $R_n$ 's wedge. This is not too much, as  $I$  spans an angle of  $\alpha = 0.3141592\dots$ ; hence, there remains a part of angle  $\alpha - 2\alpha_{\text{inters.}}^{\text{max}} = 0.1890168\dots > 0.0038786\dots = \alpha'$  in the middle.

The other kind of disk  $D \in \mathcal{D} \setminus \{D_n\}$  intersecting with  $I$  is centered inside the wedge of  $R_n$  and its radius  $r$  is bounded by  $1/8 < r \leq 1$ . If there exists only one such disk, due to the same calculation as above it can only intersect with a part of  $I$  of angle  $2\alpha_{\text{inters.}}^{\text{max}}$ . Hence, either to the left or to the right there remains a part of  $I$  of angle  $\alpha/2 - 2\alpha_{\text{inters.}}^{\text{max}} = 0.0319372\dots$  not intersected by any disk  $\tilde{D} \in \mathcal{D} \setminus \{D_n\}$  with radius  $\tilde{r} > 1/1280$ . This is much more than the necessary angle  $\alpha' = 0.0038786\dots$ ; hence, we can find a valid circular region  $R_{n+1}$ .

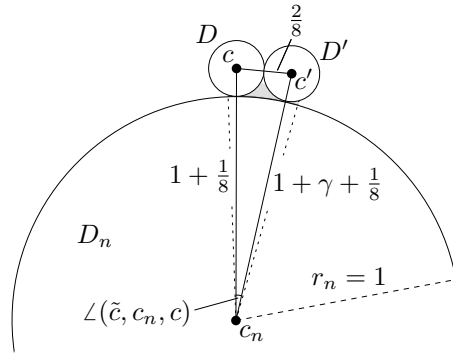


Figure B.16: The minimum angle  $\angle(c', c_n, c)$  between two big disks,  $D$  and  $D'$ , from  $\mathcal{D}$  centered inside  $R_n$ 's wedge is attained in this situation.

Consider Figure B.16. If there are at least two such disks,  $D$  and  $D'$ , the angle  $\angle(c', c_n, c)$  between the rays connecting  $c_n$  to their centers is minimal, if  $r = r' = 1/8$ , if  $D$  and  $D'$  touch each other, and if one of them only touches  $I$  and the other one touches  $D_n$ . We get

$$\angle(c', c_n, c) \geq \arccos \left( \frac{\left(1 + \frac{1}{8}\right)^2 + \left(1 + \gamma + \frac{1}{8}\right)^2 - \left(\frac{2}{8}\right)^2}{2 \left(1 + \frac{1}{8}\right) \left(1 + \gamma + \frac{1}{8}\right)} \right) = 0.2222675\dots$$



Hence, in between two such disks, there remains a part of  $I$  of angle at least

$$0.2222675\dots - 2\alpha_{\text{inters.}}^{\max} = 0.0971251\dots,$$

more than enough space for a valid circular region  $R_{n+1}$ , because an angle of  $\alpha' = 0.0038786\dots$  would suffice.

This completes the induction step if  $R_n$  is a crescent. If there exists a medium size disk  $D$  centered inside  $R_n$ 's wedge and intersecting  $I$ , then we can find a valid crescent region  $R_{n+1} \subset R_n$ . If no such disk exists, we can find a valid circular region  $R_{n+1} \subset R_n$ . Furthermore, in both cases, we have  $r_{n+1} \leq (1/8)r_n$ .

### B.2.3 Induction Step: $R_n$ circular

If  $R_n$  is a circular region, the induction step is easier. To facilitate notation, we assume  $r(R_n) = 1$ , which can be reached by scaling. This implies  $r_n = 1/2$ . In this case, we define  $I$  to be the disk with radius  $3/4$  which is concentric with  $R_n$ , i.e.  $I := R_n^{\frac{3}{4}}$ , as shown in Figure B.17. Let  $D$  be the largest disk (or one of the largest disks) from  $\mathcal{D}$  biting into  $I$ . And let  $r$  denote its radius.

If  $r < 3/8$ , we define  $R_{n+1} := I$  and  $r_{n+1} := 3/8$ . Clearly this is a valid circular region of radius  $3/4$  because no disk  $D \in \mathcal{D}$  with radius  $r > 3/8$  bites into it. Otherwise, we have  $3/8 \leq r \leq 1$ .

If  $D$  has a crescent which is fully contained in  $I$ , this crescent is a valid region  $R_{n+1}$  with  $r_{n+1} := r \leq r_n$ , as no disk  $\tilde{D} \in \mathcal{D}$  with radius  $\tilde{r} > r$  bites into  $I$  by definition of  $D$ , hence no such disk bites into the crescent contained in  $I$ .

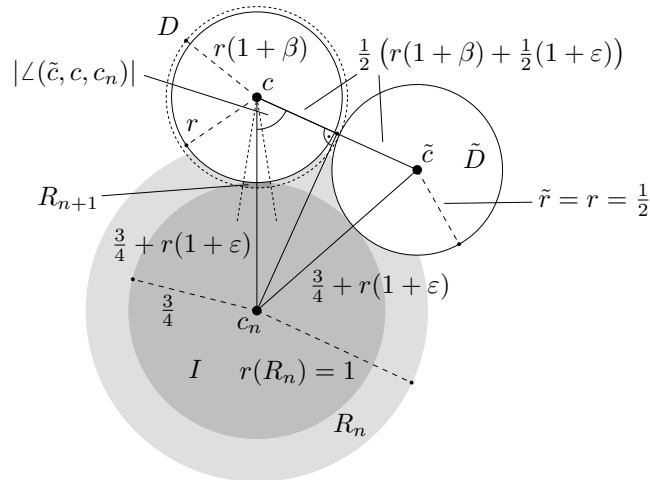


Figure B.17: If  $R_n$  is circular, we consider the largest disk  $D \in \mathcal{D}$  biting into  $I := R_n^{\frac{3}{4}}$ . It has a crescent  $R_{n+1}$  which is not bitten by any disk  $\tilde{D} \in \mathcal{D}$  with radius  $\tilde{r} > r = r(D)$ . The situation shown here minimizes  $\angle(\tilde{c}, c, c_n)$ .

In the remaining case, the disk  $D \in \mathcal{D}$  with radius  $r \leq r_n = r(R_n)/2$  bites into  $I$ , but there is no full crescent of  $D$  in  $I$ . We want to state the arguments for this case explicitly, although

they might seem trivial, and they are left to the reader in the original article.

We can find a crescent  $R_{n+1}$  of  $D$  such that no disk  $\tilde{D} \in \mathcal{D}$  with radius  $\tilde{r} > r$  bites into  $R_{n+1}$ . We choose the crescent for  $R_{n+1}$  whose axis hits  $c_n$ , the center of  $R_n$ . The disk  $D$  cannot contain  $c_n$ , because then, due to  $r < r_n = 1/2$ , there would be a crescent of  $D_n$  fully inside of  $I$ .

If there was a disk  $\tilde{D} \in \mathcal{D}$  with radius  $\tilde{r} > r$  biting into the crescent  $R_{n+1}$ , it could not bite into  $I$ , because that would contradict the definition of  $D$ . We show that there cannot exist such a disk  $\tilde{D}$  biting into  $R_{n+1}$  but not into  $I$ .

First, we want to prove a lower bound to the angle  $\angle(\tilde{c}, c, c_n)$  between the centers  $c$  of  $D$ ,  $c_n$  of  $R_n$ , and  $\tilde{c}$  of such a disk  $\tilde{D}$  biting into  $D^{1+\beta}$ .

We consider the triangle  $\triangle(\tilde{c}, c, c_n)$ . The side length  $|\tilde{c}c_n|$  is bounded by

$$|\tilde{c}c_n| > \frac{3}{4} + (1 + \varepsilon)\tilde{r} > \frac{3}{4} + (1 + \varepsilon)r$$

because  $\tilde{D}$  does not bite into  $I$  and  $\tilde{r} > r$ . If the other side lengths of the triangle remain constant, the angle  $\angle(\tilde{c}, c, c_n)$  is minimal if  $|\tilde{c}c_n|$  is minimal, i.e.  $|\tilde{c}c_n| = \frac{3}{4} + r(1 + \varepsilon)$  because  $\tilde{D}$  does not bite into  $I$ .

In the considered situation, it is easy to see that  $\angle(\tilde{c}, c_n, c) < 90^\circ$ . Hence, by arguments analogous to the ones from Figure B.12 on page 181, the angle  $\angle(\tilde{c}, c, c_n)$  is minimal if  $|cc_n|$  is maximal. This means  $|cc_n| = \frac{3}{4} + r(1 + \varepsilon)$ , as  $D$  has to bite into  $I$ .

Therefore, in order to find a lower bound to  $\angle(\tilde{c}, c, c_n)$  it suffices to consider an isosceles triangle  $\triangle(\tilde{c}, c_n, c)$  where  $|cc_n| = |\tilde{c}c_n| = \frac{3}{4} + r(1 + \varepsilon)$ . Then, the angle  $\angle(\tilde{c}, c, c_n) = \angle(c, \tilde{c}, c_n)$  is minimized if the angle  $\angle(\tilde{c}, c_n, c)$  is maximized, which is the case if  $|\tilde{c}c|$  is maximal. We can use the upper bound

$$|\tilde{c}c| \leq \tilde{r}(1 + \varepsilon) + r(1 + \beta) \leq \frac{1}{2}(1 + \varepsilon) + r(1 + \beta),$$

because  $\tilde{D}$  has to bite into  $D^{1+\beta}$ , and because  $\tilde{r} \leq r_n = 1/2$ . Plugging everything together yields

$$\angle(\tilde{c}, c, c_n) \geq \arccos\left(\frac{\frac{1}{2}(\frac{1}{2}(1 + \varepsilon) + r(1 + \beta))}{\frac{3}{4} + (1 + \varepsilon)r}\right). \quad (\text{B.3})$$

The function on the right-hand side is plotted in Figure B.18. We get

$$\angle(\tilde{c}, c, c_n) > 1.1.$$

As the angle  $\angle(\tilde{c}, c, p)$  for any  $p \in D^{1+\beta}$  bitten by  $\tilde{D}$  is less or equal  $\alpha_{\text{bitten}}\left(\frac{3}{8}, \frac{1}{2}\right)$ , cf. (B.1), we get

$$\begin{aligned} \angle(c_n, c, p) &\geq \angle(\tilde{c}, c, c_n) - \angle(\tilde{c}, c, p) \geq 1.1 - \alpha_{\text{bitten}}\left(\frac{3}{8}, \frac{1}{2}\right) \\ &= 0.8430463\dots > 0.1570796\dots = \frac{\alpha}{2}. \end{aligned}$$

Hence, no such disk  $\tilde{D}$  bites into the crescent  $R_{n+1}$ .

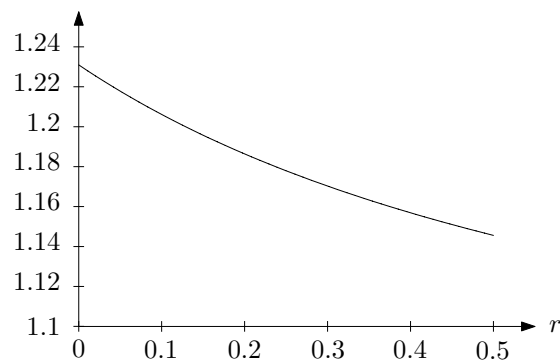


Figure B.18: If  $D \in \mathcal{D}$  is the largest disk with radius  $r \leq 1/2$  biting into  $I$ , and  $\tilde{D} \in \mathcal{D}$  is another disk with radius  $\tilde{r} > r$  biting into  $D^{1+\beta}$  but not into  $I$ , the angle  $\angle(\tilde{c}, c, c_n)$  is bounded from below by the function from (B.3), which is plotted here.

This concludes the induction step if  $R_n$  is a circular region. Note that in this case we might have  $r_{n+1} = r_n$ . However, in the next step, the current region will be a crescent. And by what we have seen before, this implies  $r_{n+2} \leq (1/8)r_{n+1}$ . This shows that for every  $n$ , we have  $r_{n+2} \leq (1/8)r_n$ , which guarantees  $r_n \rightarrow 0$ .

Hence, the arguments from Section B.1 prove Theorem 5.5.

### B.3 Final Remark

Like the authors of the original article, here, we did not try to optimize the constants to achieve an optimal value for  $\tilde{\Lambda}$ . This would be some further tedious work.

However, it seems one can significantly reduce the value of  $\alpha$ , i.e., one can make the crescent regions shorter, because the inequalities from Section B.2.2.2 are not tight. The reduction of  $\alpha$  could then be used to reduce  $\varepsilon$  without harming the inequalities from Section B.2.2.1.

The induction step for circular  $R_n$  from Section B.2.3 seems not to be a real problem at all. There is so much space in the inequalities that one should be able to change the constants significantly without doing harm to these arguments.

# List of Symbols

Symbol	Explanation	First Used
$\angle(v_1, v_2)$	the smaller angle between $v_1$ and $v_2$	(2.3), p. 40
$\angle ABC$	the smaller angle between $BA$ and $CA$	Sect. 4.3, p. 121
$\angle(A, B, C)$	ditto	Sect. 4.3, p. 121
$X + Y$	Minkowski sum of $X, Y \subset \mathbb{R}^2$	(2.7), p. 47
$ pq $	Euclidean distance between $p$ and $q$	Sect. 1.1, p. 1.1
$[a, b]$	closed interval	Sect. 2.1, p. 28
$[u, v]$	determinant of $2 \times 2$ -matrix	(2.17), p. 58
$\langle u, v \rangle$	scalar product of vectors $u$ and $v$	Def. 2.4.2, p. 33
ALG	(costs of) online algorithm	Sect. 1.3.2, p. 11
$b_C(v)$	$v$ -breadth	Def. 2.4.2., p. 33
$B_\varepsilon(p)$	$\varepsilon$ -ball/disk centered at $p$	pp. 17, 40
$\text{Bis}(p, q)$	bisector of $p$ and $q$	Sect. 2.4, p. 39
$\bar{c}$	arc-length parameterization of $C$	Sect. 2.1, p. 30
$\dot{c}_{\parallel}^*(t)$	component of $\dot{c}^*(t)$ parallel to $c^*(t)$	(3.2), p. 84
$\dot{c}_{\perp}^*(t)$	component of $\dot{c}^*(t)$ orthogonal to $c^*(t)$	(3.2), p. 84
$c_{\text{ALG}}$	competitive ratio of ALG	Sect. 1.3.2, p. 11
$C$	considered class of curves	Sect. 2.1, p. 28
$C_F$	the flower (a particular curve)	Sect. 3.2.2, p. 107
$C_H$	(boundary cycle of a) hexagon	Fig. 5.6, p. 144
$C_p^q$	counter-clockwise path on $C$ from $p$ to $q$	Sect. 2.1, p. 30
$C_Z$	Zindler's example (a curve)	Sect. 3.2.3, p. 109
$C'$	central symmetrization of $C$	Def. 2.15, p. 47
$C^*$	halving pair transformation of $C$	Def. 2.20, p. 50
$C^\circ$	interior domain of curve $C$	Sect. 2.1, p. 29
$\hat{C}$	cap-curve	Thm. 2.33, p. 64
$C_\Delta$	rounded triangle	Sect. 3.2.1, p. 100
$C_\square$	(boundary cycle of a) square	Fig. 1.16.a, p. 18
$C_\circ$	a circle	Sect. 2.11, p. 67
$C(x)$	shortest cycle encircling $x$	Sect. 5.3.4, p. 158
$C_1 \oplus C_2$	concatenation of two curves	Sect. 2.4, p. 38
$\mathbb{C}$	the set of complex numbers	Sect. 2.10, p. 59
CAB	Continuous Angular Bisector strategy	Sect. 1.3.2, p. 12
$\text{ch}(S)$	convex hull of set $S$	Sect. 2.3, p. 37

Symbol	Explanation	First Used
$D, D(C)$	diameter	Def. 2.4.4., p. 34
$\mathcal{D}$	disk packing	Thm. 5.5, p. 154
$\mathcal{D}_A$	Apollonian packing	Sect. 5.3.6, p. 161
$\mathcal{D}_H$	hexagonal disk packing	Fig. 5.15, p. 155
$D^\lambda$	$\lambda$ -enlargement of disk packing $\mathcal{D}$	(5.8), p. 154
$d_G(p, q)$	shortest-path distance of $p$ and $q$ in $G$	Sect. 1.1, p. 1
$d_H(X, Y)$	Hausdorff distance of $X, Y \subset \mathbb{R}^2$	Sect. 4.11, p. 133
$d_E(X, Y)$	Eggleston dsitance of $X, Y \subset \mathbb{R}^2$	Sect. 4.11, p. 133
$DT(S)$	Delaunay triangulation of $S$	Sect. 1.3.5, p. 18
$\delta_{\text{graph}}(G)$	graph dilation of geometric graph $G$	(1.5), p. 17
$\delta_G(p, q)$	detour between $p$ and $q$ in $G$	(1.1), p. 2
$\delta(G)$	dilation of geometric graph $G$	(1.2), p. 2
$\delta(S)$	dilation of point set $S$	(1.3), p. 3
$\Delta$	supremum of dilation of point sets	(1.4), p. 5
$\Delta_{\text{graph}}$	supr. of graph dilation of point sets	(1.8), p. 22
$\Delta_{\text{graph}}^{\text{no Steiner}}$	dito without Steiner-points	(1.6), p. 19
$\partial R$	boundary of region $R$	Sect. 2.3, p. 37
$G_F$	hexagonal grid with flower curves	Fig. 1.5, p. 5
$G_H$	hexagonal grid	Fig. 5.6, p. 144
$G_I$	particular grid with small graph dilation	Fig. 1.20.b, p. 22
$G_\Delta$	hexagonal grid with rounded triangle	Fig. 5.8.a, p. 146
$G_\square$	square grid	Fig. 5.10, p. 149
$\eta(C)$	annulus constant of cycle $C$	(2.36), p. 72
$h, h(C)$	minimum halving distance	Def. 2.4.5., p. 34
$H, H(C)$	maximum halving distance	Def. 2.4.5., p. 34
$h_C(v)$	$v$ -halving distance	Def. 2.4.3., p. 34
$H_F$	hexagonal cycle in $G_F$	Fig. 5.9, p. 147
$H_\Delta$	hexagonal cycle in $G_\Delta$	Fig. 5.8.a, p. 146
iff	if and only if	Lem. 2.6.1., p. 35
$K_5$	complete graph of 5 vertices	Sect. 3.1.1, p. 88
$\kappa(C, p)$	curvature of curve $C$ in $p \in C$	(3.6), p. 94
LAD	Local Absolute Detour strategy	Sect. 1.3.2, p. 12
$l_C(v)$	$v$ -length	Def. 2.4.1., p. 33
$\text{lcd}(\dots)$	least common denominator	Sect. 5.2.2, p. 143
$\lambda_R(\mathcal{D})$	cover factor of $\mathcal{D}$ and $R$	(5.9), p. 155
$\lambda(R)$	cover factor of $R$	(5.10), p. 155
$\lambda_{\text{fin}}(R)$	cover factor with finite packings	Sect. 5.3.3, p. 155
$\tilde{\Lambda}$	a cover factor for $R_\square$	Thm. 5.5, p. 154
$\Lambda$	cover factor constant	(5.11), p. 155
$\Lambda_{\text{fin}}$	finite cover factor constant	(5.11), p. 155

Symbol	Explanation	First Used
$M$	midpoint curve	Def. 2.24, p. 56
$\mathcal{M}$	maximal shortest cycles in graph $G$	Sect. 5.3.4, p. 157
$M_Z$	the deltoid (midpoint curve of $C_Z$ )	Sect. 3.2.3, p. 109
$M_\Delta$	midpoint curve of $C_\Delta$	Sect. 3.2.1, p. 102
$\dot{m}_\parallel(t)$	component of $\dot{m}(t)$ parallel to $c^*(t)$	(3.2), p. 84
$\dot{m}_\perp(t)$	component of $\dot{m}(t)$ orthogonal to $c^*(t)$	(3.2), p. 84
$\text{MDT}(S)$	minimum dilation triangulation of $S$	Sect. 1.3.5, p. 18
$\mathbb{N}$	the set of natural numbers	Sect. 2, p. 30
OPT	(costs of) optimal offline algorithm	Sect. 1.3.2, p. 11
$\xi_G(p, q)$	shortest path between $p$ and $q$ in $G$	Sect. 5.3.1, p. 152
$P$	$\{-9, -8, \dots, 9\} \times \{-9, -8, \dots, 9\}$	Fig. 5.16.a, p. 157
$\hat{p}$	halving partner of $p$	Sect. 2.2, p. 32
$Q_1$	square $[-9, 9] \times [-9, 9] \subset \mathbb{R}^2$	Fig. 5.16.a, p. 157
$Q_2$	square $[-8, 8] \times [-8, 8] \subset \mathbb{R}^2$	Fig. 5.16.a, p. 157
$Q_F$	point set on edges of $G_F$	Fig. 5.11, p. 151
$Q_\square$	point set on edges of $G_\square$	Fig. 5.10, p. 149
$\mathbb{R}$	the set of real numbers	Sect. 1.1, p. 1
$r, r(C)$	inradius	Def. 2.4.6., p. 34
$R, R(C)$	circumradius	Def. 2.4.6., p. 34
$r(\mathcal{D})$	maximum radius of packing $\mathcal{D}$	Sect. 5.3.3, p. 155
$r_\kappa(C, p)$	radius of curvature of $C$ in $p \in C$	Sect. 3.1.3, p. 94
$R(S)$	bounding box of set $S \subset \mathbb{R}^2$	(1.9), p. 23
$R(x)$	interior of shortest cycle encircling $x$	Sect. 5.3.4, p. 158
$\overline{R}$	closure of the region $R$	Sect. 2.6, p. 44
$R^{90^\circ}$	matrix of rotation $90^\circ$ ccw.	Sect. 2.2, p. 31
$R_\square$	a square of side length 4	Sect. 5.3.3, p. 155
$s_C(v)$	support function of cycle $C$	(4.13), p. 134
$\mathcal{S}$	shortest cycles in graph $G$	Sect. 5.3.4, p. 157
$\mathbb{S}^1$	unit circle	Sect.2.2, p. 31
$S_n$	vertex set of regular $n$ -gon	pp. 4, 19, 139
$v \perp w$	vectors $v$ and $w$ are orthogonal	Sect. 2.9, p. 57
$v \parallel w$	vectors $v$ and $w$ are parallel	Sect. 2.9, p. 57
$w, w(C)$	width	Def. 2.4.4., p. 34
$\omega(p, C)$	winding number	Sect. 2.10, p. 59

# List of Open Problems

## Chapter 1: Introduction

**Open Problem 1.** (p. 19) *What is the worst-case dilation of any Euclidean Delaunay triangulation? Is it smaller than 2, thereby leading to a better upper bound to  $\Delta_{\text{graph}}^{\text{no Steiner}}$ ? Can one prove better lower and upper bounds than*

$$1.5708 \approx \frac{\pi}{2} \leq \sup_{S \subset \mathbb{R}^2, |S| < \infty} \delta_{\text{graph}}(\text{DT}(S)) \leq \frac{8}{3\sqrt{3}} \frac{\pi}{2} \approx 2.4184 ?$$

**Open Problem 2.** (p. 22) *Find better upper and lower bounds to  $\Delta_{\text{graph}}$  than*

$$1.0000047 < \Delta_{\text{graph}} < 1.1247.$$

## Chapter 2: Closed Curves

**Open Problem 3.** (p. 55) *What is the infimum of  $|C^*|/|C|$ ?*

## Chapter 3: Zindler Curves

**Open Problem 4.** (p. 105) *Does the rounded triangle  $C_{\Delta}$  minimize  $A/h^2$  amongst convex Zindler curves? Does it maximize  $|C|/h$ ?*

## Chapter 4: Halving Distance

**Open Problem 5.** (p. 117) *What is the supremum of  $h/r$ ?*

**Open Problem 6.** (p. 126) *What is the infimum of  $H/|C|$ ?*

**Open Problem 7.** (p. 127) *Are there convex cycles besides Zindler curves, curves of constant breadth and equilateral triangles attaining  $H = w$ ?*

**Open Problem 8.** (p. 128) *Are there other convex cycles besides circles attaining  $H = 2r$ ?*

**Open Problem 9.** (p. 132) *What is the supremum of  $h^2/A$ ?*

## Chapter 5: Point Sets

**Open Problem 10.** (p. 140) *Given an arbitrary finite point set  $S \subset \mathbb{R}^2$ , is there always a geometric graph  $G_S$  of smallest dilation embedding  $S$ ? How can we construct  $G_S$ ? Or how can we compute  $\delta(S)$ ?*

**Open Problem 11.** (p. 155) Prove  $\Lambda \geq \underline{\Lambda}$  or  $\Lambda_{\text{fin}} \geq \underline{\Lambda}_{\text{fin}}$ , for better lower bounds  $\underline{\Lambda}$ ,  $\underline{\Lambda}_{\text{fin}} > 1.00001!$  Which better upper bounds can be proved?

**Open Problem 12.** (p. 160) How can one prove better upper and lower bounds to the dilation constant  $\Delta$ ? Can we even determine the correct value of  $\Delta$ ?

**Open Problem 13.** (p. 164) What is the cover factor  $\lambda_{\mathbb{R}^2}(\mathcal{D}_A)$  of the Apollonian packing  $\mathcal{D}_A$ ? Is the Apollonian packing the best option, i.e., do we have  $\Lambda = \lambda_{\mathbb{R}^2}(\mathcal{D}_A)$ ?



# List of Figures

1.1	Detour situation in Bonn. . . . .	1
1.2	Three given sites in a SimCity screenshot. . . . .	2
1.3	Network of streets in a SimCity screenshot. . . . .	3
1.4	Optimal embeddings of the point sets $S_n$ . . . . .	4
1.5	A grid of small dilation based on hexagons. . . . .	5
1.6	Attempts to embed $S_5$ with small dilation. . . . .	6
1.7	A halving pair and the halving pair transformation. . . . .	7
1.8	The midpoint curve of an U-shaped cycle. . . . .	7
1.9	Rounded triangle $C_\Delta$ and dual curve of constant breadth. . . . .	9
1.10	The history of dilation. . . . .	10
1.11	A robot searching for a destination $t$ in a street-polygon. . . . .	12
1.12	Search for the kernel of a polygon by strategy CAB. . . . .	12
1.13	Longest curve with increasing chords. . . . .	13
1.14	Non-contractible set $S \subset \mathbb{R}^3$ of dilation $< \frac{\pi}{2}$ . . . . .	15
1.15	Simple link of two ropes. . . . .	16
1.16	Differences between geometric and graph dilation. . . . .	18
1.17	Delaunay triangulations. . . . .	19
1.18	MDT of $S_{21}$ and Delaunay triangulation of $\tilde{S}_{4n}$ . . . . .	20
1.19	Dilation center of three points. . . . .	21
1.20	Grids of small graph dilation. . . . .	22
1.21	Iterated line segment intersections. . . . .	22
1.22	A minimum Manhattan network. . . . .	24
2.1	Breadth quantities of an isosceles, right-angled triangle. . . . .	27
2.2	Dilation of a cycle attained by a pair of points. . . . .	30
2.3	Dilation maximum sequence converging to a single point. . . . .	31
2.4	A halving pair for every direction. . . . .	33

2.5	Halving pair distance and non-unique halving pairs. . . . .	34
2.6	Proving that maximum breadth equals maximum length. . . . .	35
2.7	Proving that minimum breadth equals minimum length. . . . .	36
2.8	Cycles with arbitrarily big and infinite dilation. . . . .	38
2.9	Case 2 in the proof of Lemma 2.10. . . . .	38
2.10	Three regions in the proof of Lemma 2.10. . . . .	39
2.11	Bisector argument in the proof of Lemma 2.10. . . . .	39
2.12	The angles at a detour maximum. . . . .	41
2.13	Illustrating the proof of Theorem 2.12. . . . .	42
2.14	Angle analysis in the proof of Theorem 2.12. . . . .	43
2.15	The quantities $h$ and $H$ of a centrally symmetric cycle. . . . .	44
2.16	Proving $h_C(v) \geq l_C(v)$ for a convex, symmetric $C$ . . . . .	45
2.17	Symmetric $C$ with $b_C(\alpha) \neq \sqrt{h'^2(\alpha) + h^2(\alpha)}$ . . . . .	46
2.18	Example for central symmetrization. . . . .	46
2.19	Proof of $b_{C'}(v) \leq b_C(v)$ . . . . .	48
2.20	An unsymmetric example curve satisfying $h(C) = w(C)$ . . . . .	50
2.21	An example of halving pair transformation. . . . .	50
2.22	Halving pair transformation may increase $v$ -length. . . . .	51
2.23	Halving pair transformation may increase dilation. . . . .	52
2.24	Proving the convexity of $C^*$ for convex $C$ . . . . .	52
2.25	Proving $b_{C^*}(v) \leq b_C(v)$ . . . . .	53
2.26	An example satisfying $r(C^*) < r(C)$ . . . . .	54
2.27	An example satisfying $r(C^*) > r(C)$ . . . . .	54
2.28	The derived curves $C^*$ and $M$ of an equilateral triangle. . . . .	56
2.29	Illustration of Holditch's theorem. . . . .	58
2.30	Winding numbers of an oriented closed curve. . . . .	59
2.31	Cap-curve and plot of new bound to dilation of cycles. . . . .	65
2.32	Dilation of a circle. . . . .	67
2.33	Upper bound to the dilation of cycles. . . . .	68
2.34	Dilation of a cycle contained in a thin annulus. . . . .	71
2.35	Upper bound to the dilation of a cycle in a thin annulus. . . . .	73
2.36	Distance arguments on two rays. . . . .	73
2.37	Minimum and maximum halving distance of a triangle. . . . .	74
2.38	Proving formulas for the dilation of triangles. . . . .	75
2.39	Dilation of a regular $2k$ -gon. . . . .	77

2.40	Dilation of a regular $(2k - 1)$ -gon. . . . .	78
2.41	Plot of the dilation of regular polygons. . . . .	79
3.1	Intuition: Convex Zindler curves have small dilation. . . . .	81
3.2	Rounded triangle $C_\Delta$ and Flower $C_F$ . . . . .	82
3.3	Basic movements for curves of constant halving distance. . . . .	84
3.4	Three possible parts of a Zindler curve. . . . .	86
3.5	No translation parts for convex Zindler curves. . . . .	87
3.6	Translation parts although halving chords in $\overline{C^\circ}$ . . . . .	88
3.7	Basic movements for curves of constant area halving distance. . . . .	89
3.8	Proving strict convexity of curves of constant breadth. . . . .	93
3.9	Curvature of a Parabola. . . . .	94
3.10	Curvature of convex curves of constant breadth. . . . .	95
3.11	Reuleaux-triangle. . . . .	97
3.12	Ellipsoid of density $1/3$ floating in water. . . . .	98
3.13	A log and a rounded triangle floating in water. . . . .	99
3.14	Construction of rounded triangle $C_\Delta$ . . . . .	100
3.15	Tractrix curve. . . . .	102
3.16	Midpoint curve $M_\Delta$ of rounded triangle. . . . .	103
3.17	Rounded pentagon. . . . .	107
3.18	Construction of the flower $C_F$ . . . . .	107
3.19	Deltoid. . . . .	109
3.20	Zindler's example curve. . . . .	110
4.1	Maximum halving distance $H$ of an isosceles triangle. . . . .	118
4.2	The construction in Lemma 4.4. . . . .	120
4.3	Proving Theorem 4.1. . . . .	121
4.4	First step in the proof of $H \leq \frac{3}{2}R$ . . . . .	123
4.5	The maximum height of a triangle in the unit circle is $\geq 3/2$ . . . . .	125
4.6	Constructing continuously moving extreme points. . . . .	128
4.7	Proving $h(v) \geq l(v)/2$ . . . . .	129
4.8	An example for $h/w \searrow 1/2$ . . . . .	129
4.9	An example attaining $h/r \searrow 1$ . . . . .	130
4.10	Comparing $h^2/A$ of a circle and an equilateral triangle. . . . .	132
4.11	Proving the continuity of $h_C(v)$ . . . . .	135
4.12	Proving the continuity of $h_C(v)$ for line segments. . . . .	136

5.1	Optimal embedding of three points. . . . .	140
5.2	Dilation of optimal embeddings of $S_n$ . . . . .	140
5.3	Proving that a detour maximum is mutually visible. . . . .	141
5.4	Bad embedding with the induced rectangular grid. . . . .	142
5.5	Embedding into a square grid. . . . .	143
5.6	Embedding into a hexagonal grid. . . . .	144
5.7	Failed improvement attempts of hexagonal grid. . . . .	145
5.8	Hexagonal grid with rounded triangle. . . . .	146
5.9	Hexagonal grid with flower. . . . .	147
5.10	Embedding any point set in a scaled, perturbed square grid. . . . .	149
5.11	Embedding any point set in a scaled, perturbed grid $\zeta G_F$ . . . . .	151
5.12	A shortest path of a graph embedding $S_n$ inside an ellipse. . . . .	153
5.13	A graph of small dilation embedding $S_n$ contains a cycle. . . . .	153
5.14	Graphs of small dilation cannot have only circular faces. . . . .	154
5.15	Cover factor of hexagonal disk packing. . . . .	155
5.16	Ideas behind the proof of the improved lower bound. . . . .	157
5.17	Every point $x \in Q_2$ is encircled by a cycle. . . . .	157
5.18	Properties of the shortest cycles. . . . .	158
5.19	Good disk packing, not inducing a graph of small dilation. . . . .	161
5.20	Apollonian packing. . . . .	162
5.21	Cover Factor of first iteration of Apollonian packing. . . . .	163
A.1	Proving the existence of an area-bisecting parameterization. . . . .	167
A.2	The angle-value $\alpha$ of the supporting line(s) through $c(\tau)$ . . . . .	171
B.1	A crescent-type region $R_n$ of the disk $D$ . . . . .	174
B.2	Definition of first region $R_1$ . . . . .	175
B.3	Constructing $R_{n+1}$ if medium size disk intersects $I$ . . . . .	175
B.4	Constructing $R_{n+1}$ if no medium size disk intersects $I$ . . . . .	176
B.5	The corner points $u, v$ and $w$ of the crescent $R_{n+1}$ . . . . .	176
B.6	Minimum angle $\alpha_D(\tilde{v})$ where $D$ leaves $R_n$ . . . . .	177
B.7	The maximal angle $\angle(c, c_n, w)$ . . . . .	178
B.8	The flaw in the original proof. . . . .	179
B.9	The definition of $\alpha_{\text{bitten}}(r, \tilde{r})$ . . . . .	179
B.10	The maximal angle $\angle(c_n, c, \tilde{c})$ . . . . .	180
B.11	The minimum distance between $D^{1+\beta}$ and right border of $R_n$ . . . . .	180

---

B.12 Monotonicity of $\angle(c_n, c, \tilde{c})$ with respect to $ c\tilde{c} $ . . . . .	181
B.13 A Plot of a lower bound to the angle $\angle(c_n, c, \tilde{c})$ . . . . .	182
B.14 Choosing a valid circular region $R_{n+1}$ inside $I$ . . . . .	183
B.15 A big disk intersecting $I$ from outside $R_n$ 's wedge. . . . .	184
B.16 The minimum angle between two big disks intersecting $I$ . . . . .	184
B.17 Induction step for circular $R_n$ . . . . .	185
B.18 Bounding the angle $\angle(\tilde{c}, c, c_n)$ if $R_n$ is circular. . . . .	187



# Bibliography

- [1] A. Abrams, J. Cantarella, J. H. Fu, M. Ghomi, and R. Howard. Circles minimize most knot energies. *Topology*, 42(2):381–394, 2003.
- [2] P. K. Agarwal, R. Klein, C. Knauer, S. Langerman, P. Morin, M. Sharir, and M. Soss. Computing the detour and spanning ratio of paths, trees and cycles in 2d and 3d. *Discrete & Computational Geometry*, 2007. To appear.
- [3] P. K. Agarwal, R. Klein, C. Knauer, and M. Sharir. Computing the detour of polygonal curves. Technical Report B 02-03, Freie Universität Berlin, Fachbereich Mathematik und Informatik, 2002.
- [4] D. Aharonov and K. Stephenson. Geometric sequences of discs in the Apollonian packing. *Algebra i Analiz, Russian Academy of Sciences, dedicated to Goluzin*, 9(3):104–140, 1997.
- [5] L. V. Ahlfors. *Complex Analysis*. McGraw-Hill, 2nd edition, 1966.
- [6] O. Aichholzer, F. Aurenhammer, C. Icking, R. Klein, E. Langetepe, and G. Rote. Generalized self-approaching curves. *Discrete Appl. Math.*, 109:3–24, 2001.
- [7] H. W. Alt. *Lineare Funktionalanalysis*. Springer, Berlin, Heidelberg, 3rd edition, 1999.
- [8] E. L. Annette Ebbers-Baumann, Rolf Klein and A. Lingas. A fast algorithm for approximating the detour of a polygonal chain. In F. M. auf der Heide, editor, *Proc. 9th Annu. European Sympos. Algorithms*, volume 2161 of *LNCS*, pages 321–332, Berlin, 2001. Springer.
- [9] B. Aronov, M. de Berg, O. Cheong, J. Gudmundsson, H. Haverkort, and A. Vigneron. Sparse geometric graphs with small dilation. In V. Diekert and B. Durand, editors, *Proc. 16th International Symposium on Algorithms and Computation*, volume 3827 of *LNCS*, pages 50–59. Springer, 2005.
- [10] H. Auerbach. Sur un problème de M. Ulam concernant l'équilibre des corps flottants. *Studia Math.*, 7:121–142, 1938.
- [11] R. Ault. Metric characterization of circles. *Amer. Math. Monthly*, 81:149–153, 1974.
- [12] F. Aurenhammer and R. Klein. Voronoi diagrams. In J.-R. Sack and J. Urrutia, editors, *Handbook of Computational Geometry*, pages 201–290. Elsevier Science Publishers B.V. North-Holland, Amsterdam, 2000.

- [13] I. Bárány. Problem 1. Auburn geometry mini-workshop, held at Auburn University, Alabama, October 1997.
- [14] M. Benkert, T. Shirabe, and A. Wolff. The minimum Manhattan network problem: Approximations and exact solutions. In *Proc. 20th European Workshop on Computational Geometry*, pages 209–212, March 2004.
- [15] M. Benkert, F. Widmann, and A. Wolff. The minimum Manhattan network problem: A fast factor-3 approximation. In J. Akiyama, M. Kano, and X. Tan, editors, *Proc. 8th Japanese Conf. on Discrete and Computational Geometry*, volume 3742 of *LNCS*, pages 16–28. Springer, October 2005.
- [16] M. Benkert, F. Widmann, A. Wolff, and T. Shirabe. The minimum Manhattan network problem: Approximations and exact solutions. *Computational Geometry: Theory and Applications*, 2006. To appear.
- [17] P. Berman. On-line searching and navigation. In A. Fiat and G. Woeginger, editors, *Online Algorithms: The State of the Art*, volume 1442 of *LNCS*, pages 232–241. Springer, 1998.
- [18] K. G. Binmore. On Turan’s lemma. *Bull. London Math. Soc.*, 3:313–317, 1971.
- [19] W. Blaschke. *Kreis und Kugel*. Veit, Leipzig, 1916. Later editions: Chelsea, New York, 1955; de Gruyter, Berlin, 1956.
- [20] W. Blaschke and H. R. Müller. *Ebene Kinematik*. Verlag von R. Oldenbourg, München, 1956.
- [21] T. Bonnesen. *Les problèmes des isopérimètres et des iséiphanes*. Gauthier et Villars, Paris, 1929.
- [22] T. Bonnesen and W. Fenchel. *Theorie der konvexen Körper*. J. Springer, Berlin, Germany, 1934. Reprinted Chelsea, New York, 1948.
- [23] A. Borodin and R. El-Yaniv. *Online Computation and Competitive Analysis*. Cambridge University Press, 1998.
- [24] J. Bourgain. On Lipschitz embedding of finite metric spaces in Hilbert space. *Israel Journal of Mathematics*, 52(1–2):46–52, 1985.
- [25] D. W. Boyd. Improved bounds for the disk-packing constant. *Aeq. math.*, 9:99–106, 1973.
- [26] C. B. Boyer. *A History of Mathematics*. John Wiley & Sons, 1968.
- [27] A. Broman. Holditch’s theorem - A fresh look at a long-forgotten theorem. *Mathematics Magazine*, 54(3):99–108, 1981.
- [28] P. B. Callahan and S. R. Kosaraju. A decomposition of multidimensional point sets with applications to  $k$ -nearest-neighbors and  $n$ -body potential fields. *J. ACM*, 42:67–90, 1995.



- [29] J. Cantarella, R. B. Kusner, and J. M. Sullivan. On the minimum ropelength of knots and links. *Inventiones Math.*, 150(2):257–286, 2002.
- [30] A. L. Cauchy. Note sur divers théorèmes relatifs à la rectification des courbes et à la quadrature des surfaces. *C. R. Acad. Sci. Paris*, 13:1060–1065, 1841. [Oeuvres complètes (1), Vol. 6 (Gauthier-Villars, Paris, 1888) 369–375].
- [31] G. D. Chakerian. A characterization of curves of constant width. *Amer. Math. Monthly*, 81:153–155, 1974.
- [32] G. D. Chakerian and P. R. Goodey. Inequalities involving convex sets and their chords. *Annals of Discrete Mathematics*, 20:93–101, 1984.
- [33] G. D. Chakerian and H. Groemer. Convex bodies of constant width. In P. M. Gruber and J. M. Wills, editors, *Convexity and its Applications*, pages 49–96. Birkhäuser, Boston, 1983.
- [34] O. Cheong, H. Haverkort, and M. Lee. Computing a minimum-dilation spanning tree is NP-hard. In *Proc. Computing: The Australasian Theory Symposium (CATS)*, 2007. To appear.
- [35] V. Chepoi, K. Nouioua, and Y. Vaxès. A rounding algorithm for approximating minimum Manhattan networks. In *8th International Workshop on Approximation Algorithms for Combinatorial Optimization Problems and 9th International Workshop on Randomization and Computation*, volume 3624 of *LNCS*, pages 40–51. Springer, August 2005.
- [36] L. P. Chew. There is a planar graph almost as good as the complete graph. In *Proc. 2nd Annu. ACM Sympos. Comput. Geom.*, pages 169–177, 1986.
- [37] L. P. Chew. There are planar graphs almost as good as the complete graph. *J. Comput. Syst. Sci.*, 39:205–219, 1989.
- [38] R. Courant and F. John. *Introduction to Calculus and Analysis*, volume 1. Interscience Publishers, John Wiley & Sons, New York, 1965.
- [39] R. Courant and F. John. *Introduction to Calculus and Analysis*, volume 2. Interscience Publishers, John Wiley & Sons, New York, 1974.
- [40] H. P. Croft, K. J. Falconer, and R. K. Guy. *Unsolved Problems in Geometry*. Springer, 1991.
- [41] P. Dale, P. Eades, X. Lin, and N. C. Wormald. Measuring motion planning strategies. In *Abstracts First Canadian Conference on Computational Geometry*, page 8, 1989.
- [42] G. Das and D. Joseph. Which triangulations approximate the complete graph? In *Proc. International Symposium on Optimal Algorithms*, volume 401 of *LNCS*, pages 168–192. Springer, 1989.
- [43] M. de Berg, M. van Kreveld, M. Overmars, and O. Schwarzkopf. *Computational Geometry: Algorithms and Applications*. Springer-Verlag, Berlin, Germany, 2nd edition, 2000.

- [44] E. Denne, Y. Diao, and J. M. Sullivan. Quadriseccants give new lower bounds for the ropelength of a knot. *Geometry and Topology*, 10:1–26, 2006.
- [45] E. Denne and J. M. Sullivan. The distortion of a knotted curve. Preprint at <http://www.arxiv.org/abs/math.GT/0409438>, September 2004.
- [46] M. P. do Carmo. *Differential Geometry of Curves and Surfaces*. Prentice Hall, Englewood Cliffs, NJ, 1976.
- [47] D. P. Dobkin, S. J. Friedman, and K. J. Supowit. Delaunay graphs are almost as good as complete graphs. *Discrete Comput. Geom.*, 5:399–407, 1990.
- [48] A. Dumitrescu, A. Ebberts-Baumann, A. Grüne, R. Klein, and G. Rote. On geometric dilation and halving chords. In *9th International Workshop on Algorithms and Data Structures*, volume 3608 of *LNCS*, pages 244–255. Springer, 2005.
- [49] A. Dumitrescu, A. Ebberts-Baumann, A. Grüne, R. Klein, and G. Rote. On the geometric dilation of closed curves, graphs and point sets. *Computational Geometry: Theory and Applications*, 36:16–38, 2007.
- [50] A. Dumitrescu, A. Grüne, and G. Rote. Improved lower bound on the geometric dilation of point sets. In *Abstracts 21st European Workshop Comput. Geom.*, pages 37–40. Technische Universiteit Eindhoven, 2005.
- [51] P. Eades, X. Lin, and N. C. Wormald. Performance guarantees for motion planning with temporal uncertainty. Technical Report 173, Dept. of Computer Science, Univ. of Queensland, St. Lucia, Queensland, Australia, 1990.
- [52] P. Eades, X. Lin, and N. C. Wormald. Performance guarantees for motion planning with temporal uncertainty. In *Proc. 13th Australian Computer Science Conference*, pages 78–87, 1990.
- [53] P. Eades, X. Lin, and N. C. Wormald. Performance guarantees for motion planning with temporal uncertainty. *Australian Computer Journal*, 25(1):21–28, 1993.
- [54] A. Ebberts-Baumann, A. Grüne, M. Karpinski, R. Klein, C. Knauer, and A. Lingas. Embedding point sets into plane graphs of small dilation. In *Algorithms and Computation: 16th International Symposium, ISAAC 2005*, volume 3827 of *LNCS*, pages 5–16. Springer, December 2005.
- [55] A. Ebberts-Baumann, A. Grüne, M. Karpinski, R. Klein, C. Knauer, and A. Lingas. Embedding point sets into plane graphs of small dilation. *International Journal of Computational Geometry & Applications*, 2007. To appear.
- [56] A. Ebberts-Baumann, A. Grüne, and R. Klein. On the geometric dilation of finite point sets. In *14th Annual International Symposium on Algorithms and Computation*, volume 2906 of *LNCS*, pages 250–259. Springer, 2003.
- [57] A. Ebberts-Baumann, A. Grüne, and R. Klein. Geometric dilation of closed planar curves: A new lower bound. In *Abstracts 20th European Workshop Comput. Geom.*, pages 123–126. Universidad de Sevilla, 2004.

- [58] A. Ebbers-Baumann, A. Grüne, and R. Klein. The geometric dilation of finite point sets. *Algorithmica*, 44:137–149, 2006.
- [59] A. Ebbers-Baumann, A. Grüne, and R. Klein. Geometric dilation of closed planar curves: New lower bounds. *Computational Geometry: Theory and Applications*, 2007. To appear.
- [60] A. Ebbers-Baumann, R. Klein, C. Knauer, and G. Rote. The geometric dilation of three points. Unpublished manuscript, April 2006.
- [61] A. Ebbers-Baumann, R. Klein, E. Langetepe, and A. Lingas. A fast algorithm for approximating the detour of a polygonal chain. *Computational Geometry: Theory and Applications*, 27:123–134, 2004.
- [62] J. Edwards. *A Treatise on the Integral Calculus*, volume I. Chelsea Publishing Company, New York, 2nd edition, 1930.
- [63] H. G. Eggleston. *Convexity*. Cambridge University Press, Cambridge, England, 1958.
- [64] H. G. Eggleston. The maximal length of chords bisecting the area or perimeter length of plane convex sets. *Jour. London Math. Soc.*, 36:122–188, 1961.
- [65] D. Eppstein. Dilation-free planar graphs. The Geometry Junkyard, <http://www.ics.uci.edu/~eppstein/junkyard/dilation-free/>, 1997.
- [66] D. Eppstein. Spanning trees and spanners. In J.-R. Sack and J. Urrutia, editors, *Handbook of Computational Geometry*, pages 425–461. Elsevier Science Publishers B.V. North-Holland, Amsterdam, 2000.
- [67] D. Eppstein and K. A. Wortman. Minimum dilation stars. In *Proc. 21st ACM Symp. Comp. Geom.*, pages 321–326, 2005.
- [68] N. Eriksson and J. C. Lagarias. Apollonian packings: Number theory II. Spherical and hyperbolic packings. *Ramanujan Journal*, 2007. To appear.
- [69] K. J. Falconer. *The geometry of fractal sets*. Cambridge University Press, Cambridge, 1985.
- [70] M. Farshi, P. Giannopoulos, and J. Gudmundsson. Finding the best shortcut in a geometric network. In *Proc. 21st ACM Symp. Comp. Geom.*, pages 327–335, 2005.
- [71] G. Fejes Tóth and W. Kuperberg. Packing and covering with convex sets. In P. M. Gruber and J. M. Wills, editors, *Handbook of Convex Geometry*, volume B, chapter 3.3, pages 799–860. Elsevier Science, Amsterdam, 1993.
- [72] A. Fiat and G. Woeginger, editors. *Online Algorithms: The State of the Art*, volume 1442 of *LNCS*. Springer, 1998.
- [73] B. Fuglede. Bonnesen’s inequality for the isoperimetric deficiency of closed curves in the plane. *Geom. Dedicata*, 38:283–300, 1991.
- [74] M. R. Garey and D. S. Johnson. *Computers and Intractability: A Guide to the Theory of NP-Completeness*. W. H. Freeman, New York, NY, 1979.

- [75] H. Geppert. Über einige Kennzeichnungen des Kreises. *Mathematische Zeitschrift*, 46:117–128, 1940.
- [76] P. Goodey. Area and perimeter bisectors of planar convex sets. Unpublished manuscript, June 2005.
- [77] P. R. Goodey. A characterization of circles. *Bull. London Math. Soc.*, 4:199–201, 1972.
- [78] P. R. Goodey. Mean square inequalities for chords of convex sets. *Israel Journal Math. Soc.*, 42:138–152, 1982.
- [79] R. L. Graham, J. C. Lagarias, C. L. Mallows, A. Wilks, and C. H. Yan. Apollonian packings: Number theory. *J. Number Theory*, 100:1–45, 2003.
- [80] R. L. Graham, J. C. Lagarias, C. L. Mallows, A. Wilks, and C. H. Yan. Apollonian circle packing: Geometry and group theory, I. The Apollonian group. *Discrete & Computational Geometry*, 34:547–585, 2005.
- [81] R. L. Graham, J. C. Lagarias, C. L. Mallows, A. Wilks, and C. H. Yan. Apollonian circle packing: Geometry and group theory, III. Higher dimensions. *Discrete & Computational Geometry*, 35:37–72, 2006.
- [82] R. L. Graham, J. C. Lagarias, C. L. Mallows, A. Wilks, and C. H. Yan. Apollonian circle packing: Geometry and group theory, II. Super-Apollonian group and integral packings. *Discrete & Computational Geometry*, 35:1–36, 2006.
- [83] P. Gritzmann and V. Klee. Inner and outer  $j$ -radii of convex bodies in finite-dimensional normed spaces. *Discrete Comput. Geom.*, 7:255–280, 1992.
- [84] H. Groemer. Stability of geometric inequalities. In P. M. Gruber and J. M. Wills, editors, *Handbook of Convex Geometry*, volume A, pages 125–150. North-Holland, Amsterdam, Netherlands, 1993.
- [85] M. Gromov. Homotopical effects of dilatation. *J. Differential Geometry*, 13:303–310, 1978.
- [86] M. Gromov. *Structures Métriques des Variétés Riemanniennes*, volume 1 of *Textes math.* CEDIC / Fernand Nathan, Paris, 1981. Edited by J. Lafontaine and P. Pansu.
- [87] M. Gromov. Filling Riemannian manifolds. *J. Differential Geometry*, 18:1–147, 1983.
- [88] M. Gromov. *Metric Structures for Riemannian and Non-Riemannian Spaces*, volume 152 of *Progress in Mathematics*. Birkhäuser, Boston, 1998. Edited by J. Lafontaine and P. Pansu. Extended English translation of “Structures Métriques des Variétés Riemanniennes”.
- [89] P. M. Gruber. Aspects of approximation of convex bodies. In P. M. Gruber and J. M. Wills, editors, *Handbook of Convex Geometry*, volume A, chapter 1.10, pages 319–345. Elsevier Science, Amsterdam, 1993.
- [90] P. M. Gruber. The space of convex bodies. In P. M. Gruber and J. M. Wills, editors, *Handbook of Convex Geometry*, volume A, chapter 1.9, pages 301–318. Elsevier Science, Amsterdam, 1993.

- [91] B. Grünbaum and G. C. Shephard. *Tilings and Patterns*. W. H. Freeman, New York, NY, 1987.
- [92] A. Grüne. Umwege in Polygonen. Diplomarbeit, Rheinische Friedrich-Wilhelms-Universität Bonn, 2002.
- [93] A. Grüne and S. Kamali Sarvestani. On the density of iterated line segment intersections. Technical Report 004, Department of Computer Science I, University of Bonn, 2005.
- [94] A. Grüne and S. Kamali Sarvestani. On the density of iterated line segment intersections. In *Abstracts 22nd European Workshop Comput. Geom.*, pages 39–42, 2006.
- [95] A. Grüne, R. Klein, and E. Langetepe. Computing the detour of polygons. In *Abstracts 19th European Workshop Comput. Geom.*, pages 61–64. University of Bonn, 2003.
- [96] A. Grüne, R. Klein, C. Miori, and S. Segura Gomis. Chords halving the area of a planar convex set. *Mathematical Inequalities and Applications*, 2007. To appear.
- [97] J. Gudmundsson, C. Levcopoulos, and G. Narasimhan. Approximating minimum Manhattan networks. In D. S. Hochbaum, K. Jansen, J. D. P. Rolim, and A. Sinclair, editors, *Randomization, Approximation, and Combinatorial Algorithms and Techniques, Proceedings RANDOM-APPROX '99*, volume 1671 of *LNCS*, pages 28–38. Springer, August 1999.
- [98] J. Gudmundsson, C. Levcopoulos, and G. Narasimhan. Approximating a minimum Manhattan network. *Nordic J. Comput.*, 8:219–232, 2001.
- [99] J. Gudmundsson, G. Narasimhan, and M. Smid. Fast pruning of geometric spanners. In V. Diekert and B. Durand, editors, *Proc. 22nd Annual Symposium on Theoretical Aspects of Computer Science*, volume 3404 of *LNCS*, pages 508–520. Springer, 2005.
- [100] J. Gudmundsson and M. Smid. On spanners of geometric graphs. In L. Arge and R. Freivalds, editors, *10th Scandinavian Workshop on Algorithm Theory*, volume 4059 of *LNCS*, pages 388–399. Springer, July 2006.
- [101] H. Herda. A conjectured characterization of circles. *Amer. Math. Monthly*, 78:888–889, 1971.
- [102] H. Herda. A characterization of circles and other closed curves. *Amer. Math. Monthly*, 81:146–148, 1974.
- [103] K. E. Hirst. The Apollonian packing of circles. *Journal London Math. Soc.*, 42:281–291, 1967.
- [104] R. H. Holditch. Geometrical theorem. *The Quarterly Journal of Pure and Applied Mathematics*, II:38, 1858.
- [105] J. Hoschek. Räumliche Zindlerkurven. *Math. Balcanica*, 4:253–260, 1974.
- [106] F. Hurtado. Personal communication. March 2004.

- [107] C. Icking, T. Kamphans, R. Klein, and E. Langetepe. On the competitive complexity of navigation tasks. In H. Bunke, H. I. Christensen, G. D. Hager, and R. Klein, editors, *Sensor Based Intelligent Robots*, volume 2238 of *LNCS*, pages 245–258, Berlin, 2002. Springer.
- [108] C. Icking and R. Klein. Competitive strategies for autonomous systems. In H. Bunke, T. Kanade, and H. Noltemeier, editors, *Modelling and Planning for Sensor Based Intelligent Robot Systems*, pages 23–40. World Scientific, Singapore, 1995.
- [109] C. Icking and R. Klein. Searching for the kernel of a polygon: A competitive strategy. In *Proc. 11th Annu. ACM Sympos. Comput. Geom.*, pages 258–266, 1995.
- [110] C. Icking, R. Klein, and E. Langetepe. Searching for the kernel of a polygon: A competitive strategy using self-approaching curves. Technical Report 211, Department of Computer Science, FernUniversität Hagen, Germany, 1997.
- [111] C. Icking, R. Klein, and E. Langetepe. Self-approaching curves. Technical Report 217, Department of Computer Science, FernUniversität Hagen, Germany, 1997.
- [112] C. Icking, R. Klein, and E. Langetepe. An optimal competitive strategy for walking in streets. In *Proc. 16th Sympos. Theoret. Aspects Comput. Sci.*, volume 1563 of *LNCS*, pages 110–120. Springer, 1999.
- [113] C. Icking, R. Klein, and E. Langetepe. Self-approaching curves. *Math. Proc. Camb. Phil. Soc.*, 125:441–453, 1999.
- [114] C. Icking, R. Klein, E. Langetepe, S. Schuierer, and I. Semrau. An optimal competitive strategy for walking in streets. *SIAM J. Comput.*, 33:462–486, 2004.
- [115] I. M. Jaglom and W. G. Boltjanski. *Konvexe Figuren*. VEB Deutscher Verlag der Wissenschaften, Berlin, 1956.
- [116] W. Johnson and J. Lindenstrauss. Extensions of Lipschitz maps into a Hilbert space. *Contemp. Math.*, 26:189–206, 1984.
- [117] S. Kamali. On the density of iterated segment intersections. Diplomarbeit, Rheinische Friedrich-Wilhelms-Universität Bonn, 2005.
- [118] T. Kamphans. *Models and Algorithms for Online Exploration and Search*. Dissertation, University of Bonn, 2006. Available at [http://hss.ulb.uni-bonn.de/diss\\_online/math\\_nat\\_fak/](http://hss.ulb.uni-bonn.de/diss_online/math_nat_fak/).
- [119] J. M. Keil. Approximating the complete Euclidean graph. In *Proc. 1st Scand. Workshop Algorithm Theory*, volume 318 of *Lecture Notes Comput. Sci.*, pages 208–213. Springer, 1988.
- [120] J. M. Keil and C. A. Gutwin. Classes of graphs which approximate the complete Euclidean graph. *Discrete Comput. Geom.*, 7:13–28, 1992.
- [121] E. Kiliç and S. Keleş. On Holditch’s theorem and polar inertia momentum. *Commun. Fac. Sci. Univ. Ank. Series A*, 43:41–47, 1994.

- [122] C. Kimberling. Encyclopedia of triangle centers. <http://faculty.evansville.edu/ck6/encyclopedia/>.
- [123] C. Kimberling. *Triangle Centers and Central Triangles*, volume 129 of *Congressus Numerantium*. Utilitas Mathematica, Winnipeg, Canada, 1998.
- [124] A. Klein. Applet 'Minimum Dilation Triangulation'. Geometry Lab, <http://www.geometrylab.de/>, 2006.
- [125] A. Klein. Effiziente Berechnung einer dilationsminimalen Triangulierung. Diplomarbeit, Rheinische Friedrich-Wilhelms-Universität Bonn, 2006.
- [126] R. Klein. Walking an unknown street with bounded detour. *Comput. Geom. Theory Appl.*, 1:325–351, 1992.
- [127] R. Klein. *Algorithmische Geometrie*. Springer, Heidelberg, 2nd edition, 2005.
- [128] R. Klein, C. Knauer, G. Narasimhan, and M. Smid. Exact and approximation algorithms for computing the dilation spectrum of paths, trees, and cycles. In *Algorithms and Computation: 16th International Symposium, ISAAC 2005*, volume 3827 of *LNCS*, pages 849–858, Berlin / Heidelberg, December 2005. Springer.
- [129] R. Klein and M. Kutz. Computing geometric minimum-dilation graphs is NP-hard. In *Proc. 14th International Symposium on Graph Drawing*, LNCS. Springer, September 2006. To appear.
- [130] R. Klein and M. Kutz. The density of iterated crossing points and a gap result for triangulations of finite point sets. In *Proc. 22nd ACM Symp. Comp. Geom.*, pages 264–272. ACM Press, 2006.
- [131] M. Köhler. Berechnung minimaler Manhattan-Netzwerke. Diplomarbeit, Rheinische Friedrich-Wilhelms-Universität Bonn, 2006.
- [132] T. Komorowski. Berechnung der graphentheoretischen Dilation. Diplomarbeit, Universität Bonn, 2004.
- [133] T. Kubota. Einige Ungleichheitsbeziehungen über Eilinien und Eiflächen. *Sci. Rep. Tōhoku Univ.*, 12:45–65, 1923.
- [134] K. Kuperberg, W. Kuperberg, J. Matousek, and P. Valtr. Almost-tiling the plane by ellipses. *Discrete & Computational Geometry*, 22(3):367–375, 1999.
- [135] R. B. Kusner and J. M. Sullivan. On distortion and thickness of knots. In S. G. Whittington, D. W. Sumners, and T. Lodge, editors, *Topology and Geometry in Polymer Science*, volume 103 of *IMA Volumes in Math. and its Applications*, pages 67–78. Springer, 1998.
- [136] S. Lang. *Complex Analysis*. Addison-Wesley, Reading, Massachusetts, 1977.
- [137] S. Langerman, P. Morin, and M. A. Soss. Computing the maximum detour and spanning ratio of planar chains, trees, and cycles. In *Abstracts 11th Fall Workshop Comp. Geom.*, 2001.

- [138] S. Langerman, P. Morin, and M. A. Soss. Computing the maximum detour and spanning ratio of planar paths, trees, and cycles. In *Proc. 19th Symp. Theoret. Aspects. Comput. Sci.*, pages 250–261, 2002.
- [139] D. G. Larman and P. McMullen. Arcs with increasing chords. *Proc. Camb. Phil. Soc.*, 72:205–207, 1972.
- [140] S. R. Lay. *Convex Sets and their applications*. John Wiley & Sons, New York, 1972.
- [141] J.-H. Lee and K.-Y. Chwa. Tight analysis of a self-approaching strategy for the online kernel-search problem. *Inform. Process. Lett.*, 69:39–45, 1999.
- [142] J.-H. Lee, C.-S. Shin, J.-H. Kim, S. Y. Shin, and K.-Y. Chwa. New competitive strategies for searching in unknown star-shaped polygons. In *Proc. 13th Annu. ACM Sympos. Comput. Geom.*, pages 427–429, 1997.
- [143] N. Linial, E. London, and Y. Rabinovich. The geometry of graphs and some of its algorithmic applications. *Combinatorica*, 15:215–245, 1995.
- [144] E. H. Lockwood. *A Book of Curves*. Cambridge University Press, Cambridge, UK, 1961.
- [145] K. L. Mampel. Über Zindlerkurven. *J. reine angew. Math.*, 234:12–44, 1969.
- [146] B. B. Mandelbrot. *The Fractal Geometry of Nature*. W. H. Freeman and Company, New York, updated and augmented edition, 1983.
- [147] J. Matoušek. *Lectures on Discrete Geometry*, volume 212 of *Graduate Texts in Mathematics*. Springer-Verlag, 2002.
- [148] C. T. McMullen. Hausdorff dimension and conformal dynamics III: Computation of dimension. *Amer. J. Math.*, 120:691–721, 1998.
- [149] J. W. Milnor. On the total curvature of knots. *Annals of Mathematics*, 52(2):248–257, September 1950.
- [150] H. Minkowski. Volumen und Oberflächen. *Math. Ann.*, 57:447–495, 1903. [Gesammelte Abhandlungen, Vol. II (Teubner, Leipzig, 1911) pp. 230–276.].
- [151] C. Miori, C. Peri, and S. S. Gomis. On fencing problems. *Journal of Mathematical Analysis and Applications*, 300(2):464–476, 2004.
- [152] H. R. Müller. Zum Satz von Holditch. In J. Tölke and J. M. Wills, editors, *Contributions to Geometry: Proc. of the Geometry-Symposium held in Siegen in 1978*, pages 330–334. Birkhäuser, Basel, 1979.
- [153] W. Mulzer. Minimum dilation triangulations for the regular  $n$ -gon. Diplomarbeit, Freie Universität Berlin, 2004.
- [154] W. Mulzer and G. Rote. Minimum weight triangulation is NP-hard. In *Proc. 21st ACM Symp. Comp. Geom.*, pages 1–10, 2006.



- [155] G. Narasimhan and M. Smid. Approximating the stretch factor of Euclidean paths, cycles and trees. Report 9, Department of Computer Science, University of Magdeburg, Magdeburg, Germany, 1999.
- [156] G. Narasimhan and M. Smid. Approximating the stretch factor of Euclidean graphs. *SIAM J. Comput.*, 30:978–989, 2000.
- [157] G. Narasimhan and M. Smid. *Geometric Spanner Networks*. Cambridge University Press, 2007. To appear.
- [158] J. Pál. Ein Minimumproblem für Ovale. *Math. Ann.*, 83:311–319, 1921.
- [159] C. H. Papadimitriou and M. Yannakakis. Shortest paths without a map. In *Proc. 16th Internat. Colloq. Automata Lang. Program.*, volume 372 of *LNCS*, pages 610–620. Springer-Verlag, 1989.
- [160] C. H. Papadimitriou and M. Yannakakis. Shortest paths without a map. *Theoret. Comput. Sci.*, 84(1):127–150, 1991.
- [161] D. Peleg and A. A. Schäffer. Graph spanners. *J. Graph Theory*, 13(1):99–116, 1989.
- [162] C. Peri and S. Vassallo. Minimal properties for convex annuli of plane convex curves. *Archiv der Mathematik*, 64(3):254–263, 1995.
- [163] K. Radziszewski. Sur les cordes qui partagent le périmètre d’un ovale en 2 parties égales. *Ann. Univ. Mariae Curie-Sklodowska Sect. A*, 8:93–96, 1954.
- [164] N. S. V. Rao, S. Karetí, W. Shi, and S. S. Iyengar. Robot navigation in unknown terrains: introductory survey of non-heuristic algorithms. Technical Report ORNL/TM-12410, Oak Ridge National Laboratory, 1993.
- [165] F. Reuleaux. *The Kinematics of Machinery: Outlines of a Theory of Machines*. Macmillan, London, 1876. Reprinted as *The Kinematics of Machinery*. New York: Dover, 1963.
- [166] A. W. Roberts. Convex functions. In P. M. Gruber and J. M. Wills, editors, *Handbook of Convex Geometry*, volume B, chapter 4.2, pages 1081–1104. Elsevier Science, Amsterdam, 1993.
- [167] G. Rote. Curves with increasing chords. *Math. Proc. Camb. Phil. Soc.*, 115:1–12, 1994.
- [168] E. Salkowski. Eine kennzeichnende Eigenschaft des Kreises. *Sitzungsberichte der Heidelberger Akademie der Wissenschaften, math.-nat. Klasse*, Jahrgang 34(14. Abhandlung), 1934.
- [169] J. R. Sangwine-Yager. Mixed volumes. In P. M. Gruber and J. M. Wills, editors, *Handbook of Convex Geometry*, volume A, chapter 1.2, pages 43–71. Elsevier Science, Amsterdam, 1993.
- [170] L. A. Santaló. *Integral Geometry and Geometric Probability*. Addison-Wesley, Reading, MA, 1976.

- [171] S. Schuierer and I. Semrau. An optimal strategy for searching in unknown streets. In *Proc. 16th Sympos. Theoret. Aspects Comput. Sci.*, volume 1563 of *Lecture Notes Comput. Sci.*, pages 121–131. Springer-Verlag, 1999.
- [172] P. R. Scott and P. W. Awyong. Inequalities for convex sets. *Journal of Inequalities in Pure and Applied Mathematics*, 1(1):6 pp., 2000. Art. 6, <http://jipam.vu.edu.au/article.php?sid=99>.
- [173] D. D. Sleator and R. E. Tarjan. Amortized efficiency of list update rules. In *Proceedings of the Sixteenth Annual ACM Symposium on Theory of Computing*, pages 488–492. ACM Press, 1984.
- [174] D. D. Sleator and R. E. Tarjan. Amortized efficiency of list update and paging rules. *Commun. ACM*, 28:202–208, 1985.
- [175] F. Soddy. The kiss precise. *Nature*, June 20, 1936.
- [176] K. Strubecker. *Differentialgeometrie I: Kurventheorie der Ebene und des Raumes*. De Gruyter, Berlin, 1955.
- [177] J. M. Sullivan. Curves of finite total curvature. *Discrete Differential Geometry*, 2007. To appear. Preprint available at [arxiv.org](http://arxiv.org).
- [178] G. v. Sz. Nagy. Über konvexe Kurven und einschließende Kreisringe. *Acta Sci. Math. Szeged*, 10:174–184, 1941–43.
- [179] G. R. Veldkamp. The isoperimetric point and the point(s) of equal detour in a triangle. *American Mathematical Monthly*, 92:546–558, 1992.
- [180] I. Vincze. Über Kreisringe, die eine Eilinie einschliessen. *Studia Sci. Math. Hungar.*, 9:155–159, 1974.
- [181] B. Wegner. Verallgemeinerte Zindlerkurven in euklidischen Räumen. *Math. Balkanica*, 6:298–306, 1976.
- [182] E. W. Weisstein. *CRC Concise Encyclopedia of Mathematics*. CRC Press LLC, Boca Raton, FL, 1999.
- [183] H. S. Witsenhausen. On closed curves in Minkowski spaces. *Proc. Amer. Math. Phys.*, 31:240–241, 1972.
- [184] I. M. Yaglom and V. G. Boltyanski. *Convex Figures*. English Translation, Holt, Rinehart and Winston, New York, NY, 1961.
- [185] R. C. Yates. *A Handbook on Curves and their Properties*. J. W. Edwards - Ann Arbor, revised edition, 1951.
- [186] K. Zindler. Über konvexe Gebilde. II. Teil *Monatsh. Math. Phys.*, 31:25–56, 1921.
- [187] C. Zong. Simultaneous packing and covering in the Euclidean plane. *Monatsh. Math.*, 134:247–255, 2002.
- [188] D. Zwillinger, editor. *Standard Mathematical Tables and Formulae*. CRC Press, Boca Raton, FL, 30th edition, 1996.

# Index

- airline distance, 1
- annulus, 7
- annulus constant, 72
- Apollonian gasket, 161
- Apollonian packing, 161
- Apollonius of Perga, 161
- Apollonius' problem, 162
- arc with increasing chords, 13
- arc-length parameterization, 30, 165
- Archimedes principle, 98
- area bisector, 89
- area halving distance, 25, 83, **115**
- area-bisecting parameterization, 89, 166
- area-halving chord, 89
- arithmetic mean of sets, 47
  
- Bárány number, 155
- bend, 162
- bisector, 39
- biting, 173
- Blaschke selection theorem, 133
- bounding box, 23
- Brunn-Minkowski theorem, 49
  
- $C$ -distance, 29
- CAB-strategy, 12
- cap-curve, 64, 65
- Cauchy, 36
- Cauchy-Crofton formula, 37
- center of gravity, 99
- center of mass, 99
- central symmetrization, 47
- centroid, 99
- circle of Apollonius, 21
- circumradius, **34**, 44
- closed curve, 29
- closure, 44
- competitive, 11
- competitive analysis, 11
- competitive ratio, 11
- concatenation, 38
- constant area halving distance, 83, 88
- constant halving distance, 81
- continuity in  $\mathcal{X}$ , 133
- contractible, 16
- convergence of compact sets, 133
- convex curve, 29
- cover factor, 155
- crescent, 174
- curvature, 94, 162
- curve
  - closed, 29
  - convex, 29
  - open, 29
  - simple, 27, 29
- curve with interior halving chords, 87
- curves of finite total curvature, 29
- cycle, 29
  
- $D$ -embedding, 24
- Delaunay triangulation, 19
- Delaunay triangulation
  - $L_1$ , 18
- deltoid, 109
- derivative, 29
- Descartes circle theorem, 162
- Descartes equation, 162
- detour, 2, 11, 29
- diameter, **34**, 34
- diametral chord, 34
- diametric points, 117
- differentiable, 29
- dilatation, 14
- dilation
  - geometric, 2, 29
  - of  $(2k - 1)$ -gon, 77
  - of  $2k$ -gon, 77
  - of circle, 66

- of convex cycle, 42
- of hexagonal grid, 144
- of improved hexagonal grid, 148
- of point set, 3, 139
- of polygon, 14
- of rectangular grid, 142
- of square grid, 143
- of triangle, 75
- dilation center, 21
- dilation spectrum, 21
- dilation-free graphs, 23
- disk packing, 154
  - hexagonal, 155
- distortion, 14–16
- duality, 97
- $\varepsilon$ -disk, 40
- embedding, **2**, 139
- envelope, 83
- equilibrium property, 99
- Euclidean distance, 1
- extremal parameterization, 94
- extremal set, 7, 66, 115
- extreme point, 93
- fencing problem, 25
- flattened circle, 67
- flower, 107
- geometric dilation, 3, 29
- graph dilation, 17
  - of point sets, 22
- $\eta$ -annulus, 69
- halving chord, 6, **32**
- halving distance, 6
  - maximum, 34
  - minimum, 34
- halving pair, 6, **32**
  - existence, 33
  - uniqueness, 33
- halving-pair parameterization, 83
- Hausdorff distance, 133
- hexagonal disk packing, 155
- hexagonal grid, 144
- Holditch's theorem, 58
- hypocycloid, 109
- iff, 35
- inradius, **34**, 44
- interior, 29
- interior domain, 29
- interior halving chords, 87
- interior of segment, 87
- intrinsic metric, 15
- Johnson-Lindenstrauss
  - flattening lemma, 24
- $K_5$ , 88
- kernel, 12
- kissing circles, 107
- Kubota, 65
- $\lambda$ -enlargement, 154
- $L_1$ -Delaunay triangulation, 18
- LAD-strategy, 12
- length of a curve, 29
- Lipschitz constant, 14
- local detour maximum, 40
- maximum halving distance, 34
- midpoint curve, 7, 56
- minimum dilation triangulation, 18
- minimum growth rate, 13
- minimum halving distance, 34
- minimum Manhattan network, 23
- Minkowski sum, 47
- mutually visible, 141
- nice parameterization, 29
- one-sided derivative, 28
- online algorithms, 11
- open curve, 29
- orthogonal, 57
- packing, 154
- parallel, 57
- parameterization, 29
  - arc-length, 30, 165
  - area-bisecting, 89, 166
  - extremal, 94
  - halving-pair, 83
  - nice, 29
  - regular, 29
- perimeter, 29

piecewise continuously differentiable, 29

radius of curvature, 94

rectangular grid, 142

regular grid, 144

regular parameterization, 29

regular polygons, 4

Reuleaux-triangle, 97

right area, 89

rope length, 16

rounded pentagon, 106

rounded triangle, 100

scalar product, 33

self-approaching, 13

simple curve, 27, 29

simple graph, 2

simultaneously packing and covering, 155

Soddy's formula, 162

spanner, 18

square grid, 142

stability result, 7, 69

star-shaped polygon, 12

Steiner's hypocycloid, 109

Steiner-point, 18

strictly convex, 93

strip, 53

support function, 134

supporting line, 33

surface area formula, 36

$t$ -spanner, 18

thickness of rope, 16

$\triangle$ -Delaunay triangulation, 18

unit circle, 31

$v$ -breadth, 33

$v$ -halving distance, 34

$v$ -length, 33

$v$ -width, 33

$w$ -chord, 34

width, 34

winding number, 59

Zindler curve, 8, 81

Zindler's example, 109